Integrated Process Development for Bio-fixation of Flue Gases (CO_2, NO and SO_2) Utilizing Microbial Route and Characterization of Products

THESIS

Submitted in partial fulfilment

of the requirements for the degree of

DOCTOR OF PHILOSOPHY

by

ABHISHEK ANAND

Under the
Supervision of

Prof. SMITA RAGHUVANSHI

and

Co-Supervision Of

Prof. SURESH GUPTA

BITS Pilani
Pilani | Dubai | Goa | Hyderabad

BIRLA INSTITUTE OF TECHNOLOGY AND SCIENCE, PILANI
2023

BIRLA INSTITUTE OF TECHNOLOGY & SCIENCE
PILANI-333031 (RAJASTHAN) INDIA

CERTIFICATE

This is to certify that the thesis entitled "Integrated Process Development for Bio-fixation of Flue Gases (CO_2, NO and SO_2) Utilizing Microbial Route and Characterization of Products" and submitted by **ABHISHEK ANAND**, ID. No. **2017PHXF0014P** for the award of Ph.D. degree of the Institute embodies the original work done by him under our supervision.

Signature of the Supervisor
Name in capital letters
Designation

Prof. SMITA RAGHUVANSHI
Professor
Department of Chemical Engineering
BITS-PILANI, Pilani Campus, India

Date:

Signature of the Co-Supervisor
Name in capital letters
Designation

Prof. SURESH GUPTA
Professor
Department of Chemical Engineering
BITS-PILANI, Pilani Campus, India

Date:

ॐ

भूर्भुवः स्वः तत्सवितुर्वरेण्यं भर्गो देवस्य धीमहि धियो यो नः प्रचोदयात्।

Rig Veda (Mandala 3.62.10)

To

My Parents,

Brothers,

Sisters-in-law,

Mahi & Ruhi

ACKNOWLEDGEMENTS

I would like to express heartfelt and earnest gratitude to my PhD supervisor **Prof. Smita Raghuvanshi**, Professor, Department of Chemical Engineering, BITS-Pilani, Pilani Campus, for her unwavering guidance, encouragement, patience, and support. Madam has supported me academically and emotionally through the rough road to finish this thesis. During my tenure, she contributed to a rewarding doctorate experience by giving me intellectual freedom in my work, supporting my attendance at various conferences, engaging me in new ideas, and demanding a high quality of work in all my endeavors. I could not have imagined having a better advisor and mentor for my Ph.D. programme.

My sincere gratitude is reserved for my Co-Supervisor, **Prof. Suresh Gupta**, Professor, Former Head, Department of Chemical Engineering, and Former Associate Dean, Academic - Undergraduate Studies Division (AUGSD) BITS-Pilani, Pilani Campus, for his invaluable insights and suggestions. His vast research knowledge and experience in the field, deep understanding, flexible and welcoming attitude have helped me throughout my research. It is truly an honour to be his student, and working under his mentorship has facilitated optimal growth of research and academics.

I would also take this opportunity to express my profound gratefulness to the members of my Doctoral Advisory Committee (DAC), Prof. Arvind Kumar Sharma, Associate Professor & Former Head, Department of Chemical Engineering, BITS- Pilani, Pilani campus, and Dr. Amit Jain, Assistant Professor, Department of Chemical Engineering, BITS-Pilani, Pilani Campus for their continuous feedback, time, patience and effort to read my thesis and provide valuable feedback and suggestions.

I would like to thank Prof. Sanjay Kumar Verma (Dean**,** Administration)**,** BITS- Pilani**,** Pilani campus**,** for providing all the lab facilities**.** Without his unconditional support**,** work related to the loop photobioreactor would not have been possible.

I am forever grateful to the administration of BITS, Pilani, Pilani Campus. My sincere regards to Prof. V. Ramgopal Rao (Vice-Chancellor), Prof. Sudhir Kumar Barai (Director, BITS, Pilani, Pilani Campus), Prof. Souvik Bhattacharya (Former Vice-Chancellor), Prof. A. K. Sarkar (Former Director**,** BITS, Pilani, Pilani Campus)**,** for facilitating me to pursue my research work at such an esteemed university. I also express my sincere gratitude to Prof. M. B. Srinivas (Dean, Academic – Graduate Studies & Research), Prof. Srinivas Krishnaswamy (Former Dean, Academic – graduate studies & research), Prof. Shamik Chakraborty (Associate Dean, Academic – Graduate Studies & Research) and Prof. Jitendra Panwar (Former Associate Dean**,** academic – graduate studies & research) for providing their valuable support throughout this my doctoral tenure.

I am grateful to be a part of the diverse and inclusive Department of Chemical engineering, BITS, Pilani. I extend my profound thanks to Prof. Pratik N. Sheth, Professor, and Head, Department of Chemical Engineering, BITS-Pilani, Pilani campus, Prof. Hare Krishna Mohanta and Prof. Banasri Roy (Former Head, Department of Chemical Engineering, BITS-Pilani, Pilani campus) for facilitating a conducive and healthy environment to conduct this research with great enthusiasm

and encouragement. I would also like to thank all the faculties of the department, Prof. Pradipta Chattopadhyay, Dr. Ajaya Kumar Pani, Dr. Bhanu Vardhan Reddy Kuncharam, Dr. Jay Pandey, Dr. Krishna C Etika, Dr. Srinivas Appari, Dr. Priya C. Sande, Dr. Mohit Garg, Dr. Sarbani Ghosh, and Dr. Somak Chatterjee for encouraging me by discussing their valuable and expert views during my mid-semester and end-semester presentations to the department.

I would like to extend my gratitude towards the office staff of the Department of Chemical Engineering, Mr. Ashok Saini for his help in technical assistance. I would like to thank Mr. Kuldeep Kumar, demonstrator, for his help in handling various analytical equipment. Thanks to Mr. Babulal Saini, Mr. Suresh Kumar Sharma, Mr. Jeevan Lal Verma, Mr. Jangvir Sheron, and Mr. Sunder Lal Harijan for their help and cooperation during this work.

I extend my special thanks to Mr. Sandeep Poonia and Dr. Shraddha Mishra, Research Scholars, Biological Science, for familiarizing me with biological experiments and helping me understand protocols used in the isolation and identification of microbial strains. I also thank Dr. Somesh Mishra for his constant support.

I would like to thank my seniors, Dr. Arun Karthick, Dr. Shweta Sharma, Dr. Saswat Kumar Pradhan, and Dr. Tapas Kumar Patra, Department of Chemical Engineering, for their support at the personal and professional level. I also thank my fellow labmates Mr. Akshya Khandelwal, Mr. Amit Kumar, Mr. Venkata Vijayan S, Mrs. Shailee Gaur, Mrs. Priya S Tanvidkar, Ms. Ajita Neogi, Mr. Anil Kumar K, Ms. Rachael Jovita Barla, Mr. Bharat Nayak and Mr. Manu Sharma. I also thank all the research scholars of our department.

I cannot do without thanking my friends at the university, Dr. Himanshu Seth, Dr. Namita Ruparel, Dr. Sachin Kumar and Dr. Bhoopendra Pandey. They made the entire duration of my doctorate not only supporting and encouraging, rather fun and adventurous. With their consistent support, the span of my doctorate seems to have flown away in no time.

I am blessed to have such amazingly supportive and loving family members, my father, Mr. Ramlakhan Prasad, my mother, Mrs. Malti Devi, my brothers, Dr. Pranav Ranjan, Mr. Praveen Kumar, Mr. Brajesh Kumar, my sisters-in-law, Mrs. Priyanka Kumari, Mrs. Shwetanka Singh and my beloved nieces Mahi and Ruhi. I wouldn’t have come this far without their emotional and tangible support. It is their patience and consistent love, that has helped achieve such great feats.

I thank the Almighty for giving me the strength and patience to work through all these years so that today I can stand proud with my head held high.

Last but not least, I want to thank me. I want to thank me for believing in me. I want to thank me for doing all this hard work to be here. I want to thank me for never quitting. I want to thank me for always being a giver and trying to give more than I receive. I want to thank me for trying to do more right than wrong. I want to thank me for just being always me.

ABHISHEK ANAND

ABSTRACT

Global warming and air pollution are significantly caused by releasing greenhouse gases (GHGs) and flue gases into the atmosphere due to anthropogenic activities. Industries like cement, coal-fired, and gas-fired power plants are the main producers of flue gases (CO_2, NO_x, and SO_x). Out of which, cement sector flue gas emissions required significant attention. Therefore, flue gas fixation from industrial sources must be accomplished. A more practical, cost-effective biological alternative is required for the simultaneous fixation and use of CO_2, NO, and SO_2. Therefore, the current work focuses on the microbiological pathway to bio-fixing flue gases (CO_2, NO, and SO_2). *Desmodesmus sp.* was used to conduct the bio-fixation investigation of CO_2 in the 34 L custom-designed loop photobioreactor at varying inlet CO_2 concentrations of 0.03%, 5%, and 10% (v/v). The gas mixture was supplied during the 12-hour light period, and the impact of the light-dark cycle on the growth of microalgal biomass was investigated. The different growth kinetic parameters for the generated biomass, including specific growth rate, biomass productivity, CO_2 fixation rate, and biochemical characteristics, lipids, carbohydrate, and protein, including chlorophyll content, were calculated. The obtained values of biomass productivity and CO_2 fixation rate include 0.185 ± 0.004 g L^{-1} d^{-1} and 0.333 ± 0.004 g L^{-1} d^{-1}, respectively, at 10% (v/v) CO_2 concentration and 0.084 ± 0.003 g L^{-1} d^{-1} and 0.155 ± 0.003 g L^{-1} d^{-1}, respectively, at 5% (v/v) CO_2 concentration. At a CO_2 concentration of 10% (v/v), the maximum amounts of carbohydrates, proteins, and lipids were obtained as $20.7 \pm 2.4\%$, $32.2 \pm 2.5\%$, and $42 \pm 1.0\%$, respectively. The current study's findings are compared with those of earlier research investigations published in the literature and indicated the viability of scaling up the method for CO_2 source reduction. The ability of bacteria to proliferate quickly and tolerate high CO_2 concentrations attracted a lot of attention to the bio-fixation of CO_2 via the bacterial route. Using domestic wastewater (DWW) as a nutrition medium and energy source will benefit the bio-fixation process. Therefore, it was determined whether using DWW instead of deionized water (DIW) would be feasible for the bio-fixation of CO_2 using *Halomonas stevensii* (H. stevensii).

Laboratory scale experiments were conducted in a suspended bioreactor (semi-continuous mode) for 6 days to evaluate the potential of *H. stevensii* towards bio-fixation of 10% (v/v) CO_2 (g) in DIW (100 mM $Na_2S_2O_3$), DWW (100 mM $Na_2S_2O_3$) and DWW (no additional sulfate). Various parameters such as biomass concentration, specific growth rate, biomass productivity, CO_2 fixation rate, carbonate ions, bicarbonate ions, optical density, pH, dry weight biomass, gaseous

phase CO_2 (g) concentration, dissolved CO_2 (g) concentration, and colony forming unit (CFU) were measured or estimated in every 24 h. *H. stevensii* grown on DWW (no additional sulfate) showed maximum specific growth rate and biomass productivity of 1.19 d^{-1} and 3.24 g L^{-1} d^{-1}, respectively, comparable with the results obtained from two other cultivation media. The possibility for the simultaneous removal of various nutrients and pollutants such as NO_3^-, NH_4^+, PO_4^{3-}, COD and SO_4^{2-} were also carried out. Fourier-transform infrared spectroscopy (FT-IR) and Gas Chromatography/Mass Spectrometry (GC-MS) analysis of cell lysate and cell-free supernatant confirmed the presence of fatty alcohols and long-chain hydrocarbons in all three cultivation media. Techno-economic analysis of the present system was carried out by estimating the total operating cost per batch and per kg of biomass produced. The assessment indicated the feasibility of using DWW as cultivation media to replace DIW and is explored further for the bio-fixation of flue gases [CO_2 (g), NO (g), and SO_2 (g)] using bacterial species.

The bio-fixation of individual and simultaneous flue gas mixtures (C, N, S, CN, CS and CNS) by the bacterial consortium (*Bacillus tropicus* SSLMC1, *Bacillus cereus* SSLMC2) isolated from the extreme environment of Sambhar Salt Lake using DWW as a nutrient and energy source was carried out in a laboratory-scale semi-continuous suspended bioreactor (3 L). The parameters include carbonate, bicarbonate, nitrate, nitrite, sulfate, optical density, pH, dissolved CO_2 (l) concentration, CFU, biomass concentration, specific growth rate, biomass productivity, and gas fixation rate were measured or calculated using standard techniques. The higher value of biomass productivity (4.39 g L^{-1} d^{-1}) and maximum specific growth rate (5.89 d^{-1}) for CNS gas mixture validated the utilization of bacterial consortium for the simultaneous bio-fixation of flue gases. The simultaneous utilization efficiency of organic and inorganic components [BOD, COD, PO_4^{3-}, NO_3^-, NO_2^-, CO_3^{2-}, SO_4^{2-} and Fe (II)] present in DWW using bacterial consortium was obtained in the range of 89.91% - 100% for all flue gas mixtures. The FT-IR and GC-MS analysis of cell lysate and cell-free supernatant were conducted to find the likely functional groups present after the bio-fixation study and to confirm the presence of fatty acids, fatty alcohols, and long-chain hydrocarbons. Carbon and Nitrogen balance in all the bio-fixation studies validated the bacterial consortium's utilization of CO_2 (g) and NO (g) for their growth and to produce organic compounds as by-products. Based on the experimental results and product analysis, the possible mechanism for the bio-fixation of CO_2 (g) and NO (g) was also proposed. The results were compared with the previous studies in terms of bio-kinetic parameters, indicating the feasibility of bacterial

consortium for the simultaneous bio-fixation of CO_2 (g), NO (g) and SO_2 (g) utilizing DWW as a nutrient and energy source. The flue gas fixation ability of bacterial consortium at higher gaseous concentration and in the presence of DWW can be understood to be one of the sustainable options for the simultaneous bio-fixation of CO_2 (g), NO (g), and SO_2 (g), wastewater treatment, and production of value-added products. The present study concludes that utilizing DWW as a nutrient and energy source by bacterial consortium indicated the process feasibility for industrial flue gas treatment. The obtained by-products from bio-fixation studies suggest that it can partially replace the requirement of conventional fuels.

Keywords: *Bio-fixation; Simulated flue gas* [CO_2 (g), NO (g) and SO_2 (g)]*; Domestic wastewater; Deionized water; Desmodesmus sp.; Halomonas stevensii; Bacterial consortium; Loop photobioreactor; Suspended bio-reactor; Biomass productivity; lipid; Thiosulfate; Ferrous ions; Biomass; Products identification, Material balance; Fixation mechanism.*

TABLE OF CONTENTS

LIST OF FIGURES

LIST OF TABLES

NOMENCLATURE

C_C	Carbon content in biomass	
CFU	Colony forming unit	CFU mL^{-1}
M_C	Molecular weight of carbon	g $mole^{-1}$
M_C, in	Mass of C supplied as CO_2(g)	g
M_C, go	Carbon left in gaseous phase as CO_2 at the end of study	g
M_C, bo	Carbon assimilated as biomass	g
M_C, CO_2 (l)	Dissolved CO_2 in aqueous phase	g
M_{Cin},CO_2 (g)	Mass of CO_2 (g) present in the head space of bioreactor	g
M_{Cin},CO_2 (l)	CO_2 present in dissolved form in the liquid media	g
M_{CO2}	Molecular weight of CO_2	g
P_{max}	Biomass productivity	g L^{-1} d^{-1}
R.R_{CO2}	Actual CO_2 removal efficiency	% w/w
R^2	Co-relation factor	
R_{CO2}	CO_2 (g) fixation rate	g $_{CO2}$ L^{-1} d^{-1}
X_{max}	Maximum biomass obtained in terms of dry weight	g L^{-1}
y_{in}	Initial concentration of CO_2 (g)	% v/v
y_{CO2}, final	Initial (t = 0) head space CO_2 concentration	% v/v
y_{CO2}, in	Final (t = t_x) head space CO_2 concentration	% v/v
$y_{CO2,}$ out	Final concentration of CO_2	% v/v
T	Temperature	^oC
C	CO_2 10 % (v/v) balanced with moisture-free air	
N	[NO (750 ppm) + rest N_2] 95% + Air (5%)	
S	[SO_2 (150 ppm) + rest N_2] 95 % + Air (5%)	
CN	[(CO_2 10% (v/v) + NO (750 ppm) + rest N_2] 95% + Air (5%)	
CS	[(CO_2 10 % (v/v) + SO_2 (150 ppm) + rest N_2] 95 % + Air (5%)	
CNS	[CO_2 10 % (v/v) + NO (760 ppm) + SO_2 (140 ppm) + rest N_2] 95 % + Air (5%)	

Greek Symbols

μ_{max}	Specific growth rate	d^{-1}
η_{CO2}	CO_2 (g) removal efficiency	% v/v

Abbreviations

16S rRNA	16S ribosomal RNA
ATR	Attenuated total reflectance
CA	Carbonic anhydrase
CCM	Carbon concentration mechanism
CCS	Carbon capture and sequestration
CCU	Carbon capture and utilization
DIC	Dissolved inorganic carbon
DO	Dissolved oxygen
FAME	Fatty acid methyl ester
FT-IR	Fourier-transform infrared spectroscopy
GC-MS	Gas chromatography and mass spectroscopy
GHGs	Greenhouse gases
MSM	Minimal salt media
LPM	Liter per minute
PBR	Photobioreactor
NCBI	National center for biotechnology information
SSE	Solvent-solvent extraction
SSL	Sambhar salt lake
STP	Sewage treatment plant
vvm	Vessel volumes per minute
OD	Optical density
DWW	Domestic wastewater
DIW	Deionized water
NO_x	Nitrogen oxides
SO_x	Sulfur oxides

Chapter 1

Introduction

A brief background of the basis of the problem statement, flue gas fixation using conventional techniques and their limitations, wastewater utilization as growth media, hypothesis as well as research objectives of the present work are summarized in this chapter.

1.1 Greenhouse gas (CO_2), criteria pollutants (NO_x, SO_x) and their environmental impacts

The rapid pace of industrialization, population expansion, and unplanned urbanization have significantly contributed to severe environmental pollution in the past few decades. Flue gases are mainly generated by burning fossil fuels such as natural gas, fuel oil, and coal. The flue gas composition depends on the fuel type, combustion techniques, and cleaning methods applied to the exhaust gases. Flue gas typically comprises of nitrogen (N_2) (more than two-thirds), carbon dioxide (CO_2), water vapour, excess oxygen (O_2), NO_x, SO_x, CO, C_xH_y, PM, heavy metals, chlorine, fluorine, and their compounds (Simoneit et al., 2000). The flue gas is mainly generated from industries such as coal-fired power plants, gas-fired power plants, and cement plants. Out of which, flue gas emissions from the cement industry requires serious attention. The cement industry generates around 6% of the CO_2 emissions globally, having 10-15% CO_2 concentration, with an estimated release of 0.9 tons of CO_2 per tonne of cement (Borkenstein et al., 2011). The flue gases from the cement industry also contain NO_x [nitric oxide (600-800 ppm) and nitrogen dioxide (350 ppm)] and SO_x (150 ppm). In general, NO_x contains 95% NO and 5% NO_2; however, SO_x has 96-98% SO_2 and rest SO_3 (Hende et al., 2012). CO_2, the primary greenhouse gas (GHGs), represents 77% of the total GHGs emissions (IPCC 2021; https://www.CO_2.earth/, 2021) in the earth's atmosphere and plays a vital role in global warming. GHGs have become a significant concern in the present century (Rahman et al., 2017). The intergovernmental panel on climate change (IPCC) suggests the complete elimination of CO_2 (g) emissions by 2050 to retain the temperature of the earth below a 1.5-degree guardrail (Williamson, 2016; Yadav et al., 2017).

CO_2 has an atmospheric lifetime of 50 to 200 years (Hamiit et al., 2020), and the higher CO_2 (g) concentration in the earth's atmosphere has a physical, ecological, and biological impact (Rosenzweig et al., 2008). This largely contributes to global warming that affects human health

and causes injury, mass migration, economic disruption, malnutrition, social unrest and displacement (Zhou et al., 2017). An increase of CO_2 (g) concentration up to 450 ppmv–600 ppmv (parts per million volumes) would result in an irreversible dry climate. Increasing CO_2 (g) concentration up to 600 ppm in the twenty-first century would raise the sea level from 0.4 to 1 m (Solomon et al., 2009). The accumulation of CO_2 (g) in oceans has resulted in ocean acidification, another mankind-induced problem due to increased CO_2 (g) concentration in the earth's atmosphere. The changing pH of the sea has adversely affected the climate and marine biota to a more significant extent (Baumann et al., 2012).

Inhalation of NO_x may cause heart disease and respiratory diseases such as emphysema and bronchitis. NO_x significantly contributes to the urban air's photochemical smog, acid rain formation, and tropospheric ozone formation. It also participates in eutrophication and ozone removal from the stratosphere, resulting in increased ultraviolet radiation reaching the earth's surface, which causes several skin diseases (Kampa et al., 2008; Hende et al., 2012; Deng et al., 2013). The emissions of sulfur oxides (SO_x) not only endanger people's health but also instigates various environmental problems, such as acid smog formation and acid rain (Lin et al., 2015). SO_x are the leading cause of the degradation of the ozone layer. Sulfur dioxide also contributes to respiratory problems, particularly in youngsters and the elderly (Chiang et al., 2016; Ghozikali et al., 2016).

Hence, the industrial emissions of flue gas, mainly CO_2, NO and SO_2 into the atmosphere resulted in global warming, acid rain, ozone layer depletion, and many more environmental problems. Therefore, flue gas fixation from industrial sources is an urgent need of the hour.

1.2 Existing abatement techniques and their limitations

The available control technologies for flue gas fixation are industrially applicable and are being worked with a research perspective. The abatement technologies for flue gas fixation can be categorized into three types: fuel treatment/replacement, combustion variation, and post-combustion method. Different physicochemical and biological processes for CO_2, NO, and SO_2 abatement, their advantages, and limitations, are summarized in Table 1.1. The physical method of direct injection into subsurface natural reservoirs, as well as the chemical technique of gas scrubbing with alkaline or amine solutions, are not considered cost-effective or environmental friendly (Zhou et al., 2017). There are three biological techniques available for the abatement of CO_2 from flue gases: (1) forestation, (2) oceanic fertilization, and (3) microalgae-based sequestration. Forestation has the limitation of very limited CO_2 sequestration, large land area requirement, and food supply. Oceanic fertilization has the limitations of high cost, high level of uncertainty, impact on ocean eco-system (change in plankton structures), and possible trigger of methane production. The main disadvantages of the microalgae-based system include low efficiency of open pond cultivation system, unavailability and heterogeneous distribution of light, expensive closed system, lower efficiency at an industrial scale, toxicity of gases present in exhaust (Mishra et al., 2017; Zhou et al., 2017).

The NO abatement treatment technologies include selective catalytic reduction (SCR) and selective non-catalytic reduction (SNCR) methods. These expensive methods add significant environmental impacts when treating large air flow rates containing low concentrations of NO due to intensive energy usage (Table 1.1) (Lopez et al., 2013). There are various methods available for the reduction of SO_2 emissions. Some are pretreatment processes such as reducing fuel sulfur through raw material processing or fuel change, increasing stack height, and dispersion of source

location through proper planning and zoning of industrial areas. The most common post-treatment technique is flue gas desulfurization (FGD), which is efficient for SO_2 treatment, it often generates additional wastes or requires additional chemical and energy inputs (Table 1.1) (Philip et al., 2003). NO and SO_2 can also be treated simultaneously using DESONOX or SNOX methods, combining catalytic reduction for NO and catalytic oxidation for SO_2 (Kenneth, 2019). The physico-chemical $DeSO_x$ methods have certain drawbacks, such as higher capital and energy costs, regeneration costs of sulfate and oxide (if catalysts are employed), poor SO_3 removal (50%), higher amount of water use, appreciable limestone cost, scrubber size, and increased acid mist creation (in case of wet desulphurization) (Mochida et al., 2000). The bio-fixation of NO and SO_2 present in the flue gas using microalgae is also limited as NO and SO_2 are toxic to most microalgae.

The limitations of physical and chemical methods to mitigate CO_2, NO, and SO_2 lead researchers to look for a more economical, efficient, and effective biological alternative for simultaneous fixation and utilization of CO_2, NO, and SO_2. Microalgae's use for bio-fixing flue gas has drawn significant attention since the 1990s (Negoro et al., 1991; Ma et al., 2018). However, technological challenges hinder the simultaneous bio-fixation of flue gases (CO_2, NO, SO_2) using microalgae. Few studies have found that SO_2 and NO, particularly SO_2, inhibit microalgal growth in the system (Wang et al., 2011; Jiang et al., 2013a; Li et al., 2015). Hence, important concern is the supply of SO_2 and NO into the system without pretreatment. However, desulfurization of flue gas can overcome the problem of SO_2 inhibition (Doucha et al., 2005; Douskova et al., 2009; Zhu et al., 2014). Few studies suggested the production of lipids from algal biomass utilizing a low concentration of flue gas ($\leq 0.015\%$) SO_2 and NO (Chiu et al., 2011; Kao et al., 2014; Aslam et al., 2018). The detrimental effects of SO_2 and NO on microalgae are primarily due to the reduction in system pH induced by the continuous supply of these components (Wang et al., 2011; Jiang et

al., 2013). The limitations of microalgae-based techniques for simultaneous fixation and utilization of CO_2, NO, and SO_2 lead researchers to look for an alternative technique that can overcome the microalgae-based method's shortcomings. The utilization of bacteria for the simultaneous fixation of flue gases CO_2, NO, and SO_2 is getting researcher's attention as it can overcome the limitations of microalgae-based methods. The bacterial species utilizes CO_2 as a carbon source, NO as a nitrogen source in the form of nitrite and nitrate and SO_2 as an energy source in the form of sulfate ions. The utilization of bacteria can conquer SO_2 inhibition, which is the main shortcoming of the microalgae-based technique. Also, the utilization of low concentration of flue gas in the microalgae-based process can be overthrown by the utilization of bacterial species for flue gas fixation as CO_2 remains the sole carbon source and SO_2 remains the sole energy source during the process. Therefore, flue gas fixation using the bacterial route remains efficient as it has many advantages over physio-chemical techniques and microalgae-based methods, such as no requirement of additional energy, no production of secondary pollutants, rapid growth rate, and it can tolerate higher concentration of flue gases (Passos et al., 2015; Mishra et al., 2016).

The bacterial route of flue gas fixation requires higher nutrient consumption and directly affects the process's overall cost. The demand for higher nutrient consumption can be overcome by using growth media prepared in wastewater as it has many nutrients that the bacterial species can utilize as a nutrient and energy source for their growth and formation of products. Hence, if adequately tailored, the bacterial-based process can become a low-cost and environmentally friendly alternative to conventional and microalgal methods for the simultaneous bio-fixation of flue gases such as CO_2, NO, and SO_2.

1.3 Wastewater utilization as growth media

Since the human population in urban, suburban, and rural regions has been overgrown, an enormous amount of freshwater is widely consumed. As a result, surface and groundwater get contaminated by the discharge of domestic wastewater (DWW) (Rawat et al., 2011; Passos et al., 2015). There is enough carbon, nitrogen, phosphorus, and other minerals in the DWW to induce eutrophication and other environmental problems (Rawat et al., 2011). The released DWW is required to be treated before its discharge.

The challenges, such as the use of expensive inorganic nutrients, and the unavailability of a large amount of freshwater, prohibit the large-scale implementation of microbial-based flue gas fixation (Mishra et al., 2016; Moreira et al., 2016). This may be due to the requirement of a considerable amount of water and costly inorganic nutrients for microbial cultivation. The higher cost of nutrients directly affects the overall profitability of biofuel production. Microbial-based wastewater treatment is a greener and more ecological option over traditional methodologies, as microbes have a higher nutrient-eliminating ability and produce microbial biomass for biofuel production using nutrient-rich DWW. These microbes utilize phosphorous, nitrogen, and sulfate ions, which are the main contributors to eutrophication (Nayak et al., 2016a; Ma et al., 2019). Nutrients present in DWW can be utilized as the growth media nutrients for the microbial fixation of flue gases (CO_2, NO, SO_2). This process provides the solution for flue gas fixation and wastewater treatment. The utilization of concomitant sulfate, nitrite, and nitrate ions from DWW as a nutrient source may lead to a significant cost reduction of microbial cultivations. Few previous studies demonstrated the utilization of wastewater by cyanobacteria as a nutrient source for biofuel production (Figueroa et al., 2008; Cai et al., 2013; Ferreira et al., 2017; Nayak et al., 2018). Previous studies have shown the application of thiosulfate salt and ferrous ion (Fe (II)) as an energy

source for the bio-fixation of CO_2 by utilizing *Halomonas stevensii* and *Bacillus cereus,* respectively (Mishra et al., 2016, 2017).

The higher cost of nutrient sources and energy substrate has a direct impact on the overall profitability of the biofuel production process. Thus, nutrients present in DWW can be utilized as the growth media for the microbial fixation of flue gas (CO_2, NO, SO_2).

1.4 Motivation

Conventionally, algae can be cultivated in an open culture system (raceway ponds) or a closed system (photobioreactors). The disadvantage of raceway ponds compared to the closed photobioreactor is lower productivity due to the carbon limitation (Nayak et al., 2016b). Closed photobioreactors provide higher biomass productivity and prevent outside contamination. Given the benefits of closed systems over open ponds, various photobioreactors (from laboratory to industrial scale) have been developed. Even though many photobioreactors have been studied, only a small number of these reactors can efficiently use solar energy for mass algal production. Most outdoor photobioreactors have exposed lightning surfaces, such as flat-plate, horizontal, and inclined tubular photobioreactors. Bubble-column, airlift, and stirred-tank photobioreactors offer high scalability, but their application in outdoor cultures is limited due to their low illumination surface areas (Achinas et al., 2020). Many photobioreactors appear simple to run at the laboratory scale; however, a few have been successfully scaled up at the pilot scale. Maintaining optimal light, temperature, mixing, and mass transfer in photobioreactors makes these scale-up techniques extremely difficult. The absence of effective photobioreactors is a primary blockage to mass algae production. Overcoming these limitations, loop bioreactors are efficient reactors that provide uniform and good mixing without mechanical agitation and ease of operation. These are mainly

Table 1.1 Different techniques for CO_2, NO, and SO_2 abatement

Process	Techniques	Advantage	Limitations	References
CO_2				
Physical	Membrane separation	Easy continuous operation	Energy inefficient, membrane fouling and blockage, high cost	(Beedlow et al., 2004; Hyvonen et al., 2007)
	Geologic injection	Help in the generation of sustainable geothermal energy	Requirement of geological and geomorphological environment, gas leakage over time (several thousand years), high cost	
	Oceanic injection	Strong carbon sink	Gas leakage over time (several hundred years), threaten the lives of non-swimming marine organisms, requirement of high-cost injection techniques	
Chemical	Chemical absorption	High efficiency	Large equipment size requirements, high energy requirements, high cost	(Lal, 2008; Ho et al., 2010; Kita et al., 2004)
	Mineral carbonation	High storage security	Requirement of a large amount of reagent, not cost-effective	
	Chemical adsorption	High carbon dioxide uptake, efficient under humid conditions	High adsorbent cost, high energy-intensive process, unable to capture the low concentration of CO_2	
Biological	Forestation	Pure natural process, no equipment required, environment friendly	Limited CO_2 sequestration, large land area requirement, potential threat to biological diversity and food supply	(Salek et al., 2013)
	Oceanic fertilization	Increase fish stocks via increasing primary production, reduce GHGs along with slow down the climate change	High cost, high level of uncertainty, impact on ocean eco-system (change in plankton structures), possible trigger of methane production	(Tang et al., 2014)

	Microalgae-based Sequestration	It can be cultivated on non-fertile land with unit CO_2 fixation capacity 10–50 times higher than terrestrial plants, production of value-added products	Sensitive to toxic substances in exhaust gases, expensive process for reactor design and algal biomass harvesting	(Silva et al., 2015)
NO				
Chemical	SCR, SNCR	Higher NO_x control efficiency and reactions within a lower and broader temperature range	Intensive energy usage, expensive methods	(Lopez et al., 2013)
SO_2				
Physicochemical	FGD	Flue-gas desulfurization (FGD) may remove 90% or more of the SO_2 in the flue gases	Generation of additional waste, requires additional chemical and energy inputs	(Philip et al., 2003)

constructed of transparent materials such as glass, plexiglass, polyvinyl chloride (PVC), acrylic PVC, or polyethylene (Kumar et al., 2011; Huang et al., 2017). Loop reactors are cylindrical vessels that mix multiphase fluids without the impeller action. The advantages of the loop reactor are better mixing without impellers and an adequate illumination surface, which allow these reactors to overcome the limitations of flat-plate, horizontal, and inclined tubular photobioreactors. Another significant advantage is the energy savings, as the impellers are not required in loop reactors (Sharma et al., 2016). The literature studies indicated that the application of loop bioreactors for CO_2 fixation using microalgae is limited. Most of the studies are confined to bench-scale reactors. Hence, there is an enormous scope to utilize the pilot-scale closed-loop photobioreactor for CO_2 fixation using microalgae.

The concept of using microalgae for the bio-fixation of flue gas has drawn significant attention since the 1990s (Negoro et al., 1991; Ma et al., 2018). However, technological challenges hinder the simultaneous bio-fixation of flue gases (CO_2, NO, SO_2) using microalgae. Few studies have found that SO_2 and NO, particularly SO_2, inhibit microalgal growth in the system (Wang et al., 2011; Jiang et al., 2013; Li et al., 2015). Bio-fixation of CO_2 using a bacterial route and simultaneous production of different value-added products is a well-established method (Bharti et al., 2014; Mishra et al., 2016, 2017, 2018). The biological treatment of nitric oxide (NO) using bacterial species is a well-known process. The denitrifying bacteria have been utilized for NO removal from flue gas (Barnes et al., 1995; Kumaraswamy et al., 2005; Jiang et al., 2008; Han et al., 2016; Li et al., 2016; Zheng et al., 2016). Since the late 1980s and early 1990s, researchers have been designing biological methods to reduce SO_2 (Dasu et al., 1989; Lee et al., 1994; Kaufman, 1997). The majority of the research is mainly focused on the SO_2 removal by bacteria (Gasiorek, 1994; Lee et al., 1994; Philip et al., 2003; Li et al., 2017; Papi et al., 2018; Zhang et al.,

2015b, 2018). One study has reported the simultaneous removal of CO_2 and NO from flue gas in a biofilter using bacteria (Xu et al., 2022). However, the utilization of bacterial species for the simultaneous removal of CO_2 and SO_2 needs to be explored. The literature studies indicated that the application of microalgae for flue gas fixation has many limitations. Most of the studies utilizing bacterial route are confined to individual CO_2, NO and SO_2 fixation. To the best of our knowledge, the simultaneous bio-fixation of flue gas **(**CO_2, NO, SO_2) using bacterial species has rarely been studied. Hence, there is an enormous scope to utilize the bacterial route for flue gas bio-fixation.

In one of the studies, Mishra et al. (2016) showed the utilization of *Bacillus cereus* SM1 for CO_2 (g) fixation. Another study revealed the use of *Bacillus* sp. ISTS2 for CO_2 fixation and biofuel generation (Sundaram et al., 2015). The previous studies showed the utilization of thiosulfate salt and ferrous ion (Fe (II)) as an energy source by *Halomonas stevensii* and *Bacillus cereus,* respectively, for the bio-fixation of CO_2 (Mishra et al., 2016, 2017). The removal of SO_2 by *Bacillus* genus was investigated by Li et al. (2017) and Zhang et al. (2018). The utilization of nitrate (NO_3^-) and nitrite (NO_2^-) by the *Bacillus* genus as a nitrogen source was also established (Remde et al., 1991; Rout et al., 2017; Uddin et al., 2021; Saha et al., 2022;). The reported studies were focused on individual CO_2 (g) fixation or SO_2 (g) fixation or NO_3^- and NO_2^- utilization by different *Bacillus* species. The literature studies suggest that the *Bacillus* genus can be a potential candidate for CO_2, NO, and SO_2 bio-fixation. The simultaneous removal of flue gas (CO_2, NO, SO_2) using the genus *Bacillus* is yet to be investigated.

Microbial cultivation needs enormous amounts of nutrients to grow; these nutrients are provided as growth media prepared in fresh water. The scarcity of fresh water is limiting the microbial cultivation process. The utilization of DWW can overcome the problems of the availability of fresh

water for growth media and the supply of nutrients. To the best of our knowledge, no study has been carried out for the simultaneous bio-fixation of flue gas (CO_2, NO, SO_2) using growth media prepared in DWW. Hence, the utilization of concomitant nutrients present in DWW as growth media and energy sources (SO_3^{2-}, Fe(II)) for the simultaneous bio-fixation of CO_2, NO, and SO_2 is the need of the hour.

The biofilter and biotrickling filter systems have been extensively used for flue gas purification purposes (Barnes et al., 1995; Flanagan et al., 2002; Wang et al., 2006; Xiao et al., 2017; Wen et al., 2019). However, due to excess biomass depositions, biofilter and biotrickling filter systems have operating limitations, such as bed clogging, gas mixing, and pressure drop (Littlejohns et al., 2010). These shortcomings become more apparent when operated for an extended period or high intake load (Clarke et al., 2009; Lebrero et al., 2012). Similar to other fixed-bed reactors, it was observed that the attachment of the fillers was the primary cause of clogging and gas channeling. This problem can be overcome by replacing fixed fillers with suspended carriers. As a result, it could prevent gas channeling and bed clogging. This type of reactor is referred to as a suspended bioreactor. A suspended bioreactor's use for the simultaneous bio-fixation of flue gas (CO_2, NO, SO_2) has rarely been studied. Hence, there is a vast scope to utilize the suspended bioreactor for flue gas bio-fixation.

To give commercial value to the fixation process, the analysis of by-products obtained from flue gas fixation studies and utilization of domestic wastewater as growth media is an exciting area to think of and requires serious attention. In recent years, no work has been discussed on developing a downstream processing strategy for the economic recovery of metabolites from flue gas utilizing bacterial consortium. The utilization of bacterial consortium isolated from the extreme

environment of Sambhar Salt Lake for simultaneous flue gas (CO_2, NO, SO_2) fixation in a suspended bioreactor is yet to be investigated.

1.5 Research objectives

Thus, the objectives of the present study are:

1. To carry out CO_2 (g) fixation studies utilizing *Desmodesmus* species in a pilot scale, custom-designed loop photobioreactor.
2. To check the feasibility of Domestic Wastewater (DWW) utilization as growth media and energy source for the bio-fixation of CO_2 using *Halomonas stevensii*.
3. To develop an economically viable integrated system for bio-fixation of simulated flue gas (CO_2, NO, and SO_2) by utilizing DWW as a growth media and energy source.
4. To perform the semi-continuous studies for the bio-fixation of simulated flue gases in suspended bio-reactor and to develop an appropriate downstream strategy for the recovery of products.

1.6 Thesis organization

The objectives are accomplished by initially carrying out the detailed literature review on available studies for microalgal CO_2 fixation in different types of bioreactors, individual and simultaneous bio-fixation of flue gas (CO_2, NO, SO_2) using bacteria, utilization of different bioreactors for NO, and SO_2 removal and utilization of DWW as growth media, which is given in chapter 2. The details on growth media formulation, semi-continuous studies, by-product analysis techniques, downstream processing strategy and design of loop photobioreactor are described in chapter 3. The results related to CO_2 fixation using *Desmodesmus* species in loop photobioreactor, CO_2 bio-fixation using *Halomonas stevensii*, flue gas (CO_2, NO, SO_2) bio-fixation using bacterial consortium in suspended bioreactor and downstream processing strategy are discussed in chapter

4. Chapter 5 deals with the summary of the work and important conclusions drawn from the present study. The thesis organization are also shown in the flowchart for better understanding (Fig. 1.1).

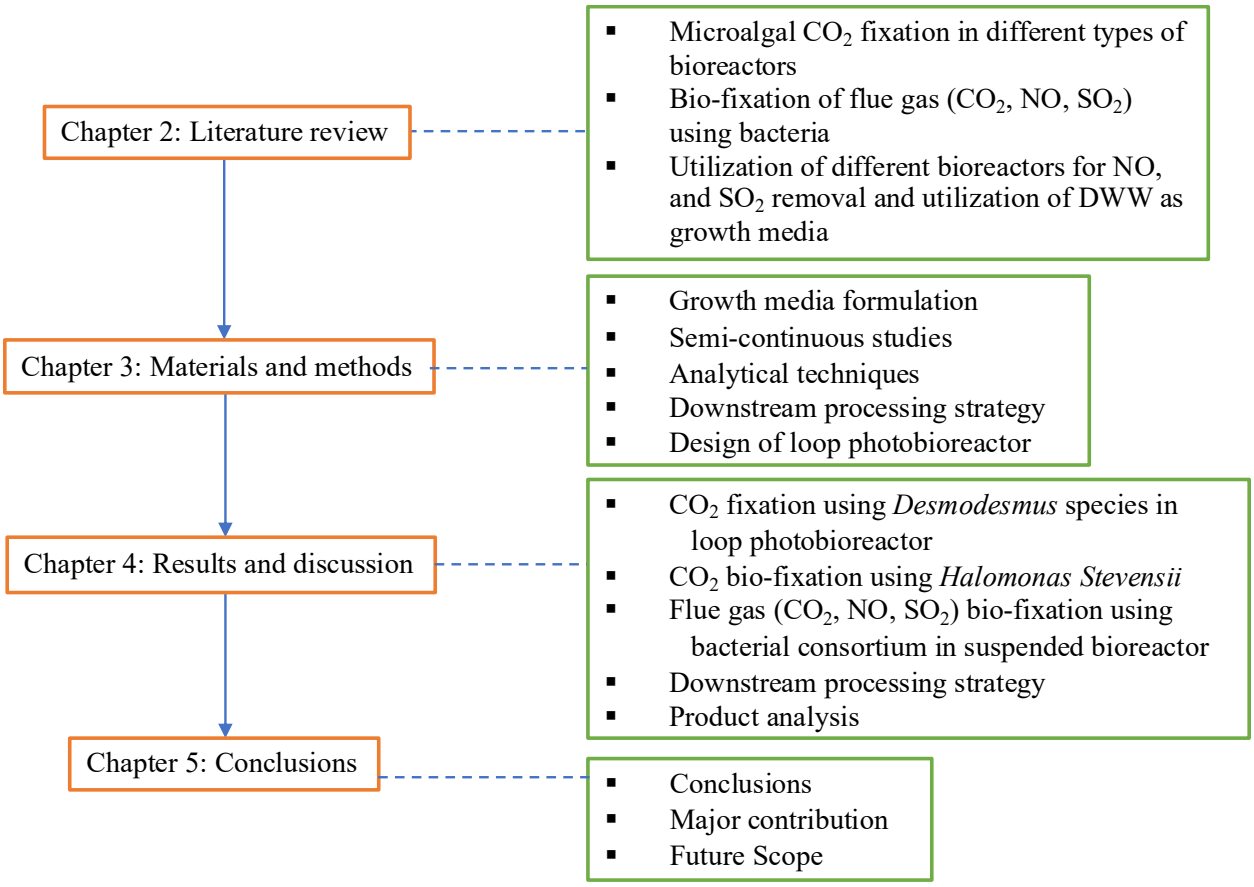

Fig. 1.1 Pictorial representation of thesis organization

Chapter 2

Literature Review

CO_2 bio-fixation studies utilizing microalgae in different bioreactors, CO_2, NO, and SO_2 bio-fixation studies using bacterial species, simultaneous flue gas fixation studies using bacterial species, gaps, and scope of the present work are described in this chapter.

2.1 Microalgal CO_2 fixation in different types of bioreactors

Over the last decade, extensive work has been carried out on the bio-fixation of carbon dioxide (CO_2) in different bioreactors. The previous studies reported from the lab and pilot scale bioreactors for CO_2 fixation using microalgae are summarized in Table 2.1 and discussed in the following section.

Ho et al. (2010) isolated seven *Scenedesmus obliquus* from a freshwater lake in southern Taiwan, and CO_2 fixation efficiency was evaluated in a 1-L glass-made photobioreactor. *Scenedesmus obliquus* CNW-N and AS-6-1 showed a maximum specific growth rate of 1.019 and 1.065 d^{-1} and maximum biomass concentration of 2.63 and 1.90 g L^{-1}, respectively, under 20% (v/v) CO_2 (g). The maximum CO_2 utilization rate for *Scenedesmus obliquus* CNW-N and AS-6-1 were found to be 0.3902 and 0.2902 g L^{-1} d^{-1}, respectively, which showed the opportunity of two different species of *Scenedesmus obliquus* for the bio-fixation of CO_2.

Chlorella sp. has been tested to produce precursors for biodiesel, biomass accumulation, calcite formation, and CO_2 fixation (Fulke et al., 2010). The experiments were carried out in a 3-L airlift photobioreactor at different CO_2 concentrations (0.03%, 3%, 10%, and 15%), and lipid productivity was found in the range of 20-27.3 mg L^{-1} d^{-1}. FT-IR, SEM, and XRD were used for the characterization of produced calcite. FAME content was characterized by GC- FID, which confirmed the presence of palmitic acid (C16:0), docosapentaenoic acid (C22:5), and docosahexaenoic acid (C22:6). The higher calorific value (29 kJ g^{-1}) of produced oil makes it a potential alternative candidate of alternate fuel.

Table 2.1 CO_2 bio-fixation studies incorporating different species of microalgae in different bioreactors

S.No.	Microbial Species (Microalgae)	CO_2 % (v/v)	Reactor Type	Products	References
1	*Scenedesmus obliquus CNW-N and AS-6-1*	20	Photobioreactor	_	(Ho et al., 2010)
2	*Chlorella sp.*	3-15	Airlift Photobioreactor	Lipid -20–27.3%	(Fulke et al., 2010)
3	*Scenedesmus obliquus WUST4*	20	Airlift Photobioreactor	_	(Li et al., 2011)
4	*Chlorella emersonii*	15	pH-Stat Photobioreactor	_	(Borkenstein et al., 2011)
5	*Synechocystis aquatilis TISTR8612*	5	Airlift Photobioreactor	Lipids -18.58%	(Kaiwan-arporn et al., 2012)
6	*Chlorella PY-ZU1*	15	Column Bioreactor	_	(Cheng et al., 2013)
7	*Scenedesmus obtusiusculus*	10	Bubble Column Photobioreactor	Lipid - 55.7%	(Toledo-Cervantes et al., 2013)
8	*Chlorella vulgaris P12*	6.5	Bubble Column Photobioreactor	_	(Anjos et al., 2013)
9	*Chlorella sp. MTF-15*	26	Photobioreactor	Lipid - 0.961 g L^{-1}	(Kao et al., 2014)
10	*Chlorella sorokiniana*	12	Photobioreactor	Lipids - 31 mg L^{-1}	(Lizzul et al., 2014)
11	*Chlorella sp.*	5	Bubble Column Photobioreactor	_	(Yadav et al., 2015)
12	*Desmodesmus sp. 3Dp86E-1*	20	Glass Column Reactor	_	(Solovchenko et al., 2015)
13	*Chlorella sp*	20	Bubble Column Photobioreactor	Lipids -20.9 ± 1.7% Protein -30.5 ±0.5% Carbohydrate-13.2%	(Li et al., 2015)

14	*Nannochloropsis oculata*	12	Photobioreactor	_	(Razzak et al., 2015)
15	*Chlorella. Vulgaris*	15	Luminescent Photobioreactor	Lipids -36.6%	(Mohsenpour et al., 2016)
16	*Scenedesmus sp.*	2.5	Photobioreactor	Lipids -35.6% Carbohydrate-10.4%	(Nayak et al., 2016b)
17	*Chlorella sp. BTA 9031*	4–15	Photobioreactor	Lipid -5.3−22.4%	(Mondal et al., 2017)
18	*Chlorella vulgaris*	2	Airlift Photobioreactor	_	(Sadeghizadeh et al., 2017)
19	*Coelastrum sp.*	12	Airlift Photobioreactor	Lipid -37.91% Carbohydrate-58.4%	(Mousavi et al., 2018)
20	*Spirulina platensis*	2.5–20	Pilot Scale Photo-bioreactor	_	(Almomani et al., 2019)
21	*Chlorella vulgaris*	2.5	Photobioreactor	Lipid - 516.6 mg L^{-1} d^{-1}	(Fu et al., 2019)
22	*Chlorella Vulgaris*	7	Bubble Column Photobioreactor	_	(Barahoei et al., 2020)
23	*Scenedesmus obliquus*	10	Vertical Column Photobioreactor	Protein - 9.66±1.20	(Aghaalipour et al., 2020)
24	*Spirulina strains*	10	Columnar Photobioreactor	_	(Zhu et al., 2021)
25	*Scenedesmus acutus NCIM5584, Micractinium pusillum*	15	Bubble Column Laboratory Scale Photobioreactor	Lipid - 32%	(Chauhan et al., 2022)

Li et al. (2011) grew a *Scenedesmus obliquus* strain (*S. obliquus* WUST4) with a UV mutagenesis technique that can bear a high concentration of CO_2 (20% (v/v)) and has a high CO_2 fixation ability. The pilot-scale microalgal CO_2 fixation system was developed in a 100-L airlift photobioreactor that can mitigate the CO_2 generated by coke combustion. The maximum CO_2 removal was obtained up to 67%. Thus, *S. obliquus* WUST4 showed its applicability for CO_2 fixation from the flue gas.

Borkenstein et al. (2011) cultivated a green alga, *Chlorella emersonii*, in the presence of cement plant flue gas under photoautotrophic environments. The study was conducted in a semi-continuous mode 5.5 L pH-stat photobioreactor. The microalgal dry biomass and CO_2 fixation were obtained as 2.00 g L^{-1} and 3.25 g L^{-1}, respectively.

Synechocystis aquatilis TISTR8612 (*S. aquatilis*) was cultured to investigate CO_2 fixation rate, biomass production, and extraction of lipids. The experiments were performed in three steps. First optimal growth conditions were examined in a flask study. Second, CO_2 fixation rate in batch mode was determined in an airlift photobioreactor (PBR). At last, a continuous study was carried out in an airlift PBR to estimate CO_2 fixation rate, biomass production, and lipid extraction. The optimum pH, temperature and luminance for the cultivation of *S. aquatilis* were obtained as 8, 30 ^oC and 4 klx, respectively. Batch experiments at 5% inlet CO_2 yielded a maximum CO_2 fixation rate at a space velocity of 14 min^{-1}. The continuous study showed the maximum biomass production rate of 0.932 g L^{-1} d^{-1}, CO_2 fixation rate of 5.3 g L^{-1} d^{-1}, and lipid yield of 18.58% at an inlet CO_2 concentration of 8%. The extracted fatty acids were mainly comprised of saturated and polyunsaturated fatty acids. Thus, *S. aquatilis* is best grown in a continuous photobioreactor for lipid extraction (Kaiwan-arporn et al., 2012).

The green microalga, *Chlorella vulgaris* P12 was cultivated by Anjos et al. (2013) in 110 mL bubble column photobioreactors at different CO_2 concentrations (2%-10%) with aeration rates of

0.1 vvm to 0.7 vvm. The study aimed to maximize the CO_2 bio-fixation rate. The maximum CO_2 fixation rate of 2.22 g L^{-1} d^{-1} was reported after 7 days of cultivation using 6.5% CO_2 at 0.5 vvm and 30 ^oC. The final biomass concentration and maximum biomass productivity of microalgae were affected by the different cultivation conditions, but there were no significant differences obtained in the biochemical composition of microalgal cells.

Scenedesmus obtusiusculus was isolated from Cuatro Cienegas, Mexico springs, and was cultivated in bubble-column photobioreactors. The experiments were carried out in batch operation mode at 10% carbon dioxide (CO_2) concentration and showed a maximum CO_2 fixation rate of 0.970 g L^{-1} d^{-1}. The maximum biomass productivity, maximum biomass concentration, and lipid productivity were obtained as 0.500 g L^{-1} d^{-1}, 6 g L^{-1}, and 55.7 % on a dry weight basis, respectively. Thus, the microalga has the biotechnological potential to produce lipids for biodiesel production (Toledo-Cervantes et al., 2013).

Cheng et al. (2013) mutated the *Chlorella pyrenoidosa* by nuclear irradiation combined with CO_2 domestication to improve biomass productivity and CO_2 fixation at 15% (v/v) CO_2. The biomass yield of *Chlorella pyrenoidosa* was increased by 53.1% after nuclear irradiation under air bubbling. The maximum growth, fixation rate, and CO_2 fixation efficiency of domesticated mutant (*Chlorella* PY-ZU1) were found to be 0.68 g L^{-1} d^{-1}, 1.54 g L^{-1} d^{-1} and 32.7 %, respectively, under enhanced light transmission and culture mixing in the photobioreactor. Optimization of the bioreactor and growth conditions of *Chlorella* PY-ZU1 improved biomass production and CO_2 fixation from flue gas.

Kao et al. (2014) investigated the biomass and lipid productivity of *Chlorella* sp. MTF-15. The strain was cultivated in flue gas from a coke oven, hot stove, or power plant in the steel plant of the China Steel Corporation in Taiwan. The microalgal cells were cultivated in a column-type

glass-fabricated photobioreactor with a working volume of 1 L. The microalgal strain obtained a maximum specific growth rate of 0.827 d^{-1} for coke oven gas and maximum lipid production of 0.961 g L^{-1} for hot stove gas. The study suggested that *Chlorella* sp. MTF-15 could efficiently utilize CO_2, NO_x, and SO_2 in the flue gases. The findings of this study proved that the flue gas composition and the operating strategy impacted the microalgal strain's growth capacity, lipid production, and fatty acid compositions.

A comparative study of microalgal CO_2 fixation at different concentrations of pure and flue gas CO_2 was accomplished using *Chlorella* sp. in the bubble column photobioreactor (Yadav et al., 2015). A significant improvement in the overall biomass production (21–36%) was achieved at 5% CO_2 (v/v). CO_2 fixation rate, total carbohydrate, and protein contents were increased when photobioreactors were arranged in series. The bio-fixation efficiency was improved by 54% with the adopted strategies. The work provides the basis for reducing flue gas CO_2 for synthesizing algal biomass, carbohydrates, and proteins for various possible uses.

Li et al. (2015) cultivated two *Chlorella* sp. strains, AE10 and AE20, which can tolerate higher concentrations of CO_2 with higher fixation ability. These strains were developed using 31 cycles of adaptive laboratory evolution (ALE) under 10% and 20% CO_2 concentration, respectively. All the experiments were performed at 28 ± 0.5 °C in the bubble column photobioreactor. AE10 and AE20 showed better growth in 30% CO_2, and the maximum biomass concentration was obtained as 3.68 ± 0.08 g L^{-1}. The biomass concentration of AE10 was 1.22 times of AE20 and 2.94 times of *Chlorella* sp. The chlorophyll contents of AE10 and AE20 were considerably higher than the *Chlorella* sp. at 30% CO_2 concentration. The effects of the ALE approach on the biochemical components of *Chlorella* cells were also studied. The study demonstrated ALE as an effective way to improve the higher tolerance of CO_2.

Mohsenpour et al. (2016) discussed the effect of CO_2 aeration in luminescent photobioreactors (red, blue, yellow, and green) on biomass production, CO_2 fixation rate, pH, cell's vital elements (carbon, nitrogen, hydrogen), and lipid content. The effect of pure air aeration (0.03% CO_2) on the CO_2 fixation rate was minimal. The maximum lipid content of 36.6% for *G. membrancea* was reported at 15% CO_2 in blue light. Lipid production of *G. membranacea* almost doubled when aerated with 15% CO_2, compared to aeration with 5% CO_2 for all photobioreactors. The lipid content was increased nearly six times in yellow PBR when it was aerated with 5% and 15% CO_2. This study focused on the combined effects of light quality through spectral conversion, and CO_2 aeration, on biomass production, lipid accumulation, and elemental contents of microalgae.

The integrated system for CO_2 fixation, wastewater remediation, and biomass feedstock generation for sustainable biofuel application using *Scenedesmus* sp. was developed in closed and open culture systems. The *Scenedesmus* sp. was cultured in the photobioreactor, which generated 35.6% lipid and 10.4% carbohydrate with a 46.1% increase in biomass productivity (0.1857 ± 0.0073 g L^{-1} d^{-1}) at a CO_2 concentration of 2.5%. The bio-remediation of ammonium, nitrate, phosphate, and COD was obtained as 95%, 66%, 72%, and 93%, respectively. The open culture system was supplied with 2.5% CO_2, which generated 24.1% lipid and 19.2% carbohydrate. The biomass productivity (0.0971 ± 0.0027 g L^{-1} d^{-1}) at 2.5% CO_2 aeration was increased by 36% compared to the control run. The presence of C16-C18 fatty acid concentration indicated high-grade biofuel. Thus, the sustainable, environmental friendly, and economically advantageous method for producing biofuels while simultaneously sequestering CO_2 and valorizing wastewater was developed and standardized as "green processes" (Nayak et al., 2016b).

Mondal et al. (2017) performed the experiments to optimize operating conditions for maximizing CO_2 sequestration by *Chlorella sorokiniana* BTA 9031 at different temperature ranges of 20–40

°C, light intensities of 30–100 μmol m^{-2} s^{-1}, and CO_2 concentrations (4–15%) in the photobioreactor. This study investigated the possibilities of lipid accumulation for biodiesel production. The Central Composite Design (CCD) approach of Response Surface Methodology (RSM) was used to optimize these three critical operational parameters. The maximum biomass and lipids were obtained at optimum conditions of 28.26 °C temperature, 76.64 μmol m^{-2} s^{-1} light intensity, and 4% CO_2 concentration. The maximum CO_2 bio-fixation rate was obtained as 0.235 g L^{-1} d^{-1} under optimal conditions.

Mousavi et al. (2018) investigated the efficiency of freshly isolated microalgae, *Coelastrum* sp. SM for a higher concentration of CO_2 (6, 12, and 16%) fixation and nutrient removal. *Coelastrum* sp. ability to produce carbohydrates, lipids, and biodiesel during the process was examined. The microalgae were cultured in an airlift photobioreactor in the presence of wastewater and 12% CO_2 concentration. The maximum biomass productivity and CO_2 fixation rate were obtained as 0.267 g L^{-1} d^{-1} and 7.248 g L^{-1} d^{-1}, respectively. The removal efficiency for total Kjeldahl nitrogen (TKN), total phosphorous (TP), nitrate, and COD were obtained as 84.01, 100, 86.811, and 73.084%, respectively. The maximum amount of lipids and carbohydrates were obtained as 37.91 and 58.45%, respectively. The composition of fatty acids methyl ester (FAME) of the microalga suggests the *Coelastrum* sp. SM was a potential candidate for biodiesel production and CO_2 bio-fixation.

Fu et al. (2019) developed a techno-economic model suggesting that LED-based PBRs can be a realistic approach for converting CO_2 into value-added biomass. *Chlorella vulgaris* were cultivated in different-sized photobioreactors (PBRs) and established a strategy to increase CO_2 fixation under light-emitting diode illumination by adding a small amount of sugar to the system. The low-level glucose dosing led to a 10% increase in CO_2 fixation and photoautotrophic growth-

driven biomass production. The photoautotrophic growth rate was enhanced by 14% when urea was used as the sole nitrogen source. The maximum amount of neutral lipids production was obtained as 0.516 g L^{-1} d^{-1} at optimized conditions.

Barahoei et al. (2020) utilized a modified gas-feeding bubble column photobioreactor for CO_2 fixation and microalgae cultivation. The optimum values of temperature, pH, light intensity, aeration rate, light-dark cycle, and time were obtained as 25 °C, 8, 49.95 μmol m^{-2} s^{-1}, 0.5 LPM, and 16−8 h, respectively. The parameters were optimized using the response surface methodology. The effect of bubble size on CO_2 capture and microalgae growth rate was investigated using two air spargers with various aperture sizes. The maximum biomass productivity and CO_2 bio-fixation rate were increased by 57% and 56% by increasing the CO_2 concentration from 3 to 7%, respectively. The maximum productivity, microalgae concentration, and CO_2 bio-fixation rate of *Chlorella vulgaris* at 7% CO_2 with small bubble size were obtained as 0.337 g L^{-1} d^{-1}, 4.244 g L^{-1}, and 0.6337 g L^{-1} d^{-1}, respectively. The CO_2 utilization efficiency for smaller bubble sizes was 35% more than that of the larger bubbles.

Zhu et al. (2021) isolated three different strains of the genus *Spirulina* (LAMB171, LAMB172, and LAMB220), and those were grown to varying concentrations of CO_2 (2, 5,10, and 15%) in a columnar photobioreactor. This study also examined the ideal strain for CO_2 bio-fixation and production of value-added products such as carotenoids, C-phycocyanin (C-PC), and allophycocyanin (A-PC). The maximum value of biomass concentration and carbon dioxide fixation rate for all three species were achieved at 10% CO_2 concentration. Chlorophyll a, carotenoids, C-PC, and A-PC content for 2% and 5% CO_2 were comparatively higher than in the control run. LAMB220 was the most effectively mitigated CO_2 in three strains because of the

higher biomass productivity and excellent C-fixation capability. However, LAMB171 and LAMB172 were more suitable for pigment production at 10% CO_2 concentration.

Chauhan et al. (2022) isolated 13 different microalgal strains to evaluate the acclimatization capacity of microalgal strains in flue gas compounds by analyzing growth capacity and photosynthetic ability. The experiments were performed in a 2 L custom-made bubble column laboratory scale photobioreactor (PBR) in a semi-continuous mode. The two microalgal strains, *Micractinium pusillum* KMC8 and *Scenedesmus acutus* NCIM5584 were found to be promising for CO_2 bio-fixation and neutral lipid accumulation. The *Micractinium pusillum* KMC8 showed a higher biomass yield (1.32 g L^{-1}), neutral lipid accumulation (32%), enhanced CO_2 utilization efficiency (3.07%), and higher CO_2 fixation rate (0.13679 g L^{-1} d^{-1}) post-acclimatization.

2.2 Bacterial fixation of flue gases (CO_2, NO, SO_2)

Using the bacterial route, limited or no studies are available for the simultaneous bio-fixation of CO_2, NO, and SO_2. The subsequent sections discuss the bacterial fixation of CO_2, NO, and SO_2.

2.2.1 CO_2

Bio-fixation of CO_2 using bacterial species is a well-established process, and extensive work has been carried out in this field. The previous studies reporting CO_2 fixation using different species of bacteria are summarized in Table 2.2 and are discussed in the following sections.

Bharti et al. (2014) cultivated *Serratia* sp. ISTD04 in the presence of sodium bicarbonate as a sole carbon source and examined the potential of *Serratia* sp. for CO_2 fixation and production of value-added products. The bacterium's CO_2 fixation efficiency was measured by the enzymatic activity of carbonic anhydrase and ribulose-1,5-bisphosphate carboxylase/oxygenase (RuBisCO). The produced hydrocarbons (0.487 mg mg^{-1} per unit cell of dry biomass) were in the range of C13–C24, and lipids (0.647 mg mg^{-1} per unit cell of dry biomass) were in the range of C15–C20,

indicating the presence of carbon chain length equivalent to the light oil and biodiesel, respectively. Unsaturated (55%) and saturated (45%) organic compounds were characterized with GC–MS, FT-IR, and NMR spectroscopy. *Serratia* sp. ISTD04 was found to be a potential candidate for lipid synthesis for biodiesel production.

Bacillus sp. strain ISTS2 was enriched in a chemostat for CO_2 bio-fixation and biosurfactant production in the presence of sodium bicarbonate and CO_2 (g) as a carbon source. CO_2 fixation efficiency of *Bacillus* sp. was observed by the enzymatic activity of carbonic anhydrase and ribulose-1,5-bisphosphate carboxylase/oxygenase (RuBisCO). Surface and interfacial tension measurements, emulsification stability tests, hydrophobicity tests, contact angle measurements, bacterial adhesion to hydrocarbon, and purification by silica gel column (60–120 mesh) were used to assess biosurfactant production capabilities at 100 mM $NaHCO_3$ and 5% CO_2 concentration. The crude biosurfactant of *Bacillus* sp. was demonstrated by thin layer chromatography (TLC) and gas chromatography-mass spectrometry (GC-MS) to be made up of lipopeptides and free fatty acids (FA), and it contains five different types of fatty acids (FA) with chain lengths ranging from C14 to C19. Thus, to utilize industrial CO_2 as a substitute substrate, *Bacillus* sp. strain IST2 has shown the potential as a sustainable option (Sundaram et al., 2015).

Mishra et al. (2016) isolated *B. Cereus* SM1 from the sewage treatment plant (STP) of BITS Pilani and performed a 5-day batch study to evaluate the efficiency of CO_2 fixation. The inlet concentration of CO_2 was 13 ± 1 % (v/v), and the maximum removal efficiency was obtained as 84.6 (±5.76) % at 100 ppm of Fe[II] ion concentration. Fourier Transformation Infrared Spectroscopy (FT-IR) and GC-MS were utilized to check the presence of fatty acids and hydrocarbons in cell lysate and cell-free supernatant. The hydrocarbons and fatty acids were observed in the range of C_{11}–C_{22} and C_{11}–C_{19}, respectively. The biodiesel yield was found as 86.5

(±0.048) %. The approximate material and energy balance for the CO_2 fixation process was also discussed. The relevance of *B. Cereus* SM1 for industrial use has been demonstrated for biodiesel production through the transesterification process.

Mishra et al. (2017, 2018) isolated *Halomonas stevensii* from Sambhar Lake, Rajasthan (India), to check the CO_2 fixation efficiency at 5%, 10%, and 15% CO_2 concentration in shake flask and laboratory scale bio-reactor and the ability to produce value-added products during the process. The maximum CO_2 removal efficiency was obtained as 98% for the flask study and 100% for the laboratory scale study at 15 (±1) % (v/v) inlet CO_2 concentrations. The obtained biomass was explored for different functional groups and value-added products using FT-IR and GC-MS. Thus, *Halomonas stevensii* was proposed to be a potential candidate for producing value-added products and gaseous-phase CO_2 fixation in the presence of thiosulfate ion $S_2O_3^{2-}$ as an energy source.

2.2.2 NO

Limited studies were available for the bio-fixation of NO utilizing bacterial species. The previous studies reporting NO fixation in the biofilter and biotrickling column using different species of bacteria are summarized in Table 2.3 and are discussed in the following sections.

Jiang et al. (2009) described the construction of a biotrickling filter system for the treatment of nitric oxide (NO) by *Pseudomonas putida* SB1. The experiments were performed on a lab-scale biotrickling filter for a higher NO concentration in the aerobic environment. The maximum NO removal was 82.9–94.2%, with inlet NO and oxygen concentrations of 400 ppm and 2-20%, respectively. A kinetic relationship between oxygen concentration and biological NO elimination confirmed the primary involvement of microbial metabolism. The study showed that it is possible to remove NO from flue gas via the aerobic denitrification process in a biotrickling filter.

Yang et al. (2013) isolated *Chelatococcus daeguensis* TAD1 in a lab-scale biotrickling filter to investigate the effect of nitrate, oxygen, and carbon sources on the nitrification and denitrification rate. The maximum nitrification and denitrification rate were observed as 0.03008 g-N L^{-1} h^{-1} and 0.1008 g-N L^{-1} h^{-1}, respectively. TAD1 was also checked for NO_x removal in the actual scenario in a coal-fired power plant into a pilot-scale biotrickling filter. For the actual NO_x gas from coal-fired power plants, the higher removal efficiency of 86.7% at 45–50°C was acquired. Thus, *Chelatococcus daeguensis* TAD1 was found suitable for NO_x removal from the acutal flue gases under thermophilic conditions.

Zhang et al. (2013) studied the ability of a hollow-fibre membrane bioreactor (HMBR) for NO treatment from the simulated flue gas. The maximum NO removal efficiency of 86% and elimination capacity of 0.702 g NO m^{-2} day^{-1} for an inlet NO concentration of 2.680 g m^{-3} were achieved. The bacterial population in HMBR was sensitive to pH, and the optimum pH value was obtained as 8. The inlet oxygen concentration adversely affects NO elimination capacity and removal efficiency. In contrast, SO_2 showed no such influence on the process. Analysis of the microbial population showed the presence of denitrifying bacteria in the HMBR. This study indicated that the denitrifying HMBR was a viable option for NO removal.

Zheng et al. (2016) showed a different approach for NO_x removal at different oxygen concentrations by isolated bacterial strain *Pseudomonas aeruginosa* PCN-2. A biotrickling filter and *Pseudomonas aeruginosa* PCN-2 showed higher NO_x removal efficiency of 96.74% for an inlet NO concentration of 500 ppm and O_2 concentration of 10%. Thus, the isolated strain *Pseudomonas aeruginosa* PCN-2 could be a promising candidate for treating NO_x flue gas in a biotrickling filter.

Han et al. (2016) designed a suspended biofilter to remove nitrogen oxides (NO_x) from simulated flue gas under thermophilic conditions. The NO removal efficiency and maximum elimination capacity were achieved as 90% and 146.9 g m^{-3} h^{-1}, respectively. The inlet NO concentration and NO loading ranged from 0.2–2 g m^{-3} and 8.2–164 g m^{-3} h^{-1}, respectively. 16S rRNA MiSeq sequencing of microbial community structure confirmed the bacterial population in the biofilm.

Wang et al. (2018) designed a new AnammoxDeNOx process to remove NO_x in flue gas. The performance of the AnammoxDeNOx process indicated a maximum NO_x removal efficiency of 87–96% for inlet NO concentration of 100–500 ppm utilizing simulated ammonium wastewater. There was a slight decrease in NO_x removal efficiency for the same inlet NO concentration when *Anammox bacteria* (*C. brocadia*) was grown in municipal wastewater. Thus, this process can efficiently remove NO_x from flue gas.

2.2.3 SO_2

Bio-fixation of SO_2 utilizing bacterial species in the biofilter column is scarce. The previous studies reporting SO_2 fixation in the biofilter column utilizing different species of bacteria are summarized in Table 2.4 and are discussed in the following sections.

Zhang et al. (2015b) utilized a bench-scale thermophilic biofilter for SO_2 removal at 60 °C and also analyzed the bacterial structure formed in the biofilter during the process. The maximum SO_2 removal efficiency was 93.10% with an inlet SO_2 concentration of 100 - 200 mg m^{-3}. The water-containing rate of the packing materials has dramatically affected the removal efficiency of SO_2 in the biofilter. The maximum elimination capacity of 50.67 g m^{-3} h^{-1} was obtained at SO_2 loading rate of 51.44 g m^{-3} h^{-1}. The bacterial community analysis showed the abundant presence of desulfurization and thermophilic bacteria. Thus, biofiltration in a thermophilic biofilter proved to be a promising treatment option at high-temperature SO_2.

Li et al. (2015) developed an integrated bioreactor with two different zones, a suspended zone and an immobilized zone, to treat SO_2 and to investigate the integrated bioreactor's performance and microbial characteristics. The SO_2 removal efficiency was achieved as 85% in both zones with an inlet SO_2 concentration of 102 mg m^{-3}. The average removal capacity of SO_2 in the suspended zone and immobilized zone of the bioreactor was 2.80 g m^{-3} h^{-1} and 1.50 g m^{-3} h^{-1}, respectively. The 16S rDNA analysis of the microbial community revealed the presence of desulfurization bacteria in both zones. *Paenibacillus* sp. was present in both zones, whereas *Ralstonia* sp. was present in the suspended zone only. Thus, the integrated bioreactor can be potentially used for a waste gas treatment containing hydrophilic compounds.

Zhang et al. (2015a) checked the performance of thermophilic biofilter for SO_2 removal. Thermophilic desulfurization bacteria were used as inoculum for the study. At steady state, the maximum SO_2 removal efficiency and maximum elimination capacity were achieved as 90% and 48.39 g m^{-3} h^{-1}, respectively. The temporal shift in the bacterial community was determined through polymerase chain reaction-denaturing gradient gel electrophoresis and DNA sequence analysis. The sulfate-reducing bacteria (SRB) in the bacterial population in the thermophilic biofilter was caused by the anaerobic environment and the sulfate formation.

Li et al. (2017) designed an integrated bioreactor with a suspended and immobilized zone to treat SO_2. The effects of operational conditions such as SO_2 loading, temperature, and pH on bioreactor performance and bacterial population composition were investigated. The combined action of both reactor zones increased the SO_2 removal efficiency up to 85% with inlet SO_2 loading of 91–117 mg m^{-3}. Both reactor zones were dominated by desulfurization bacteria such as *Paenibacillus* sp. and *Lysinibacillus* sp. The differences in injected SO_2 concentration and supported mode of

microbial survival indicated that the bacterial community composition and abundance changed considerably across two different zones.

Papi et al. (2018) studied the ability of sulfate-reducing bacteria, *Desulfovibrio desulfuricans,* for gaseous sulfur dioxide removal. SO_2 was generated in laboratory-scale bioreactors by chemical reaction. Three kinetics (in triplicate) were obtained in batch mode with loads of 15, 20, and 25 mmol of SO_2 produced in the gas phase per litre of culture medium to assess the biological reduction. The experimental results indicated 100% SO_2 reduction for all the tested loads.

2.2.4 Simultaneous bacterial fixation of flue gases (CO_2, NO, SO_2)

The previous studies reporting simultaneous bio-fixation of flue gases in the biofilter and biotrickling column with different species of bacteria are summarized in Table 2.5 and are discussed in the following sections.

Han et al. (2010) investigated the removal capacity of the co-culture of sulfate-reducing bacteria and anaerobic denitrifying bacteria isolated from landfill leachate for simultaneous removal of NO_x and SO_2 from exhausted gas. The co-culture system established a faster NO removal rate and higher stability when H_2S generated by sulfate-reducing bacteria was used as a sole electron donor for anaerobic denitrifying bacteria. The maximum removal of NO and SO_2 was obtained as 92 and 95% at inlet NO and SO_2 concentrations as 4 g m^{-3} and 1% (v/v), respectively. It was observed that a lower gas flow rate and a higher NO concentration might result in a higher NO removal rate.

Zhou et al. (2013) investigated the effects of sodium acetate and glucose on the microbes from the simultaneous flue gas desulfurization and denitrogenation tandem biotrickling process. The sulfite oxidation rate was increased for the acidophiles. However, carbon sources promoted total microbial growth for the neutrophiles, and sodium acetate significantly enhanced nitrite consumption. The maximum removal of NO and SO_2 was obtained as 86.7 and 47.2%,

respectively, at inlet NO and SO_2 concentration ranges as 0.5-1 g m^{-3} and 3-5 g m^{-3}, respectively. The study contributes valuable information to improve the simultaneous purification of SO_2 and NO_x.

Wang et al. (2015) used the bacterial consortium to check the O_2 effects (4, 8, 12, 16 and 20%) on SO_2 and NO removal in the biotrickling column. The SO_2 removal efficiency from mixed gas (SO_2 and NO_x) reached 100% for all five O_2 concentrations. When the O_2 concentration rose from 4 to 20%, the average NO_x removal efficiency increased from 49.28 to 80.85%. The maximum removal percentage for NO was 80.85% for an initial concentration of 2.5-3 g m^{-3}, and SO_2 was 47.2% with an initial concentration of 1.5-2 g m^{-3}.

Sun et al. (2019) investigated the biofilter efficiency for the simultaneous removal of nitric oxide (NO) and sulfur dioxide (SO_2) under thermophilic (48 ± 2 °C) micro-oxygen (3 vol%) conditions. SO_2 and NO inlet concentrations remained the same for the whole cultivation period at 0.5 g m^{-3} and 0.3-0.7 g m^{-3}, respectively. The maximum removal efficiency of NO and SO_2 were 98.08% and 99.61%, respectively. The relative abundance of sulfate-reducing bacteria was related to the rate of sulfur conversion.

Xie et al. (2021) investigated the removal performance of flue gas (CO_2, SO_2, and NO_x) and nitric-sulfur compound's conversion efficiency in the biofilter liquid phase. The influent CO_2, SO_2, and NO concentration was 14-15.5%, 19-20 g m^{-3}, and 0.9-1 g m^{-3}, respectively. Simulated industrial wastewater was used as a spray solution. The maximum flue gas removal efficiency for CO_2, SO_2, and NO was 75.23%, 100%, and 82.81%, respectively, under the optimal operating conditions of biofilter (pH- 9 and L/G- 3). The microbial population exploration results showed the presence of a bacterial community. Thus, the biofiltration system provides an economically feasible strategy for flue gas purification and increases the potential for industrial application.

Table 2.2 Bacterial fixation of CO_2 in different types of reactors under different growth media

S.No.	Bacterial species	Carbon source	Growth media prepared in	Reactor Type	References
1	*Serratia* sp. ISTD04	Sodium bicarbonate	Distilled water	Glass vessel	(Bharti et al., 2014)
2	*Bacillus* sp. ISTS2	5% CO_2 (g), $NaHCO_3$	Distilled water	Shake flask	(Sundaram et al., 2015)
3	*B. cereus* SM1	13 ± 1% CO_2 (g)	Distilled water	Erlenmeyer flask	(Mishra et al., 2016b)
4	*Serratia* sp. ISTD04	Sodium bicarbonate, Glucose	Distilled water	Microscopic visualization	(Kumar et al., 2016)
5	*Pseudomonas aeruginosa* SSL-4	17±0.8% CO_2 (g)	Distilled water	Erlenmeyer flask	(Mishra, et al., 2017)
6	*Halomonas stevensii*	15 (±1) % CO_2 (g)	Distilled water	Erlenmeyer flask	(Mishra et al., 2017)
7	*Halomonas stevensii*	15 % (v/v) CO_2 (g)	Distilled water	Laboratory scale bio-reactor	(Mishra et al., 2018)

Table 2.3 Bacterial fixation of NO under different conditions

S.no.	Bacterial species	NO concentration	NO removal %	Reactor Type	References
1	*Pseudomonas putida*	400ppm	82.9–94.2	Biotrickling filter	(Jiang et al., 2009)
2	*Chelatococcus daeguensis* TAD1	298.5–893.8 mg NO_x m^{-3}	86.7	Biotrickling filter	(Yang et al., 2013)
3	*Mixed consortium*	2680 mg m^{-3}	86	hollow-fibre membrane bioreactor	(Zhang et al., 2013)
4	*Pseudomonas* sp.	0−670 mg m^{-3}	-	Biofilter column	(Liu et al., 2014)
5	*Mixed consortium*	112–1202 mg m^{-3}	96.4	thermophilic membrane biofilm reactor	(Wei et al., 2016)
6	*Mixed consortium*	400 ppm	95	Biofilter column	(Li et al., 2016)

7	*Pseudomonas aeruginosa PCN-2*	100–500 ppm	91.94–96.74	biotrickling filter	(Zheng et al., 2016)
8	*Mixed consortium*	200–2000 mg m^{-3}	90	suspended biofilter	(Han et al., 2016)
9	*Anammox bacteria* (*C. Brocadia*)	100-500 ppm	87.11	Biofilter reactor	(Wang et al., 2018)

Table 2.4 Bacterial fixation of SO_2 in a different type of reactor

S.No.	Bacterial species	SO_2 concentration	SO_2 removal %	Reactor Type	References
1	*Mixed consortium*	100 - 200 mg m^{-3}	93.10	Biofilter column	(Zhang et al., 2015b)
2	*Paenibacillus* sp., *Ralstonia* sp.	102 mg m^{-3}	85	Integrated bioreactor	(Li et al., 2015)
3	*Mixed consortium*	1%	90	Biofilter column	(Zhang et al., 2015a)
4	*Mixed consortium*	100–200 mg m^{-3}	98	Biofilter column	(Zhang et al., 2017)
5	*Mixed consortium*	91–117 mg m^{-3}	85	Integrated bioreactor	(Li et al., 2017)
6	*Mixed consortium*	-	-	Biofilter column	(Zhang et al., 2018)
7	*Desulfovibrio desulfuricans*	15–25 mmol	100	Laboratory scale bio-reactor	(Papi et al., 2018)

Table 2.5 Simultaneous bio-fixation of flue gases (CO_2, NO, SO_2) using bacteria

S.No.	Bacterial species	Flue gas concentration	Removal %	Reactor Type	References
1	*Sulfate-reducing* and *Denitrifying* bacteria	NO- 4 g m^{-3} SO_2- 1%	NO- 92 SO_2- 95	Biotrickling filter	(Han et al., 2010)
2	*Sulfate-reducing* and *Denitrifying* bacteria	NO- 2 g m^{-3} SO_2- 2 g m^{-3}	NO- 92 SO_2- 95	Biotrickling filter	(Han et al., 2011)
3	*Mixed consortium*	NO- 0.5-1 g m^{-3} SO_2- 3-5 g m^{-3}	NO- 86.7 SO_2- 47.2	Biotrickling filter	(Zhou et al., 2013)
4	*Mixed consortium*	NO- 2.5-3 g m^{-3} SO_2- 1.5-2 g m^{-3}	NO- 80.85 SO_2- 47.2	Biotrickling filter	(Wang et al., 2015)
5	*Mixed consortium*	NO- 0-0.5 g m^{-3} SO_2- 0-0.8 g m^{-3}	NO- 96.5 SO_2- 95.6	Biotrickling filter	(Wen et al., 2019)
6	*Sulfate and Nitrate reducing bacteria*	NO- 0.3-0.7 g m^{-3} SO_2- 0.5 g m^{-3} CO_2- 14-15.5%	NO- 98.08 SO_2- 99.61 CO_2- 75.23	Biofilter column	(Sun et al., 2019)
7	*Mixed consortium*	SO_2- 19-20 g m^{-3} NO- 0.9-1 g m^{-3}	SO_2- 100 NO- 82.81	Biofilter column	(Xie et al., 2021)

2.3. Gaps and scope in existing research

2.3.1 CO_2 fixation using microalgae

Conventionally, algae are cultivated in raceway ponds or photobioreactors. The closed photobioreactors have drawn researcher's attention more than raceway ponds as they allow better control of the growing environment and efficiency than open culture systems. The closed photobioreactors mostly yielded higher biomass productivity and prevented outside contamination (Ugwu et al., 2002). Only a few photobioreactors are used for biomass bulk production as other bioreactors have certain limitations such as control in culture conditions, restricted availability of light, shear stress to algal culture, pH gradient, dissolved oxygen concentration, CO_2 concentration, and lower mass transfer rates (Ugwu et al., 2002; Achinas et al., 2020).

Loop photobioreactors can overcome the limitations of conventional photobioreactors. Loop photobioreactors are tubular photobioreactors in which continuous homogeneous mixing is carried out by constant bubbling of the different gaseous mixtures and recirculation of liquid. These are mainly constructed of transparent materials such as glass, plexi glass, polyvinyl chloride (PVC), acrylic PVC, or polyethylene (Kumar et al., 2011; Huang et al., 2017). The growth media carrying biomass with a gaseous stream circulates in a loop from one column to another without using any mechanical impeller in the loop photobioreactor. The advantages include simple construction, easy operation, defined mixing, rapid and uniform distribution of reaction components, adequate mass transfer rates, and scale-up procedures.

The literature studies (section 2.1) indicated that the application of loop bioreactors for CO_2 fixation using microalgae is limited or nil. Most of the studies are confined to bench-scale reactors. Hence, this becomes an important gap where the novelty is incorporated in terms of developing the pilot-scale closed-loop photobioreactor for CO_2 fixation utilizing microalgae.

2.3.2 Flue gas (CO_2, NO, SO_2) fixation using bacteria

The bio-fixation studies reported in the literature were mainly focused on the individual fixation of CO_2, NO, and SO_2 using MSM prepared in distilled water in a shake flask or a bioreactor on batch mode (section 2.2.1, 2.2.2, 2.2.3, and 2.2.4).

The utilization of bacterial consortium isolated from the extreme environment of Sambhar Salt Lake for simultaneous flue gas (CO_2, NO, SO_2) fixation is scarce, which is of industrial importance. Also, no reported studies discussed the utilization of suspended bioreactors for flue gases (CO_2, NO, and SO_2) bio-fixation by bacteria and the simultaneous production of value-added products during the process. To the best of our knowledge, the utilization of wastewater to prepare growth media for simultaneous bio-fixation of flue gases (CO_2, NO, and SO_2) is not studied. Limited studies were performed to develop a downstream processing strategy for the economic recovery of metabolites from flue gas utilizing bacterial consortium. Hence these are the identified gaps of simultaneous bio-fixation studies of CO_2, NO, and SO_2 by bacterial species.

The novelty of the work is simultaneous bio-fixation of flue gases (CO_2, NO, and SO_2) utilizing the bacterial consortium. A suspended bioreactor can overcome the limitations of the biofilter column for the simultaneous bio-fixation of flue gases (CO_2, NO, and SO_2). The utilization of domestic wastewater for MSM preparation as growth media was explored. Moreover, the area of product recovery using downstream processing from obtained biomass during bio-fixation of flue gases (CO_2, NO, and SO_2) required investigation. To give commercial value to the bio-fixation process, the analysis of by-products obtained from flue gas fixation studies and utilization of domestic wastewater as growth media is novelty of the process and requires attention.

Chapter 3

Materials and Methods

This chapter is divided into two parts. The first part explains the materials and methods for CO_2 fixation using microalgae. The second part describes the materials and methods for CO_2 fixation using *Halomonas stevensii* (*H. stevensii*) and flue gas (CO_2, NO, SO_2) fixation using bacterial consortium.

3.1 Glassware, plastic ware, and chemicals

The glassware and plastic wares utilized in the present work are given in Table 3.1. The chemicals used in this study were of analytical grade and are listed in Table 3.2.

3.2 CO_2 fixation using *Desmodesmus* species

This section provides the details of the materials and methods for CO_2 fixation using *Desmodesmus* species in a loop photobioreactor. It includes the procurement of microalgal species, media preparation, enrichment, semi-continuous studies, analytical methods for measurement of different parameters, and product analysis.

3.2.1 Media and inoculum preparation

Desmodesmus sp. MCC34 [KF731760.1] used in the present work was collected from the Environment and Microbiology lab of BITS Pilani, Pilani Campus, Rajasthan, India. The strain was isolated from the local water bodies of Pilani, Rajasthan, as reported by Nagappan et al. (2016).

BG-11 Medium (Table 3.3) was used as cultivation media for the growth of the strain. Trace metal mix was comprised of boric acid, zinc sulfate, copper sulfate, sodium molybdate, cobalt nitrate, and manganese chloride. The solid media was used for plating and was prepared by adding 1.5 g L^{-1} (1.5%) agar to the cultivation media. The conditioned media was autoclaved at 121 ^{o}C and 15 psi for 15 min and was used for further studies.

Table 3.1 List of glassware and plastic wares used in the present work

S.No.	Glassware/plastic ware	Make
1	Beakers (100 mL, 250 mL, 500 mL, 1 L,)	Borosil®
2	Conical flask (100 mL, 250 mL, 500 mL, 1 L, 2L)	Borosil®
3	Measuring cylinder (10 mL, 50 mL, 100 mL, 500 mL, 1 L)	Borosil®
4	Test- tubes (10 mL, 50 mL, 100 mL)	Borosil®
5	Pipette (10 mL, 50 mL)	Borosil®
6	Petri dish	Borosil®
7	Centrifuge bottle (15 mL, 50 mL, 500 mL)	Tarson®
8	Accupipet (0.1-1 mL)	Tarson®

Table 3.2 List of chemicals used in the present work

S. No.	Chemicals	Make	Use
1	Dipotassium hydrogen phosphate (K_2HPO_4)	Himedia®	
2	Citric acid ($C_6H_8O_7$)	Himedia®	
3	Ferric ammonium citrate ($C_6H_{5+4y}FexNyO_7$)	Himedia®	
4	Ethylenediaminetetraacetic acid (EDTA) $[CH_2N(CH_2CO_2H)_2]_2$	Himedia®	
5	Sodium nitrate ($NaNO_3$)	Himedia®	
6	Magnesium sulfate ($MgSO_4.7H_2O$)	Himedia®	Cultivation media
7	Calcium chloride ($CaCl_2$)	Himedia®	(Microalgal studies)
8	Sodium carbonate (Na_2CO_3)	Himedia®	
9	Boric acid (H_3BO_3)	Himedia®	
10	Zinc sulfate ($ZnSO_4$)	Himedia®	
11	Copper sulfate ($CuSO_4$)	Himedia®	
12	Sodium molybdate (Na_2MoO_4)	Himedia®	
13	Cobalt nitrate ($Co(NO_3)_2$)	Himedia®	
14	Manganese chloride ($MnCl_2$)	Himedia®	
15	Dipotassium hydrogen phosphate (K_2HPO_4)	Himedia®	
16	Potassium nitrate (KNO_3)	Himedia®	
17	Ammonium chloride (NH_4Cl)	Himedia®	Minimal salt media
18	Sodium chloride (NaCl)	Himedia®	(MSM) preparation
19	Sodium thiosulfate ($Na_2S_2O_3$)	Himedia®	
20	Sodium hydroxide (NaOH)	Himedia®	pH adjustment
21	Hydrochloric acid (HCl)	Himedia®	
22	Nutrient broth (peptone, beef extract, NaCl)	Himedia®	Inoculum preparation
23	Glucose ($C_6H_{12}O_6$)	Himedia®	Enrichment

24	Agar A	Himedia®	Solidifying agent
25	Methanol (CH_3OH)	Himedia®	
26	Sulfuric acid (H_2SO_4)	Himedia®	
27	Glucose ($C_6H_{12}O_6$)	Himedia®	
28	Phenol (C_6H_6O)	Himedia®	
29	Sodium hydroxide (NaOH)	Himedia®	
30	Reagent A (500 µL of 1:1:1:1 ratio of CTC (0.1 % $CuSO_4 \cdot 5H_2O$ + 0.2 % NaK tartrate +10 % Na_2CO_3), 10 % SDS, 0.8 M NaOH and dH_2O)		Product analysis
31	Reagent B (250 µL of a solution of one volume of Folin–Ciocalteu reagent and five volumes of dH_2O)		
32	Bovine serum albumin (BSA)	Himedia®	
33	Chloroform ($CHCl_3$)	Himedia®	
34	Potassium bromide (KBr)	Himedia®	

Table 3.3 Components of BG-11cultivation media

S.No.	Chemical	Amount (g /mL L^{-1})
1	Dipotassium hydrogen phosphate (K_2HPO_4)	0.04
2	Citric acid ($C_6H_8O_7$)	0.006
3	Ferric ammonium citrate ($C_6H_{5+4y}FexNyO_7$)	0.006
4	EDTA	0.001
5	Sodium nitrate ($NaNO_3$)	1.5
6	Magnesium sulfate ($MgSO_4.7H_2O$)	0.075
7	Calcium chloride ($CaCl_2$)	0.036
8	Sodium carbonate (Na_2CO_3)	0.002
9	Trace metal mix	1

The inoculum was grown at a constant temperature of 26 ± 1 °C and the light intensity of 67 µmol photon m^{-2} s^{-1} in the laboratory for ten days. The purity of the grown culture was checked using repeated streaking on BG-11 plates. The culture with an optical density close to unity was used as inoculum for conducting the experiments in a custom-designed loop photobioreactor. The optical density of the culture was measured at a wavelength of 650 nm ($OD_{650\ nm}$) to determine the cell concentration using a UV-Vis spectrophotometer (Evolution 201, Thermo Scientific, USA). The calibration curve was prepared between the dry weight of biomass versus optical density to measure the cell concentration. The mathematical co-relation between dry weight of biomass and optical density was obtained as $y = 0.7666\,x + 0.0711$ with R^2 value of 0.98 for 0.03% and 5% CO_2 concentration and $y = 0.6838\,x + 0.6244$ having R^2 value of 0.73 for 10% CO_2 concentration. Where y and x represent the dry weight of biomass and optical density, respectively.

3.2.2 Loop photobioreactor setup

The loop photobioreactors are tubular photobioreactors in which continuous homogeneous mixing is carried out by constant bubbling of the different CO_2 (g) concentration mixtures. The growth media carrying biomass along with a gaseous stream circulates in a loop from one column to another column without using any mechanical impeller. The reactor has the following advantages: simple construction, easy operation, defined mixing, rapid and uniform distribution of reaction components, adequate mass transfer rates, and scale-up procedures.

The loop photobioreactor was designed and made up of glass which consists of two column units with dimensions of 2.03 meter (m) length, 0.105 m inner diameter and 0.12 m outer diameter with a total volume of 34 L and a working volume of 26 L. Sunlight was used as the energy source during the process. The study used 1.25 L of enriched culture as inoculum volume, with an optical density (OD) of 0.82. The experiments were performed in semi-continuous mode. The cultivation

media was mixed with inoculum and transferred to the photobioreactor column at once before the start of the experiments. The gas mixture was supplied on an intermittent basis. The schematic diagram of the loop photobioreactor is given in Fig. 3.1. A photograph of the actual setup is shown in Fig. 3.2.

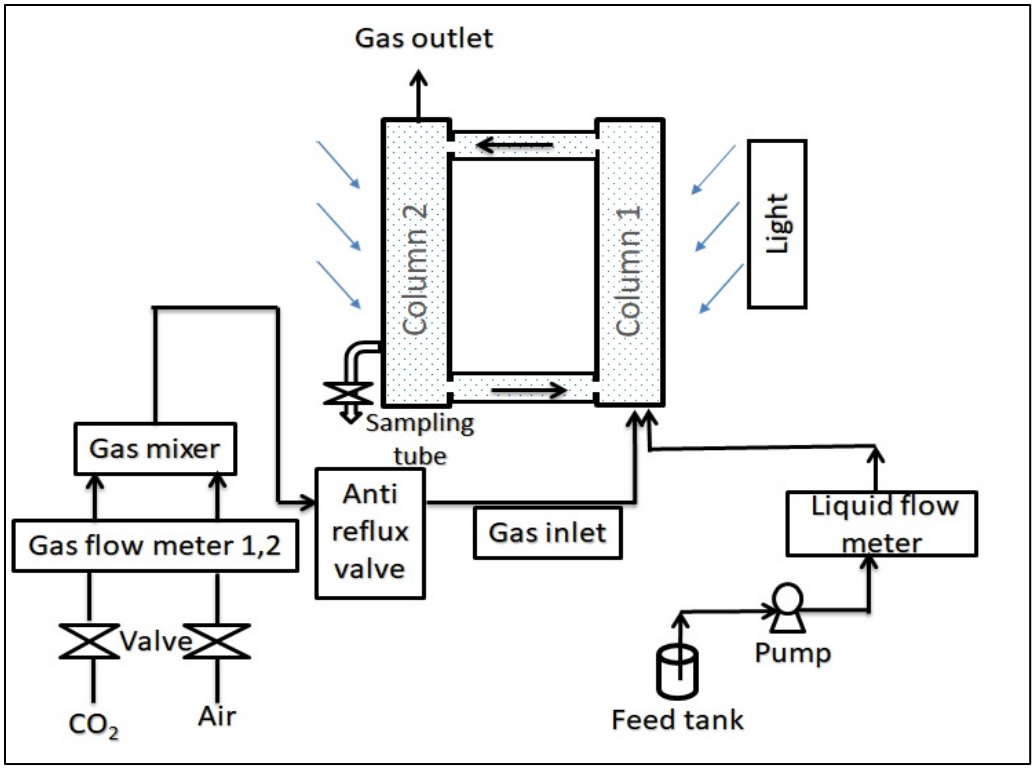

Fig. 3.1 Schematic diagram of custom-designed loop photobioreactor

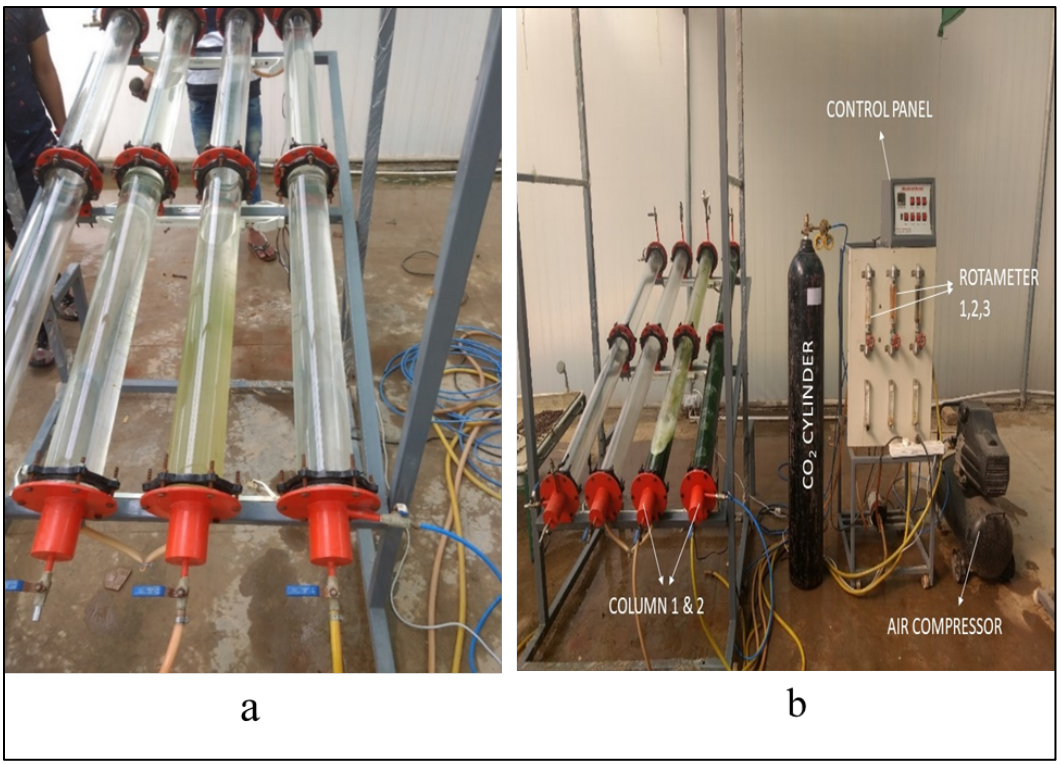

Fig. 3.2 Setup of loop photobioreactor: (a) at day zero after inoculation; (b) at day 12 – last day of the incubation period used for the CO_2 bio-fixation study

3.2.3 CO_2 bio-fixation studies

The experimental design of microalgae cultivation is shown in Fig.3.3. CO_2 bio-fixation experiments utilizing *Desmodesmus* species were carried out at 0.03 % (atmospheric), 5% and 10% (v/v) CO_2 concentrations in a loop photobioreactor. The gas mixture was supplied on a 12- h aeration cycle through the gas inlet port of the photobioreactor equipped with the sparger. The gas mixture was fed during the light period, and its supply was stopped during the dark period. The semi-continuous study was performed in a loop photobioreactor for 12 days, and the temperature was maintained at ambient conditions of 30–35 °C. A gas mixture comprising CO_2 (g) and compressed moisture-free air was supplied to photobioreactor as the sole carbon source. The initial pH was maintained in the range of 7 to 9 for the optimal growth of *Desmodesmus* sp., which increased the solubility of CO_2 in the aqueous phase. The gas flow rate into the reactor was maintained at 0.15 vvm (4 L min^{-1}). Once the microalgae reached the stationary phase, the culture was separated by filtering with muslin cloth and was rinsed with distilled water. The algal biomass was freeze-dried and preserved at -20 °C for further studies. The parameters such as pH, dry weight biomass, and colony forming unit (CFU) were measured every 24 h duration (after a complete light and dark cycle). The optical density (OD_{650nm}) was measured twice a day (after the completion of the light cycle and dark cycle). The various growth kinetic parameters such as biomass concentration, specific growth rate, biomass productivity, and CO_2 fixation rate were also estimated to check the microalgal growth. The effect of the light and dark cycles on the growth of microalgal biomass was also understood. The biochemical properties such as chlorophyll content, lipid, carbohydrate and protein were determined for the obtained biomass. The control run was performed using ambient air (0.03% CO_2) while keeping other operating conditions constant.

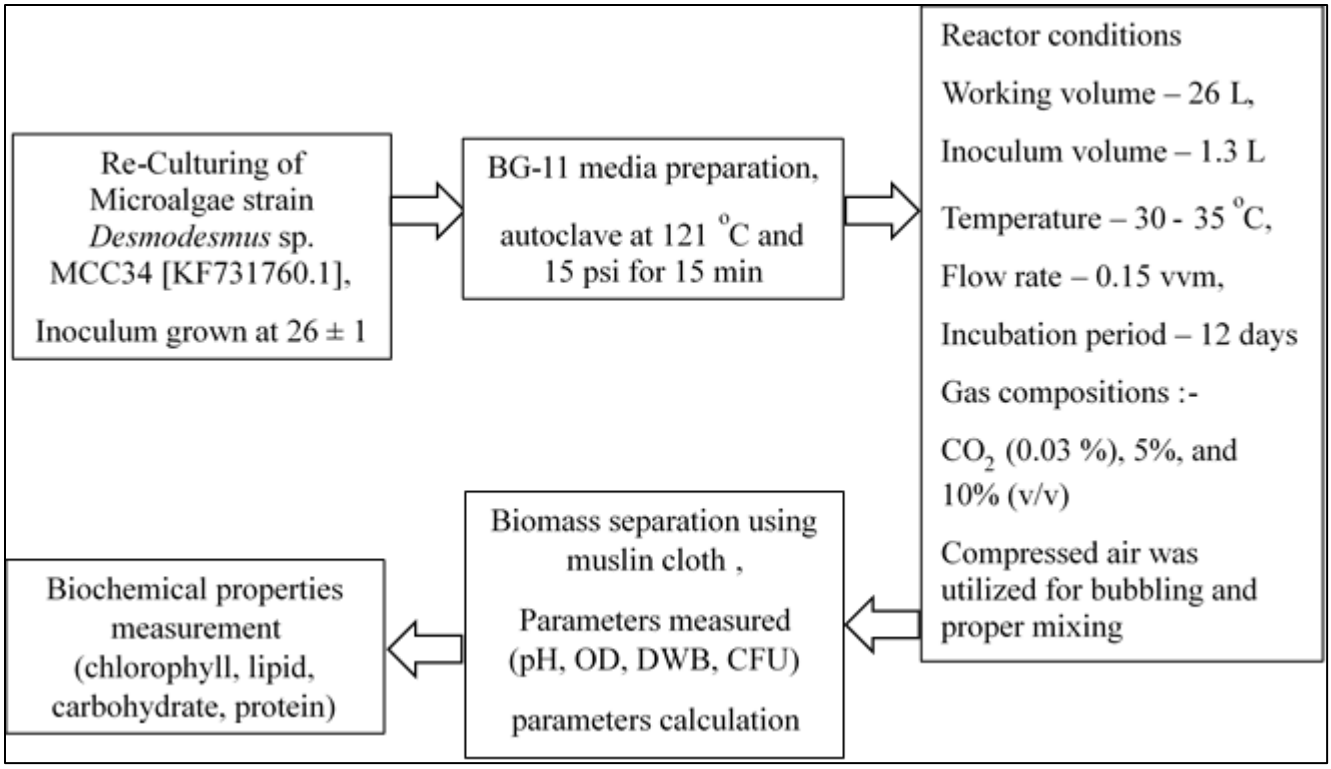

Fig. 3.3 Experimental design of microalgae CO_2 fixation studies

3.2.4 Analytical methods

3.2.4.1 CO_2 (g) measurement

The gas-phase analysis was performed to evaluate the CO_2 fixation efficiency of *Desmodesmus* sp. The inlet and outlet CO_2 concentration was measured by Gas chromatography (Model: GC-2014, Shimadzu) (Bhowmick et al., 2019). The GC comprised of Porapak-q columns having a total length of 2 m and an internal diameter of 1/8 inch. The column injector and thermal conductivity detector (TCD) temperature were maintained at 45 ^{o}C, 100 ^{o}C, and 120 ^{o}C, respectively. Helium (He) was used as carrier gas at the flow rate of 12 mL m^{-1}, having a negative polarity. The inlet and outlet concentration of CO_2 was analyzed on the alternative days. The CO_2 fixation efficiency was derived using Equation (Eq.) (3.1)

$$CO_2 \text{fixation efficiency} = \left(\frac{CO_{2\text{inlet}} - CO_{2\text{outlet}}}{CO_{2\text{inlet}}}\right) \times 100\ \% \quad (3.1)$$

3.2.4.2 Biomass concentration measurement

The dry weight biomass and optical density were measured to evaluate the biomass yield of *Desmodesmus* sp. 50 mL of aliquot culture was collected in every 24 h for dry weight biomass and pH measurement. The dry weight biomass (g L^{-1}) was measured using the standard filtration process (Abou-Shanab et al., 2013; Sundaram et al., 2015). The filtrate obtained was utilized for further studies. The contamination was checked via a colony-forming unit (CFU) after plating the grown culture. pH of the culture was measured using a digital pH meter (Eco Testr pH 2, Eutech Instruments, USA).

3.2.4.3 Determination of growth kinetic parameters

The biomass productivity (P) was calculated by using Eq. 3.2:

$$P = \frac{X_t - X_0}{t_t - t_0} \quad (3.2)$$

Where X_t is the cell concentration (g L^{-1}) at the end of the cultivation cycle (t_t), and X_0 is the initial cell concentration (g L^{-1}) at t_0 (day). The specific growth rate μ_{max} (day^{-1}) was calculated using Eq. 3.3 (Abreu et al., 2012; Anjos et al., 2013).

$$\mu_{max} = \frac{\ln N_2 - \ln N_1}{t_2 - t_1} \tag{3.3}$$

Where N_1 and N_2 are the concentrations of the cells at the beginning (t_1) and the end (t_2) of the exponential growth phase, respectively (Anjos et al., 2013; Basu et al., 2013). $C_1O_{0.48}H_{1.83}N_{0.11}P_{0.01}$ was used as the microalgal biomass molecular formula (Tang et al., 2011). As per the reported studies, it is assumed that 1 g of produced algal biomass ($C_1O_{0.48}H_{1.83}N_{0.11}P_{0.01}$) is equivalent to capturing 1.88 g of CO_2. Hence, the CO_2 fixation rate (g L^{-1} d^{-1}) was determined from Eq. 3.4 (Mohsenpour et al., 2016; Nayak et al., 2016a).

$$\text{Fixation rate of } CO_2 = 1.88 \times P_{\text{overall}} \tag{3.4}$$

Where $P_{overall}$ is the overall biomass productivity. The CO_2 utilization efficiency was obtained from Eq. 3.5.

$$CO_2\ utilization\ efficiency = \frac{fixation\ rate\ of\ CO_2}{CO_{2_{in}}\ rate} \times 100 \tag{3.5}$$

3.2.4.4 Determination of chlorophyll content

Fifty millilitres of algal culture sample were collected in the falcon tube and centrifuged for 10 minutes (min.) at 4000 rpm. The supernatant was discarded, and the pellet was stored at -20 °C until further use. During the extraction step, the pellet was re-suspended in 90% methanol. It was further assisted by sonication for cell lysis under dark conditions in the ice bath (to prevent chlorophyll degradation from light). The control parameters followed during the sonication were 1 min time and a 60% duty cycle. The snap freezing method in liquid nitrogen gave the thermal shock, and the whole process was repeated for ten cycles to maximize the extraction yield. This

step was followed by centrifugation at 4000 rpm for 10 min., and the pellet was dried and stored. One milligram of dried algal biomass was taken in the falcon tube, and a mixture of 90% methanol and 10% millipore water was added to maintain the volume of 10 mL. The tube was kept in the water bath for 20 min, and then it was stored at 4 °C for the incubation period of 24 h. The absorbance of the obtained supernatant was measured at 652 and 665 nm using a spectrophotometer. Methanol was used as a blank solution in a UV-Vis spectrophotometer. Chlorophyll a (Chl a) and chlorophyll b (Chl b) concentrations were determined according to Eq. 3.6 and 3.7 (Lichtenthaler et al., 2001).

$$\text{Chl a } (\text{mg L}^{-1}) = (16.72 \times \text{absorbance}_{665\text{nm}}) - (9.16 \times \text{absorbance}_{652\text{nm}}) \quad (3.6)$$

$$\text{Chl b } (\text{mg L}^{-1}) = (34.09 \times \text{absorbance}_{652\text{nm}}) - (15.28 \times \text{absorbance}_{665\text{nm}}) \quad (3.7)$$

3.2.5 Product analysis

3.2.5.1 Total carbohydrate (CHO) content

A 5 mL sample was taken and centrifuged at 5 °C for 10 min at 4000 rpm, and the obtained supernatant was discarded. The pellets were washed with deionized water and stored at -20 °C for further studies. Then, 0.5 mL of 2.5 M H_2SO_4 was added to the pellet to carry out primary hydrolysis (polysaccharides to monosaccharides) (Mecozzi, 2005; Wang et al., 2018). The samples were incubated in a boiling water bath for 2 h. The columns were cooled at room temperature, and hydrolysate was diluted with deionized water to make it to the volume of 5 mL. The particular step was centrifuged at 4000 rpm, and the supernatant was collected. The phenol-sulfuric method was applied to determine the total content of carbohydrates in biomass (Dubois et al., 1956). The calibration plot was drawn at different glucose concentrations (0–0.1 mg mL^{-1}). Two-millilitre aliquots of diluted supernatant and standard solution were mixed with 1 mL of 5% aqueous phenol in a 15 mL falcon tube. Then, 5 mL of concentrated sulfuric acid was added to all tubes and

vortexed for 10 s. All falcon tubes were kept at room temperature for 10 min, and later tubes were placed in the water bath at 30 °C to develop a yellow-golden colour. The absorbance value was measured at 490 nm in a UV-Vis spectrophotometer (Varshney et al., 2018).

3.2.5.2 Total protein content

The Folin–Lowry method was used for the total protein determination using white pellets obtained after pigment extraction (Lowry et al., 1951). The pellet was pretreated with 1% SDS/0.1M NaOH in 500 µL. The resuspended pellet mixed with reagent A, 500 µL of 1:1:1:1 ratio of CTC [(0.1 % $CuSO_4 \cdot 5H_2O$ + 0.2 % NaK tartrate +10 % Na_2CO_3), 10 % SDS, 0.8 M NaOH, and dH_2O] and the tubes were kept at room temperature for 10 min. After adding reagent B (250 µL of a solution of one volume of Folin–Ciocalteu reagent and five volumes of dH_2O) to the samples, tubes were instantly vortexed and allowed to stand at room temperature for 30 min. The OD was measured at 750 nm for 0.5 mL of 1 % SDS/0.1 M NaOH. The standard curve was prepared for the determination of the total amount of protein by dissolving different concentrations of bovine serum albumin (BSA) in 1% SDS/0.1 M NaOH (0–1.0 mg mL^{-1}) (Varshney et al., 2016).

3.2.5.3 Total lipid content

The total lipid content of the biomass was quantified gravimetrically using the Bligh and Dyer method with slight modifications (Bligh and Dyer, 1959). The pellets were separated from the 50 mL culture after centrifugation at 4000 rpm for 10 min at 4 °C and were stored at -20 °C for further analysis. The pellet was suspended in 2.4 mL deionized water, followed by 3 mL chloroform and 6 mL methanol. Later, it was subjected to sonication by placing the mixture in the ultrasonic bath for 20 min. Further, 3 mL of each deionized water and chloroform were added to maintain the final ratio of 2:2:1.8. The final mixture was centrifuged for 10 min at 2000 rpm. The organic bottom layer of chloroform was carefully extracted after centrifugation, transferred into a pre-weighted

vial, and preserved overnight for solvent evaporation in the fume hood. The vial was re-weighted until dry to determine the overall lipid quantity. These steps were carried out at room temperature as per the reported procedure (Varshney et al., 2018).

3.3 CO_2 bio-fixation using *H. stevensii*

3.3.1 Wastewater sampling and analysis

The discharge section of the secondary clarifier of the sewage treatment plant (STP) at Birla Institute of Technology and Science (BITS), Pilani (28º220000N, 75º360000E), Pilani campus, Rajasthan, India, was selected to obtain the domestic wastewater (DWW). STP entails using physical, chemical, and biological processes to remove contaminants such as organic compounds, inorganic compounds, and heavy metal ions from wastewater. DWW contains various nutrients and ions, such as nitrate, phosphate, and sulfate ions. Different microbes utilize these ions as nutrient and energy sources for their growth. DWW was collected before the experiments and brought to the laboratory in sterile sample bottles to avoid contamination and was kept at 4 ºC until further use.

Initially, the collected DWW was filtered with a GF/C Whatman cellulose membrane filter of 0.22 µm pore size to remove the suspended solid impurities. Further, the filtered DWW was autoclaved at 121 ºC and 15 psi for 15 min. to avoid foreign contaminants. After filtration and sterilization of DWW, the pH was 8.1 ± 0.1. The filtered autoclaved DWW was then analyzed for its physical and chemical properties such as BOD, COD, N-NO_3, N-NO_2, P-PO_4, HCO_3^-, CO_3^{2-}, OH^-, and SO_4^{2-}, dissolved oxygen (DO), total dissolved solids (TDS), conductivity, and salinity by adapting the standard procedure available in American Public Health Association (APHA) handbook (APHA, 2003). A brief description of the measurement of N-NO_3, N-NO_2, P-PO_4, HCO_3^-, SO_4^{2-} and BOD is discussed in the following section.

Nitrate content was determined at a wavelength of 220 nm and 275 nm using the UV–vis spectrophotometer. OD was measured against DIW, and the sample was diluted before the measurement. The final OD due to NO_3^- was calculated by $OD_{220} - 2 \times OD_{275}$. Sodium nitrate was used as the standard at a concentration range of 0–30 mg L^{-1}.

Nitrite was measured spectrophotometrically at 540 nm. The standard solution was prepared by adding $NaNO_2$ in DIW of varying concentrations from 1 to 10 mg L^{-1}. Nitrite was measured by adding 1 mL sulphonamide solution and 1 mL 1-Naphthyl ethylenediamine dihydrochloride (NEDD) in 0.5 ml of DWW sample. OD was measured against a mixture of DI water, sulphonamide solution and NEDD.

Phosphorus was measured by the stannous chloride method. Ammonium molybdate (80 µL) and stannous chloride reagent (10 µL) were added to 1 mL of wastewater sample. Then the sample was incubated for 10–12 min, and the absorbance was measured at 690 nm (OD_{690}) using the UV-Vis spectrophotometer. The concentration of phosphorus P-PO_4 was measured using a standard graph of mono-potassium phosphate at a concentration range of 0-10 mg L^{-1}.

Bi-carbonate and carbonate were measured using a titration-based method. In 25 mL sample, 2 or 3 drops of phenolphthalein indicator were added for the solution to turn pink and titrated with the standard 0.5 N H_2SO_4 solution until it turned colourless. Afterwards, one drop of methyl orange was added till it turned orange. The solution was again titrated with standard 0.5 N H_2SO_4 till it turned pink. P-alkalinity and M-alkalinity were calculated using standard formulas given in the APHA handbook. Then, based on P-alkalinity and M-alkalinity, bi-carbonate and carbonate were measured.

Sulfate was measured using a UV-Vis spectrophotometer. 8 mL of buffer solution (30 g magnesium chloride + 5 g sodium acetate + 1 g potassium nitrate + 20 mL acetic acid + 1000 mL

DI water) and 0.06 g barium chloride were added in 20 mL of DWW sample and stirred for one hour. After stirring solution was filtered, and OD was measured at 420 nm. DI water was utilized as a blank for OD measurement.

60 mL of DWW sample was added to 540 mL of aerated water. 300 mL- 300 mL transferred in two different BOD bottles. One bottle was kept in a BOD incubator for three days at 27 ^{o}C. Immediately, another bottle was used to measure the dissolved oxygen (DO). After three days, DO was measured for the bottle kept in a BOD incubator and tested for dissolved oxygen remaining. DO was measured by titration-based method. The sample was titrated against thiosulfate using the starch indicator.

In addition, the presence of possible heavy metals (Ni, Zn, Fe) in wastewater was investigated using atomic absorption spectroscopy (AA-7000, Shimadzu, Japan). The analysis mentioned above of DWW was conducted in duplicates.

3.3.2 Procurement of *H. stevensii* and inoculum preparation

The bacterial strain *H. stevensii* [KP 163920] was collected from the environment engineering lab of the Chemical Engineering Department, BITS Pilani, Pilani Campus, Rajasthan, India. The strain was isolated from the Sambhar Salt Lake, Rajasthan, India, and a detailed procedure for isolation and enrichment was reported by Mishra et al., (2017).

The minimal salt media (MSM) was prepared as the cultivation medium of bacteria by dissolving the following salts (g L^{-1}): K_2HPO_4 - 1, KNO_3 -1, NH_4Cl – 3 mM, and NaCl - 35 in two different aqueous mediums. Three different types of cultivation medium were prepared for the bio-fixation of CO_2 using *H. stevensii* (Table 3.4). The pH of the cultivation mediums was initially maintained at 10 using a stock solution of 1 M NaOH. The MSM prepared was then autoclaved and used in

further studies. The solid media for plating was prepared by adding 2 % (w/v) agar to the nutrient broth.

The nutrient broth containing peptone -5 g L^{-1}, beef extract -3 g L^{-1}, and NaCl -5 g L^{-1} dissolved in DI water was utilized to enrich bacterial culture. The inoculum was grown for 16 h at 37 ± 1 °C at 120 rpm. The purity of the grown culture was checked using the streaking method on nutrient agar plates. Freshly prepared inoculum with an optical density close to unity was used for conducting experiments. The optical density of the culture was measured at a wavelength of 600 nm ($OD_{600\ nm}$) using a UV-Vis spectrophotometer (Evolution 201, Thermo Scientific, USA) to determine the cell concentration.

3.3.3 Bioreactor setup

The suspended bioreactor has a working volume of 2 L and a headspace of 1 L. The reactor accessories include a control panel, air sparger, antifoam probe, pH probe, and impeller. The control of the bioreactor temperature, pH, and agitation speed was automatic. The buffer solutions at pH 4, 7, 10, and 12 were used to calibrate the pH meter. Gas cylinders with different gaseous compositions were connected to the inlet port of the bioreactor, consisting of a sparger at the bottom of the bioreactor. The schematic of the experimental setup of the bioreactor used in the present study is shown in Fig. 3.4, and the photograph of the semi-continuous bioreactor setup is shown in Fig. 3.5.

Table 3.4 Details of three different cultivation medium

Experiment Run No.	Cultivation medium	Aqueous medium	MSM (g L^{-1})	$Na_2S_2O_3$ (g L^{-1})	
				External	Total
1	DIW (100 mM $Na_2S_2O_3$)	Deionized water (DIW)	K_2HPO_4 - 1, KNO_3 -1, NH_4Cl - 0.160, NaCl - 35	24.50	24.50
2	DWW (100 mM $Na_2S_2O_3$)	Domestic wastewater (DWW)		22.05	24.50
3	DWW (no additional sulfate)	Domestic wastewater (DWW)		-	2.45

3.3.4 Experimental studies for bio-fixation of CO_2

The adaptability of bacterial species in the DWW environment was investigated by performing three experimental runs in duplicates (Table 3.4). The CO_2 bio-fixation experiments were performed in semi-continuous mode. 100 mL of the preliminary enriched culture having an OD of 1.25 ± 0.3 was used as the bacterium inoculum (section 3.3.2). A gas mixture comprising 10% of (v/v) CO_2 (g) and 90% of compressed moisture-free air (g) was utilized as a source of CO_2 (g) in the bioreactor. The gas mixture was supplied continuously with an aeration rate of 4 vvm through the gas inlet port of the bioreactor equipped with a sparger. The studies were performed for 6 days in the bioreactor programmed at 120 rpm and 37 ^{o}C. Various parameters such as carbonate ions, bicarbonate ions, optical density, pH, dry weight biomass, gaseous phase CO_2 (g) concentration, dissolved CO_2 (g) concentration, and CFU were measured in every 24 h. The control run was performed without the addition of inoculum to ensure that *H.stevensii* was solely responsible for the decrease in the concentration of CO_2 (g) at the outlet.

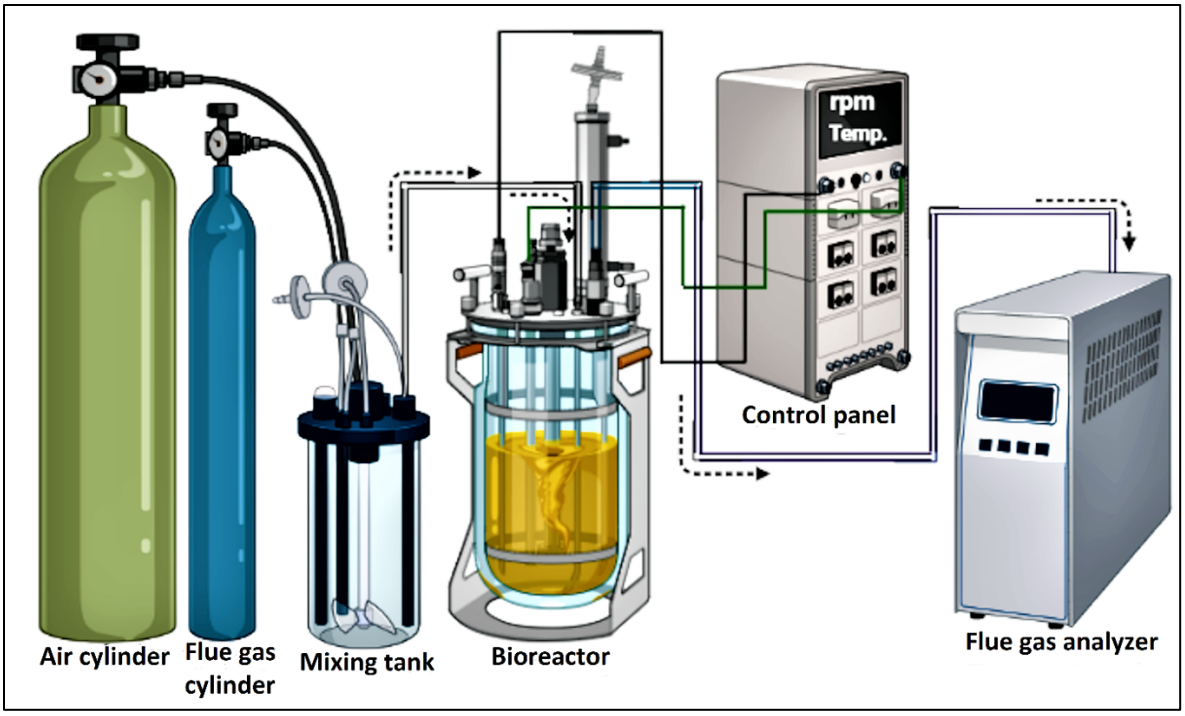

Fig. 3.4 Schematic diagram of semi-continuous bioreactor for the bio-fixation study of CO_2

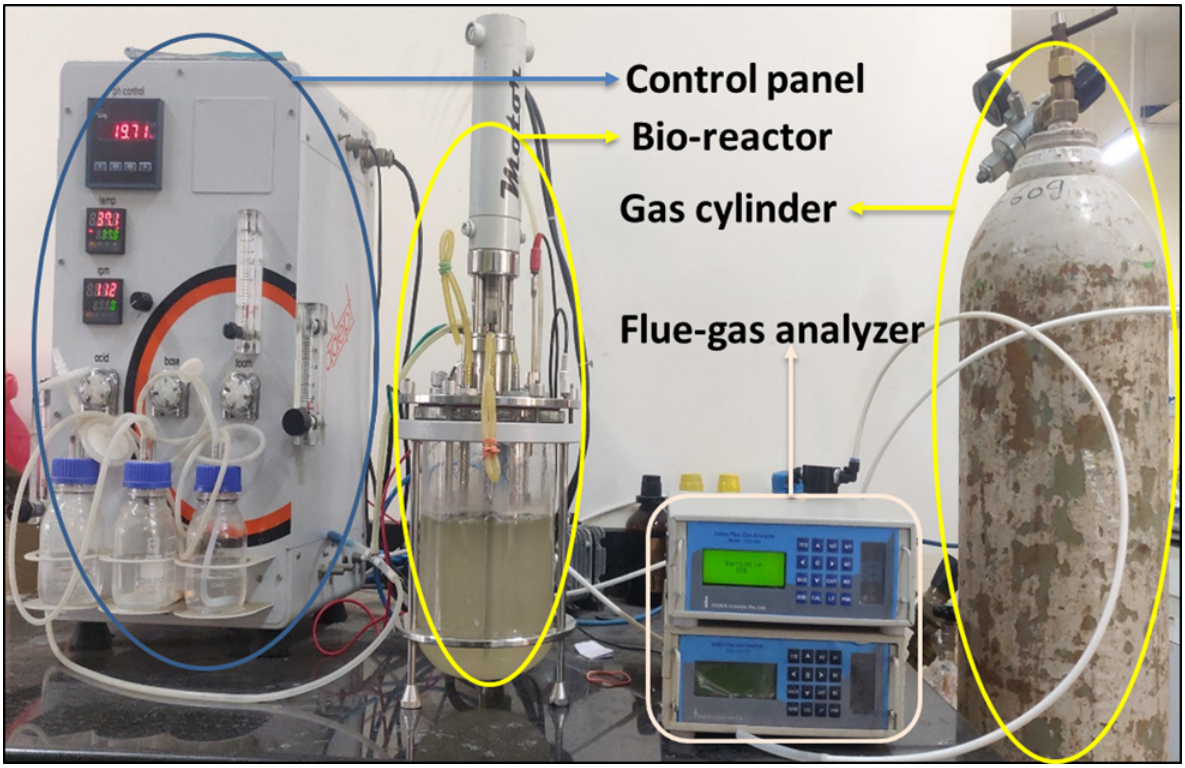

Fig. 3.5 The photograph of the semi-continuous bioreactor used for the CO_2 bio-fixation study

3.4 Flue gas (CO_2, NO, SO_2) bio-fixation using bacterial consortium

3.4.1 Microbial culture

3.4.1.1 Site selection

Bio-fixation of industrial flue gas demands mesophilic and/or thermophilic microorganisms. The extreme environment of Sambhar Salt Lake (SSL) satisfies the hour's need as microbes present in SSL can survive at a high temperature of 60 ^{o}C. In addition, the Sambhar Salt Lake is a natural habitat for halotolerant and halophilic microorganisms. Due to the habitat's high salinity, alkalinity, and thermophilic nature, SSL was chosen as a sample collection site for bacterial isolation.

In September 2019, soil and water samples were collected separately in sterile sample bottles from Sambhar Salt Lake, Rajasthan, India. The geographical coordinates of the lake are 26°58′N 75°05′E, and it is located 80 km (50 mi) southwest of the city of Jaipur and 64 km (40 mi) northeast of Ajmer, Rajasthan. The total salinity of the lake water ranges from 7% (w/v) to 35% (w/v) and has a pH value of 9.5 ± 2 (Pal et al., 2019; Sar et al., 2021; Upasani et al., 1990). Sambhar Lake's salinity significantly contributes to sulfates, carbonates, bicarbonates, chlorides, sodium, and potassium salts. The total suspended solids in the collected water sample range from 0.7 to 2.8% (w/v) (Joshi et al., 2011). The collected samples were kept at ambient temperature in the dark and were taken to the laboratory in autoclaved sample bottles. These samples were stored at 4 ^{o}C until further use.

3.4.1.2 Media preparation

The enrichment of bacterium culture from the Sambhar Salt Lake sample was carried out utilizing MSM prepared in distilled water that has the following composition (g L^{-1}): NaCl – 35, KNO_3 –

1, K_2HPO_4 – 1, NH_4Cl – 0.160, $Na_2S_2O_3$ – 24.50 (Mishra et al., 2017). 2 L of MSM prepared in distilled water was autoclaved. The pH value was found to be 9 ± 1.

The cultivation of bacterial consortium was done in MSM prepared in filtered DWW by dissolving the following salts (g L^{-1}): KNO_3 – 1, K_2HPO_4 – 1, NH_4Cl – 0.160, and NaCl – 35. The MSM was autoclaved at 121 ^oC and 15 psi for 15 min. in a vertical autoclave (MSW-101, Macro Scientific Works, India). The pH of the autoclaved cultivation media was found to be 8 ± 0.3. The solid media for plating was prepared as discussed in section 3.3.2.

3.4.1.3 Enrichment, isolation, and identification of bacterium species

The enrichment, isolation, and identification procedure of bacterium species is shown in Fig. 3.6. The water sample (20 mL) obtained from Sambhar Salt Lake was mixed thoroughly with 2 L of autoclaved MSM prepared in distilled water and transferred to a pH controlled 3 L capacity bio-reactor. The bacteria present in the water sample were grown inside the bio-reactor for the first 4 days in the presence of glucose (10 g L^{-1}) as a carbon source. Later, simulated flue gas containing 95% [CO_2 10% (v/v) + NO (750 ppm) + SO_2 (147 ppm) + rest N_2] + 5% air was provided continuously at an aeration rate of 0.25 vvm (0.5 L min^{-1}) via the gas inlet port for the next 3 days. The temperature and agitation speed inside the bio-reactor was maintained at 37 ^oC and 120 rpm, respectively. The optical density was measured daily at 600 nm with a UV-vis spectrophotometer (Evolution 201, Thermo Scientific, USA) to check the bacterial growth. The media without inoculum was used as a blank during the absorbance measurement. The viability of the bacterial culture was tested by estimating the grown culture's colony-forming unit (CFU). Bacterial culture acclimatized with flue gas and obtained after the 7^{th} day of study was utilized as inoculum for further studies. The culture was also used for species isolation and identification.

Morphologically two different bacterium species (SSLMC1 and SSLMC2) were observed in the culture and were isolated using the streak plate method. The plates of pure cultures were prepared and sent to Anuvanshiki sequencing, New Delhi, India, for amplification of 16S rRNA gene sequencing. The acquired sequence was compared with the other microbial sequences using the Basic Local Alignment Search Tool (BLAST-N) available at the National Center for Biotechnology Information (www.ncbi. nlm.nih.gov) and submitted to Gen-Bank. The closest match found in the pair-wise alignment in the BLAST result was used to determine the taxonomic affiliation of the chosen isolate. The phylogenetic tree was constructed using MEGA version 11.0 (64-bit) software using the Neighbor-Joining (NJ) method with 1000 bootstrap replicates and aligned using CLUSTAL-X.

3.4.2 Bioreactor setup

The detail of the suspended bioreactor utilized for the bio-fixation of flue gases (CO_2, NO, SO_2) is given in section 3.3.3.

3.4.3 Experimental studies

The main aim of this research work was the simultaneous bio-fixation of flue gases in a suspended bioreactor using a bacterial consortium isolated from the extreme environment of SSL. For the given purpose, a different combination of gases (CO_2, NO, and SO_2) were utilized for bio-fixation studies. The bio-fixation efficiency of the bacterial consortium in a semi-continuous mode was checked for the following six gas mixtures:

1) C: CO_2 10 % (v/v) balanced with moisture-free air
2) N: [NO (750 ppm) + rest N_2] 95% + Air (5%)
3) S: [SO_2 (150 ppm) + rest N_2] 95 % + Air (5%)
4) CN: [(CO_2 10% (v/v) + NO (750 ppm) + rest N_2] 95% + Air (5%)

5) CS: [(CO_2 10 % (v/v) + SO_2 (150 ppm) + rest N_2] 95 % + Air (5%)

6) CNS: [CO_2 10 % (v/v) + NO (760 ppm) + SO_2 (140 ppm) + rest N_2] 95 % + Air (5%)

All experiments were performed with MSM prepared in DWW without adding any external energy source (Fe(II), SO_3^{2-}). The aeration was carried with the compressed air and simulated gas. The details of experiments performed with different gas mixtures are represented in Fig 3.7. The respective gas mixture was supplied via a gas inlet port based on a 12 h aeration cycle at a 0.25 vvm aeration rate. The hydraulic retention time was estimated as 4 min, and the study was conducted for 192 h, except for N and CN gas mixture (168 h). The bioreactor was programmed at 120 rpm and 37 ^oC. 100 mL of the acclimatized enriched culture with the optical density (OD) of 1.1 ± 0.2 was used as the inoculum (Section 3.4.1.3). 50 mL sample was collected after every 12 h interval from the bioreactor, out of which 30 mL was used to estimate the dry weight of biomass. The same amount (50 mL) of MSM prepared in DWW was replenished after each sampling to maintain the constant volume inside the bioreactor. The parameters, such as carbonate, bicarbonate, nitrate, nitrite, sulfate, optical density, pH, dissolved CO_2 (l) concentration, and colony forming unit (CFU), were measured using standard techniques (section 3.5). The control run was carried out without inoculum to ensure that the decreased flue gas (CO_2, NO, and SO_2) concentration at the bioreactor outlet was due to bacterial activity.

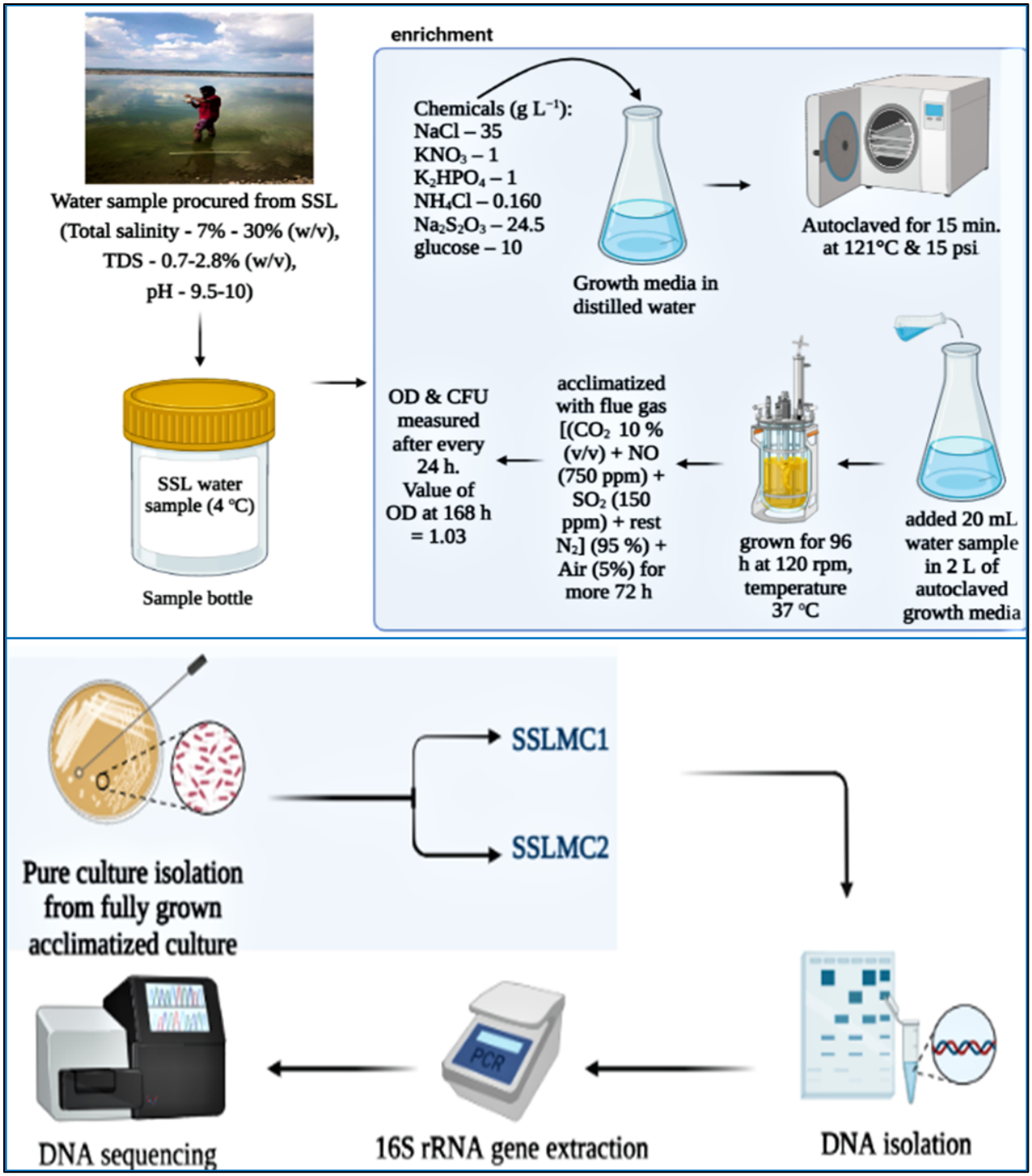

Fig. 3.6 Steps for enrichment, isolation, and identification procedure of bacterium species

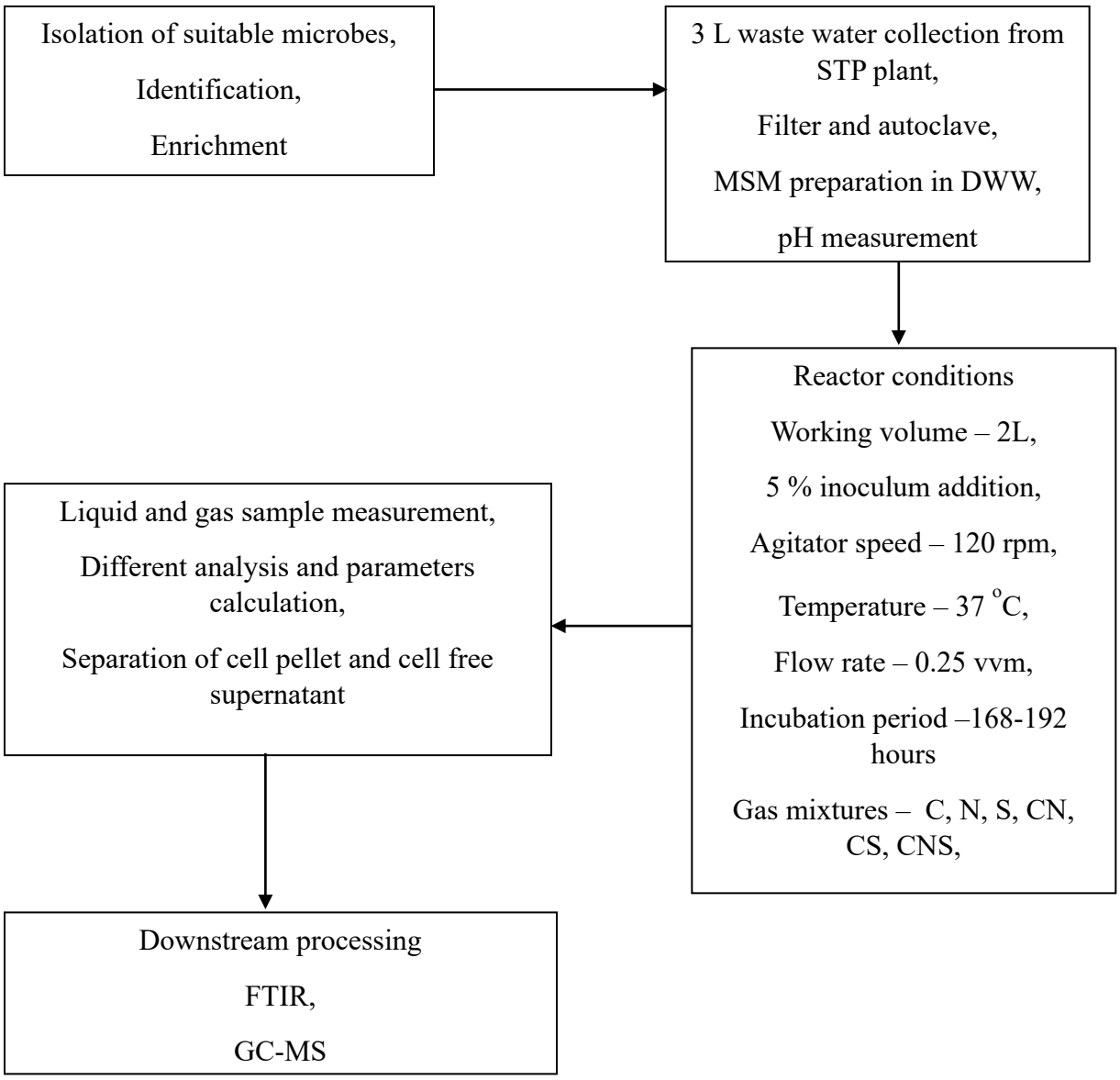

Fig. 3.7 Experimental studies for flue gas bio-fixation using bacterial consortium on semi-continuous mode

3.5 Analytical methods

The optical density was measured at 600 nm with a UV-Vis spectrophotometer (Evolution 201, Thermo Scientific, USA). The culture pH was measured with a digital pH meter (Eco Testr pH 2, Eutech Instruments, Thermo Scientific, USA). The concentration of dissolved CO_2 was measured using a dissolved CO_2 analyzer (Portable version, OxyGuard, USA). The concentration of carbonate, bicarbonate, sulfate, nitrite, and nitrate was measured using a standard protocol given in the APHA handbook (APHA, 2003). The colony forming unit (CFU) was calculated by the colony counter (DB-1246, Decibel Dynamics Ltd., India).

3.5.1 CO_2 (g), NO (g), SO_2 (g) measurement

The inlet and outlet gaseous phase CO_2 (g) concentration were measured using gas chromatography (GC) (Model: GC-2014, Shimadzu, Japan) for the bio-fixation of CO_2 using *H. stevensii* as per the procedure given in section 3.2.4.1.

The gaseous phase concentration of flue gas (CO_2, NO, and SO_2) at the inlet and outlet of the bioreactor was measured using a flue gas analyzer (Model: FGA 53X; make INDUS Scientific, Mumbai, India).

The gas phase analysis was performed to evaluate the CO_2 fixation efficiency of *H. stevensii* and flue gas (CO_2, NO, and SO_2) bio-fixation by bacterial consortium. The fixation efficiency was evaluated using Eq. 3.8 (Chen et al., 2016).

$$\eta_{gas} = \frac{y_{gas,in} - y_{gas,out}}{y_{gas,in}} \times 100\% \quad (3.8)$$

where, $y_{gas,in,}$ and $y_{gas,out}$ are the initial and final concentrations of gases, respectively.

3.5.2 Biomass growth measurement

The biomass growth rate of the bacterium culture was estimated in terms of the optical density (absorbance) and dry weight (g L^{-1}). A total of 30 mL of microbial suspension was filtered through an oven-dried, pre-weighed 0.22 µm GF/C Whatman cellulose membrane filter, dried at 50 °C, and then re-weighted to calculate the biomass dry weight (DW, g L^{-1}). The calibration curve of optical density OD and the dry weight of biomass (g L^{-1}) was drawn for all studies and obtained mathematical co-relations are given in Table 3.5.

The biomass productivity (P_{max}, g L^{-1} d^{-1}) and the specific growth rate (μ, d^{-1}) were derived using Eqs. 3.9 and 3.10, respectively (Barahoei et al., 2020).

$$P_{max} = \frac{(X_t - X_o)}{t_1 - t_0} \tag{3.9}$$

Where, X_{to} is the concentration of biomass (g L^{-1}) at the beginning (t_o), and X_{t1} is the concentration of biomass (g L^{-1}) at the end of the cultivation period (t_1), respectively.

$$\mu_{max} = \frac{\ln(X_{t1}) - \ln(X_{t0})}{t_1 - t_0} \tag{3.10}$$

The fixation rate of CO_2 (g) (R_{CO_2}, g L^{-1} d^{-1}) was calculated using Eq. 3.11.

$$R_{CO_2} = C_c \; P_{max} \; \frac{M_{CO_2}}{M_c} \tag{3.11}$$

Where, M_{CO_2} and M_C are the molecular weight of CO_2 and the atomic weight of carbon, respectively. The carbon content C_c is taken as 0.34, obtained using the typical molecular formula ($C_6H_{12}O_7N$) of microbial biomass (Rittmann, 2012).

The fixation rate of NO (g) (R_{NO} g L^{-1} d^{-1}) was calculated using Eq. 3.12.

$$R_{NO} = Nc \; P_{max} \; \frac{M_{NO}}{M_N} \tag{3.12}$$

Where, M_{NO} and M_N is the molecular weight of NO and the atomic weight of nitrogen, respectively. The nitrogen content N_c is taken as 0.12, obtained using microbial biomass's typical molecular formula ($C_5H_7O_2N$) (Rittmann, 2012).

Actual utilization efficiency (R. R_{gas}) of different gases was derived using Eq. 3.13.

$$utilization\ efficiency = \frac{fixation\ rate\ of\ gas}{gas_{in}\ rate} \times 100 \quad (3.13)$$

3.5.3 Nutrient utilization

The concentrations of nutrients were measured at the end of the incubation period. The samples obtained post-incubation were centrifuged at 10,000 rpm for 20 min. at 4°C. The supernatant obtained after centrifugation was filtered through a 0.22 µm cellulose membrane filter. The filtrate obtained was utilized to analyze different nutrient concentrations such as COD, BOD, NO_3^-, PO_4^{3-}, NO_2^- and SO_4^{2-} using standard protocols (section 3.3.1). The percentage utilization and the rate of utilization of nutrients were derived using Eqs. 3.14 and 3.15 (Nayak et al., 2016b; Bhowmick et al., 2019).

$$Nutrient\ removal\ (\%) = 100\ (\frac{C_o - C_i}{C_o}) \quad (3.14)$$

$$Rate\ of\ nutrient\ utilization\ \ (mg\ d^{-1}L^{-1}) = \frac{C_o - C_i}{\Delta t} \quad (3.15)$$

Where, C_o and C_i are the average values of concentrations of nutrients at the beginning and the end of the cultivation period, respectively. Δt represents the cultivation period in days.

3.6 Product analysis

3.6.1 Biomass harvesting and product recovery

The cultures (2 L) collected from the bio-fixation process were utilized for biomass harvesting and product recovery. The experimental procedure followed for biomass harvesting and product recovery is shown in Fig. 3.8. The collected cultures after incubation were centrifuged at 10,000

rpm for 20 min at 4 °C. The recovered supernatants were kept at 4 °C for subsequent product recovery. The biomass collected from the centrifugation process was utilized for cell lysis. Chloroform and methanol (2:1 v/v) as solvents were used to recover the products from the cell pellet. After the addition of solvent into the biomass, it was subjected to phase separation in the orbital incubator shaker for 2-3 h at 120 rpm and 37 °C. The separating funnel was used to separate the organic phase (extract). The separated organic phase (lipids) was concentrated on a rotary evaporator (R-210, BUCHI, Switzerland) and shifted to a pre-weighed glass test tube. The obtained thickened sample was filtered and preserved at 4 °C for Gas Chromatography-Mass Spectrometry (GC-MS) analysis. The products from the supernatant were extracted with a similar methodology followed for cell lysate. The obtained cell lysate and supernatant from biomass harvesting were utilized for Fourier-transform infrared spectroscopy (FT-IR) analysis.

3.6.2 FT-IR analysis

The obtained cell lysate and cell-free supernatant were utilized for FT-IR analysis. The possible functional groups prevailing in the cell lysate and cell-free supernatant from all the studies were determined using FT-IR (Model – Frontier, Perkin Elmer, India) equipped with Attenuated Total Reflectance (ATR) accessory (GladiATR, PIKE Technologies, Inc.). The cell lysate and supernatant were converted to powder form by a freeze-drying process using a lyophilizer (Cool safe55, Scanvac). FT-IR was performed by placing dried powdered samples onto the ATR crystals with a resolution of 4 cm^{-1} in the spectral range of 400–4000 cm^{-1} (Mishra et al., 2018). The FT-IR analysis of all samples was performed in duplicates.

Table 3.5 Mathematical co-relation obtained for dry weight and optical density for different gas mixtures

S.No.	Gaseous mixtures	Mathematical cor-relation	R^2 value
1	C	DW = 8.7688 OD + 0.2634	0.9053
2	S	DW = 13.576 OD + 0.0276	0.9627
3	N	DW = 6.4997 OD + 0.4321	0.9122
4	CS	DW = 7.8879 OD – 0.3309	0.9292
5	CN	DW = 13.390 OD – 1.1515	0.9487
6	CNS	DW = 11.944 OD – 1.5685	0.9011

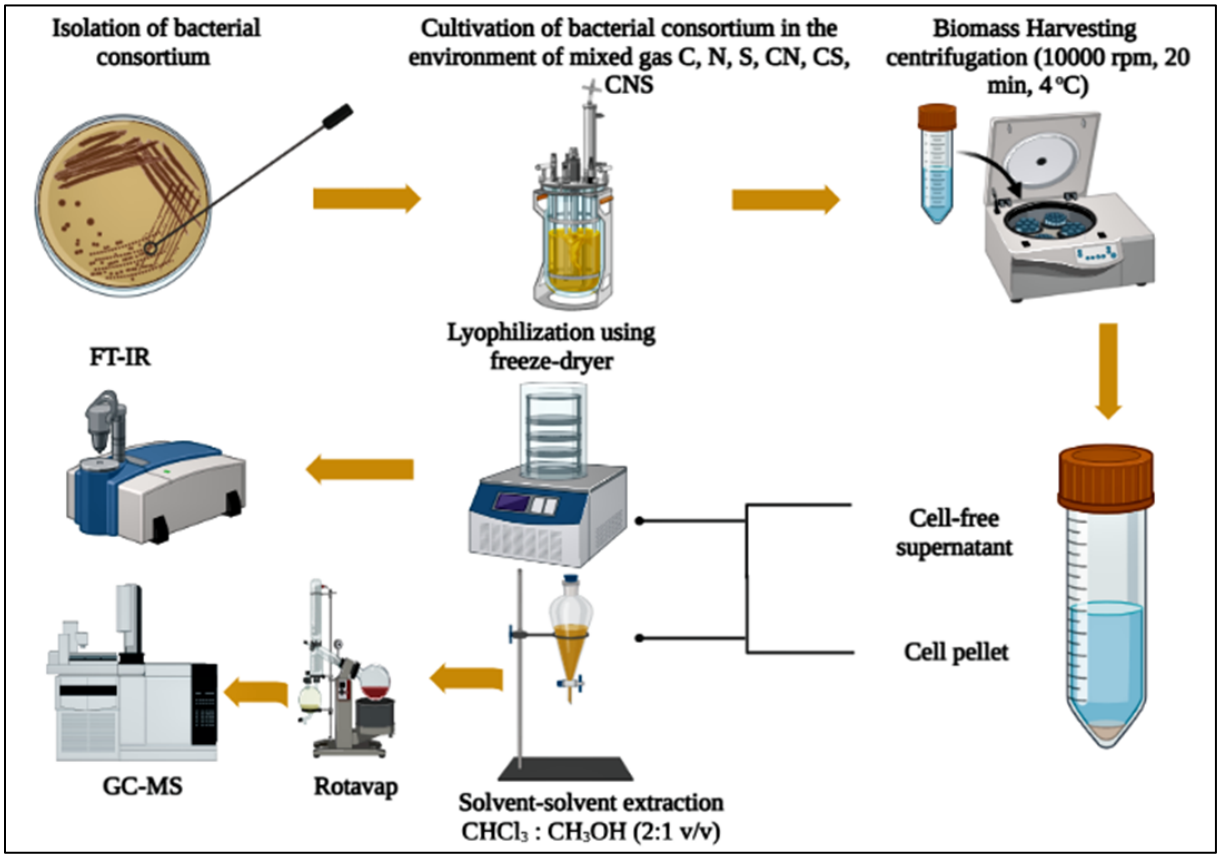

Fig. 3.8 Flow sheet for biomass harvesting and product recovery used during semi-continuous studies

3.6.3 GC-MS analysis

The thickened samples of cell lysate and cell-free supernatant were subjected to Gas chromatography-mass spectroscopy (GC-MS) analysis (QP-2010 Plus, Shimadzu, Japan) to identify value-added products produced during bio-fixation of gaseous components. The details of operating conditions for GC-MS analysis are given in Table 3.6. The column name DB-5 MS has a film thickness of 0.25 µm, an internal diameter of 0.25 mm and a length of 30 m was used. The carrier gas (Helium) was used at a flow rate of 1.21 mL min^{-1}. The initial and final column temperature was set as 80 ^oC and 250 ^oC, respectively. The column temperature increased at a rate of 10 ^oC min^{-1}. The GC-MS interface and ion source temperatures were 280 ^oC and 110 ^oC. The MS operating conditions were scan mode, start m/z 40.00, end m/z 650, scan speed 1250 and event time 0.5 s. The initial and final analysis were 5 min and 35 min, respectively. The obtained data were compared with the inbuilt standard mass spectra library system (NIST-05 and Wiley-8) of GC-MS.

3.7 Approximate material balance

The material balance in the existing system can be helpful in theoretically estimating the actual amount of CO_2 and NO assimilated as carbon and nitrogen into biomass. The actual CO_2 and NO utilization efficiency of microorganisms can be further calculated using the given carbon and nitrogen balance. The material balance in a semi-continuous batch reactor system considers the unutilized gas, which is present in gaseous form, dissolved gas and the gas exiting the reactor continuously. It also considers the amount of gas utilized by microorganisms which are assimilated as biomass. $M_{C_{in}}$, $M_{N_{in}}$, $M_{C_{go}}$and $M_{N_{go}}$ was calculated using the ideal gas law.

To calculate the actual utilization of carbon and nitrogen by the microorganism, the carbon and nitrogen material balance in the bio-reactor were carried out using Eq. 3.16 and Eq. 3.17, respectively:

$$M_{C_{in}} = M_{C_{go}} + M_{C_{bo}} + Dissolved\ C\ as\ (aq)\ CO_2 \quad (3.16)$$

$$M_{N_{in}} = M_{N_{go}} + M_{N_{bo}} + Dissolved\ N\ as\ (aq)NO \quad (3.17)$$

Where, $M_{C_{in}}$ and $M_{N_{in}}$ is the mass of carbon and nitrogen input as CO_2 and NO, respectively, $M_{C_{go}}$ and $M_{N_{go}}$ are carbon and nitrogen left in the gaseous phase as CO_2 and NO, respectively, at the end of the cultivation period, and $M_{C_{bo}}$ and $M_{N_{bo}}$ carbon and nitrogen are assimilated as biomass.

The material balance for sulfur was not calculated as sulfur is utilized as an energy source in the form of sulfate ions.

Table 3.6 Different operating conditions for the GC-MS study

Operating parameters	Operating conditions
Column Name	DB-5 MS
Column Film Thickness	0.25 μm
Column Internal Dia.	0.25 mm
Column Length	30 m
Carrier Gas	Helium (He)
Pressure	86.5 kPa
Flow Rate	1.21 mL min^{-1}
Split Ratio	10
Column Temperature (Initial, Final, Rate)	80 °C, 250 °C, 10 °C min^{-1}
GC-MS Interface Temperature	280 °C
Ion Source Temperature	110 °C

Chapter 4

Results and Discussion

This chapter describes the results of CO_2 bio-fixation studies using *Desmodesmus* sp. at different CO_2 concentrations [0.03%, 5%, 10% (v/v)], bio-fixation of CO_2 using *H. stevensii* in three different cultivation media, and flue gas fixation using bacterial consortium in MSM prepared in DWW. The products formed during CO_2 bio-fixation studies using *Desmodesmus* sp. were analyzed by estimating total carbohydrates, proteins, and lipids. The value-added products formed during bio-fixation of CO_2 using *H. stevensii* in three different cultivation media and flue gas fixation using bacterial consortium in MSM prepared in DWW were analyzed using downstream processing strategies. This chapter of the thesis presents the findings of these experiments.

The parts of results from this work have been published in Sustainability journal -: https:// doi.org/10.3390/su13179882 and Journal of Environmental Chemical Engineering -: https://doi.org/10.1016/j.jece.2021.105116.

4.1 CO_2 fixation using *Desmodesmus* species

The semi-continuous studies analyzed the growth performance of *Desmodesmus* sp. for 12 days, for three different CO_2 concentrations, 0.03%, 5%, and 10% (v/v), in a loop photobioreactor. The obtained results from these studies have been analyzed and summarized in the following sections.

4.1.1 Effect of CO_2 concentrations on gaseous phase fixation efficiency

CO_2 (g) was continuously measured at the gas outlet port of the photobioreactor, and CO_2 fixation efficiency on an alternate-day basis was calculated using Eq. 3.1 and is represented in Fig. 4.1 for two different CO_2 concentrations (5% and 10%). A significant increase in gaseous phase fixation efficiency was observed on the initial days (2 days) of bioreactor operation at both CO_2 concentrations. This may be due to the fact that the media pH was maintained at 10 at the start of the bio-fixation process, and CO_2 has higher solubility in water at higher media pH. Hence, a significant amount of gaseous phase CO_2 was initially utilized to maintain the equilibrium CO_2 concentration in the liquid phase. The gaseous phase CO_2 (g) fixation was nearly constant after day four. The fixation efficiency for 5% CO_2 concentration is more than that for 10% CO_2 concentration, which may be due to the higher initial CO_2 concentration. The excess CO_2 would escape from the photobioreactor (Barahoei et al., 2020). The maximum gaseous phase fixation efficiencies were obtained as 85.69% and 61.72% in the case of 5% and 10% initial CO_2 concentration, respectively. The CO_2 fixation efficiency for 0.03% CO_2 (ambient air) inlet concentration was not measured as the whole amount of CO_2 was utilized during the process.

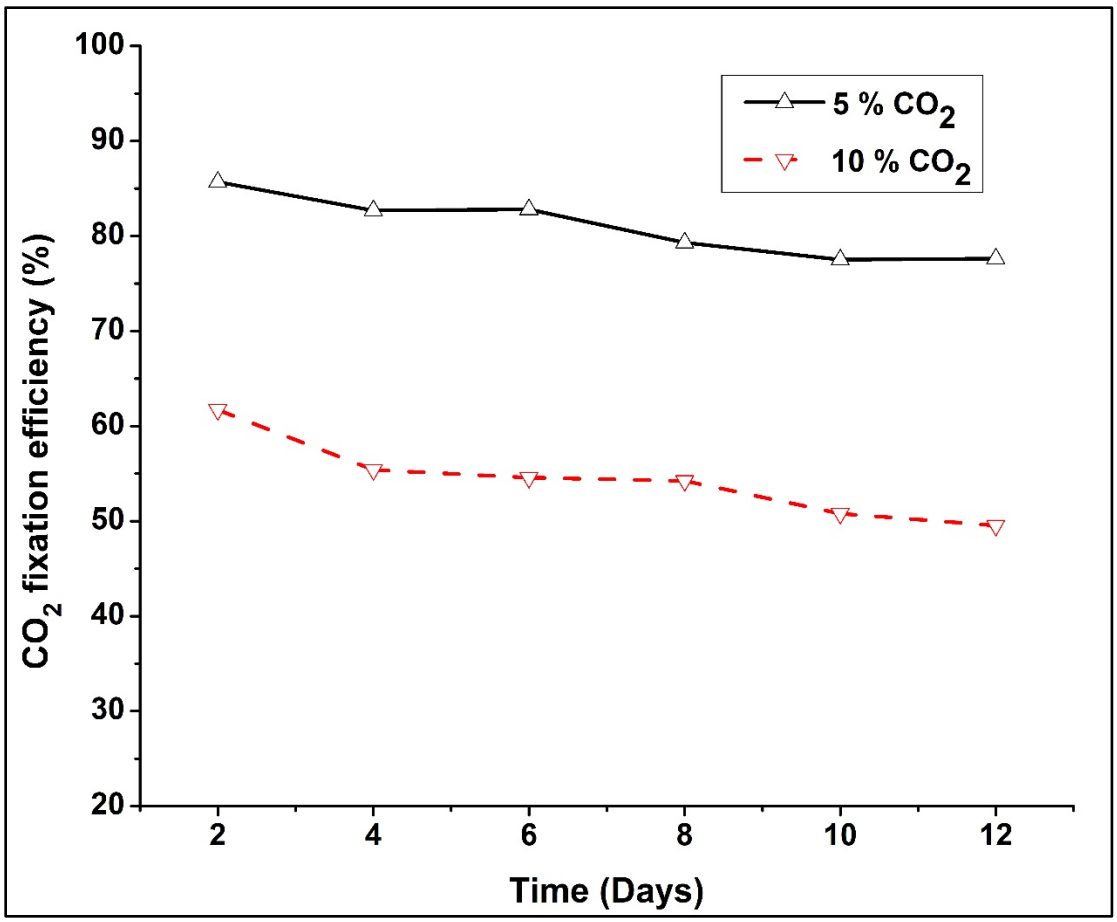

Fig. 4.1 CO_2 (g) fixation efficiency at the outlet of reactor for 5 and 10% initial CO_2 concentration

4.1.2 Effect of CO_2 Concentration on biomass growth rate and optical density

Desmodesmus sp. growth performance in the presence of different CO_2 concentrations (0.03%, 5%, and 10% v/v) was examined in a loop photobioreactor and obtained results are presented in Fig. 4.2. The microalgae showed a short lag phase of 1 to 3 days, which indicated the suitability of gaseous CO_2 fixation by *Desmodesmus* sp. as a carbon source. The trend shows increased growth in the exponential phase for ten days at different concentrations of CO_2 due to the presence of the appropriate amount of nutrients for cell growth in the reactor.

After 12 days of incubation, culture supplemented with 10% (v/v) CO_2 showed 1.903 ± 0.038 g L^{-1} of cell concentration on a dry cell weight (DCW) basis, which is higher as compared to the culture grown at 0.03% of CO_2 v/v (0.96 ± 0.039 g L^{-1}) and 5% CO_2 v/v (1.219 ± 0.040 g L^{-1}). The cell concentration in cultures supplied with 5% CO_2 and 10% CO_2 was higher than the cultures with ambient air conditions, suggesting that CO_2 as a carbon source facilitated the microalgae growth (Bligh and Dyer, 1959; Yadav et al., 2015). A similar trend was reported for CO_2 fixation in precious reported studies (Kaiwan-arporn et al., 2012; Wang et al., 2014).

The results are also plotted to understand the light and dark cycle (L/D cycle) on biomass growth rate in terms of optical density (OD_{650nm}) at three different CO_2 concentrations and are given in Fig 4.3. The values of optical density were measured twice a day in 12 h intervals (Widdel, 2010). The maximum OD values were obtained during the light cycle as 0.60 ± 0.017, 0.81 ± 0.016, and 1.99 ± 0.010 and during the dark cycle as 0.56 ± 0.016, 0.57 ± 0.017, and 1.76 ± 0.009 at 0.03% CO_2, 5% CO_2, and 10% CO_2 concentrations, respectively. The increased absorbance values during the light cycle compared to the dark cycle confirmed that the photosynthesis process is enhanced during the day and microalgal growth is better during the light period. The increase in the biomass concentration values during the day cycle is due to the increased cell growth which is greatly

dependent on the sunlight intensity (Chae et al., 2006). The photosynthetic efficiency of microalgae at intermittent illumination is to be higher as compared to continuous illumination, provided that the parameters of the L/D cycle are tuned correctly (Xue et al., 2011; Chiarini et al., 2021). This may be because photosynthesis is a cyclic process, where a slower thermochemical process follows almost instantaneous photochemical reactions.

4.1.3 Effects of CO_2 concentration on growth kinetic parameters

4.1.3.1 Specific growth rate

The specific growth rate (μ) of the algal culture was measured using Eq. 3.3. The maximum value of μ_{max} was obtained as 0.15 ± 0.004 d^{-1} when algal cells were grown with 10% inlet CO_2 concentration. The specific growth rate was observed to be 0.07 ± 0.002 d^{-1} and 0.13 ± 0.003 d^{-1} at 0.03% and 5% inlet CO_2 concentration, respectively (Fig. 4.4). The marginal difference in the value of μ was observed when CO_2 concentration changed from 5% to 10%. The possible reason behind this could be the presence of adequate amount of nutrients for cell growth in 10% inlet CO_2 concentration. These results are as per the reported results in earlier studies (Toledo-Cervantes et al., 2013; Wang et al., 2014).

4.1.3.2 Biomass productivity

The concentration of CO_2 significantly influences the productivity of biomass. The biomass productivity was estimated for all three inlet concentrations and is shown in Fig. 4.4. It was observed that with the increase in CO_2 concentration from 0.03% to 10%, the biomass productivity value was increased from 0.018 ± 0.002 g L^{-1} d^{-1} to 0.185 ± 0.004 g L^{-1} d^{-1}. The higher availability of carbon source in 10% CO_2 concentration may be the possible reason for the increase in biomass productivity. These findings are consistent with values obtained by different studies (Tang et al., 2011; Toledo-Cervantes et al., 2013).

4.1.3.3 CO_2 fixation rate

The CO_2 fixation rate was calculated using Eq. 3.4. It was observed that the higher rate of bio-fixation of CO_2 (0.33 ± 0.004 g L^{-1} d^{-1}) was achieved when microalgae were cultured at 10% inlet concentration of CO_2 (Fig. 4.4). The CO_2 fixation rates were obtained as 0.01 ± 0.001 g L^{-1} d^{-1} and 0.15 ± 0.003 g L^{-1} d^{-1} for 0.03% and 5% of CO_2 concentration, respectively. These results are supported by the work carried out by different researchers (Chiang et al., 2011; Wang et al., 2014).

4.1.4 CO_2 utilization efficiency

Fig. 4.5 shows the utilization efficiency of CO_2 calculated using Eq. 3.5 at three different concentrations of CO_2. The CO_2 utilization efficiency was obtained as 0.06 % and 0.04 % for 5% and 10 % inlet concentration of CO_2, respectively. This indicates that the lower CO_2 concentration is more favourable for the utilization of CO_2 by *Desmodesmus* sp. The portion of the injected CO_2 may not have been used efficiently by the *Desmodesmus* sp. Therefore, at a higher CO_2 level (i.e., 10% CO_2 concentration in this study), the excess CO_2 would escape from the photobioreactor, causing less carbon capturing (Barahoei et al., 2020).

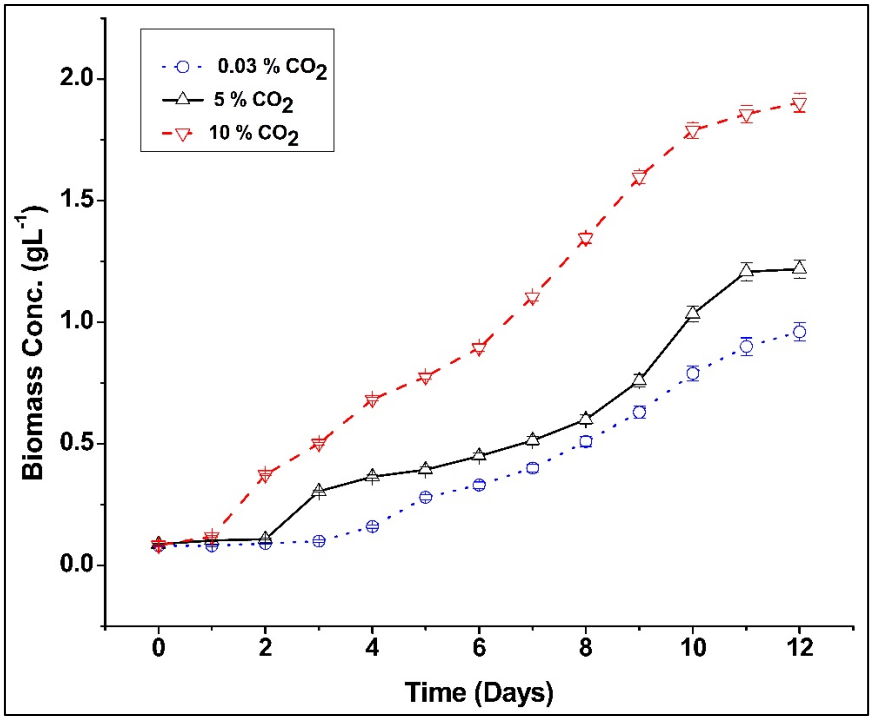

Fig. 4.2 Effect of time on cell concentration (g L^{-1}) at three different CO_2 concentrations

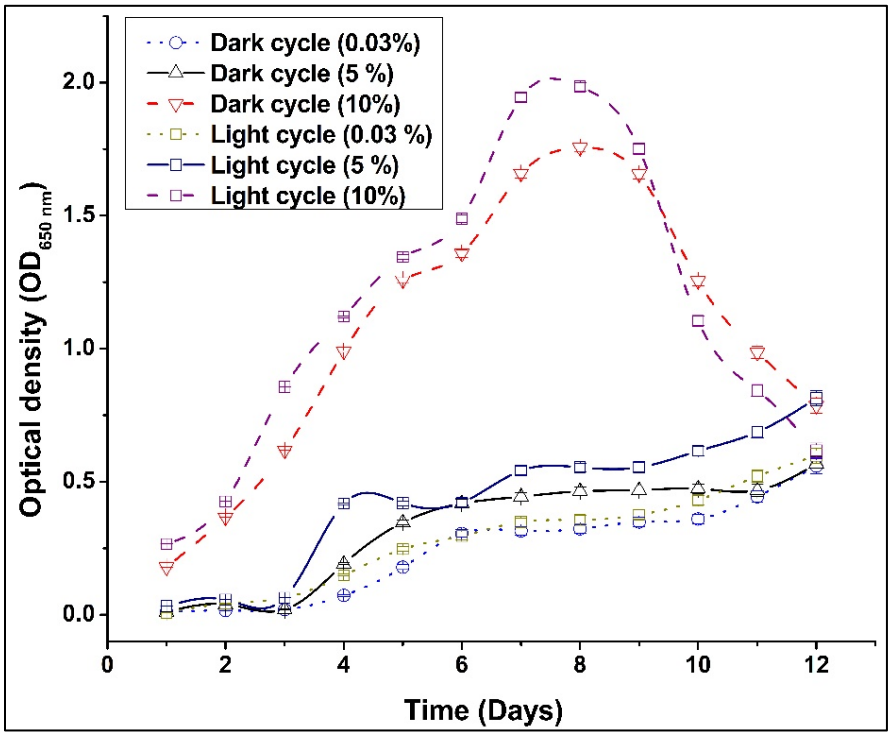

Fig. 4.3 Effect of light and dark cycle on optical density (OD) with respect to time for three different CO_2 concentrations

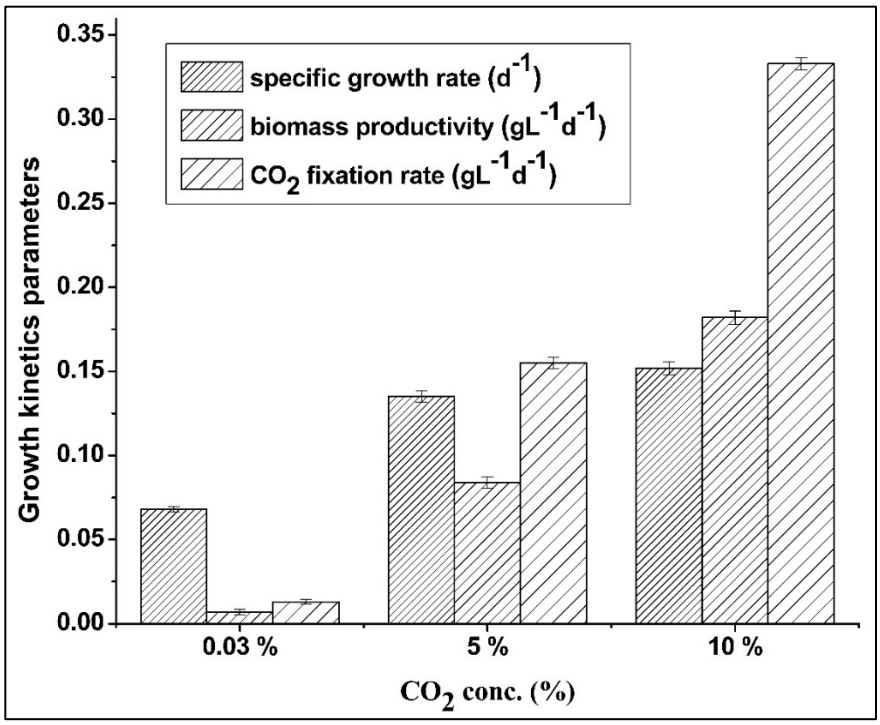

Fig. 4.4 Effect of three different CO_2 concentrations (0.03%, 5%, and 10% v/v) on the different growth kinetic parameters

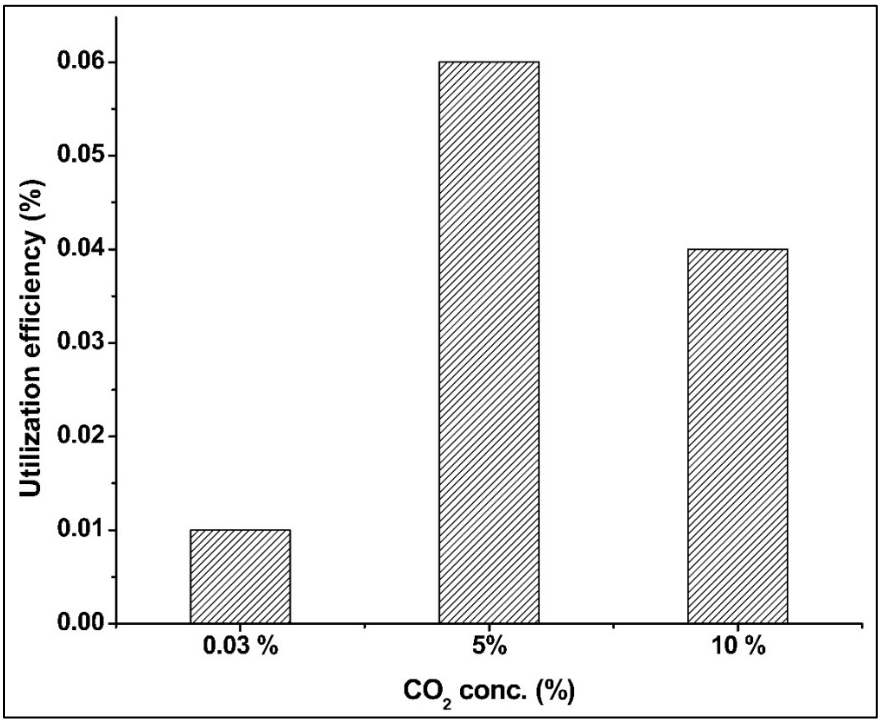

Fig. 4.5 Effect of different CO_2 concentrations (0.03 %, 5 % and 10 % v/v) on CO_2 utilization efficiency

4.1.5 Effect of CO_2 concentration on biochemical composition of *Desmodesmus* sp.

The content of lipids, total carbohydrates, proteins, and chlorophyll was estimated as macromolecular composition in the form of percentages of the total dry biomass (DCW) at three different CO_2 concentrations (0.03%, 5%, and 10% v/v). The concentration of CO_2 has a significant impact on the carbohydrate (CHO) content of microalgae (Lowry et al., 1951). The carbohydrate content of microalgae was observed as 14.6 ± 1.5%, 17.2 ± 2.0%, and 20.7 ± 2.4% of DCW at 0.03%, 5%, and 10% CO_2 (v/v) concentration, respectively (Table 4.1). The carbohydrate content in the algal biomass was significantly increased with an increase in CO_2 concentration. The different stages of growth and varying concentration of CO_2 have a greater impact on the total content of carbohydrates in the harvested algal biomass. The higher content of carbohydrates opens the possibility for further utilization of algal biomass as a substrate.

The maximum protein content of 32.3 ± 2.5% DCW was obtained when algal cells were cultivated at 10% CO_2 concentration. The protein content of 14.4 ± 1.2% and 25 ± 1.1% was obtained for algal cells at 0.03% and 5% CO_2 concentration, respectively (Table 4.1). The higher cell concentration with an increase in CO_2 concentration significantly increases the efficiency of the photosynthesis period which leads to the formation of more and more amounts of protein.

The lipid content in algal biomass was observed to increase with CO_2 concentration (Table 4.1). The maximum amount of lipid, about 42 ± 1.0% DCW, was accumulated at 10% CO_2 concentration. The lipid content was obtained as 15.5 ± 0.5% and 40 ± 2.0% for inlet CO_2 concentrations of 0.03% and 5%, respectively. The scarcity of nitrogen and phosphorus due to their continuous utilization in microalgae cultivation may be the reason for the higher lipid content (Yang et al., 2020).

The concentration of Chl a and Chl b were estimated using Eqs. 3.6 and 3.7, respectively, at 0.03%, 5%, and 10% (v/v) inlet CO_2 concentrations. Chl a and Chl b concentration varies from 0.12 ± 0.001 to 0.14 ± 0.004 mg L^{-1} and 0.15 ± 0.002 to 0.19 ± 0.005 mg L^{-1} with the increase in inlet CO_2 concentration from 0.03% to 10%, respectively (Table 4.1). The maximum amount of Chl a and Chl b was 0.14 ± 0.004 mg L^{-1} and 0.19 ± 0.005 mg $L^{-1,}$ respectively, at 10% CO_2 concentration (Table 4.1). It was observed that Chl a content is less than Chl b for all inlet CO_2 concentrations. This may be due to the fact that the chlorophyll content in the microalgae varies in response to physical and chemical factors such as light intensity, agitation, temperature, and nutrient availability (Martinez et al., 2000; Chinnasamy et al., 2009). In the present study, the microalgae species, *Desmodesmus* is a genus of green algae in the family of *Scenedesmaceae*. In green algae, Chl b absorbs energy from wavelengths of green light at 640 nm, which may be a possible reason for a higher content of Chl b in *Desmodesmus* sp. The concentration of Chl a indicates the quantity and capacity of photosynthesis activity of microalgae. It can also be used to assess the physiological state of microalgae.

4.1.6 Performance comparison of loop photobioreactor

Table 4.2 shows the comparison of the performance of the custom-designed loop photobioreactor with other reactors at different scales (bench, pilot, and large) in terms of the parameters such as biomass productivity (g L^{-1} d^{-1}), CO_2 fixation rate, and biochemical compositions (carbohydrate, protein, and lipid content) for CO_2 fixation via algal species. The maximum biomass produced (1.903 ± 0.038 g L^{-1}), biomass productivity (0.19 ± 0.004 g L^{-1} d^{-1}), and CO_2 fixation rate (0.33 ± 0.004 g L^{-1} d^{-1}) at 10% CO_2 concentration are higher or nearly the same as compared to the values reported by previous studies (Table 4.2). The carbohydrate (20.7 ± 2.4%) and protein (32.3 ± 2.5%) content obtained in the present study at 10% CO_2 concentration are comparable with the

values reported for previous studies. However, the lipid content (42 ± 1.0%) is maximum compared to the studies reported in the literature. The reactor scale of 8 L (working volume) by Sydney et al. (2010), erlenmeyer flask (0.650 L) by Tang et al. (2011), tubular batch reactor (0.660 L) by Kargupta et al. (2015) and cylindrical PBR (15 L) by Ye et al. (2018) mitigated 10-15% CO_2 concentration is showing comparable biomass produced ~1.903 g L^{-1} for the present work with 10% CO_2 concentration and 26 L reactor working volume. The comparative study of raceway pond (1000 L) with *Desmodesmus* sp. and airlift bioreactor (200 L) with *Porphyridium cruentum* shows the maximum biomass produced of 1.9 g L^{-1} and 3 g L^{-1}, respectively. The loop bioreactor indicated the possibility of further scale-up of the process for the large-scale fixation of CO_2 and simultaneous algal biomass production, leading to by-product formation. This study may be a viable solution for the source reduction of CO_2 generated from waste management systems. The higher biomass productivity and carbohydrate content may lead to the value addition of the process in biofuels as a by-product formation.

Table 4.1 Biochemical compositions of *Desmodesmus* sp. in the form of percentages of the total dry biomass (DCW) at three different CO_2 concentrations for 12 days of cultivation time

Biochemical composition	Inlet concentration of CO_2 (v/v)		
	0.03%	5%	10%
Total carbohydrates (% DCW)	14.6 ± 1.5	17.2 ± 2.0	20.7 ± 2.4
Proteins (% DCW)	14.4 ± 1.2	25 ± 1.1	32.3 ± 2.5
Lipids (% DCW)	15.5 ± 0.5	40 ± 2.0	42 ± 1.0
Chl a (mg L^{-1})	0.12	0.13	0.14
Chl b (mg L^{-1})	0.15	0.17	0.19

Table 4.2. Performance comparison of loop bioreactor in terms of various parameters with reported studies

Species	*Cultivation Time (Day)*	*Mode (Volume, L/Working Volume, L)*	*CO_2 conc. (% v/v)*	*Biomass Produced (X_{Max}) (g L^{-1})*	*Biomass Productivity (P) (g L^{-1} d^{-1})*	*CO_2 Fixation Rate (R_{CO2}) (g L^{-1} d^{-1})*	*Carbohy-drate (% DCW)*	*Protein (% DCW)*	*Lipids (% DCW)*	*References*
Chlorella sp.	8	Column Photobioreactors, (0.8)	2	1.21	0.15	0.28	-	-	-	(Chiu et al., 2008)
Chlorella vulgaris	15	Bio Flow fermenter, (11/8)	10	1.94	0.13	0.25	16.74	40.95	9.95	(Sydney et al., 2010)
Scenedesmus obliquus	6	Erlenmeyer flask, (0.650)	10	1.84	0.15	0.29	-	-	22	(Tang et al., 2011)
Chlorella sorokiniana	8	Airlift photobioreactor, (1.4)	4	1.1	0.15	-	-	-	20.93	(Kumar et al., 2014)
Scenedesm-us sp.	7	Airlift photobioreactor, (0.5)	2.5	1.3	0.19	0.35	10.4	-	35.6	(Nayak et al., 2016a)
Scenedesm-us sp.	7	Bubble-column photobioreactor, (0.5)	2.5	1.37	0.196	0.37	-	-	33.3	(Nayak et al., 2016b)
Acutodesm-us sp.	5	Erlenmeyer flasks, (0.5/0.2)	20	1.65	-	-	34.52	38.78	11.67	(Yadav et al., 2015)
A. quadrice-llulare	6	Laboratory scale photobioreactor, (0.8/0.680)	5	1.29	-	-	33.4	30.3	44	(Varshney et al., 2018)

Desmodesmus sp. MCC34	18	Raceway pond, (1000)	-	1.9	-	-	-	-	0.103	(Nagappan et al., 2016)
Porphyridium cruentum	-	Airlift tubular, (200)	-	3.0	1.50	-	-	-	-	(Yen et al., 2015)
Chlorella sorokiniana	-	Inclined tubular, (6.0)	5	1.50	1.47	-	-	-	-	(Ugwu et al., 2002)
Arthrospira platensis	-	Undular row tubular, (11)	-	-	2.70	-	-	-	-	(Carlozzi, 2003)
Haematococcus pluvialis	16	Bubble-column, (55)	-	1.4	0.06	-	-	-	-	(Lopez et al., 2006)
Chlorella pyrenoidosa	1.25	Tubular batch reactors, (0.660)	10		0.11	0.096	-	-	-	(Kargupta et al., 2015)
Chlorella PY-ZU1	4.5	Cylindrical PBR (6)	15	-	0.47	0.87	-	-	-	(Ye et al., 2018)
Desmodesmus sp.	12	Loop photobioreactor, (34/26)	0.03	0.96 ± 0.04	0.018 ± 0.002	0.013 ± 0.001	14.6 ± 1.5	14.4 ± 1.2	15.5 ± 0.5	Present study
Desmodesmus sp.	12	Loop photobioreactor, (34/26)	5	1.219 ± 0.04	0.084 ± 0.003	0.155 ± 0.003	17.2 ± 2.0	25 ± 1.1	40 ± 2.0	Present study
Desmodesmus sp.	12	Loop photobioreactor, (34/26)	10	1.903 ± 0.04	0.185 ± 0.004	0.333 ± 0.004	20.7 ± 2.4	32.3 ± 2.5	42 ± 1.0	Present study

The CO_2 bio-fixation using *Desmodesmus* species was studied in a custom-designed loop photobioreactor. The utilization of microalgae for CO_2 fixation is a well-studied research area. However, due to the slower growth rate of microalgae, the utilization of bacterial species got the attention of researchers as it can overcome the limitations of microalgae-based systems. The rapid growth rate and ability to withstand high concentrations of CO_2 by bacterial route got extensive attention in the last decades for the bio-fixation of CO_2. So, the possibility of bacterial species *H. stevensii* was explored for CO_2 bio-fixation. The organic and inorganic compounds present in DWW can be utilized as nutrients and energy sources by bacteria. So, the utilization of DWW for cultivation media preparation was explored in further studies.

4.2 CO_2 bio-fixation using *H. stevensii*

The semi-continuous studies analyzing the growth performance of *H. stevensii,* for the duration of 6 days, in the presence of 10% (v/v) CO_2 (g) concentration and different cultivation mediums (Table 3.4) were carried out in a laboratory scale bioreactor (Figs. 3.4 and 3.5). The obtained results from these studies were analyzed and are discussed in the subsequent sections.

4.2.1 Wastewater analysis

The sewage treatment plant (STP) entails using physical, chemical, and biological processes to remove contaminants such as organic compounds, inorganic compounds, and heavy metal ions from wastewater. The wastewater collected from the sewage treatment plant was analyzed for the different physio-chemical properties (section 3.3.1). The water quality parameters for domestic wastewater were estimated and are represented in Table 4.3. Data presented in the following table is the average of duplicates ± standard deviation (SD). DWW contains various nutrients and ions, such as nitrate, nitrite, phosphate, ferrous and sulfate ions in the significant amount which could be utilized by the bacterial species as nutrient and energy sources for their growth.

4.2.2 Biomass growth and CO_2 (g) bio-fixation rate in different cultivation medium

The biomass was observed to grow continuously for the overall incubation period in all three cultivation mediums (Table 3.4) at 10% inlet CO_2 concentration. The CO_2 (g) was continuously measured at the gas outlet port of the reactor and CO_2 fixation efficiency on the per day basis was calculated and is represented in Fig. 4.6 for all three cultivation mediums. The significant increase in gaseous phase fixation efficiency was observed on the first day of bioreactor operation. This may be because the solution pH was maintained as 10 at the start of the bio-fixation process and at higher solution pH, CO_2 has higher solubility in water. Hence, initially major amount of gaseous phase CO_2 was utilized to maintain the equilibrium CO_2 concentration in liquid phase. After one day, the gaseous phase CO_2 (g) fixation was observed as nearly constant. The maximum and minimum gaseous phase fixation efficiency were obtained as 18.77% and 17.79% in the case of DWW (100 mM $Na_2S_2O_3$), 18.58% and 16.30% in the case of DIW (100 mM $Na_2S_2O_3$) and 17.48% and 13.8% with DWW (no additional sulfate), respectively. The reason for nearly constant removal efficiency could be due to the higher gas flow rate (4 vvm) and hence, the change in the gaseous phase concentration of CO_2 may not be significant.

The biomass growth of *H. stevensii* in terms of dry weight (g L^{-1}) was measured for all cultivation medium conditions and is shown in Fig. 4.7. The maximum biomass concentration was found to be 7.72 g L^{-1} in the case of DIW (100 mM $Na_2S_2O_3$), 6.71 g L^{-1} in the case of DWW (100 mM $Na_2S_2O_3$) and 5.31 g L^{-1} with DWW (no additional sulfate). The cultivation medium with no external addition of sulfate source has shown the lowest value of biomass produced may be due to the less availability of sulfate ions. The inherently present sulfate ions might have been consumed by the bacteria after the initial days of cultivation and hence, the biomass produced was less as compared to other two culture medium. The availability of the energy substrate and the growth of

microbes were observed to be directly related to the amount of CO_2 (g) adopted by the cellular biomass concentration (Mishra et al., 2018). The existence of the adequate amount of energy and carbon substrate has shown a continuous rise in biomass concentration. The CO_2 utilization efficiency in the case of DWW (100 mM $Na_2S_2O_3$) was found to be 13.90%. However, cultivation media DWW (no additional sulfate) showed the CO_2 utilization efficiency was found to be 11.70% which is comparable with the result of DWW (100 mM $Na_2S_2O_3$). The utilization efficiency in both the cases of DIW (100 mM $Na_2S_2O_3$) and DWW (100 mM $Na_2S_2O_3$) was found to be equal and suggested that DIW could be replaced by DWW. Hence *H. stevensii* can be cultivated in the DWW without any considerable change in the efficiency of the process.

The bio-kinetic parameters such as maximum biomass concentration (g L^{-1}), maximum specific growth rate (μ_{max}), maximum biomass productivity (P_{max}), maximum CO_2 fixation rate and CO_2 (g) utilization efficiency (RR_{CO2}) were estimated and are presented in Table 4.4. The culture supplemented with DIW (100 mM $Na_2S_2O_3$) showed the sustained growth for the overall period of cultivation. The total biomass concentration after the six-day of the study was found to be maximum (7.72 g L^{-1}) with the μ_{max}, P_{max}, R_{CO2}, and η_{CO2} value of 1.02 d^{-1}, 2.83 g $L^{-1}d^{-1}$, 3.52 and 13.90%, respectively. The biomass productivity, specific growth rate and CO_2 (g) fixation rate in the case of DIW (100 mM $Na_2S_2O_3$) were maximum on the second day of the run whereas, in the other two cases, these parameters were maximum on the first day of the run. The possible reason for this may be the naturally available nutrients and bi-carbonate ions present in the DWW. The presence of bi-carbonates in the cultivation medium might help to grow the bacteria as it is very easy to utilize. Therefore, a higher value of μ_{max} and P_{max} were observed as 1.37 d^{-1} and 3.14 g $L^{-1}d^{-1}$, respectively in the case of DWW (100 mM $Na_2S_2O_3$). This study suggested the possible

utilization of DWW in place of DIW for the preparation of cultivation medium and providing the possible simultaneous solution of CO_2 fixation and wastewater treatment.

The change in the pH, bicarbonates, and carbonates for all three cultivation mediums with time were plotted and are shown in Figs. 4.8 and 4.9. The pH was decreased from 10 to 6.6, 7.0, and 7.1 for DIW (100 mM $Na_2S_2O_3$), DWW (100 mM $Na_2S_2O_3$) and DWW (no additional sulfate), respectively, after one day. At higher pH, OH^- ions present in water reacts with aqueous CO_2 to form bicarbonate ions. The lower utilization of bicarbonates by *H. stevensii* during first day and a higher rate of formation of carbonic acid may be the reason for the decrease in pH value of cultivation mediums (Bong et al., 2001). Further, the pH of the medium was increased from 6.8 to 7.2, 7.4 to 7.6 and 7.1 to 7.2 for DIW (100 mM $Na_2S_2O_3$), DWW (100 mM $Na_2S_2O_3$) and DWW (no additional sulfate), respectively at the end of the second day. This might be due to the increase in the utilization rate of HCO_3^- with time by *H. stevensii* (Mishra et al., 2018). Later, no significant changes were observed in the pH value of all three cultivation mediums.

The variation in free CO_2 (l) concentrations at various time intervals of cultivation for different cultivation mediums is shown in Fig. 4.10. During the initial period of cultivation (0-2 days), the amount of dissolved CO_2 in aqueous phase was higher due to less utilization of CO_2 by microbial species. For 2-5 days, change is minimal due to higher utilization of dissolved CO_2 by microbes and at the last cultivation day (5-6 days), again the amount of aqueous phase CO_2 increased due to low utilization of CO_2 as the biomass growth decreased.

Table 4.3 Characteristics of DWW used in the experiments

Parameters	Concentrations
$N–NO_3$ (mg L^{-1})	28.98 ± 1.5
$N–NO_2$ (mg L^{-1})	1.1 ± 0.4
$P–PO_4$ (mg L^{-1})	2.6 ± 0.1
Cl^- (mg L^{-1})	179 ± 4
BOD (mg L^{-1})	362 ± 8
COD (mg L^{-1})	3176 ± 36
SO_4^{2-} (mg L^{-1})	463.84 ± 8
Ni (mgL^{-1})	0.258 ± 0.01
Zn (mgL^{-1})	0.237 ± 0.02
Fe (II) (mgL^{-1})	0.021
DO (ppm)	5.5 ± 0.2
Salinity (ppm)	1.097 ± 0.1
TDS (ppm)	0.073
Conductivity (millisemens cm^{-1})	1.363 ± 0.01
HCO_3^- (mgL^{-1})	0
CO_3^{2-} (mgL^{-1})	600 ± 25
OH^- (mgL^{-1})	600 ± 25

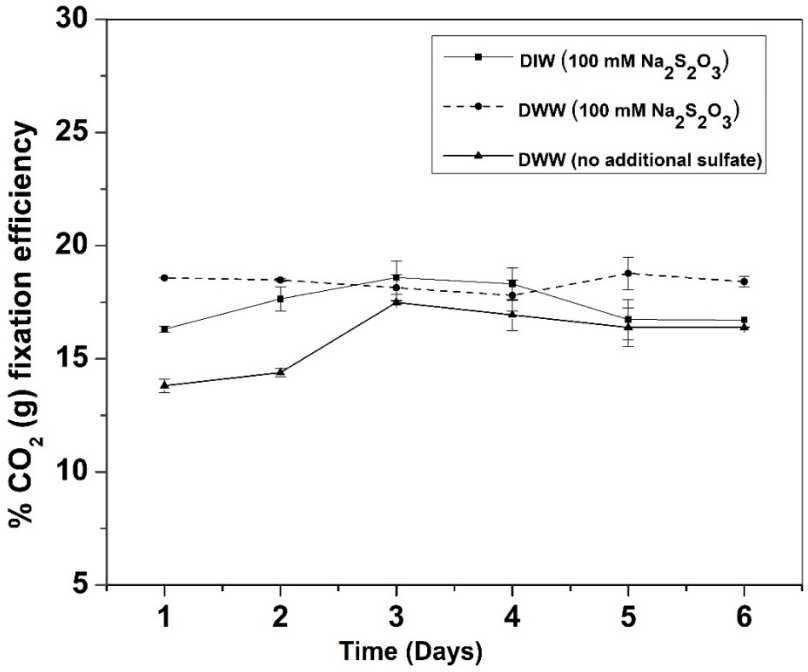

Fig. 4.6 CO_2 (g) fixation efficiency per day at the outlet of reactor in each case

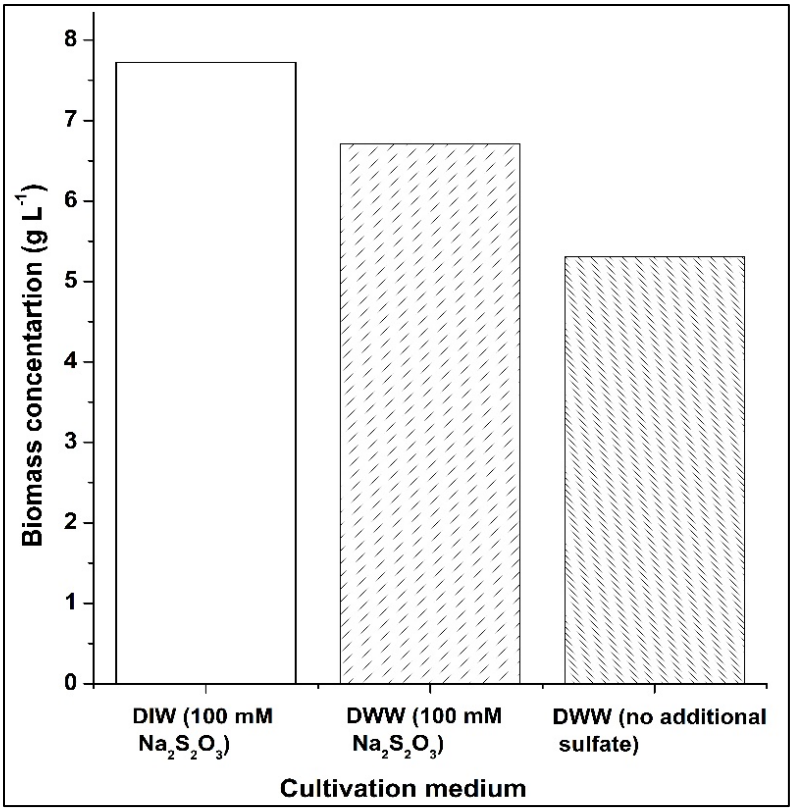

Fig. 4.7 Concentration of biomass obtained at different cultivation medium

Table 4.4 Comparison of biomass yield, maximum biomass concentration, specific growth rate, biomass productivity, CO_2 (g) fixation rate and CO_2 (g) utilization efficiency for different cultivation mediums used in the study

Parameters/culture conditions	Synthetic media		
	DIW (100 mM $Na_2S_2O_3$)	DWW (100 mM $Na_2S_2O_3$)	DWW (no additional sulfate)
Maximum biomass Concentration (g L^{-1})	7.72	6.71	5.31
Maximum specific growth rate (d^{-1})	1.02 (day 2)	1.37 (day 1)	1.19 (day 1)
Maximum biomass Productivity (g $L^{-1}d^{-1}$)	2.83 (day 2)	3.14 (day 1)	3.24 (day 1)
Maximum CO_2 (g) fixation rate (g $L^{-1}d^{-1}$)	3.52 (day 2)	3.92 (day 1)	4.04 (day 1)
CO_2 (g) utilization efficiency (%)	13.90	13.90	11.70

There is an increasing trend for HCO_3^- for first four days for DIW (100 mM $Na_2S_2O_3$) and then it was found to decrease (Fig 4.8). The concentration of HCO_3^- was found to increase for first two days for DWW (no additional sulfate) and then got decreased on third day and remained stationary for the last three days. While HCO_3^- concentration by DWW (100 mM $Na_2S_2O_3$) showed more or less the similar trend as that of DIW (100 mM $Na_2S_2O_3$). The amount of bi-carbonate ions is directly related to CO_2 fixation efficiency. At day one of the cultivation period, there is a substantial increase in bicarbonate ion and fixation efficiency values. The possible reason behind this may be the higher solubility of CO_2 that leads to the formation of more amount of bicarbonate ions. After 3rd day, there is no noticeable change in bi-carbonate ions as the CO_2 fixation efficiency values reached to steady state.

However, the concentration of CO_3^{2-} was observed to get nearly constant after the initial days of study and was found to increase slowly towards the end. This can be substantiated by the pH dependency of carbonate alkalinity formation. At pH value of approximately 8, it showed more bicarbonate alkalinity and less carbonate alkalinity. With a decrease in pH value, the bicarbonate alkalinity was found to increase, due to which there was less concentration of carbonates in comparison to bicarbonates in the present case. At very low pH values or at highly acidic conditions, there was more formation of CO_2 alkalinity, which was found to decrease with an increase in pH (Mishra et al., 2018).

4.2.3 Nutrient utilization capacity at varying cultivation conditions

The removal efficiency and removal rate of various nutrients such as NO_3^-, Cl^-, PO_4^{3-}, COD, BOD and SO_4^{2-} by *H. stevensii* at different cultivation conditions was determined after sixth day of the cultivation period (Table 4.5). The elimination capacity of NO_3^-, Cl^-, PO_4^{3-} was obtained in the range of 95–99.5% for all cultivation conditions. The sulfate elimination capacity of *H. stevensii*

in the cases of DWW (100 mM $Na_2S_2O_3$) and DIW (100 mM $Na_2S_2O_3$) was found to be more than 99% and with DWW (no additional sulfate) was found to be 18.18%. Low sulfate (energy source) removal in case of DWW (no additional sulfate) could be due to the lesser microbial activity and hence, lesser utilization of sulfate ions. The nitrate and the chloride ions consumption was found to be nearly equal in all cases (more than 95%). The concentration of nutrients present in effluent streams after treatment was found to be well below the discharge limit norms of the country. Hence, these results confirmed the survival of *H.stevensii* in domestic wastewater. The higher values of obtained BODs are 66.5% and 55.5% as reported in the case of DWW (100 mM $Na_2S_2O_3$) and DWW (no additional sulfate) in comparison to the DIW (100 mM $Na_2S_2O_3$). This may be due to the fact that DWW naturally has more amount of organic matter, unlike DIW. Hence, the oxygen required to degrade the organic matter should be more in case of wastewater, which is in agreement with the obtained results. The percentage removal of COD was found to be highest as 17.2% in case of DWW with 100 mM sulfate ions. The results obtained for the significant removal of organic and inorganic substances confirmed that *H. stevensii* can be utilized for wastewater purification along with CO_2 fixation.

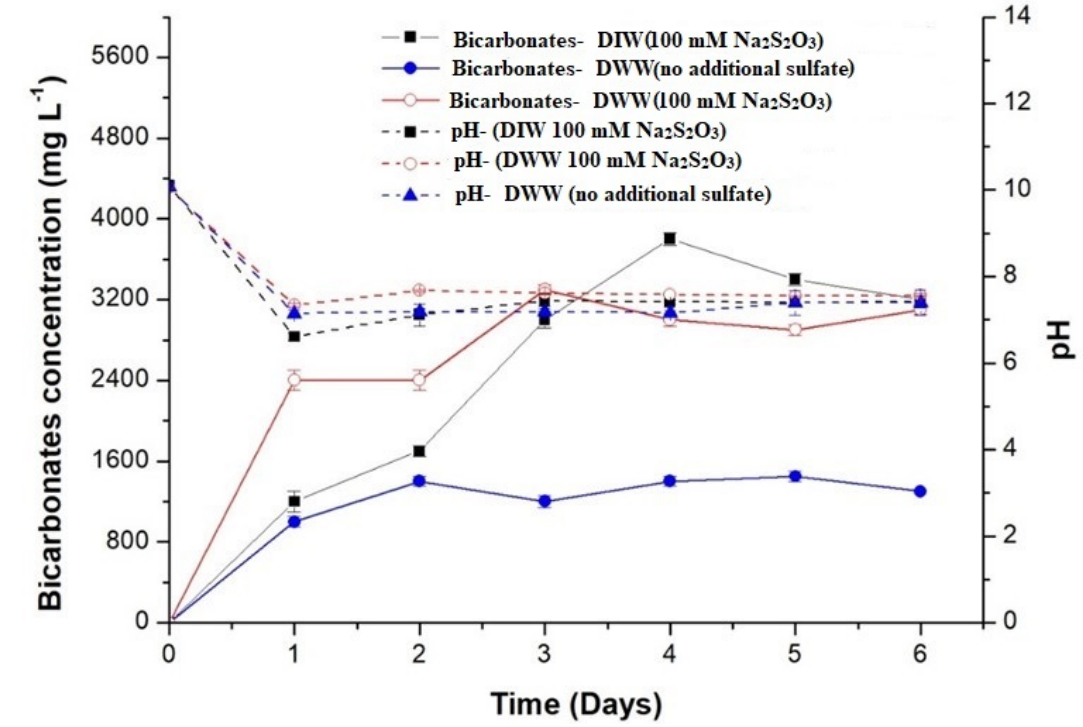

Fig. 4.8 Concentration of bicarbonates and pH at different time intervals

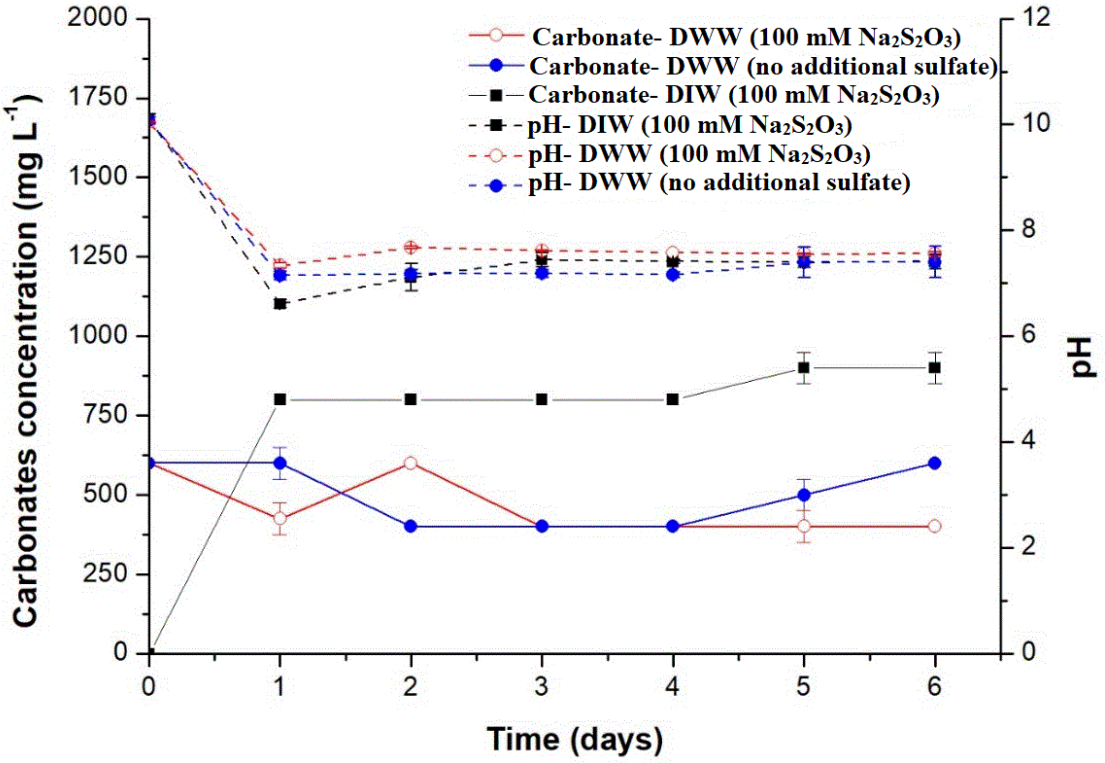

Fig. 4.9 Concentration of carbonates and pH at different time intervals

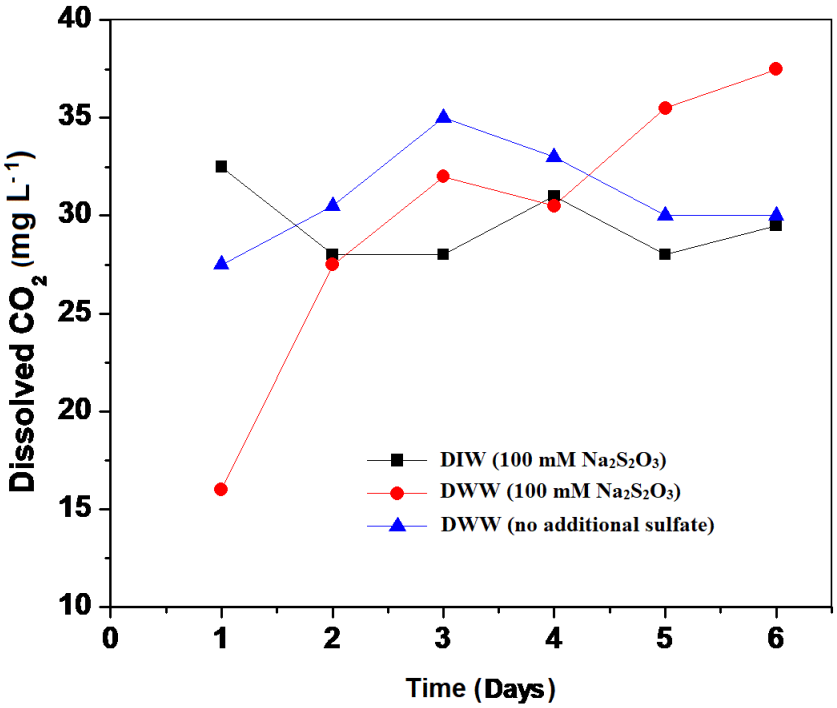

Fig. 4.10 Dissolved CO_2 (g) concentration at different time

Table 4.5 Percentage removal efficiency of various organic and inorganic parameters at the end of the study

Parameters	Initial concentration (mg L^{-1})	Cultivation conditions					
		Removal efficiency (%)			Nutrient removal rate g L^{-1} d^{-1}		
		DIW (100 mM $Na_2S_2O_3$)	DWW (100 mM $Na_2S_2O_3$)	DWW (no additional sulfate)	DIW (100 mM $Na_2S_2O_3$)	DWW (100 mM $Na_2S_2O_3$)	DWW (no additional sulfate)
$N–NO_3$	28.98 ± 1.5	98.73	98.82	99.21	10.20	10.23	10.37
$P–PO_4$	2.6 ± 0.1	98.72	98.49	99.19	0.16	0.17	0.16
Cl^-	179 ± 4	95.6	99.6	95.4	5.58	5.81	5.57
SO_4^{2-}	463.84 ± 8	99.9	99.9	18.18	1600	1600	0.02
BOD	362 ± 8	11.05	66.5	55.5	0.01	0.04	0.03
COD	3176 ± 36	7.36	17.2	7.2	0.04	0.09	0.04

4.2.4 Carbon balance

The total amount of carbon provided to the system was estimated based on the difference of inlet and outlet concentration of CO_2 (g) using ideal gas law and was estimated as 203.8 g. The concentration of CO_2 (g) at the outlet of the bioreactor was measured regularly every 24 h. The time-weighted average of the outlet percentage CO_2 (g) was then multiplied with the total CO_2 (g) supplied as carbon into the system to calculate the total amount of carbon leaving the system as gaseous CO_2 (g). The total amount of carbon present in the liquid phase was in the form of bicarbonates and carbonates ions along with total carbon consumed and is equal to the amount of carbon assimilated as biomass and extracellular products. The results are summarized and are shown in Table 4.6. The difference in LHS and RHS came out in the range of 12.32–16.38 g after substituting these values in Eq. 3.16. This may be due to the assimilation of some amount of carbon in the fatty acids and alcohols as extracellular products and their presence was confirmed by FTIR and GC-MS.

4.2.5 CO_2 fixation mechanism

One of the approaches of CO_2 fixation mechanism by bacterial route is elaborated in the earlier study. Primarily the CO_2 fixation mechanism is discussed with the autotrophic organisms impacting the carbon cycle globally. The plants are considered as primary producers for long time and hence, de novo, the reductive pentose phosphate cycle or rPP cycle is directly linked with photosynthesis. The light is essential for CO_2 fixation, and it suggests that all photosynthetic microorganisms follow rPP pathway to fix CO_2. However, Sergei Winogradsky (founder of modern microbiology) discovered that autotrophy via rPP cycle is also carried out by energy harnessed from inorganic molecules as electron donors, process which is an example of chemolithoautotrophy (Dworkin, 2012). It has been understood that there are five CO_2 fixation pathways other than rPP cycle, which are discovered for CO_2 fixation by microorganisms in nature.

These comprised of (1) the Wood–Ljungdahl Pathway (WLP, operated by acetogens to convert CO_2:H_2, CO or other C1 feedstock's into Acetyl-CoA) (2) the reductive (or reverse) tricarboxylic acid pathway (3) the dicarboxylate 4-hydroxybutyrate pathway (4) 3-hydroxypropionate/4-hydroxybutyrate or HP/HB cycle and (5) the 3-hydroxypropionate bicycle pathway (Berg, 2011; Fuchs, 2011; Saini et al., 2011). One of the study discusses how bacteria was found to utilize arsenic as electron donor for fixing CO_2 in the form of HCO_3^- to the biomass (Oremland et al., 2017). The different studies have suggested the fixation of CO_2 and its distribution in cytosolic pool by bacterium in the absence of light utilizing electron donor as energy substrate (Santoro et al., 2013; Kwon et al., 2015; Dyksma et al., 2016). Thus, CO_2 fixation utilizing electron donor as energy substrate is possible. Hence in the present study, it can be understood that CO_2 is getting accumulated into the cytosolic pool of bacterial species *H. stevensii* by harnessing the energy of thiosulfate ion $S_2O_3^{2-}$. The GC-MS analysis suggested the significant presence of hydrocarbons and fatty alcohols in all the samples.

4.2.6 Comparison with existing literature

The performance of *H. stevensii* for CO_2 fixation in the present work was compared with the performance of the reported studies. The values of maximum biomass produced (X_{max}) (g L^{-1}), maximum biomass productivity (P_{max}) (g L^{-1} d^{-1}) and maximum CO_2 fixation rate (R_{CO2}) (g L^{-1} d^{-1}) at different concentration of inlet gases reported in literature are summarized in Table 4.7. The X_{max}, P_{max} and R_{CO2} are obtained in the range of 7.7–1.3 g L^{-1}, 3.92–1.55 g L^{-1} d^{-1} and 4.01–0.12 g L^{-1} d^{-1}, respectively for different microalgae and cyanobacteria species. The values of X_{max}, P_{max} and R_{CO2} for all three cultivation conditions DIW (100 mM $Na_2S_2O_3$), DWW (100 mM $Na_2S_2O_3$), and DWW (no additional sulfate) used in the present study are found to be more than the results obtained from the reported studies. The maximum CO_2 fixation rate (R_{CO2}) is found to be in the

range of 3.75 ± 0.3 which is higher than the previous work for the *H. stevensii* and lower than the values estimated for *Chlorella vulgaris* and *Scenedesmus* strains of algae.

The higher air flowrate, higher CO_2 tolerance, potential to grow in wastewater along with better CO_2 (g) fixation ability of *H. stevensii* can make it a viable technique for the simultaneous fixation of CO_2, wastewater treatment and production of valuable chemicals which indicates the feasibility for the overall concept of bio-refinery.

4.2.7 Techno-economic assessment

The feasibility of the proposed process was evaluated by carrying out the techno-economic assessment for replacing DIW with DWW as a cultivation media in the laboratory and pilot scale process and is discussed in the subsequent sections. The cost analysis was mainly based on the operating cost by considering the fact that cost associated with manpower, bioreactor and maintenance can be same for the process operation for all cultivation media.

The costs of chemicals, different types of water and CO_2 were taken from HiMedia and Merck catalogue (2018–2019) (Robert et al., 1997; Grima et al., 2003), respectively for the laboratory scale process and are given in Table 4.8. The operating cost for a batch of 2 L working volume reactor was estimated for all three cultivation media conditions. The maximum cost of DIW (100 mM $Na_2S_2O_3$) was found to be \$0.8526 per batch and DWW (no additional sulfate) had a minimum of \$0.4461 per batch operating cost. This higher cost in case of DIW was obtained due to the cost of thiosulfate ions. The operating cost of DWW (100 mM $Na_2S_2O_3$) was less than the DIW (100 mM $Na_2S_2O_3$) which may be due to fact that additional thiosulfate was added in DWW to maintain the 100 mM concentration. The operating cost was also estimated for the production of 1 kg of biomass in laboratory scale process and is represented in Table 4.8. The operating cost of DIW (100 mM $Na_2S_2O_3$) (\$55.202) and DWW (100 mM $Na_2S_2O_3$) (\$57.624) was obtained nearly equal to produce one kg of biomass. However, the operating cost per kg of biomass was obtained

significantly less in DWW (no additional sulfate) ($42.56) as compared to other two cultivation conditions. The techno-economic analysis for laboratory scale process has indicated the feasibility for the replacement of DIW with DWW. This fact was also established by carrying out the same analysis for 500 times scaled-up process for all the three cultivation media.

In scaled-up process, the parameters such as initial pH, temperature, gaseous flow rate, initial CO_2 concentration, stirrer speed and cultivation period were kept same as laboratory scale process. The total volume and working volume of bioreactor were considered as 1500 L and 1000 L, respectively. The commercial cost of chemicals was obtained from import and export data of India obtained from Zauba link (www.Zauba.com). Different types of water and CO_2 cost were considered same as laboratory scale process. However, the cost of power in terms of electricity was estimated by considering the power required for pumping, to run centrifuge and for agitator in the commercial scale process as it may be significant for large scale operations. The cost of one unit of electricity in kWh is assumed to be $0.081 in the present work (Purbia et al., 2019). The operating cost per batch of experiment and per kg of biomass was calculated for all the three culture media and is reported in Table 4.8. Cost estimation for commercial-scale processes ascertains the fact that DIW (100 mM $Na_2S_2O_3$) can be replaced with DWW for industrial scale operations. The added advantage of using DWW as cultivation media reduces the manpower cost and the capital cost for reverse osmosis (RO) process which may be required for wastewater treatment.

Table 4.6 Different forms of carbon present in the bioreactor

Culture conditions	DIW (100 mM $Na_2S_2O_3$)	DWW (100 mM $Na_2S_2O_3$)	DWW (no additional sulfate)
Total carbon supplied to the bioreactor in grams ($M_{C,in}$), g	203.8	203.8	203.8
Total carbon assimilated as biomass in grams ($M_{C,bo}$), g	15.44	13.42	10.62
Total carbon present in the form of dissolved CO_2 in the aqueous phase (M_{C,CO_2}), g	8.26	7.08	3.86
Carbon coming out continuously at the outlet of reactor ($M_{C,out}$), g	166.04	170.98	172.94
Net	13.26	12.32	16.38

Table 4.7 Comparison of maximum specific growth rate, biomass productivity, CO_2 (g) fixation rate and maximum biomass concentration at different cultivation conditions with reported studies

Species	Mode	CO_2 (g) conc. (% v/v)	Max. biomass Produced (X_{Max}) (g L^{-1})	Biomass productivity (P) (g L^{-1} d^{-1})	CO_2 fixation rate (Rco_2) (g L^{-1} d^{-1})	References
Spongiochloris	Air-lift PBR	-	2.93	1.5 ± 0.3	2.92	(Abid et al., 2017)
Chlorella vulgaris	Bubble column PBR	15	1.976	0.282	0.35-4.0	(Chen et al., 2018)
Chlorella PY-ZU1	Bubble column PBR	15	4.03	0.518	0.94	(Cheng et al., 2016)
Chlorella sorokiniana	Air-lift PBR	5	4.4	0.338	1.21	(Kumar et al., 2012)
H. Stevensii	Laboratory scale bio-reactor	15 (±1)	2.16 (±0.11)	1.55 (±0.04)	1.94 (±0.044)	(Mishra et al., 2017)

H. Stevensii in DIW (100 mM $Na_2S_2O_3$)	Laboratory scale bio-reactor	10 (±1)	7.72	2.83	3.52	Present study
H. Stevensii in DWW (100 mM $Na_2S_2O_3$)	Laboratory scale bio-reactor	10 (±1)	6.71	3.14	3.92	Present study
H. Stevensii in DWW (no additional sulfate)	Laboratory scale bio-reactor	10 (±1)	5.31	3.92	4.01	Present study

Table 4.8 Operating cost per batch and per kg biomass of laboratory scale and commercial scale process for all the three cultivation media [Case 1: DIW (100 mM $Na_2S_2O_3$), Case 2: DWW (100 mM $Na_2S_2O_3$) and Case 3: DWW (no additional sulfate)]

Process		Operating cost in $/ batch			Operating cost in $/kg of biomass		
		Case 1	Case 2	Case 3	Case 1	Case 2	Case 3
Laboratory Scale	Chemicals	0.8442	0.77	0.4454	54.67	57.148	41.524
	DIW	0.0016	-	-	0.1033	-	-
	CO_2 (g)	0.0007	0.0007	0.0007	0.4144	0.4774	0.6034
	Total cost ($)	0.8526	0.7707	0.4461	55.202	57.624	42.56
Commercial Scale	Chemicals	42.49	37.05	15.53	5.509	5.5272	2.93
	DIW	0.868	-	-	0.113	-	-
	Wastewater	-	0.021	0.021	-	0.0031	0.004
	CO_2 (g)	3.213	3.213	3.213	0.4158	0.4788	0.6048
	Power	0.7	0.7	0.7	0.0924	0.1064	0.1344
	Total Cost ($)	47.278	40.99	19.472	6.1292	6.1152	3.6722

The requirement of freshwater in bacterial cultivation for flue gas bio-fixation becoming a limiting step in the scaled-up process. The utilization of organic and inorganic compounds present in DWW as nutrient and energy source and the preparation of cultivation media in DWW can overcome the problem of freshwater requirement. The present work indicated the feasibility of replacing DIW with DWW and utilizing the concomitant inorganic compounds of wastewater as a nutrient and energy source for the growth of bacteria can be one of the viable options. Hence, the utilization of DWW for the preparation of cultivation media for the bio-fixation of flue gases using bacterial species can be explored.

4.3 Flue gas (CO_2, NO, SO_2) bio-fixation using bacterial consortium (*Bacillus cereus* and *Bacillus tropicus*)

4.3.1 Molecular identification and characterization of isolated bacterium consortium

The isolates SSLMC1 and SSLMC2 were identified by 16S rRNA gene sequence analysis. The gene sequence of the isolate was used to construct a phylogenetic tree and characteristic bacteria of related taxa and are shown in Fig. 4.11 a and b. Neighbour-joining algorithm was used to calculate topology. Homology searches in GenBank using BLAST for strains SSLMC1 and SSLMC2 have shown the closest homology of 97.97% and 96.81% with *Bacillus tropicus* (Accession No. MK332324.1) and *Bacillus cereus* (Accession No. KR819403.1), respectively at query coverage of 93-94%. The nucleotide sequences were deposited to the NCBI GenBank database with accession no. OP028074.1 (*Bacillus tropicus* SSLMC1) and OP032651.1 (*Bacillus cereus* SSLMC2). A subdivision group of the genus *Bacillus* is *Bacillus cereus* group and phylum *Firmicutes* currently includes 12 closely related species. *Bacillus tropicus* belongs to the *Bacillus cereus* group having the same physiological and biochemical characteristics (Du et al., 2017; Lai et al., 2017).

4.3.2 Wastewater analysis

The concentration of different physio-chemical properties of DWW such as BOD, COD, $N\text{-}NO_3^-$, $N\text{-}NO_2^-$, $P\text{-}PO_4$, HCO_3^-, CO_3^{2-}, OH^-, SO_4^{2-}, Ni, Zn, Fe (II), dissolved oxygen (DO), salinity, total dissolved solid (TDS), and conductivity were measured, and their values are reported in Table 4.3.

4.3.3 Estimation of fixation efficiency

4.3.3.1 C, N and CN gas mixtures

The biomass was visible constantly throughout the cultivation period. CO_2 (g) and NO (g) concentrations were analyzed twice a day at the gas inlet and outlet of the reactor to estimate the fixation efficiency and are represented in Fig. 4.12 for all three gaseous mixtures (C, N, and CN). A substantial increase in fixation efficiency of CO_2 and NO was observed during the initial h (0-36 h) of bioreactor operation for all three gaseous combinations. This may be due to the dissolution of CO_2 and NO in aqueous media to achieve equilibrium between the aqueous phase and gaseous phase concentration of CO_2 and NO. Later, no significant change in the value of fixation efficiency was observed as the dissolution of CO_2 and NO from the gaseous phase to the aqueous phase was equal to the rate of utilization of dissolved components by bacterial consortium. In the initial incubation period, NO (g) fixation efficiency was obtained comparatively lower than the CO_2 (g) fixation efficiency as the solubility of NO (0.056 gL^{-1}) in water is lesser as compared to CO_2 (1.782 g L^{-1}) and hence, the availability of NO to the bacterial consortium was obtained less in the aqueous phase (Skalska et al., 2010; Hende et al., 2012). The fluctuations in the fixation efficiency were due to the on/off cycle of inlet gases. The maximum CO_2 (g) fixation efficiency was obtained as 66.65% for the CN mixture compared to the 56.99% for the C mixture. For NO (g), 93.44% fixation efficiency for the CN mixture was observed compared with 86.58% for the N mixture. Hence, for both CO_2 (g) and NO (g), CN mixture showed higher fixation efficiency than C and N

mixtures. This could be due to the concurrent utilization of NO as a nutrient source and CO_2 as a carbon source and resulted in better removal efficiency in the simultaneous input of both gases.

4.3.3.2 C, S and CS gas mixtures

The fixation efficiency was calculated twice a day for all three gaseous mixtures, (C, S and CS), by measuring CO_2 (g) and SO_2 (g) concentration at the inlet and outlet of the bioreactor and is represented in Fig. 4.13. There was a significant increase in the fixation efficiency values for all the gaseous compositions after 6 h of the incubation period. It is well known that CO_2 and SO_2 are soluble in water (Hende et al., 2012; Du et al., 2019). First, CO_2 and SO_2 are getting dissolved in aqueous media and are forming bicarbonate and sulfate ions, respectively. The formed bicarbonate and sulfate ions are utilized as carbon and energy source by the bacterial consortium. After 36 h of the incubation period, no significant change was observed in the fixation efficiency values. This may be due to the dissolution of CO_2 and SO_2 from the gaseous phase to the aqueous phase and is equal to the rate of utilization of dissolved components by microbes. The on/off cycle of inlet gases caused fluctuations in the fixation efficiency. The maximum CO_2 (g) fixation efficiency was obtained as 93.81% for CS gas mixture as compared to 56.99% for C gas mixture. However, 91.35% fixation efficiency was observed for SO_2 in S gas mixture compared to 88.92% in CS gas mixture which is approximately the same. The results confirmed that the bacterial consortium can simultaneously fix CO_2 and SO_2 (Mishra et al., 2017).

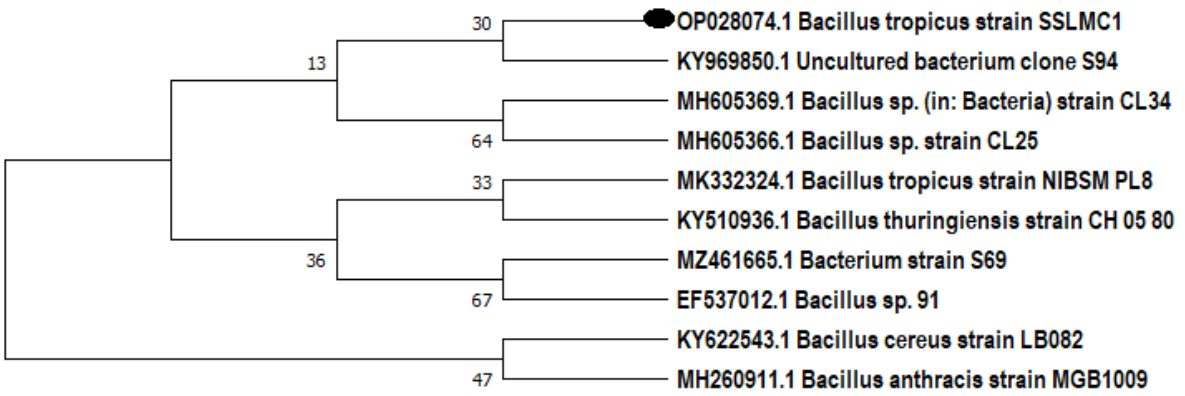

(a)

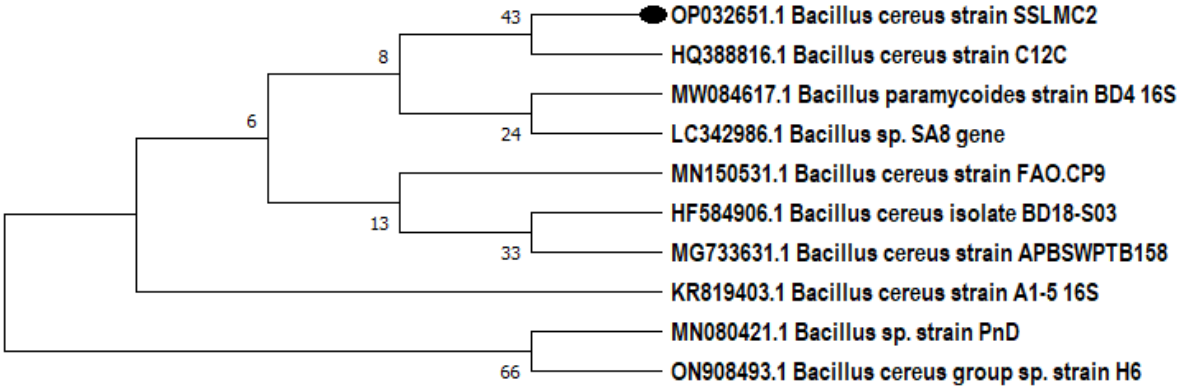

(b)

Fig. 4.11 16S rRNA gene sequences based phylogenetic tree displaying the relationships between (a) *Bacillus* and *Bacillus tropicus* SSLMC1 and (b) *Bacillus* and *Bacillus cereus* SSLMC2 and its related phylogenetic neighbors

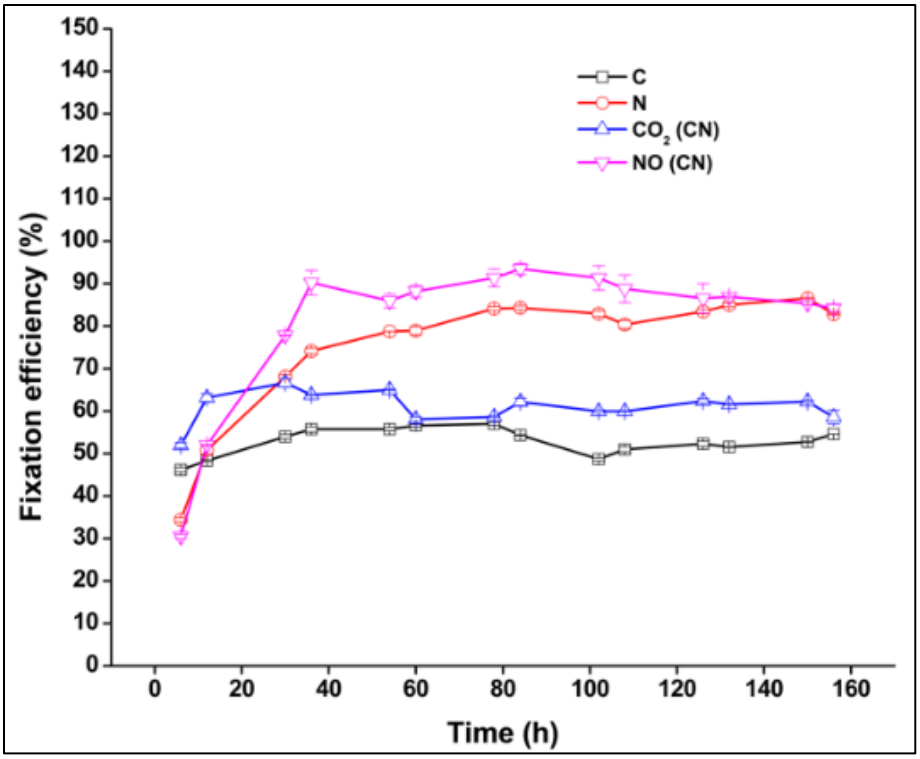

Fig. 4.12 Fixation efficiency variation with respect to time for C, N and CN gas mixture

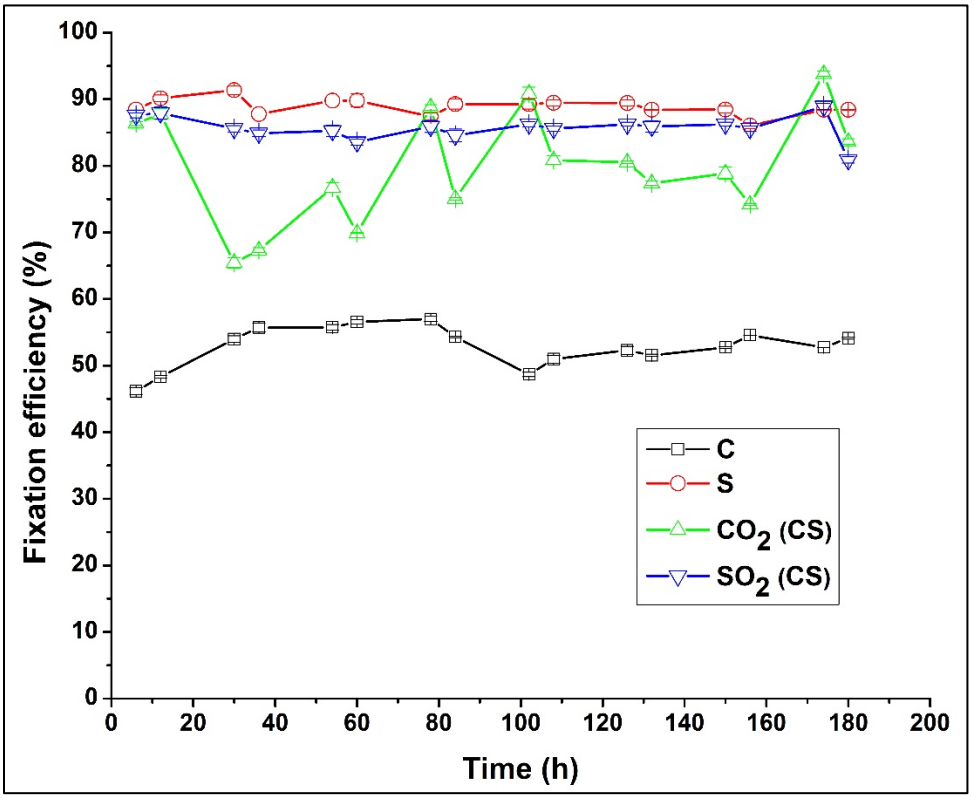

Fig. 4.13 Fixation efficiency variation with respect to time for C, S and CS gas mixture

4.3.3.3 CNS gas mixture

Fig. 4.14 illustrates the fixation efficiency of the bacterial consortium with simulated flue gas (CNS) mixture. All three gases (CO_2, NO, and SO_2) were measured twice a day with the flue gas analyzer at the inlet and outlet of the bioreactor, and fixation efficiency was calculated. The supply of simulated flue gases was intermittent. The maximum fixation efficiency of CO_2, NO and SO_2 was found to be 92.1%, 96.91%, and 84.64%, respectively. These values are much higher than those reported studies (Chiu et al., 2011; Kao et al., 2014; Xie et al., 2021). NO fixation efficiency was obtained comparatively lesser than the SO_2 and CO_2 fixation efficiency, as the solubility of NO is less than the other two gases (Skalska et al., 2010; Hende et al., 2012; Du et al., 2019). After 6 h of the incubation period, the fluctuations in fixation efficiency were due to the intermittent supply of gases.

Enhancing the gas-liquid contact area, contact period (including increasing liquid depth), lowering bubble size and gas flow rate has been proven helpful in achieving a higher flue gas removal efficiency and a higher fixation rate by microbial biomass (Nagase et al., 1998; Ryu et al., 2009; Kumar et al., 2014). The higher removal efficiencies of 92.1% for CO_2, 96.91% for NO and 84.64% for SO_2 were achieved in this study and are justified by a deeper bacterial suspension (13 cm), smaller bubble size (the diffuser pore size was < 100 μm), lower flue gas flow rate (0.25 vvm), and, most importantly, intermittent flue gas injection regulated manually. In most of the earlier studies, flue gas was supplied continually, preventing the gas from dissolving adequately in water (Arbib et al., 2013). As a result, flue gas may readily escape into the environment, which lowers the fixation efficiency. CO_2 removal efficiency of 4.7% and 25% were reported for continuous gas supply (Kao et al., 2014; Kumar et al., 2014).

The higher removal efficiencies of 60% CO_2, 70% NO and 50% SO_2 were achieved during the intermittent flue gas supply (Chiu et al., 2011). Therefore, intermittent injection of simulated flue gas was proven more effective for bio-fixation than continuous injection. A portion of the carbon, sulfur, and nitrogen from the dissolved CO_2, NO and SO_2 in the culture medium was absorbed by the microbial cells, while a portion was left in the bacterial suspension during the simulated flue gas injection phase. Therefore, the CO_2, NO and SO_2 fixation efficiencies were partially obtained differently from the utilization efficiencies. The bacterial cells constantly consume the carbon, nitrogen and sulfur sources from the dissolved CO_2, NO and SO_2 during the non-injection phase. Hence, the intermittent flue gas aeration strategy for cultivation could enhance bacterial growth and increase the utilization of CO_2, NO and SO_2 in the flue gas.

4.3.4 Estimation of biomass growth and various bio-kinetics parameters

4.3.4.1 C, N and CN gas mixtures

The biomass growth of bacterial consortium in terms of dry weight (g L^{-1}) was calculated for all three gaseous compositions (C, N, and CN). The maximum biomass concentration was found as 4.92 g L^{-1}, 7.1 g L^{-1}, and 4.95 g L^{-1} for the C, N, and CN gas mixtures, respectively. Biomass concentration for N mixture was higher than C and CN mixture. The possible reason behind this may be the utilization of NO (g) as the nitrogen source in the form of nitrate or nitrite for cell growth (Hende et al., 2012; Kao et al., 2014). The value of produced biomass for CN mixture was almost equal to C mixture, suggests that the bacterial consortium can efficiently mitigate CO_2 (g) and NO (g) simultaneously. The quantity of CO_2 (g) acquired by the cellular biomass concentration was closely correlated with the availability of the energy substrate and the growth of microorganisms (Mishra et al., 2017). The concomitant thiosulfate and ferrous ion (Fe (II)) present in the DWW were utilized as an energy source by the bacterial consortium. A sufficient amount

of carbon, nitrogen and energy source has led to a continuous increase in biomass concentration. The CFU of the final day culture was calculated as 19×10^{11}, 8×10^{11}, and 13×10^{11} for C, N, and CN mixture, respectively. CFU values suggested that the bacterial consortium is viable at the end of the bio-fixation period. The utilization efficiency of CO_2 (g) and NO (g) in the case of C and N mixtures was found to be 14.07% and 11.23%, respectively, which is less than the utilization efficiency obtained for CO_2 (18.05%) and NO (13.63%) from CN mixture. The utilization efficiency for the simultaneous removal of CN mixture study was comparatively higher than the other two studies that suggest the successful utilization of bacterial consortium for the simultaneous fixation of CO_2 (g) and NO (g).

The various bio-kinetic parameters such as biomass productivity, specific growth rate, fixation efficiency, gaseous bio-fixation rate, and utilization efficiency were calculated for all three gaseous mixtures and are presented in Table 4.9. P_{max} and μ_{max} values for the CN mixture were estimated as 4.5 g L^{-1} d^{-1} and 0.96 d^{-1}, respectively, which were higher than the C and N mixture values (Table 4.9). The maximum fixation rate for CO_2 (g) and NO (g) was calculated as 4.38 and 0.96 g L^{-1} d^{-1} from C and N mixtures, respectively. However, simultaneous removal of CO_2 (g) and NO (g) from CN mixtures resulted in a maximum fixation rate of 5.62 g L^{-1} d^{-1} for CO_2 (g) and 1.16 g L^{-1} d^{-1} for NO (g). Biomass productivity, specific growth rate, and fixation rate for simultaneous removal of CO_2 (g) and NO (g) showed maximum values compared to the other two studies. The presence of carbon, nitrogen and energy sources in an adequate amount could be the possible reason behind this trend. This suggests that the bacterial consortium utilizes CO_2 (g) as carbon and NO (g) as a nitrogen source during the bio-fixation process.

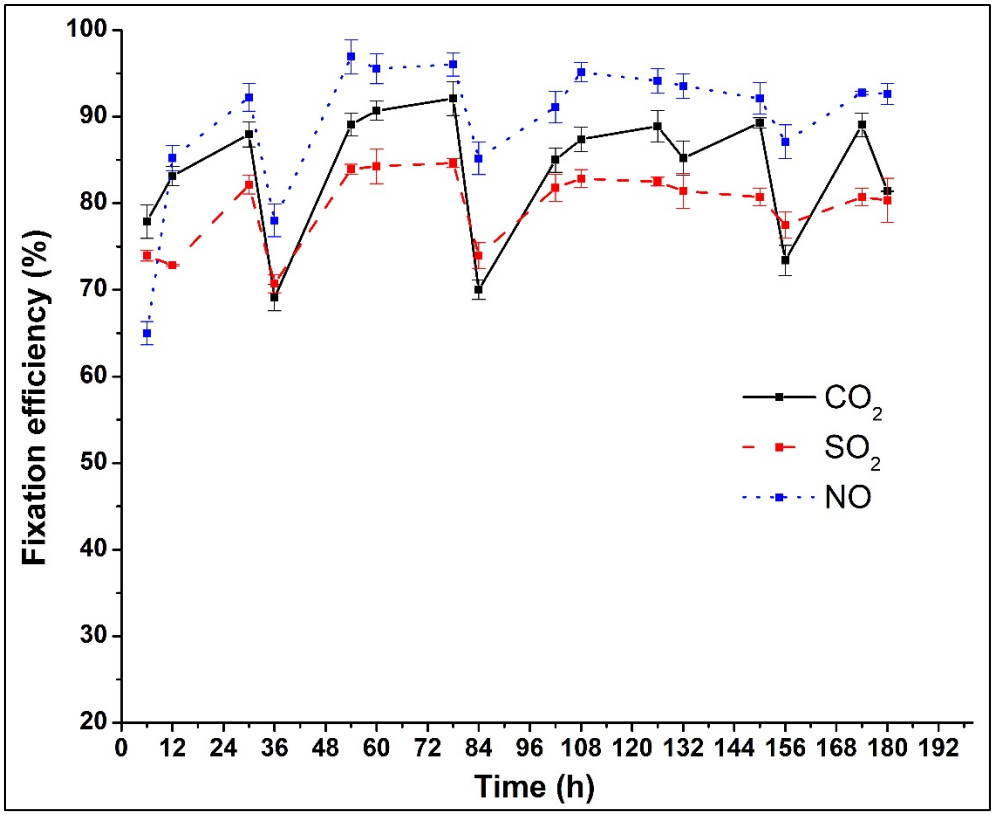

Fig. 4.14 Fixation efficiency of bacterial consortium for CNS gas mixture

Table 4.9 Bio-kinetic parameters values estimated for bio-fixation studies of C, N, and CN gas mixture

Different gaseous mixture	Maximum biomass conc. (g L^{-1})	Maximum biomass productivity (g L^{-1} d^{-1})	Maximum specific growth rate (d^{-1})	Maximum fixation rate (g L^{-1} d^{-1})	Maximum utilization efficiency
C	4.92	3.51	0.60	4.38	14.07%
N	7.1	3.73	0.92	0.96	11.23%
CN	4.95	4.50	0.96	5.62 (CO_2) 1.16 (NO)	18.05% (CO_2) 13.63% (NO)

4.3.4.2 C, S and CS gas mixtures

For each of the three gaseous mixtures, (C, S and CS) the biomass growth of the bacterial consortium was assessed in terms of dry weight (g L^{-1}) and is illustrated in Table 4.10. The dry weight biomass continues to increase with culture time for all three gaseous compositions. The maximum biomass concentration was found to be 4.92 ± 0.19 g L^{-1} in the case of C gas mixture, 3.31 ± 0.17 g L^{-1} for S gas mixture and 2.15 ± 0.52 g L^{-1} with CS gas mixture. The maximum biomass concentration for C gas mixture was obtained comparatively higher than the S and CS gas mixture. The possible reason could be the inhibition of cell growth in S and CS gas mixtures due to the presence of a higher concentration of SO_2.

The bio-kinetic parameters, maximum biomass productivity (P_{max}) and the maximum specific growth rate (μ_{max}) are presented in Table 4.10. At the end of the incubation period, the maximum P_{max} and μ_{max} for C gas mixture were found to be 3.51 g L^{-1} d^{-1} and 0.60 d^{-1}, respectively. The maximum P_{max} and μ_{max} for S gas mixture were found to be 2.31 ± 0.06 g L^{-1} d^{-1} and 1.99 ± 0.81 d^{-1}, respectively. The P_{max} and μ_{max} values for CS gas mixture were found to be 2.28 ± 0.07 g L^{-1} d^{-1} and 5.78 ± 1.07 d^{-1}, respectively. The CS gas mixture has shown the lowest but appreciable value of biomass concentration and biomass productivity as compared to the other two studies (C, S). The bacterial consortium can fix the mixture of CO_2 and SO_2 which established the fact that the bacterial consortium is utilizing CO_2 as the sole carbon source and SO_2 as energy source during the biomass growth process (Li et al., 2017).

The maximum CO_2 fixation rate for C and CS gas mixtures was 4.38 ± 0.17 g L^{-1} d^{-1}, and 2.84 ± 0.09 g L^{-1} d^{-1}, respectively. Likewise, the maximum utilization efficiency for CO_2 was obtained as 14.07% ± 0.53 and 9.14% ± 0.29 for gas mixture C and CS, respectively. The utilization efficiency

and SO_2 fixation rate cannot be calculated as molecular formula for S and CS gas mixture is not available.

4.3.4.3 CNS gas mixture

The growth performance of the bacterial consortium for CNS gas mixture was measured in terms of biomass concentration and optical density. Fig. 4.15 shows bacterial growth trends in terms of biomass concentration and optical density for the cultivation period of 192 h. The biomass concentration growth curve followed the same optical density trend for the entire period. The initial value (0 h) of biomass concentration and optical density was obtained as 0.266 g L^{-1} and 0.135, respectively. The maximum biomass concentration (24 h) of bacterial consortium with aeration of CNS gas mixture was obtained as 3.13 g L^{-1} at an optical density value of 0.371. The biomass concentration and optical density values were found to significantly increase for the initial period of (0-24 h) and decreased from 24 h to 72 h of the cultivation period. No significant changes were observed in biomass concentration and OD values. Initially, more amounts of CO_2, NO and SO_2 were dissolved in the culture medium, forming different ions such as bicarbonate, nitrate and sulfate. These ions in the medium were utilized as carbon, nitrogen, and energy source for the cellular growth of microbes. The nitrate and the sulfate ions were also utilized as nutrient and energy source for cell growth, respectively (Du et al., 2019; Xie et al., 2021). The presence of a higher amount of nutrients and energy sources was obtained during the initial cultivation hours and could be the possible reason for the significant increase in biomass concentration and OD values. After 72 h of the incubation period, no such change was observed as equilibrium was attained between the nutrients utilization by microbes and nutrients and energy source present in the dissolved form in the aqueous medium. The maximum biomass concentration (3.13 g L^{-1}) for

the present study was obtained comparatively higher than the work carried by Radmann et al. (2011) using algal culture of *chlorella sp.* (0.41-1.59 g L^{-1}).

The growth performance of the bacterial consortium for CNS gas mixture was also substantiated by calculating the maximum biomass productivity (P_{max}), maximum specific growth rate (μ_{max}), maximum fixation rate, and actual utilization efficiency and are given in Table 4.11.

The maximum biomass productivity and maximum specific growth rate for the bacterial consortium were obtained as 4.39 g L^{-1} d^{-1} and 5.89 d^{-1}, respectively for CNS gas mixture. In the CNS gas mixture, the maximum fixation rate and utilization efficiency were obtained as 5.48 g L^{-1} d^{-1} and 17.60% for CO_2 and 1.13 g L^{-1} d^{-1} and 13.29% for NO, respectively. In the present study, the maximum biomass productivity of 4.39 g L^{-1} d^{-1} was obtained much higher than the work carried out by Chiu et al. (2011) (0.64 g L^{-1} d^{-1}). The higher value of P_{max} and μ_{max} were obtained due to the abundant availability of nutrients for microbial growth due to the higher solubility of CO_2 and SO_2 in the aqueous medium (Hende et al., 2012; Du et al., 2019). The maximum CO_2 utilization efficiency of (17.60%) for the present work was comparatively higher than the previous study (3.46%−14.85%) carried out by Radmann et al. (2011) with the gaseous mixture of CO_2- 12% v/v, SO_2- 60 ppm and NO-100 ppm. The higher values of the growth parameters in the present work suggested that the bacterial consortium used in the present work is capable of the simultaneous fixation of CO_2, NO and SO_2 at higher concentrations (CO_2-10 % (v/v), NO- 760 ppm, SO_2- 140 ppm).

Table. 4.10 Comparison of maximum biomass concentration, biomass productivity, and specific growth rate for C, S, and CS gas mixture

Different gaseous mixture	Maximum biomass conc. ($g\ L^{-1}$)	Maximum biomass productivity ($g\ L^{-1}\ d^{-1}$)	Maximum specific growth (d^{-1})	Maximum fixation rate ($g\ L^{-1}\ d^{-1}$)
C	4.92 ± 0.19	3.51 ± 0.13	0.60 ± 0.21	4.38 ± 0.17
S	3.31 ±1.16	2.31 ± 0.06	1.99 ± 0.81	-
CS	2.15 ± 0.51	2.28 ± 0.07	5.78 ± 1.07	2.84 ± 0.09 (CO_2)

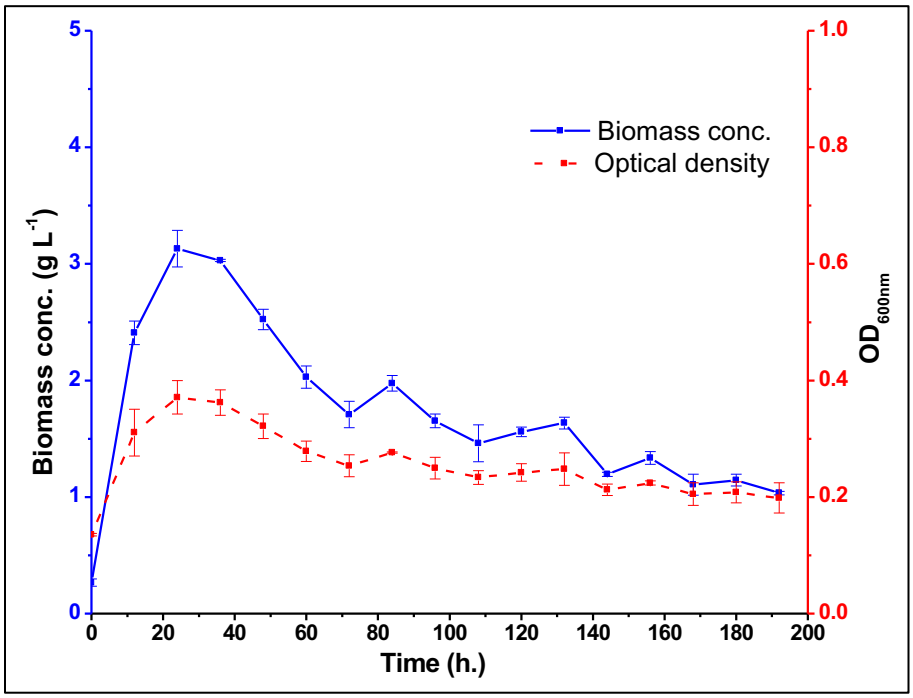

Fig. 4.15 Growth profile of bacterial consortium for CNS gas mixture

Table 4.11 Growth parameters of bacterial consortium for CNS gas mixture

Gas mixture	Maximum biomass productivity ($g\ L^{-1}\ d^{-1}$)	Maximum specific growth rate (d^{-1})	Maximum fixation rate ($g\ L^{-1}\ d^{-1}$)	Maximum utilization efficiency
CNS	4.39 ± 0.71	5.89 ± 0.97	5.48 ± 0.88 (CO_2) 1.13 ± 0.18 (NO)	17.60 ± 2.83% (CO_2) 13.29 ± 2.14% (NO)

4.3.5 Analysis of dissolved parameters

4.3.5.1 C, N and CN gas mixtures

The change in the pH, carbonates (CO_3^{2-}), and bi-carbonates (HCO_3^-) ions for C and CN mixture with different time intervals were plotted and are shown in Figs. 4.16 and 4.17. After introducing the gaseous mixture, pH of the solution decreased to 7.4 and 6.9 for C and CN mixtures, respectively. At a pH value of 10, aqueous CO_2 reacts with OH^- ions present in the solution to form HCO_3^- ions (Bong et al., 2001; Mishra et al., 2016). In the initial period of the bio-fixation process, HCO_3^- ions were less utilized by bacterial consortium, due to which the formation of carbonic acid be higher and resulted in a decrease in the pH value of culture media. Later, the equilibrium was achieved between the gas phase and liquid phase CO_2 concentration; hence, the pH value change was insignificant (Figs. 4.16 and 4.17). Due to the utilization of CO_2 by the bacterial consortium, equilibrium was shifted to dissolve additional CO_2 (g) in the medium, which increased the concentration of dissolved CO_2 (Mishra et al., 2017).

The increasing trend of HCO_3^- concentration during the initial 36 h was observed for C and CN mixture. Later, it decreased and remained almost stationary for the rest of the bio-fixation period. Initially, the concentration of CO_3^{2-} ions was found to decrease, then increase, and remain constant for the rest of the incubation period. The trend was obtained due to the pH dependency of carbonate alkalinity formation. The presence of HCO_3^- is higher than the CO_3^{2-} at a pH of approximately 7.5. The change in the pH, nitrite, and nitrate for N and CN mixture with different time intervals were plotted and is shown in Figs. 4.18 and 4.19, respectively. The pH decreased from 8.2 to 7.3 and 8 to 6.9 for N and CN mixtures, respectively, while introducing NO (g) into the reactor system. Initially, NO was dissolved in aqueous media and formed nitrite and nitrate ions. The lower utilization of nitrite or nitrate ions by the bacterial consortium during the initial period and the

simultaneous production of nitrous or nitric acid may be the possible reason for the culture media's decrease in pH value. Later, the equilibrium was attained between the NO (l) in the aqueous phase and NO (g) in the headspace of the bioreactor, and hence, no significant change in pH value was observed after 36 h of the incubation period (Du et al., 2019; Ma et al., 2019). Growth of bacterial culture was observed in the entire pH range from 6.9 to 9. However, the maximum growth was found at a pH of around 7‑8. The result corroborated with the previous study (Rout et al., 2017). The nitrite concentration is comparatively higher than the nitrate concentration for most of the incubation period. *Bacillus cereus* can utilize nitrate or nitrite ions as the sole nitrogen source for its growth. However, it utilizes more nitrate than nitrite. Some toxicity of nitrite ions towards *Bacillus cereus* could be the possible reason (Rout et al., 2017).

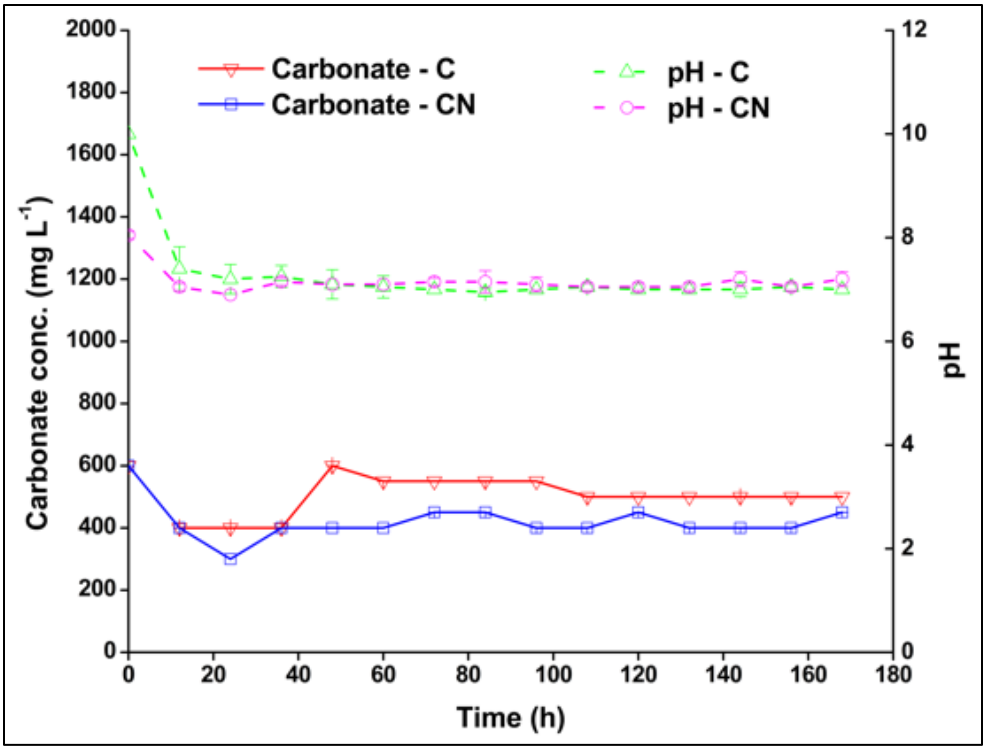

Fig. 4.16 Concentration of carbonates and pH at different time intervals

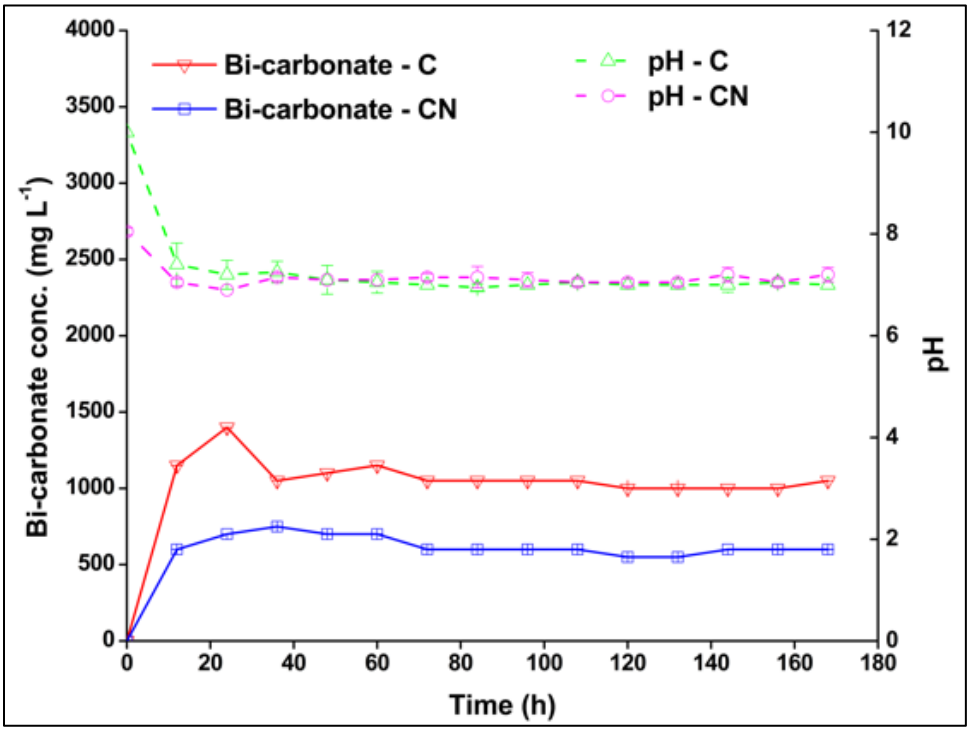

Fig. 4.17 Concentration of bi-carbonates and pH at different time intervals

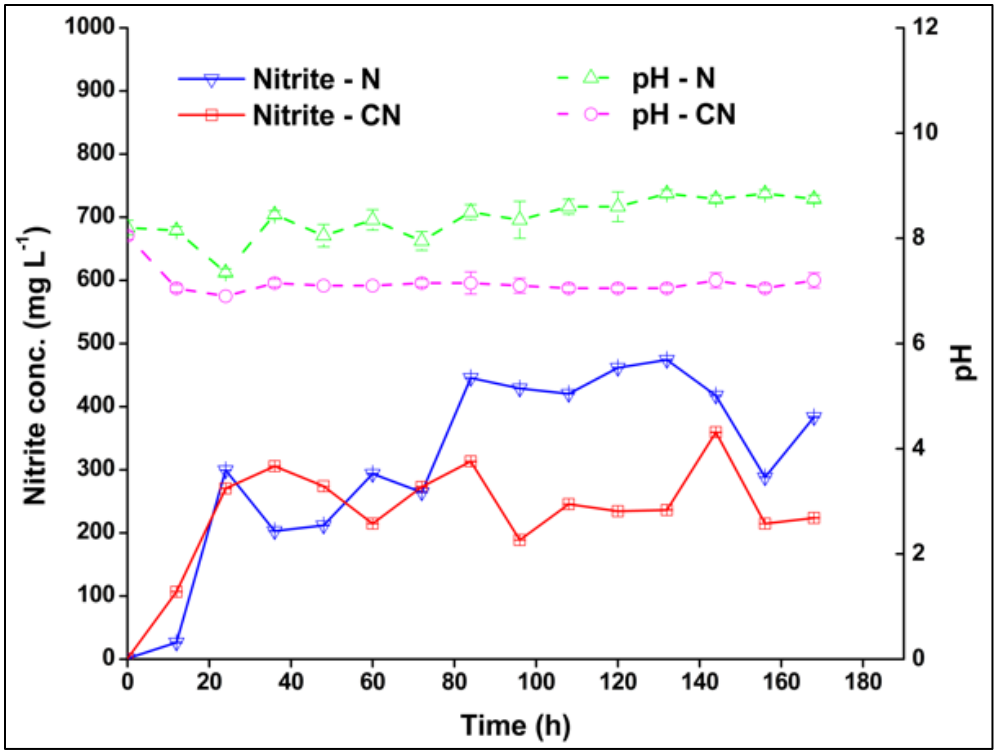

Fig. 4.18 Concentration of nitrite and pH at different time intervals

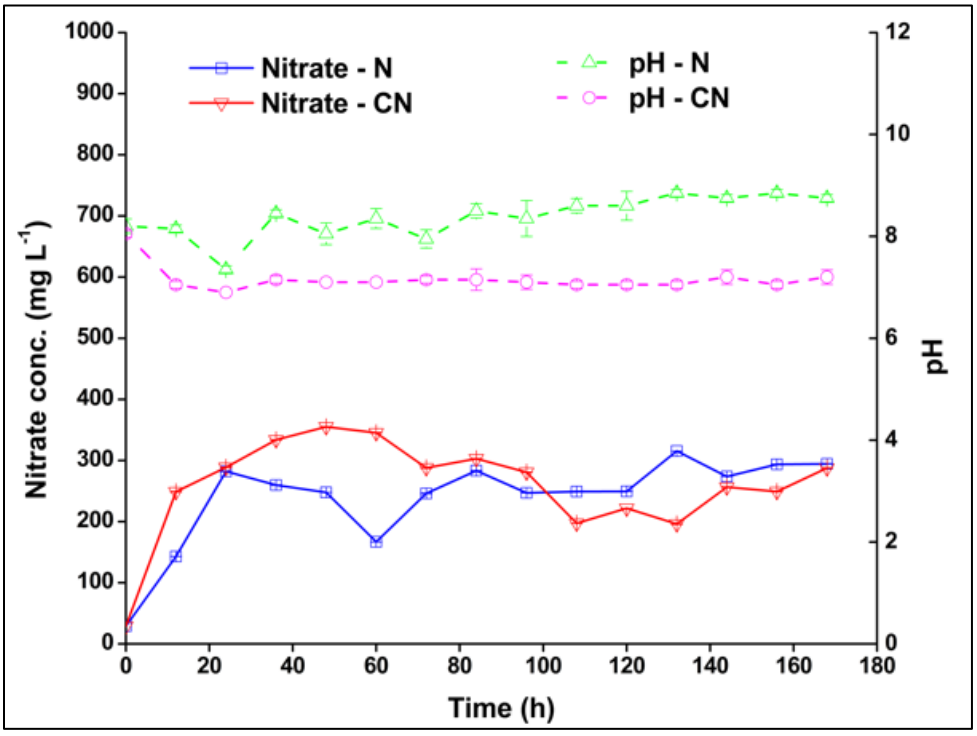

Fig. 4.19 Concentration of nitrate and pH at different time intervals

4.3.5.2 C, S and CS gas mixtures

Figs. 4.20 and 4.21 show the formation of carbonate ions, bi-carbonate ions and variation of pH with time for C and CS gas mixture. The initial pH of C gas mixture was maintained at 10 as the solubility of CO_2 at pH 10 is more. When CO_2 (g) get dissolved in aqueous media, pH was observed to decrease from 10 to 7.4. Similarly, the pH value was found to decrease from 7.8 to 7.4 for CS gas mixture. At higher pH, bicarbonate ions were formed by the reaction of OH^- ions present in water with aqueous CO_2 and a decrease in the pH value of culture media for C and CS gas mixture was observed. This could be due to the higher rate of formation of carbonic acid and lower utilization of bicarbonates by the bacterial consortium during the initial periods (Bong et al., 2001). A change in pH values for C and CS gas mixture was minimal. The possible reason could be the equilibrium obtained between aqueous phase CO_2 and gaseous CO_2 present in the headspace of the bioreactor (Mishra et al., 2017).

The concentration of carbonate ions (CO_3^{2-}) was found to decrease initially (0-36 h) and then increased after 36 h of the cultivation period and further, no such change was observed for the rest of the period. This confirmed that the carbonate alkalinity formation is pH-dependent. The concentration of bicarbonate alkalinity was higher than the carbonate alkalinity at pH 7.5. For the C and CS gas mixture, the concentration of carbonate ions was obtained comparatively lower than the concentration of bi-carbonate ions, as bicarbonate alkalinity tends to increase with a decrease in pH value.

The concentration of bicarbonate ions significantly increased till 36 h of the incubation period for C and CS gas mixture. After 36 h of the study, HCO_3^- concentration decreased and then it remained constant for the rest of the cultivation period of the C gas mixture. The HCO_3^- concentration for CS gas mixture has also shown a similar trend till 120 h, it was found to decrease and remain

constant for the rest of the periods. The possible reason could be the simultaneous utilization of bi-carbonate ions by bacterial consortium as a carbon source.

The change in the pH and sulfate concentration of S and CS gas mixture with different time intervals is plotted and shown in Fig. 4.22. After introducing SO_2 (g) into the reactor system, the pH decreased from 8.0 to 7.1 and 7.8 to 7.4 for S and CS gas mixture, respectively. SO_2 is soluble in water and acts as a weak acid. Hence, SO_2 gets dissolved in water when it passes through the aqueous media leading to the production of SO_3^{2-} and H^+. The obtained SO_3^{2-} was bio-oxidized into sulfate by microorganisms. The lower utilization of sulfate ions as energy source by the bacterial consortium during the initial period of (0−24 h) led to the formation of sulfuric acid could be the reason for the decrease of pH value of the culture media. Later, from 24-36 h of the cultivation period, the pH value increased from 7.1 to 8.3. No further significant changes in pH values were observed for S gas mixture. For CS gas mixture, no significant change was observed in pH values after 24 h of the study. The possible reason behind no change in pH values could be the rate of formation of sulfate ions becoming equal to the rate of utilization of sulfate ions by bacterial consortium.

The free CO_2 (l) concentration variation of C and CS gas mixture at various time intervals are shown in Fig. 4.23. During the initial period of cultivation (0-12 h), the amount of dissolved CO_2 in aqueous phase was higher due to less utilization of CO_2 by bacterial species. For 12-144 h, fluctuation in dissolved CO_2 was observed due to intermittent supply of C and CS gas mixture and at the last cultivation day (144-192 h), the amount of aqueous phase CO_2 decreased due to higher utilization of CO_2.

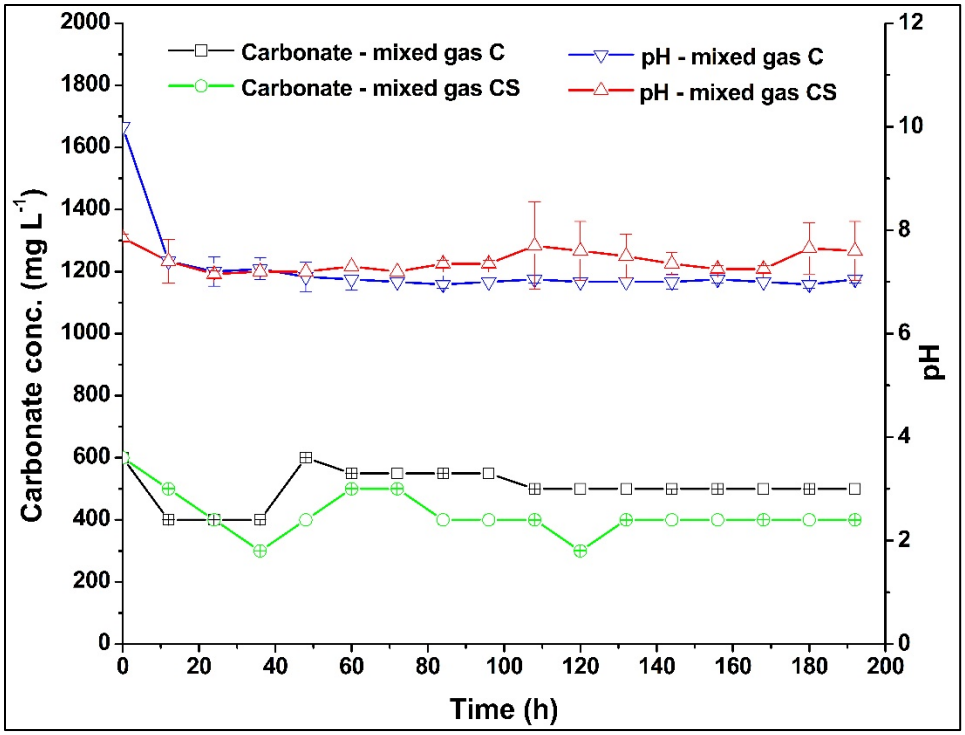

Fig. 4.20 Effect of simulated gas mixture on pH and carbonate concentration

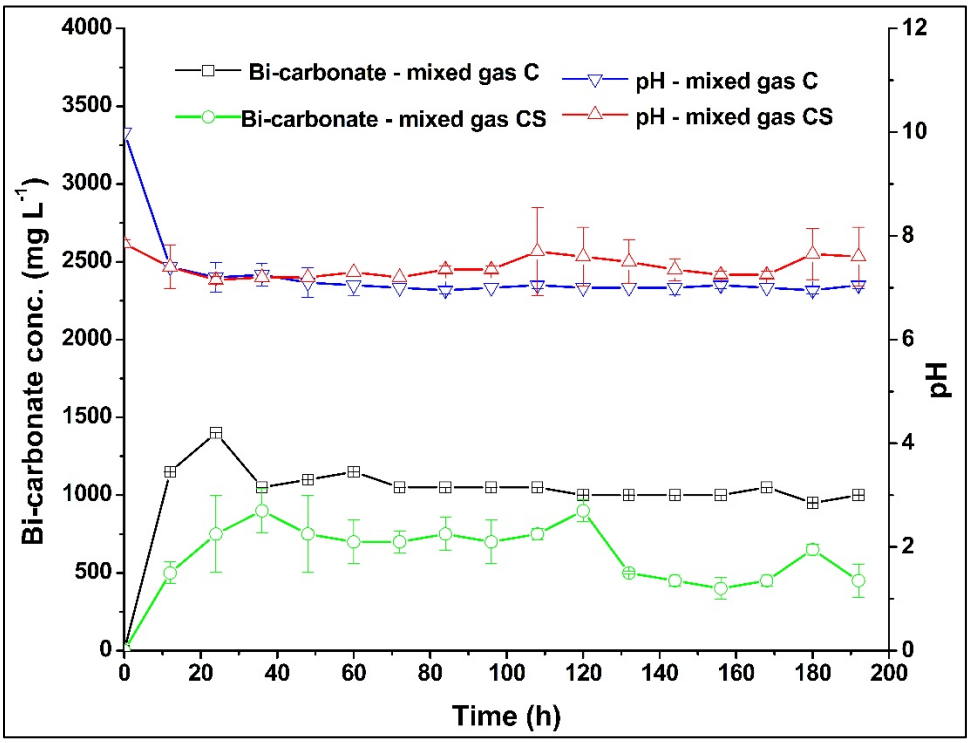

Fig. 4.21 Effect of simulated gas mixture on pH and bi-carbonate concentration

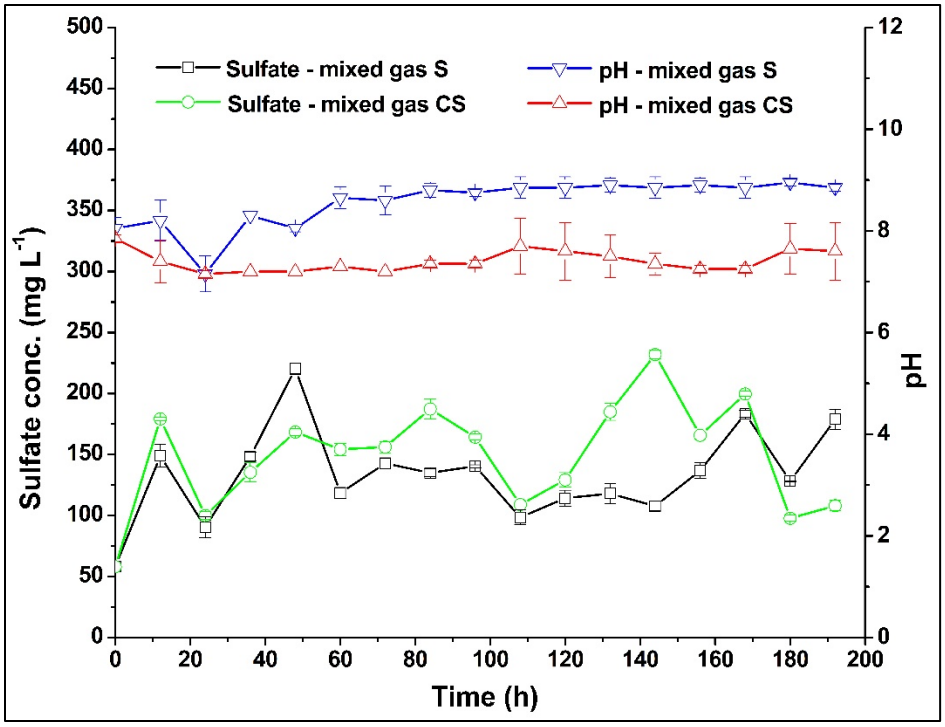

Fig. 4.22 Effect of simulated gas mixture on pH and sulfate concentration

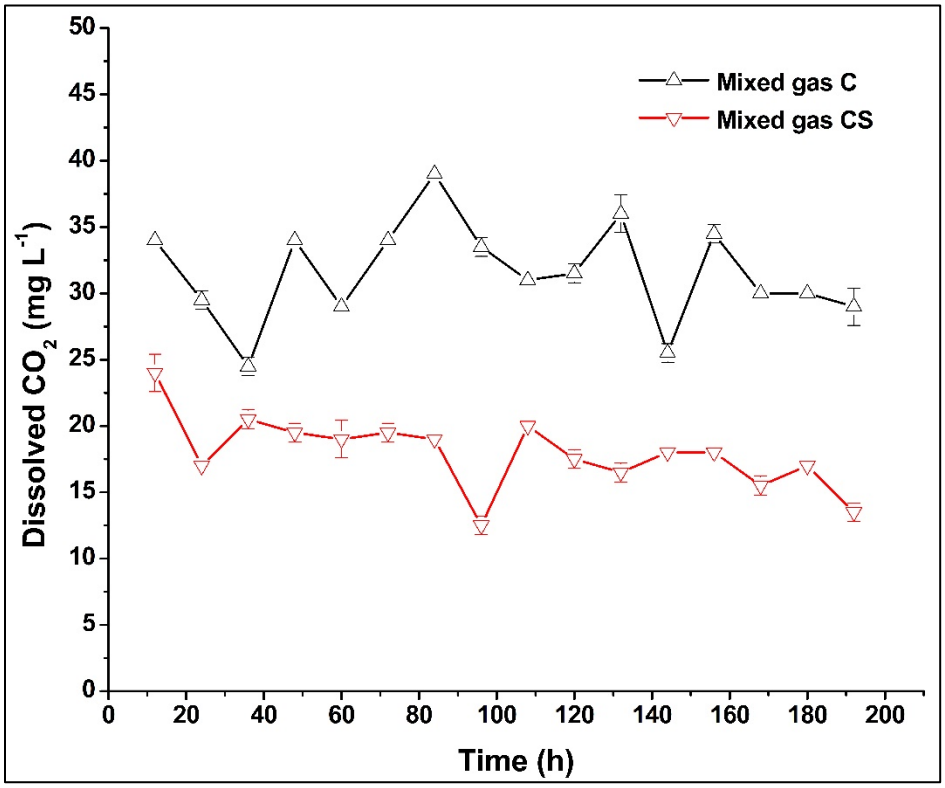

Fig. 4.23 Effect of simulated gas mixture on dissolved CO_2 concentration

4.3.5.3 CNS gas mixture

Fig. 4.24 illustrates the effect of CNS flue gas mixture on carbonate, bi-carbonate, and pH variation with respect to time. The pattern of the changes in the pH of the bacterial consortium culture was stable during the intermittent flue gas aeration. At the zeroth hour of the cultivation period, the pH of the culture medium was obtained as 7.5. After supplying the CNS gas mixture into the reactor system, bicarbonate ions were formed by the reaction of OH^- ions with aqueous CO_2. During the initial h (0-12 h), the pH of the system decreased from 7.5 to 6.9. During 48-60 h of cultivation, the pH value increased from 7 to 7.7, and no further change was observed for the rest of the cultivation period. The decrease in pH value of the culture medium was observed due to the higher rate of carbonic acid formation and lower utilization of bicarbonates by the bacterial consortium during the initial periods (Bong et al., 2001). The minimal change in pH can be explained by the equilibrium between aqueous phase CO_2 and gaseous CO_2 present in the headspace of the bioreactor (Mishra et al., 2017).

During 0-48 h of cultivation, the concentration of carbonate ions (CO_3^{2-}) decreased and later increased up to 120 h of the incubation period. No further change was seen after 120 h. This demonstrates that the formation of carbonate alkalinity is pH-dependent. At pH 7.5, the bicarbonate (HCO_3^-) alkalinity concentration was obtained higher than the concentration of carbonate alkalinity. Since bicarbonate alkalinity was found to increase with a decrease in pH value, the concentration of carbonate ions with the introduction of CNS gas mixture is relatively lesser than the concentration of bicarbonate ions. The concentration of HCO_3^- ion was found to increase considerably till 48 h of the cultivation period for simulated flue gas. After 48 h, HCO_3^- concentration decreased and then remained constant for the remaining cultivation period for CNS gas mixture.

The change in the pH, NO_2^-, NO_3^-, SO_4^{2-}, and dissolved CO_2 for CNS gas mixture with different time intervals were plotted and are shown in Figs. 4.25, and 4.26. When the culture medium was introduced to NO (g) and SO_2 (g), the medium's pH decreased from 7.5 to 6.9. Then NO and SO_2 were dissolved in the aqueous media and nitrite, nitrate, and sulfate ions were formed. The lower utilization of these ions by the bacterial consortium during the initial hours and a higher rate of formation of nitrous, nitric, and sulfuric acid could be the possible reason for the decrease in the pH value of the culture media. Later, no significant changes were observed in the pH value for CNS gas mixture.

Nitrite concentration was found to increase in 0-72 h, and it decreased in 72-192 h of the cultivation period. Nitrate concentration increased in 0-12 h, then decreased in 12-24 h, and later again increased in 24-192 h during the incubation period. The sulfate concentration increased for the duration of 0-48 h. It kept fluctuating between 48-108 h, and afterwards SO_4^{2-} concentration increased for the rest of the cultivation time. At the start of the cultivation period, a good amount of gases were getting dissolved in the aqueous media and were simultaneously utilized by the microbes as a nutrient or energy source. This could be the possible reason for the initial increase in NO_2^-, nitrate NO_3^-, and sulfate SO_4^{2-} concentration.

Fig. 4.26 shows the variation of dissolved CO_2 in the aqueous phase with respect to time. The amount of dissolved CO_2 concentration in the aqueous media is crucial for cell growth as it is the sole carbon source in the system. There is a significant change in CO_2 (l) from 0-12 h of the incubation period as more CO_2 was dissolved in the system. The fluctuation in the CO_2 (l) from 12 to 192 h may be substantiated by the intermittent supply of flue gases into the system.

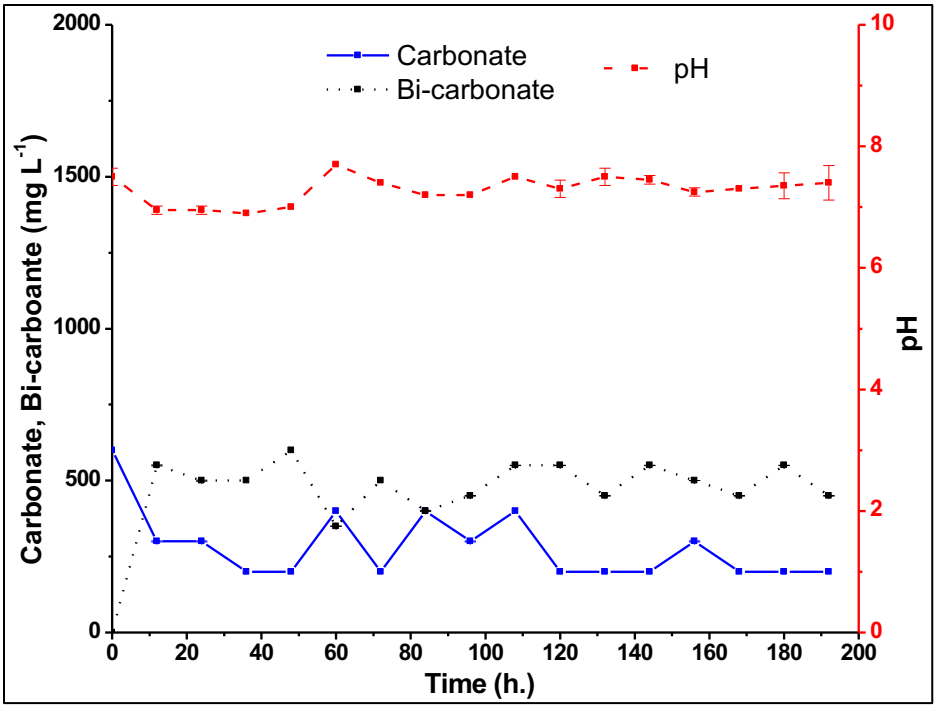

Fig. 4.24 Effects of CNS gas mixture on carbonate, bi-carbonate, and pH with respect to time

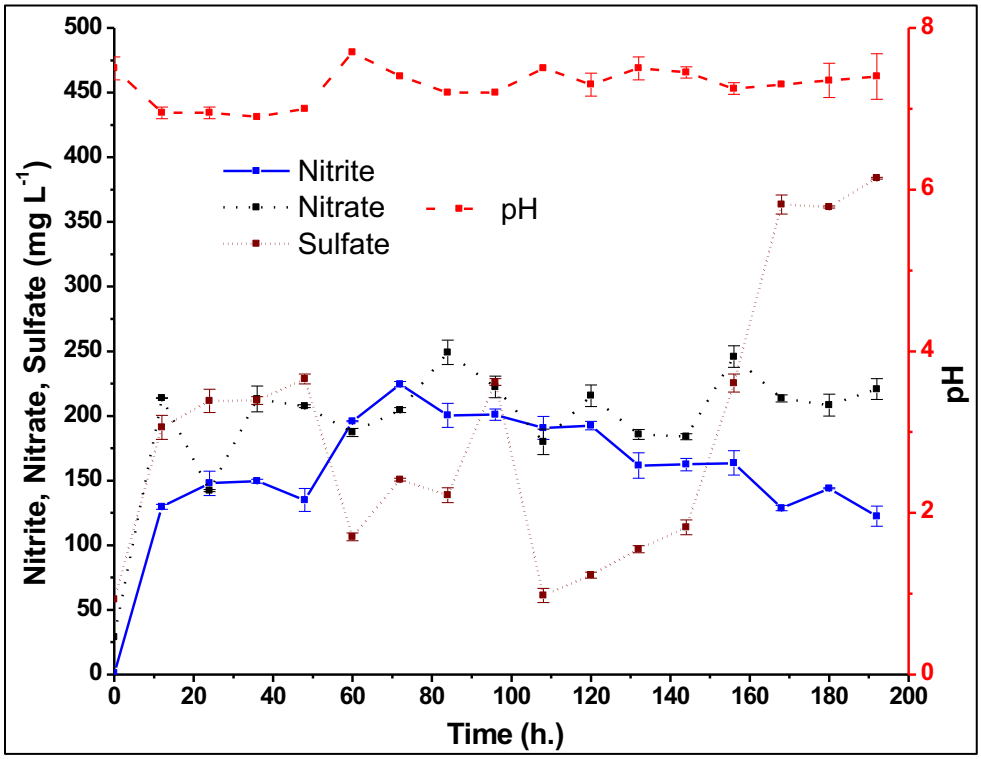

Fig. 4.25 Effects of CNS gas mixture on nitrite, nitrate, sulfate, and pH with respect to time

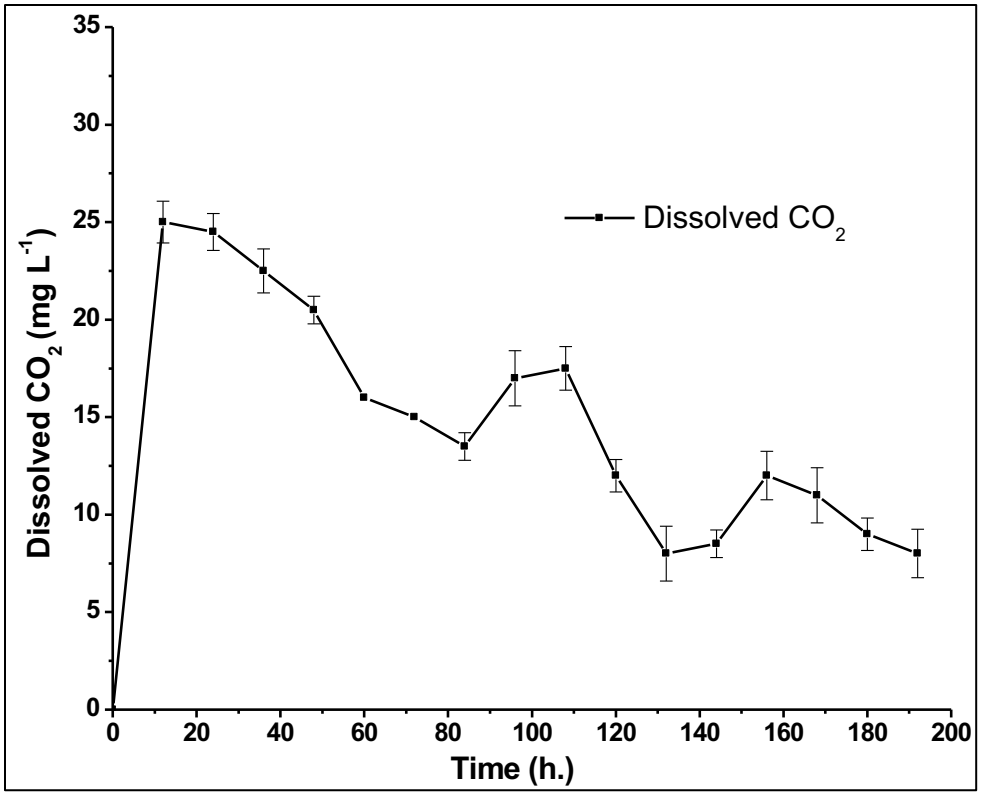

Fig. 4.26 Variation of dissolved CO_2 with respect to time

4.3.6 Nutrient utilization under different gaseous mixture

The combination of DWW with flue gas (CO_2, NO and SO_2) fixation and biomass production encourages higher microbial growth rates. Furthermore, DWW as growth media will lessen the freshwater and nutrient requirements, ultimately reducing the overall cost of the large-scale output (Razzak et al., 2015). Bacteria require essential nutrients such as carbon, nitrogen, and phosphorus for optimal growth. The utilization efficiency of various nutrients such as BOD, COD, PO_4^{3-}, SO_4^{2-}, NO_3^-, NO_2^- and Fe (II) by the bacterial consortium for different gaseous mixtures (C, N, S, CN, CS, CNS) were determined at the end of the cultivation period and are reported in Table 4.12. The utilization efficiency of BOD, COD and PO_4^{3-} was obtained in the range of 91.13% - 99.10%, 89.91% - 99.73%, and 94.30% - 98.18%, respectively for all six gas mixtures. The nutrient utilization efficiency of NO_3^- and NO_2^- was obtained in the range of 95.43% - 99.01% and 94.31% - 99%, respectively for C, S and CS gas mixtures. The higher utilization efficiency of NO_3^- and NO_2^- suggests that nitrate and nitrite ions are being utilized as a source of nitrogen for bacterial growth. The utilization efficiency for Fe (II) ion was 100% for all six gaseous mixtures. The possible reason behind this could be the lower initial concentration and utilization of Fe (II) ion as energy source during bacterial growth. The sulfate ion utilization efficiency was more than 98.21% for C, N and CN gas mixture. This suggested the utilization of sulfate ions as energy source by the bacterial consortium. The concentration of nutrients in effluent streams was determined to be considerably lower than the country's discharge limit except for BOD and COD values for N, S, CN, CS and CNS gas mixtures. The possible reason for higher values of BOD and COD could be the presence of a lower amount of oxygen in DWW for the degradation of biological and chemical pollutants. Hence, these results confirmed the use of nutrients and energy sources available in DWW by the bacterial consortium for their survival.

Table 4.12 Nutrient utilization efficiency by bacterial consortium at the end of bio-fixation period

Nutrient/energy source (mg L^{-1})	DWW concentration (mg L^{-1})	DWW concentration (after bio-fixation) (mg L^{-1})	Permissible limit (mg L^{-1})	Utilization efficiency %
C gas mixture				
$P–PO_4$	2.6 ± 0.1	0.05	1	98.18
BOD	362 ± 8	3.26	10	99.10
COD	3176 ± 36	40.33	125-150	99.73
SO_4^{2-}	464 ± 8	0.79	250	99.83
Fe (II)	0.021	0	0.3	100
$N\text{-}NO_3^-$	28.98 ± 1.5	0.20	10	99.01
$N\text{-}NO_2^-$	1.1 ± 0.4	0.01	1	99
N gas mixture				
$P–PO_4$	2.6 ± 0.1	0.08	1	97.11
BOD	362 ± 8	14,48	10	96
COD	3176 ± 36	146.63	125-150	95.37
SO_4^{2-}	464 ± 8	8.31	250	98.21
Fe (II)	0.021	0	0.3	100
S gas mixture				
$P–PO_4$	2.6 ± 0.1	0.12	1	95.2
BOD	362 ± 8	32.11	10	91.13
COD	3176 ± 36	230.89	125-150	92.73
Fe (II)	0.021	0	0.3	100
$N\text{-}NO_3^-$	28.98 ± 1.5	1.09	10	96.24
$N\text{-}NO_2^-$	1.1 ± 0.4	0.06	1	94.31
CN gas mixture				
$P–PO_4$	2.6 ± 0.1	0.13	1	94.81
BOD	362 ± 8	24.54	10	93.22
COD	3176 ± 36	51.76	125-150	98.37
SO_4^{2-}	464 ± 8	32.48	250	99.03
Fe (II)	0.021	0	0.3	100
CS gas mixture				
$P–PO_4$	2.6 ± 0.1	0.15	1	94.30
BOD	362 ± 8	29.97	10	91.72
COD	3176 ± 36	320.46	125-150	89.91
$N\text{-}NO_3^-$	28.98 ± 1.5	1.32	10	95.43
$N\text{-}NO_2^-$	1.1 ± 0.4	0.06	1	94.78
Fe (II)	0.021	0	0.3	100
CNS gas mixture				

$P–PO_4$	2.6 ± 0.1	0.13	1	95.13
BOD	362 ± 8	10.42	10	97.12
COD	3176 ± 36	260.11	125-150	91.81
Fe (II)	0.021	0	0.3	100

4.4 Product analysis

4.4.1 FT-IR analysis

The preliminary FT-IR analysis was performed in order to obtain bio-molecules from CO_2 and flue gas (CO_2, NO, and SO_2) bio-fixation studies. Culture obtained from bio-fixation studies was centrifuged, and cell pellet and supernatant were obtained. The FT-IR analysis of the cell pellet and supernatant was carried out. The biological samples are primarily complex and contain different proteins, lipids, nucleic acids, and carbohydrates. Hence, FT-IR spectrum is the result of their characteristic absorption bands and is explained in the following subsections:

4.4.1.1 Bio-fixation of CO_2 using *H. stevensii*

The FT-IR spectra of *H. stevensii* cell pellet obtained from CO_2 bio-fixation studies under three different cultivation conditions of DIW (100 mM $Na_2S_2O_3$), DWW (100 mM $Na_2S_2O_3$) and DWW (no additional sulfate) are depicted in Fig. 4.27 (Table A.1). The Peak assignment to the FT-IR spectra is carried out as per the literature (Bernhard S, 2008). The prominent peaks (3433.88, 3446.87 and 3434.21 cm^{-1}) in the region of 3700–3000 cm^{-1} indicate the presence of a significant quantity of hydroxyl groups (OH) in the structure (Fig. 4.27). These peaks correspond to the valence vibration of hydrogen-bonded with OH group, i.e., intra, inter or O–H stretching. Further, the transmittance of these peaks is approximately equal to 90%. This confirms that the number of hydrogen bond present in all the cell pellets is of same nature as per Beer–Lambert's law.

Transmittance in the region of 3000–2800 cm^{-1} is primarily due to symmetric and asymmetric stretching modes of C–H stretches, $CH_2<$ and CH_3- groups of lipids. The intensities of peak around 2960 cm^{-1} relates to CH_2 symmetric stretching and CH_2 asymmetric stretching. CH_2 symmetric and asymmetric also have peak around 2800 cm^{-1} which was not recognized in Fig. 4.27. This

may be due to the overlapping from strong OH band. Further, the region highlights the occurrence of fatty acids which is obvious from the cell wall.

The weak peak obtained at 2560 cm^{-1} in the region of 2800–1400 cm^{-1} is attributed to thiol stretch. It may be due to the formation and reduction of disulfide bonds catalyzed by thiol-disulfide exchanging enzyme (Ritz, 2002). The transmittance in the range of 2000–1900 cm^{-1} is either related to conjugate double bonds or "pseudo" symmetric alkynes as shown in Fig. 4.27. Further, the peak obtained at ~1650 and ~1547 cm^{-1} indicated the presence of amide I and amide II bands, respectively. These vibrations have originated from the amide groups (COONH) of proteins and are often an indicator of their secondary structure.

Significant heterogeneity was observed between the spectra for DIW (100 mM $Na_2 S_2O_3$), DWW (100 mM $Na_2 S_2O_3$) and DWW (no additional sulfate) in the spectral region of 1200–900 cm^{-1} and 1500–1300 cm^{-1} (Fig. 4.27). The band changes in this region are associated with main macromolecules such as carbohydrates and polysaccharides represented by glucose, fructose, and glycogen. Peaks obtained around 1200 and 1000 cm^{-1} are due to the antisymmetric and symmetric C–O and P–O areas as observed in DNA, ribonucleic acid (RNA) and phospholipids. Additionally, the peak 1450 and 834 cm^{-1} are related to the CO_3 out-of-plane deformation mode of the CO_3^{2-}. Further, as per IR peak assignment charts, C–OH stretches appear in 1400–1300 cm^{-1} region of the IR spectrum. This is in line with the peak assignments given in the literature as around 1390 cm^{-1} for CO_3^{2-} and around 1350 cm^{-1} for HCO_3^- (Jackson et al., 2009).

The cell-free supernatant obtained from CO_2 bio-fixation studies was extracted and FT-IR spectroscopy was applied in order to preliminary identify the molecules having economic benefits. The obtained FT-IR spectra of cell-free supernatant for culture conditions of DIW (100 mM Na_2

S_2O_3), DWW (100 mM $Na_2 S_2O_3$) and DWW (no additional sulfate) has shown in Fig. 4.28 (Table A.1) which indicated all four characteristic separated regions.

Region I (3700–3000 cm^{-1}) indicates strong peaks at wavenumbers 3453.97, 3451.20, 3435.09 cm^{-1}. It is attributed to the hydroxyl groups (OH) in the structure at appreciable amount (Fig. 4.28). The valence vibration of hydrogen-bonded with OH group i.e., intra, inter or O–H stretching is the reason for the obtained peaks (Bernhard S, 2008). Additionally, the transmittance of these peaks is greater than 90% for all the samples of supernatant. Thus, as per Beer-Lambert's law, number of hydrogen bond present is of same nature (Bernhard S, 2008).

In case of cell pellet, the region of 3000–2800 cm^{-1} is the region dominated by the fatty acids related to the bacterial cell membrane. The peaks around 2900 and 2800 cm^{-1} are assigned to the asymmetric or symmetric stretches of their methyl or methylene group, respectively. However, no such peaks were observed in the FT-IR spectra of the supernatant (Fig. 4.28). It may be due to the overlapping of strong –OH band with the weak signals of 2900 and 2800 cm^{-1}. It also signifies the limited amount of fatty acids present in the supernatant.

Region III (2800–1400 cm^{-1}) reflects the proteinaceous type content in the supernatant due to the two intense peaks around 1600 cm^{-1} related to the vibrations of amide I and II bands, respectively (Bernhard S, 2008). Further, 1500–1200 cm^{-1} is considered as a mixed region, as it is informative for proteins, fatty acids, and phosphate-carrying compounds (Fig. 4.28). In addition, peak at ~1230 cm^{-1} was due to the symmetric stretching of phosphodiester groups in nucleic acids or phospholipids. The peak at ~1383 cm^{-1} can be attributed to the symmetric bending of the methyl or methylene groups as well as the C–O symmetric stretching of carbohydrates (Bernhard S, 2008).

Region IV (1400–900 cm^{-1}) is shown the dominance of compounds having –OH bending vibrations, –C–O–H in-plane bending vibrations, $–CH_3$, out-of-plane bending vibrations, $–CH_2–$

wagging and twisting vibrations (Fig. 4.28). The C–OH of –COOH was indicated by the presence of vibrational bands around 1230 cm^{-1}. The spectral features of carboxylic acid in the energy range of 900–1200 cm^{-1} were caused by the vibrations of C–OH (alcohol), C–C, and C–H groups. As a whole, the FT-IR spectra predominantly indicated the functional groups associated with each region of carboxylic acid and polysaccharides (Bernhard S, 2008).

4.4.1.2 Bio-fixation of C, N and CN mixtures

The preliminary FT-IR analysis was used to identify valuable bio-molecule groups produced from bio-fixation studies for all three gaseous mixtures (C, N, and CN). The pellet was made using Potassium bromide (KBr), and FT-IR analysis of the cell pellet and cell-free supernatant was carried out. The subsequent paragraphs explain the analysis of the FT-IR spectrum for all three gaseous compositions.

Peaks were assigned to the FT-IR spectrum ranges based on the literature (Bernhard S, 2008). Figs. 4.29 and 4.30 (Table A.2) show the FT-IR spectra of cell pellet and cell-free supernatant, respectively for C, N, and CN gas mixtures. The presence of a substantial amount of hydroxyl group (OH^-) was confirmed from the prominent peaks (3460, 3451, 3449, 3443, 3439, 3302, and 3136 cm^{-1}) in the region of 3700–3000 cm^{-1} (Fig. 4.29 and 4.30). The presence of the O–H group also confirms the finding of the C–O bond near 1300–1000 cm^{-1} (Pavia et al., 2019). These peaks resemble the O–H stretching with a transmittance of nearly 99%.

The peaks were observed in the 3000–2800 cm^{-1} range suggested -CH stretching of long-chain fatty alcohols (Pavia et al., 2019). FT-IR spectrum peaks at 2900 cm^{-1} and 2800 cm^{-1} were assigned to the symmetric or asymmetric stretches of their methylene or methyl group (Fig. 4.29 and 4.30) (Pavia et al., 2019). Cell pellet peaks around 2900 cm^{-1} were only observed in the N and CN gas mixture (Fig. 4.29). This suggests the presence of fatty acids in the cell pellet. Except for mixture

C, such peaks were not found in the spectra of cell-free supernatant (Fig. 4.30). This indicated the limited presence of fatty acids in the supernatant. The two strong peaks about 1600 cm^{-1} are associated with the vibrations of the amide I and II bands. This represents the proteinaceous type presence in the cell pellet and cell-free supernatant (Bernhard S, 2008). The peaks in the range of 2000–1900 cm^{-1} were attributed to the pseudo-symmetric alkynes or conjugated double bonds.

A mixed region of 1500–1200 cm^{-1} depicted the presence of fatty acids, proteins, and phosphate-carrying compounds (Figs. 4.29 and 4.30). The symmetric bending of methylene and methyl groups and symmetric stretching of C–O of carbohydrates was attributed to the peak at 1384 cm^{-1}. The vibrational bands around 1270 cm^{-1} indicated the C–OH and COOH presence. The peak at 1200 cm^{-1} was due to the symmetric stretching of phosphodiester groups in the nucleic acid or phospholipids (Figs. 4.29 and 4.30).

For the cell pellet and cell-free supernatant, the peak at 834 cm^{-1} was attributed to the CO_3^{2-}, which was out of plane deformation mode of the CO_3^{2-}. As per the literature on the IR spectrum, the C-OH stretch occurs in the 1400–1300 cm^{-1} spectra region, which matches the peak assignment to CO_3^{2-} (1390 cm^{-1}) and HCO_3^{2-} (1350 cm^{-1}) (Bernhard S, 2008).

Thus, FT-IR spectroscopy of cell pellet and cell-free supernatant extract of bacterial consortium biomass indicated the presence of –OH, C–O, –CH, and C=C bonds as major functional groups. Hence, bio-fixation studies of C, N, and CN gas mixtures produced various organic compounds such as fatty alcohols and long-chain hydrocarbons. The structural composition obtained from FT-IR studies was further substantiated by conducting GC–MS analysis to identify and validate compounds in the cell pellet and cell-free supernatant extract.

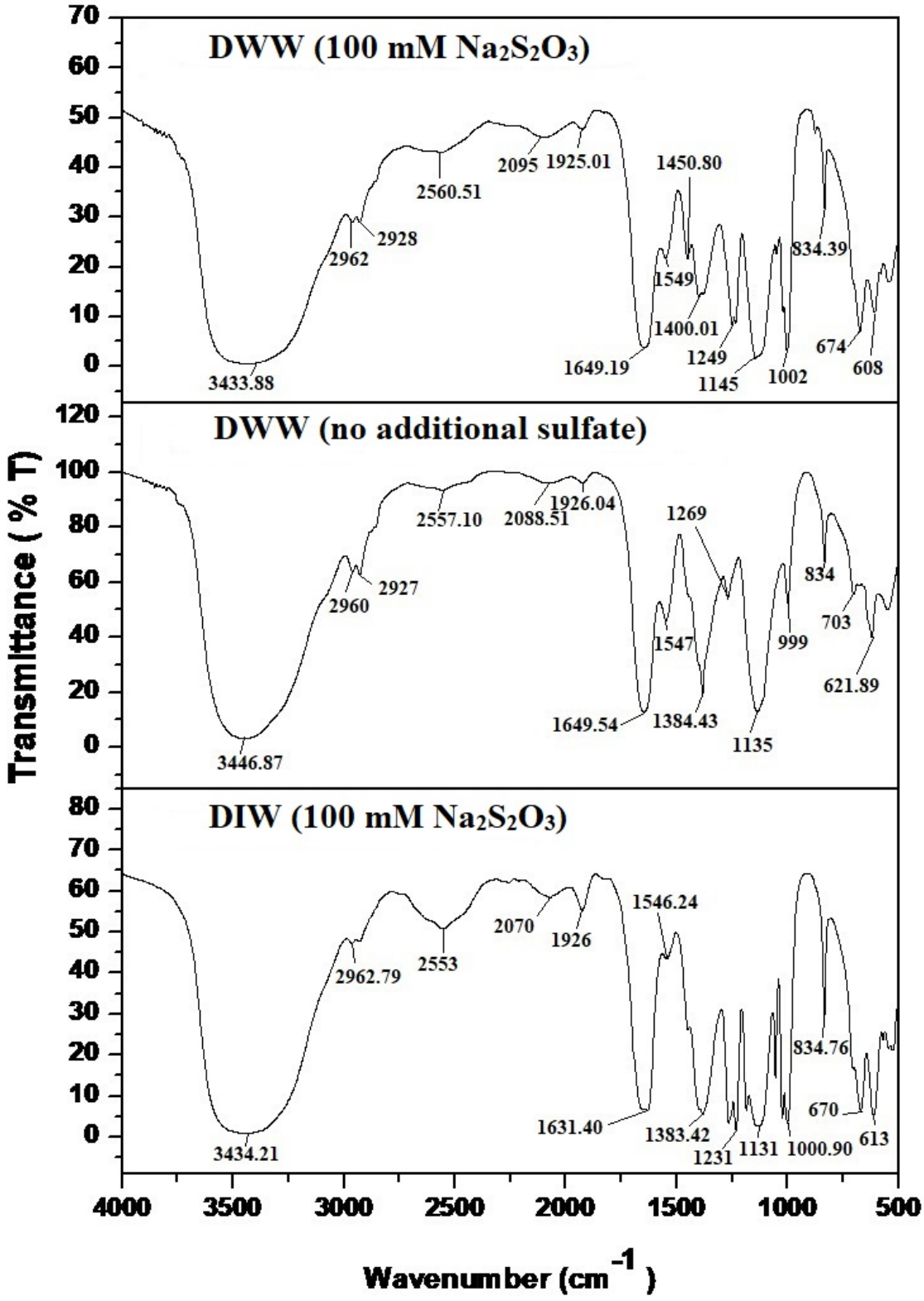

Fig. 4.27 FT-IR analysis of cell lysate at different culture conditions

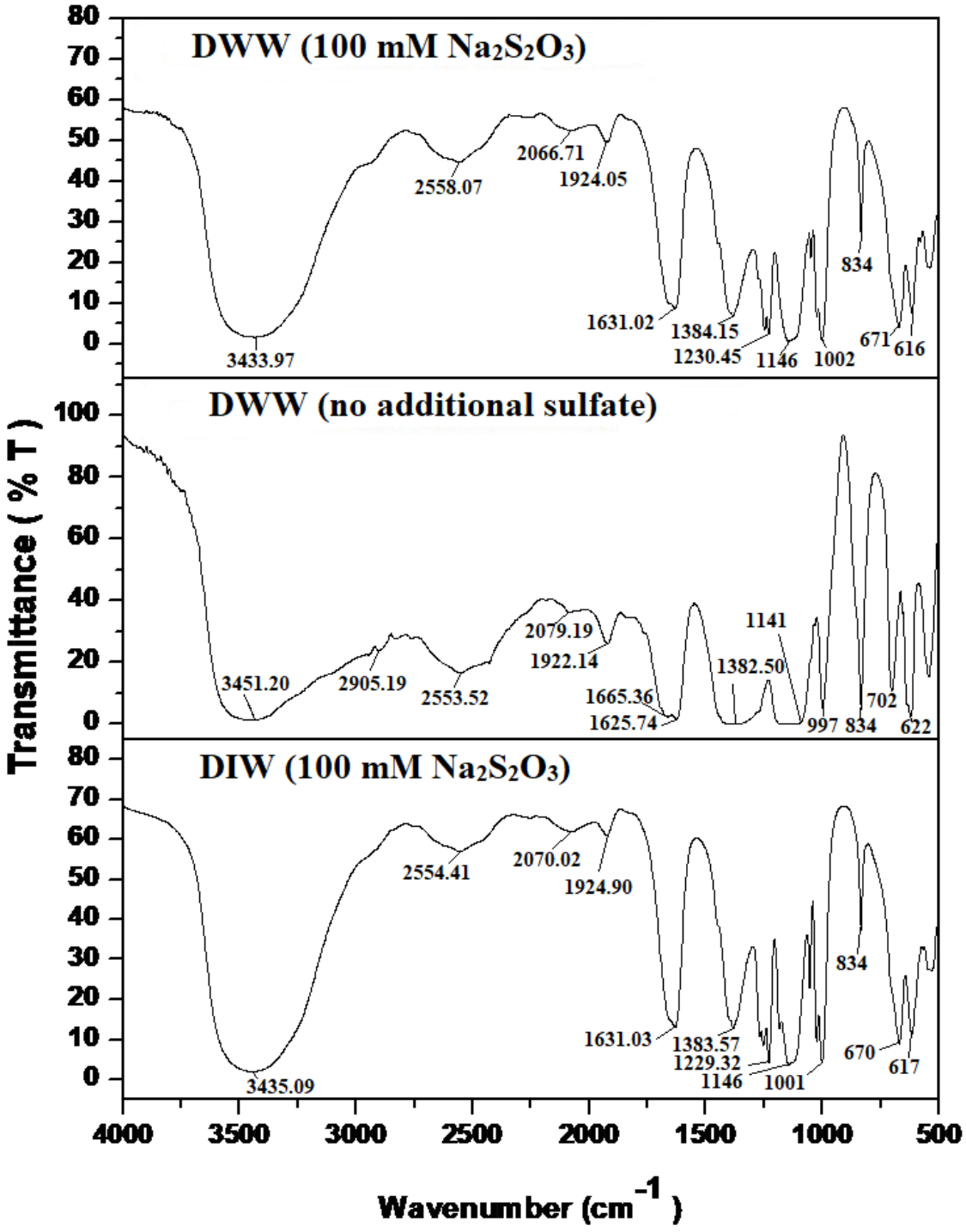

Fig. 4.28 FT-IR analysis of supernatant at different culture conditions

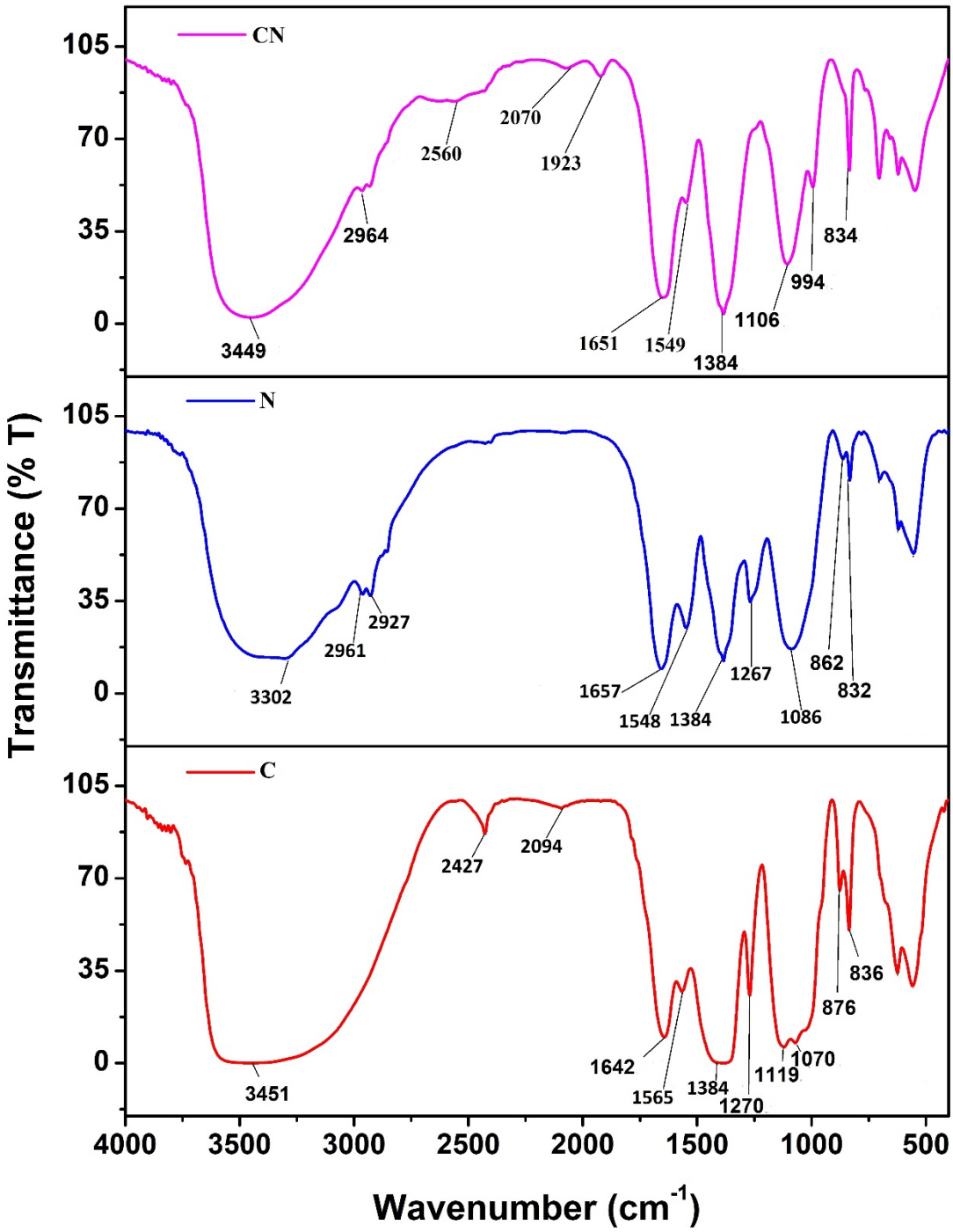

Fig. 4.29 FT-IR analysis of cell pellet at different gaseous mixture

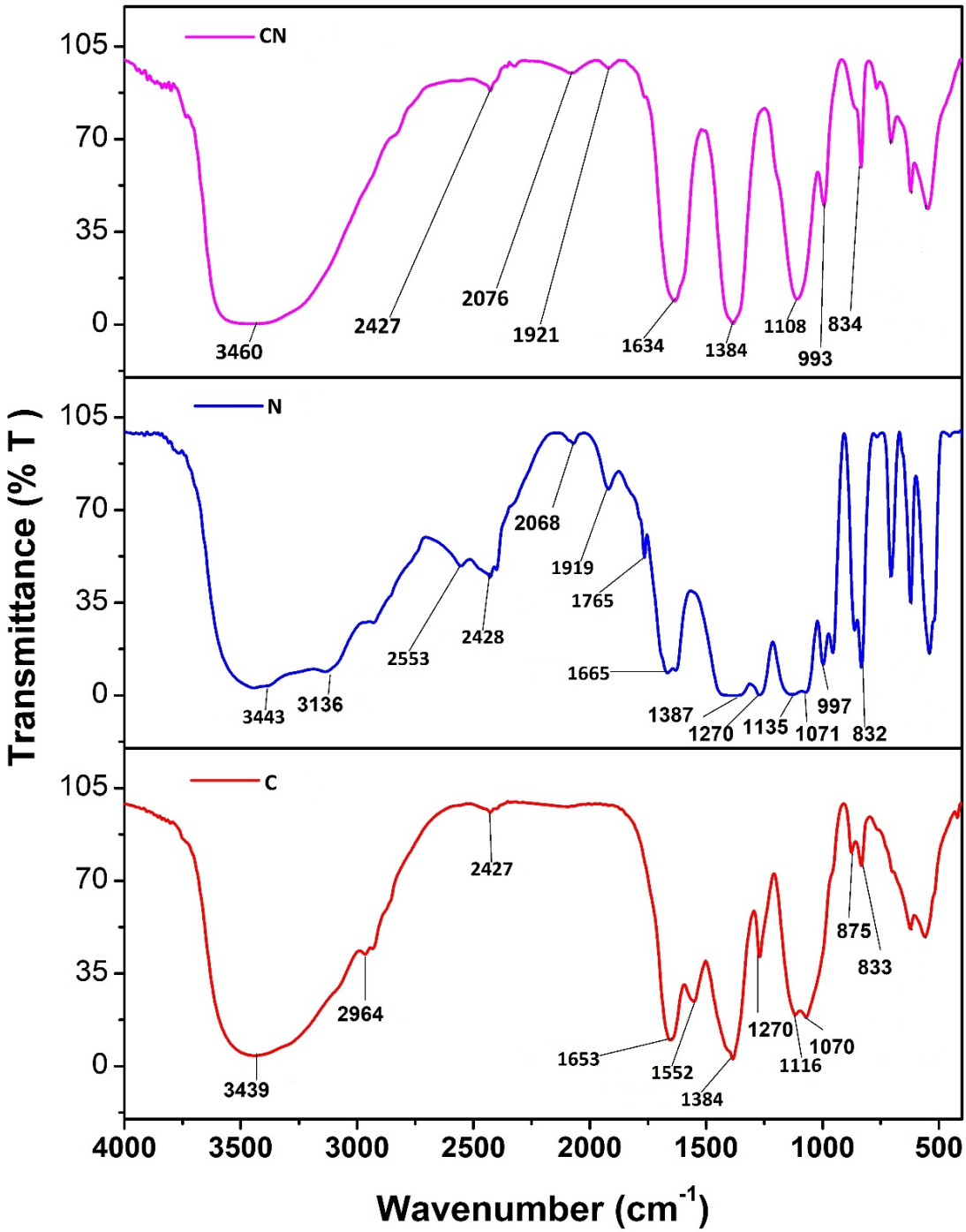

Fig. 4.30 FT-IR analysis of cell-free supernatant at different gaseous mixture

4.4.1.3 Bio-fixation of C, S and CS gas mixtures

Preliminary identification of the functional group present in the cell lysate and cell-free supernatant of gas mixture C, S and CS were analyzed using FT-IR spectroscopy. The FT-IR spectra of cell lysate and the cell-free supernatant extracts are shown in Fig. 4.31 and 4.32 (Table A.3), respectively. The existence of a wide and strong peak in the region of 3600–3000 cm^{-1} confirmed the presence of the hydroxyl group (–OH) of fatty alcohols (Fig 4.31). The peaks obtained in region 3000 –2800 cm^{-1} indicated the −CH stretching of long-chain fatty alcohols, but no peaks were found in this range for cell lysate of any of the gas mixtures. The formation and reduction of disulfide bonds referred to the thiol stretch and were obtained at 2427.84 cm^{-1} in the region of 2800–1400 cm^{-1}. The transmittance in the range of 2000–1900 cm^{-1} is either related to conjugate double bonds or "pseudo" symmetric alkynes. The wavenumber in the range of 1700–1600 cm^{-1} confirmed the− C=O group of either cell-bound fatty acids or the amide I band of proteins. Carbonate formation by CO_2 fixation has indicated the−C=O group in the region of wave number 1500 –1400 cm^{-1} (Basu et al., 2013). The presence of the O–H group confirms the finding of the C–O bond near 1300–1000 cm^{-1}. The peak in the region of 1100–1000 cm^{-1} confirmed the C−O− C and C–O stretching of the –COOH group of lipids or polysaccharides. The wavenumber in the range of 800–600 cm^{-1} confirmed the presence of compounds having an unsaturated double bond and –CH rock of long-chain alkanes (Kalsi, 2007; Pavia et al., 2019).

The FT-IR spectra for cell-free supernatant of bacterial consortium biomass showed a distinct peak in the range of 4000–500 cm^{-1} and are presented in Fig. 4.32. The peaks are divided into three different regions 3600–2500 cm^{-1}, 2000–1100 cm^{-1}, and 1000–500 cm^{-1}. The peak obtained at ~3400 cm^{-1} for C, S and CS gas mixtures has confirmed the presence of the –OH bond. The presence of the –OH group is also supported by the existence of a C–O bond in the range of 1300–

1000 cm^{-1}. For C gas mixture, the wavenumber at 2964.60 cm^{-1} represented the −CH stretching of long-chain fatty alcohols. The wavenumbers at 1653.29 for C gas mixture and 1638 for CS gas mixture indicated the presence of C=O stretch. The presence of a peak at 1633.02 cm^{-1} in the spectrum range (1656 cm^{-1} -1542 cm^{-1}) represents the C=C stretching of alkenes. The presence of a peak at ~1384 cm^{-1} for C, S and CS gas mixtures indicated either the –C=O group of carbonate ion formed due to the CO_2 bio-fixation or bending of –CH present in the aliphatic group. The strong peak was found in the region of 1200–1000 cm^{-1} and confirmed the presence of C–O vibrating stretch (Fig. 4.32). The wavenumber in the range of 800–600 cm^{-1} confirmed the presence of unsaturated double bond and –CH rock of long-chain alkanes (Kalsi, 2007; Pavia et al., 2019). Further, the transmittance of these peaks is approximately equal to 100%.

Thus, FT-IR spectroscopy of cell lysate and cell-free supernatant extract of bacterial consortium biomass indicated the existence of –OH, C–O, –CH and C=C bonds as major functional groups. Hence, bio-fixation studies of C, S and CS gas mixtures consist of various organic compounds of different fatty alcohols and long-chain hydrocarbons.

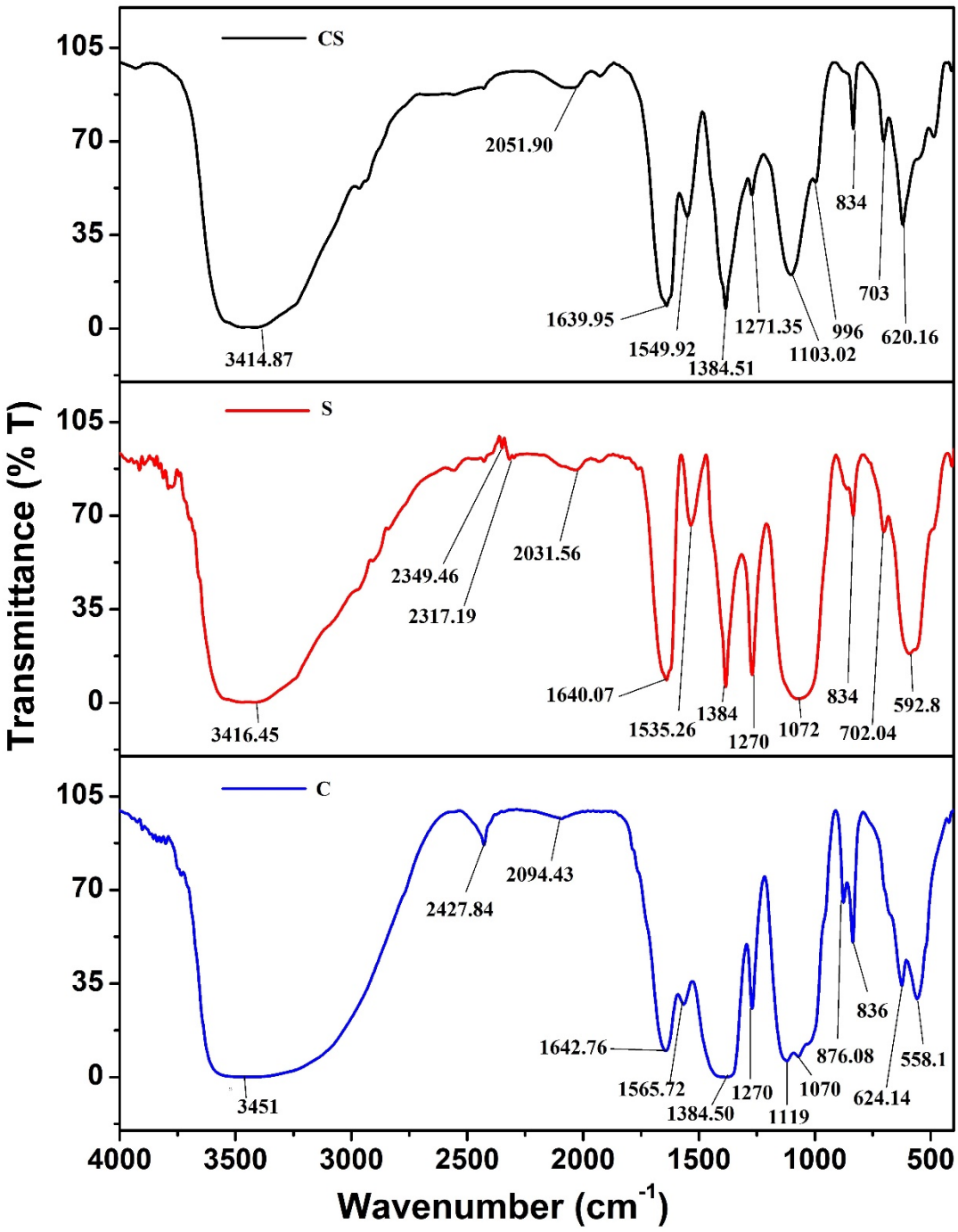

Fig. 4.31 FTIR analysis of cell lysate for C, S, and CS gas mixture

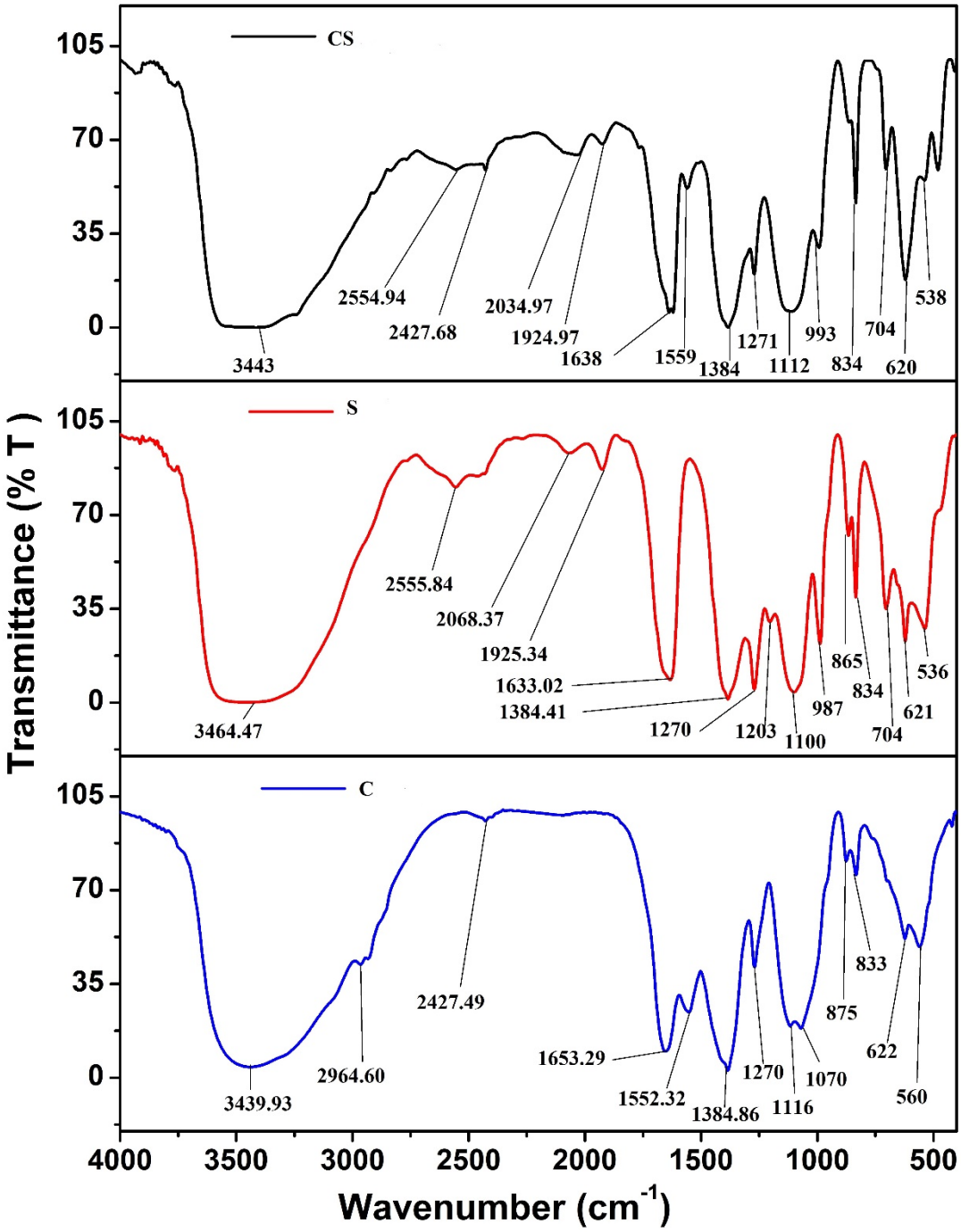

Fig. 4.32 FT-IR analysis of cell-free supernatant for C, S, and CS gas mixture

4.4.1.4 Bio-fixation of CNS gas mixture

FT-IR analysis was carried out to investigate the presence of the different functional groups in the product formed during the bio-fixation study of CNS gas mixture. Fig 4.33 (Table A.4) illustrates the FT-IR spectra of cell lysate and cell-free supernatant extract of simulated flue gas fixation studies. FT-IR spectroscopy has shown a distinct peak in the region of 4000–600 cm^{-1}.

The acquired spectra revealed a broad and prominent peak in the range of 3600-3000 cm^{-1}, which corresponds to the hydroxyl group (-OH) of fatty alcohols. The wavenumber at 2427.10 cm^{-1} in the region of 2800–1400 cm^{-1} represents the formation and reduction of disulfide bonds referred as the thiol stretch. The "pseudo" symmetric alkynes or formation of conjugate double bonds are indicated by the transmittance in the range of 2100–1900 cm^{-1}. The distinctive peak of the −C=O group represented by either the amide I band of proteins or the cell-bound fatty acids was confirmed by the wavenumber in the range of 1700–1600 cm^{-1}. Carbonate formation by CO_2 fixation was represented by the −C=O group in the region of wave number 1500 –1400 cm^{-1} (Basu et al., 2013). The existence of the O–H group was also confirmed by the C–O bond near 1300–1000 cm^{-1}. The wave number in the region of 1100–1000 cm^{-1} confirmed the C−O−C and C–O stretching of –COOH group from lipids or polysaccharides. The peaks in the range of 800–600 cm^{-1} confirmed the presence of compounds having an unsaturated double bond and –CH rock of long-chain alkanes (Kalsi, 2007; Pavia et al., 2019).

Bio-molecule representation for different group attribution is shown in Table A.5 (appendix A).

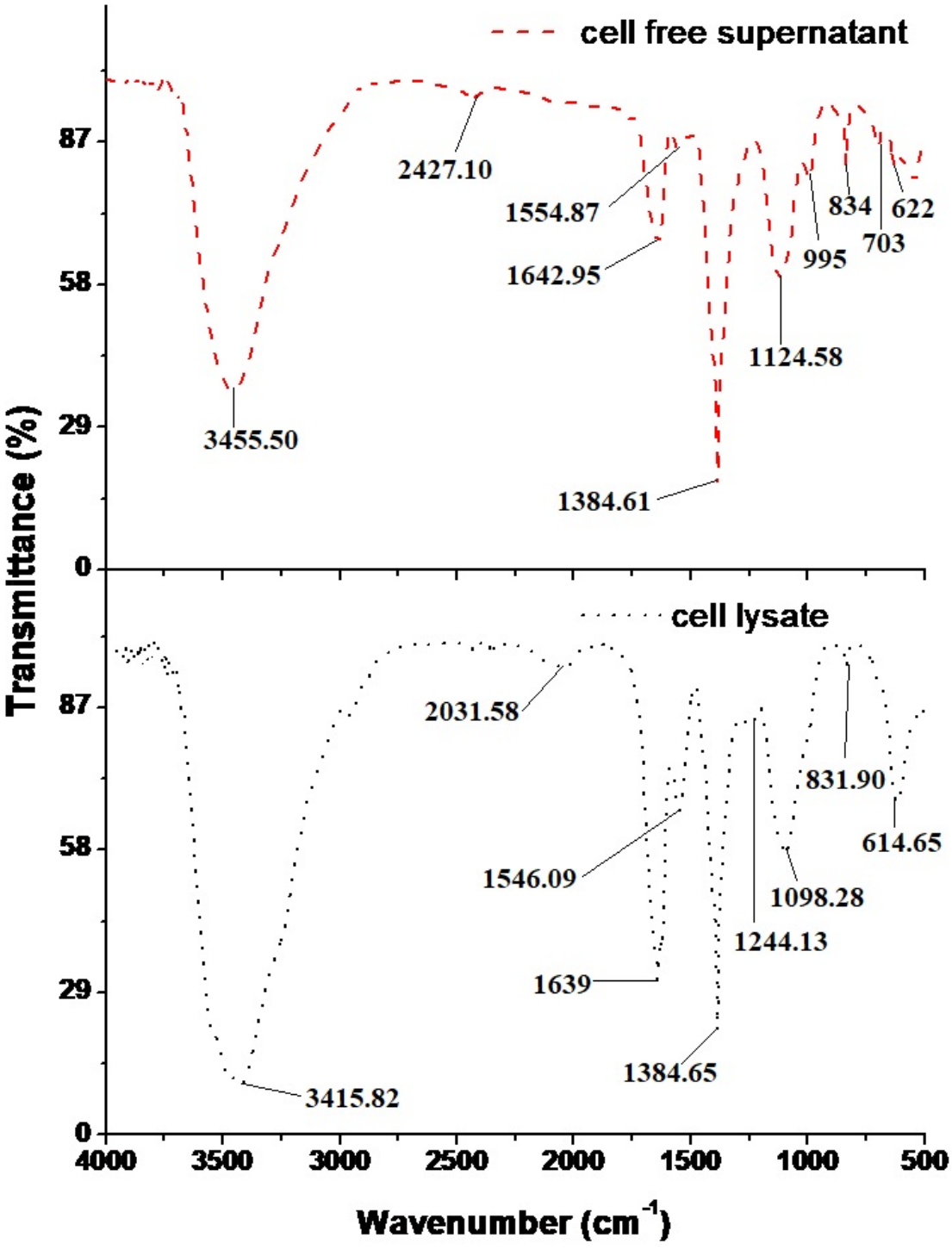

Fig. 4.33 FT-IR spectra of cell lysate and cell-free supernatant for bio-fixation of CNS gas mixture

4.4.2 GC-MS analysis

The cell lysate and supernatant obtained from CO_2 and flue gas (CO_2, NO and SO_2) bio-fixation studies are analyzed by GC-MS for identifying and confirming the different compounds present in the sample. The GC-MS technique is usually considered as specific test which gives insight about a particular substance present in a given sample. Further, this helps in developing the value addition strategy of recovering valuable compounds. The obtained spectra of GC-MS are matched with National Institute of Standards and Technology (NIST) mass spectra library and obtained results are illustrated in the subsequent subsections.

4.4.2.1 Bio-fixation of CO_2 using *H. stevensii*

The cell lysate is obtained via methodology described in Section 3.6.1 and resulting samples are analyzed with GC-MS. GC-MS analysis of the cell lysate extract of DIW (100 mM $Na_2 S_2O_3$), DWW (100 mM $Na_2 S_2O_3$) and DWW (no additional sulfate) show the presence of fatty alcohol and hydrocarbons in considerable amount with match quality ranging from 80% to 98% (Tables 4.13–4.15).

GC spectrum area of cell lysate from culture condition of DIW (100 mM $Na_2 S_2O_3$) has shown approximately 8.33% which comprised of fatty alcohols and has a carbon chain length ranging from C_8-C_{27}. The major fatty alcohols present are the compounds such as 2-Ethyl-1-hexanol (3.21%), 1-Dodecanol (0.84%), Hexadecanol (1.17%), n-Nonadecanol-1 (1.35%), Behenic alcohol (0.88%) and 1-Heptacosanol (0.88%) (Table 4.13). The fatty alcohols obtained from cell lysate extract of DWW (100 mM $Na_2 S_2O_3$) comprised of 2-Ethyl-1-hexanol (3.28%), 1-Dodecanol (0.83%), n-Tridecan-1-ol (1.20%), n-Pentadecanol (1.27%), Behenic alcohol (0.84%), 1-Heptacosanol (0.69%), and n-Tetracosanol-1 (0.41%). The total percentage areas of fatty alcohols obtained are 8.52% of the area of GC-MS spectrum (Table 4.14). The cell lysate extract obtained

from DWW (no additional sulfate) has shown the presence of 2-Ethyl-1-hexanol (2.39%), 1-Dodecanol (0.62%), n-Tridecan-1-ol (0.87%), n-Pentadecanol (1.00%), and Behenic alcohol (0.67%) (Table 4.15).

The obtained results indicated a minute increase in fatty alcohol content as the culture condition changed from DIW to DWW. It is due to the presence of such compounds, which are inherent to DWW and are utilized by *H. stevensii* for synthesizing fatty alcohols. However, the presence of thiosulfate ions shows negligible increment when DWW was used for CO_2 fixation studies. This indicated that it is not thiosulfate ions rather extreme culture conditions that drives *H. stevensii* to produce fatty alcohols (Mishra et al., 2017). Further, the percentage area of branched fatty alcohol (2-Ethyl-1-hexanol) decreased from 3.28% to 2.39% when DWW with thiosulfate was employed. This also suggests that the production of branched fatty alcohols is linked to the presence of energy source. The obtained results are in agreement with reported literature about bacterial production of fatty alcohols (Mudge, 2005; Youngquist et al., 2013). The obtained results were supported by the FT-IR analysis that highlighted the occurrence of compounds having long carbon chain length along with -OH group (Section 4.4.1.1).

GC-MS analysis of cell lysate extract of DIW (100 mM $Na_2 S_2O_3$), DWW (100 mM $Na_2 S_2O_3$) and DWW (no additional sulfate) confirmed the presence of alkane and alkene with match quality ranging from 80% to 98% (Tables 4.13–4.15). The percentage area of hydrocarbons is 5.65%, 8.73% and 8.73% of the total GC-MS spectra for cell lysate extract of DIW (100 mM $Na_2 S_2O_3$), DWW (100 mM $Na_2 S_2O_3$) and DWW (no additional sulfate), respectively. The major compounds of hydrocarbons identified are Dodecane, Tetradecane and Nonadecane (Tables 4.13–4.15). It can be seen that the % area of total hydrocarbon was found to increase with change in the cultivation condition from DIW to DWW water. However, the presence of thiosulfate ions does not show any

considerable effect on the synthesis of hydrocarbons. It may be due to the occurrence of compounds other than essential compounds in the DWW. The FT-IR spectrum of the cell lysate extract at all three culture conditions suggested the presence of hydrocarbons and is also supported by the GC-MS analysis.

The obtained result of the supernatant extract of DIW (100 mM $Na_2 S_2O_3$), DWW (100 mM $Na_2 S_2O_3$) and DWW (no additional sulfate) revealed the occurrence of fatty alcohol and branched hydrocarbons in considerable amounts with match quality ranging from 79% to 94% (Tables 4.16-4.18).

The GC-MS analysis of supernatant obtained from the culture conditions of DIW (100 mM $Na_2 S_2O_3$) showed approximately 5.54% of fatty alcohols having carbon chain length ranges from C_{12}-C_{14}. The major fatty alcohols present are the compounds such as 1-Dodecanol (4.03%) and Tetradecanol (1.51%) (Table 4.16). The fatty alcohols obtained from supernatant extract of DWW (100 mM $Na_2 S_2O_3$) are mainly n-Nonadecanol-1(0.11%) (Table 4.17). The Cell lysate extract obtained from DWW (no additional sulfate) has shown the presence of 1-Dodecanol (3.69%), n-Tridecan-1-ol (1.52%), n-Pentadecanol (0.88%), and n-Heptadecanol-1 (0.53%). This revealed the presence of 6.62% of the total GC-MS spectrum area (Table 4.18).

The obtained results indicated the increase in fatty alcohol content as the culture conditions changed from DIW to DWW. It owes to the compounds which are inherent to DWW and utilized by *H. stevensii* for synthesizing the fatty alcohols. However, the absence of thiosulfate found to affect the fatty alcohol synthesis and indicated the considerable increment when DWW was used for CO_2 fixation studies. This indicated that thiosulfate absence results in the extracellular synthesis of *H. stevensii*. Further, the branched fatty alcohol (2-Ethyl-1-hexanol) was found to be absent in the GC-MS spectra of all three culture conditions. The obtained results are confirmed by

the FT-IR analysis that highlighted the occurrence of compounds having long carbon chain length along with -OH group (Section 4.4.1.2).

Additionally, GC-MS analysis of supernatant extract of DIW (100 mM $Na_2 S_2O_3$) and DWW (no additional sulfate) indicated the presence of branched alkane and alkene with match quality ranging from 79% to 90% (Tables 4.16–4.18). The percentage area of branched hydrocarbons is obtained as 5.38% and 5.22% of the total GC-MS spectra for supernatant extract of DIW (100 mM $Na_2 S_2O_3$) and DWW (no additional sulfate), respectively. The major compounds of hydrocarbons identified are Undecane, 4,7-dimethyl-, Decane, 2,4- dimethyl-, Hexadecane and Heptadecane (Tables 4.16-4.18). The % area of total hydrocarbon found to increase with change in cultivation condition from DIW to DWW (Tables 4.16–4.18). Further, the presence thiosulfate ions do not show any considerable effect on the synthesis of hydrocarbons. However, the absence of thiosulfate ions results in the synthesis of un-branched long-chain hydrocarbons (Tables 4.16-4.18). The obtained results are in line with the FT-IR spectrum of the supernatant extract under all three culture conditions.

Hence, the isolate *H. stevensii* has shown its ability to capture CO_2 while using DWW as growth media and can also be utilized in tandem to extract valuable bio-molecule such as fatty alcohol as suggested by FT-IR and GC-MS analysis and hence, solve the dual-purpose.

Table 4.13 GC-MS analysis of cell lysate obtained from DIW (100 mM $Na_2S_2O_3$)

S.No.	Run Time	Compound	% Area	Match quality
1.	7.445	2-Ethyl-1-hexanol	3.21	98%
2.	8.62	Dodecane	0.32	95%
3.	10.040	1-Dodecanol	0.84	95%
4.	10.170	Tridecane	0.36	96%
6.	11.925	Heptadecane	0.12	88%
7.	12.885	1-Hexadecanol	1.17	96%
8.	12.995	Tetradecane	0.48	98%
9.	14.140	Hexadecane	0.39	89%
10.	14.280	Octadecane	0.28	81%
11.	14.705	Heptadecane, 8-methyl-	0.33	88%
12.	15.409	n-Nonadecanol-1	1.35	94%
13.	16.654	Nonadecane	0.56	94%
14.	17.672	Behenic alcohol	0.88	96%
15.	17.747	Heneicosane	0.56	97%
16.	18.791	Eicosane	0.61	89%
17.	19.190	Tetracosane	0.23	86%
18.	19.420	2-Methyltriacontane	0.22	81%
19.	19.721	1-Heptacosanol	0.88	93%
20.	21.960	Dotriacontane	0.15	87%
21.	26.396	Tetracontane	0.69	94%
22.	30.813	Tetrapentacontane	0.35	90%
Total Fatty Alcohol			8.33%	
Total Hydrocarbons			5.65%	

Table 4.14 GC-MS analysis of cell lysate obtained from DWW (100 mM $Na_2S_2O_3$)

S.No.	Run Time	Compound	% Area	Match quality
1.	7.447	2-Ethyl-1-hexanol	3.28	98%
2.	8.62	Undecane	0.33	95%
3.	10.045	1-Dodecanol	0.83	95%
4.	10.172	Tridecane	0.35	96%
6.	12.888	n-Tridecan-1-ol	1.20	96%
8.	12.994	Tetradecane	0.5	98%
9.	14.141	Heptadecane	0.36	90%
10.	14.279	Octadecane	0.29	80%
11.	14.704	Eicosane	0.37	91%
12.	15.410	n-Pentadecanol	1.27	94%

13	15.5	Octadecane	0.71	96%
14.	16.654	Heneicosane	0.78	95%
15.	17.674	Behenic alcohol	0.84	96%
16.	17.749	Nonadecane	0.79	95%
17.	18.791	Octacosane	0.73	92%
18.	19.215	11-Methyltricosane	0.23	85%
19.	19.420	Dotriacontane	0.42	85%
20.	19.721	1-Heptacosanol	0.69	94%
21.	20.476	Tetratetracontane	0.26	90%
22.	20.734	Octacosane	0.49	92%
23.	21.591	n-Tetracosanol-1	0.41	89%
24.	21.646	Triacontane	0.41	92%
25.	21.962	Dotriacontane	0.34	87%
26.	22.543	Heneicosane	0.32	93%
27.	26.396	Tetracontane	0.31	93%
28.	29.582	Tetrapentacontane	0.28	90%
29.	30.818	Hexatriacontane	0.46	80%
Total Fatty Alcohol			8.52%	
Total Hydrocarbons			8.73%	

Table 4.15 GC-MS analysis of cell lysate obtained from DWW (no additional sulfate)

S.No.	Run Time	Compound	% Area	Match quality
1.	7.445	2-Ethyl-1-hexanol	2.39	98%
2.	8.618	Undecane	0.26	96%
3.	10.042	1-Dodecanol	0.62	95%
4.	10.170	Dodecane	0.31	96%
5.	11.270	Dodecane, 4,6-dimethyl-	0.20	93%
6.	12.886	n-Tridecan-1-ol	0.87	96%
7.	12.994	Tetradecane	0.64	98%
8.	14.140	Heptadecane	0.54	90%
9.	14.280	Hexadecane	0.62	93%
10.	14.703	Eicosane	0.28	90%
11.	15.410	n-Pentadecanol	1.00	94%
12.	15.499	Octadecane	0.76	96%
13.	16.045	Pentadecane, 2,6,10-trimethyl	0.28	86%
14.	16.653	Heneicosane	1.20	96%
15.	17.140	Heptadecane, 8-methyl-	0.44	91%
16.	17.440	Heptadecane, 3-methyl-	0.44	86%
17.	17.673	Behenic alcohol	0.67	95%

18.	17.747	Nonadecane	0.88	96%
19.	17.817	Hexadecane, 2,6,10,14-tetramethyl-	0.56	92%
20.	18.180	Dodecane, 2-methyl-	0.33	85%
21.	18.340	13-Methylheptacosane	0.21	81%
22.	18.790	Octacosane	1.92	84%
23.	19.193	Nonadecane, 9-methyl-	0.44	89%
24.	19.786	Heneicosane	1.09	96%
25.	20.263	5,15-Dimethylnonadecane	0.20	85%
26.	20.473	Tetratetracontane	0.59	94%
27.	20.735	Octacosane	1.10	93%
28.	21.083	Pentadecane, 8-hexyl-	0.80	87%
29.	21.645	Triacontane	0.95	93%
30.	21.966	Dotriacontane	0.78	90%
31.	22.547	Heneicosane	0.67	94%
32.	26.399	Tetracontane	0.75	94%
33.	29.572	Tetrapentacontane	0.33	91%
34.	30.814	Hexatriacontane	0.27	89%
Total Fatty Alcohol			8.52%	
Total Hydrocarbons			8.73%	

Table 4.16 GC-MS analysis of supernatant extract obtained from DIW (100 mM $Na_2 S_2O_3$)

S.No.	Run Time	Compound	% Area	Match quality
1.	7.073	1-Dodecanol	4.03	91%
2.	7.206	Undecane, 4,7-dimethyl-	2.63	79%
3.	9.892	1-Tetradecanol	1.51	93%
4.	10.004	Decane, 2,4-dimethyl-	1.05	88%
5.	12.415	1-Nonadecene	0.65	89%
Total Fatty Alcohol			5.54%	
Total Hydrocarbons			5.38%	

Table 4.17 GC-MS analysis of supernatant extract obtained from DWW (100 mM $Na_2 S_2O_3$)

S.No.	Run Time	Compound	% Area	Match quality
1.	12.414	n-Nonadecanol-1	0.11	90%

Table 4.18 GC-MS analysis of supernatant extract obtained from DWW (no additional sulfate)

S.No.	Run Time	Compound	% Area	Match quality
1.	7.076	1-Dodecanol	3.69	92%
2	7.207	Dodecane	1.85	85%
3	9.893	n-Tridecan-1-ol	1.52	94%
4	9.998	Tetradecane	0.64	90%
5	12.414	n-Pentadecanol	0.88	92%
6	12.505	Hexadecane	0.37	87%
7	13.657	Heptadecane	0.75	88%
8	14.679	n-Heptadecanol-1	0.53	87%
9	14.752	Octadecane	0.52	90%
10	15.793	Heneicosane	0.51	88%
11	16.792	Eicosane	0.58	84%
Total Fatty Alcohol			6.62%	
Total Hydrocarbons			5.22%	

4.4.2.2 Bio-fixation of C, N and CN gas mixtures

GC-MS analysis of cell pellet and cell-free supernatant for all three gaseous mixtures (C, N, and CN) showed the presence of fatty alcohol and hydrocarbons in considerable amounts with match quality ranging from 84% to 100% and carbon chain lengths ranging from C_7–C_{27} (Table 4.19-4.24).

The maximum amount of fatty alcohol content in cell pellet extract was obtained as 33.33% for CN gas mixture. The amount of fatty alcohol was estimated as 28.43% and 21.24% for C and N gas mixture, respectively (Table 4.25). The amount of fatty alcohol achieved in cell-free supernatant for C, N, and CN mixture was found as 24.35%, 26.34%, and 28.59%, respectively (Table 4.25). The amount of fatty alcohol was significantly higher for the simultaneous bio-fixation of CO_2 (g) and NO (g) as compared to the individual gas component fixation. The major fatty alcohols present in cell pellet and cell-free supernatant include 1-Tertadecanol, 1-Heptacosanol, 1-Hexacosanol, 1-Decanol, 1-Pentacosanol, 1-Hexadecanol, and n-Tetracosanol-1 (Table 4.19-4.24). The acquired results are consistent with previous research on bacterial fatty alcohol production (Mudge, 2005; Youngquist et al., 2013). The results are coherent with FT-IR analysis, which revealed the presence of molecules with long carbon chains and –OH groups.

Additionally, GC-MS analysis of cell pellet and cell-free supernatant extract also confirmed the presence of alkane and alkene with match quality ranging from 83% to 100% (Table 4.19-4.24). The percentage area of hydrocarbons was 18.47%, 26.33%, and 18.64% of the total GC-MS spectra for cell pellet extract of C, N, and CN gas mixture, respectively (Table 4.25). The percentage area of hydrocarbons was obtained as 28.11%, 25.83%, and 21.97% of the total GC-MS spectra for a cell-free supernatant extract of C, N, and CN gas mixture, respectively (Table 4.25). The major compounds of hydrocarbons were identified as 1-Dodecene, Tetradecane, 1-

Pentadecene, 1-Nonadecene, 1-Heptadecene, 1-Tridecene, 1-Tetradecene and Hexadecane (Table 4.19-4.24). The obtained results align with the FT-IR results of the cell lysate and supernatant extract under all three gaseous conditions.

Hence, the bacterial consortium showed its ability to capture CO_2 (g) and NO (g) simultaneously while using domestic wastewater as growth media and energy source. The concurrent production of valuable bio-molecules like fatty alcohol and long-chain hydrocarbons makes this process be feasible and more sustainable in large-scale applications.

4.4.2.3 Bio-fixation of C, S, and CS gas mixtures

GC-MS analysis of cell lysate extract showed the presence of fatty alcohol and long-chain hydrocarbon in significant amounts with match quality ranging from 87% to 100% for C, S, and CS gas mixture (Table 4.19, 4.26-4.27). GC spectrum area of 28.43%, 18.87%, and 21.24% was comprised of fatty alcohols for C, S and CS gas mixture, respectively, and have carbon chain length ranging from C_{14} to C_{27}. For C gas mixture, fatty alcohols were mainly comprised of the compounds such as 1-Tertadecanol (5.87%), Phenol, 3,5-bis (1,1dimethylethyl)- (5.60%), 1-Heptacosanol (7.96%), n-Hexadecanoic acid (1.82%), and 1-Hexacosanol (5.99%) (Table 4.19). The S gas mixture showed the presence of 18.87% of fatty alcohol, which included 2,4-Di-tert-butylphenol (3.28%), 1-Hexadecanol (5.35%), n-Hexadecanoic acid (1.63%), 1-Heptacosanol (4.55%), and 1-Hexacosanol (3.41%) (Table 4.26). The major compounds of fatty alcohol present in the CS gas mixture were 2,4-Di-tert-butylphenol (3.33%), 1-Hexadecanol (5.56%), n-Hexadecanoic acid (3.18%), 1-Heptacosanol (4.66%), and 1-Hexacosanol (3.34%). Saturated, unsaturated, and branched hydrocarbons were found to be 21.24% of the total area of cell lysate extract. In addition, cell lysate extract of C, S, and CS gas mixture revealed the presence of long-chain hydrocarbons in the range of 18.47%, 22.13%, and 25.79% of GC spectrum area,

respectively with match quality of 83% to 100% (Table 4.19, 4.26-4.27). The major compounds present for C, S, and CS gas mixtures were 1-Tridecene, 1-Nonadecene, Floxuridine, 1-Dodecene, 1-Tetradecene, Eicosane, and 1,3,5-Trisilacyclohexane. The obtained results are coherent with FT-IR analysis, which revealed the presence of molecules with long carbon chains, hydrocarbons and -OH groups.

The GC-MS analysis of cell-free supernatant revealed the presence of fatty alcohol, alkane, and alkene in considerable amounts with match quality ranging from 86% to 100% (Table 4.22, 4.28-4.29). The GC-MS analysis of cell-free supernatant obtained for the C gas mixture study showed ~24.35% of fatty alcohols have a carbon chain length ranging from C_7-C_{27}. The major fatty alcohols present are the compounds such as Benzoic acid (1.12%), Phenol, 3,5-bis (1,1-dimethylethyl)- 1- (5.04%), n-Tetracosanol-1 (8.15%), 1-Heptacosanol (6.36%), and 1-Hexacosanol (3.29%) (Table 4.22). Fatty alcohols account for 20.39% of the area of the total extracellular cell extract for S gas mixture. The major compounds of fatty alcohols are obtained as 1-Dodecanol (1.22%), 1-Tetradecanol (3.95%), 2,4-Di-tert-butylphenol (2.60%), 1-Hexadecanol (4.96%), Hexadecanoic acid (1.38%), n-Hexadecanoic acid (1.79%), 1-Heptacosanol (3.94%), Erucic acid (0.40%), 1-Hexacosanol (2.87%), and Octadecanoic acid (1.23%) (Table 4.30). For CS gas mixture, 19.12% of GC spectrum area was present as fatty alcohols that include 1-Dodecanol (0.40%), 2,4-Di-tert-butylphenol (2.43%), 1-Hexadecanol (4.34%), Hexadecanoic acid (1.17%), n-Hexadecanoic acid (3.45%), Octadecanoic acid (1.12%), 1-Heptacosanol (3.32%), Erucic acid (0.27%), and 1-Hexacosanol (2.62%) (Table 4.29). Additionally, the saturated, unsaturated, and branched hydrocarbons were found to be 28.11%, 20.95% and 21.77% of total cell-free supernatant extract for C, S, and CS gas mixtures, respectively. The major compounds of

hydrocarbons identified are 1-Dodecene, Tetradecane, 1-Pentadecene, 1-Nonadecene, and 1-Heptadecene (Table 4.22, 4.28-4.29).

4.4.2.4 Bio-fixation of CNS gas mixture

Table 4.30 shows the GC-MS analysis of cell lysate extract for the bio-fixation study of simulated flue gas. The compounds were segregated based on their match quality and % area. The cell lysate extract from semi-continuous bio-fixation studies of simulated flue gas shows the presence of different fatty alcohol and hydrocarbons in substantial amounts with match quality ranging from 92-100% (Tables 4.30). GC spectrum area of cell lysate from CNS gas mixture study showed ~16.90% fatty alcohols and ~23.73% long chain hydrocarbons having the carbon chain length ranging from C_9-C_{54}. The primary fatty alcohols present in the cell lysate extract were comprised of 1-Dodecanol (0.56%), n-Hexadecanoic acid (3.62%), Octadecanoic acid (1.20%), 1-Heptacosanol (4.56%) and 1-Hexacosanol (3.42%) (Table 4.30). The long-chain hydrocarbons present in the cell lysate extract include 1-Tridecene (3.16%), 1-Tetradecene (3.99%), 1-Nonadecene (6.01%), Floxuridine (2.52%), and 1,3,5-Trisilacyclohexane (3.11%). Hexadecane, Heptadecane, Eicosane, Tetracosane, and Tetrapentacontane were also present in the trace amount (Table 4.30). GC-MS analysis of cell-free supernatant for the bio-fixation of simulated flue gas was illustrated in Table 4.31. The cell-free supernatant contains 13.44% fatty alcohol and 19.18% hydrocarbons of GC spectrum area with match quality ranging from 92-100% and having a carbon chain length of C_9-C_{54}. The major compounds of fatty alcohols were 1-Tetradecanol (1.74%), 2,4-Di-tert-butylphenol (3.08%), 1-Hexadecanol (3.51%), Hexadecanoic acid (3.39%), and 1-Hexacosanol (1.72%). Moreover, the saturated, unsaturated, and branched hydrocarbons were found to be in the form of Hexadecane (1.11%), Eicosane (2.08%) and 1-Heptadecene (Table 4.31).

Table 4.19 GC-MS analysis of cell lysate extract obtained from C gas mixture

S.No.	Run time	Compound	% Area	Match quality
1	5.106	1-Tridecene	1.85	100%
2	6.784	Hexadecane	0.37	100%
3	7.237	Naphthalene, 1-methyl-	0.25	99%
4	7.767	Dodecane, 4,6-dimethyl-	0.09	99%
5	9.271	1-Tetradecanol	5.87	100%
6	9.87	Heptadecane	0.14	97%
7	11.404	2,6,10-Trimethyltridecane	0.24	99%
8	11.527	Eicosane	0.59	100%
9	12.337	Phenol, 3,5-bis (1,1 dimethylethyl)-	5.60	100%
10	14.016	1-Decene, 3,3,4-trimethyl-	0.26	97%
11	14.893	Pentadecane, 2,6,10,14-tetramethyl-	0.10	95%
12	17.418	1-Chloroeicosane	0.08	96%
13	17.691	Eicosanoic acid	0.12	91%
14	17.782	Tridecane, 3-methylene-	0.16	99%
15	17.974	1-Nonadecene	10.11	100%
16	18.04	Heneicosane	0.25	98%
17	18.195	Cyclohexane, (1,2,2-trimethylbutyl)-	0.31	100%
18	18.903	Dotriacontane	0.17	99%
19	20.361	Tetracosane	0.51	100%
20	20.771	Tetrapentacontane, 1,54-dibromo-	0.24	90%
21	21.321	3-Methyldotriacontane	0.12	99%
22	21.676	n-Hexadecanoic acid	1.82	92%
23	21.867	Hexadecane, 2-methyl-	0.38	97%
24	24.185	Tetrapentacontane	0.29	98%
25	24.995	Octadecanoic acid	0.64	100%
26	25.317	1-Heptacosanol	7.96	100%
27	27.607	Triacontane, 1,30-dibromo-	0.10	83%
28	28.537	1-Hexacosanol	5.99	100%
29	30.23	Floxuridine	1.05	98%
30	32.806	1,3,5-Trisilacyclohexane	0.71	100%
31	35.594	Hexacontane	0.10	98%
32	46.301	1-Pentacosanol	0.43	100%
Total Fatty Alcohol			28.43%	
Total Hydrocarbons			18.47%	

Table 4.20 GC-MS analysis of cell pellet obtained from N gas mixture

S.No.	Run time	Compound	% Area	Match quality
1	5.039	1-Tridecene	1.58	100%
2	6.407	2,4-Dimethyldodecane	0.22	97%
3	6.743	Hexadecane	0.51	100%
4	7.195	Naphthalene, 1-methyl-	0.33	100%
5	7.735	Dodecane, 4,6-dimethyl-	0.13	99%
6	9.264	1-Tetradecene	5.32	100%
7	9.39	Tetradecane	0.25	97%
8	9.565	Naphthalene, 1,3-dimethyl-	0.15	93%
9	9.857	Dodecane, 2-methyl-	0.21	96%
10	10.552	Heptadecane	0.12	99%
11	10.766	2,6,10-Trimethyltridecane	0.19	99%
12	10.824	3-Ethyl-3-methylheptadecane	0.07	99%
13	11.524	Eicosane	0.77	100%
14	12.342	Phenol, 3,5-bis(1,1-dimethyl ethyl)-	4.85	100%
15	13.039	Heneicosane, 10-methyl-	0.05	96%
16	13.196	1-Decanol, 2-hexyl-	0.06	98%
17	14.694	Benzophenone	0.06	98%
18	14.896	Pentadecane, 2,6,10-trimethyl-	0.20	96%
19	15.684	1-Heptadecene	0.57	100%
20	15.790	Hexadecane, 2,6,10,14-tetramethyl-	0.09	98%
21	16.853	Octadecane, 5-methyl-	0.04	95%
22	17.42	1-Dodecanol, 2-hexyl-	0.06	97%
23	17.7	Tetradecanoic acid	0.12	98%
24	17.787	Tridecane, 3-methylene-	0.13	96%
25	18.052	Heneicosane	0.18	96%
26	18.908	Dotriacontane	0.14	100%
27	20.366	Tetracosane	0.48	100%
28	21.838	1-Nonadecene	12.39	100%
29	22.038	1-Decene, 3,3,4-trimethyl-	0.32	96%
30	23.105	Erucic acid	0.21	95%
31	24.192	Tetrapentacontane	0.46	98%
33	25.337	1-Heptacosanol	9.30	99%
34	27.614	5,5-Diethylpentadecane	0.25	98%
35	28.557	1-Hexacosanol	6.04	100%
36	30.228	Floxuridine	0.79	97%
37	32.806	1,3,5-Trisilacyclohexane	0.33	97%
38	46.317	1-Pentacosanol	0.60	100%
Total Fatty Alcohol			21.24%	
Total Hydrocarbons			26.33%	

Table 4.21 GC-MS analysis of cell pellet obtained from CN gas mixture

S.No.	Run time	Compound	% Area	Match quality
1	5.041	1-Tridecene	1.47	100%
2	6.746	Hexadecane	0.44	100%
3	7.197	Naphthalene, 1-methyl-	0.30	100%
4	7.736	Dodecane, 4,6-dimethyl-	0.11	99%
5	9.264	1-Tetradecanol	5.04	100%
6	9.391	Tetradecane	0.22	98%
7	9.858	Dodecane, 2-methyl-	0.19	98%
8	10.554	Heptadecane	0.11	100%
9	10.768	2,6,10-Trimethyltridecane	0.17	99%
10	10.825	3-Ethyl-3-methylheptadecane	0.07	97%
11	11.525	Eicosane	0.72	100%
12	12.336	Phenol, 3,5-bis(1,1-dimethylethyl)-	5.13	98%
13	13.787	1-Hexadecanol	8.02	100%
14	14.696	Benzophenone	0.07	98%
15	14.895	Pentadecane, 2,6,10-trimethyl-	0.20	95%
16	15.688	1-Heptadecene	0.55	100%
17	17.423	1-Chloroeicosane	0.07	96%
18	17.702	Tetradecanoic acid	0.11	98%
19	18.055	Heneicosane	0.18	98%
21	18.909	Dotriacontane	0.09	100%
22	20.513	Tetracosane	0.14	95%
23	21.841	1-Nonadecene	11.80	99%
24	21.887	Hexadecane, 2-methyl-	0.29	100%
25	22.04	Tridecane, 3-methylene-	0.10	97%
26	24.194	Tetrapentacontane	0.20	99%
27	25.204	Octadecanoic acid	1.27	84%
28	25.34	1-Heptacosanol	7.67	100%
29	25.54	1-Decene, 3,3,4-trimethyl-	0.15	97%
30	28.561	1-Hexacosanol	6.09	100%
31	32.818	1,3,5-Trisilacyclohexane	0.78	100%
32	35.597	Hexacontane	0.22	97%
Total Fatty Alcohol			33.33%	
Total Hydrocarbons			18.64%	

Table 4.22 GC-MS analysis of cell-free supernatant extract for C gas mixture

S.No.	Run time	Compound	% Area	Match quality
1	5.043	1-Dodecene	1.99	100%
2	6.433	Benzoic acid	1.12	99%
3	6.745	Dodecane, 4,6-dimethyl-	0.06	98%
4	7.202	Naphthalene, 1-methyl-	0.17	98%
5	9.264	1-Pentadecene	5.18	100%
6	9.392	Tetradecane	0.14	95%
7	11.397	2,6,10-Trimethyltridecane	0.12	97%
8	11.522	Eicosane	0.18	100%
9	12.345	Phenol, 3,5-bis(1,1-dimethyl ethyl)-	5.04	98%
10	13.779	1-Heptadecene	7.69	100%
11	14.716	Benzophenone	0.07	97%
12	15.73	1-Tetradecanol	0.30	99%
13	15.985	Heptadecane	0.56	97%
14	16.078	Hexadecane, 1-iodo-	0.09	96%
15	17.706	Oleic Acid	0.09	98%
16	17.789	1-Undecene, 9-methyl-	0.15	95%
17	18.05	Heneicosane	0.17	93%
18	20.367	Decane, 1-iodo-	0.08	98%
19	21.829	1-Nonadecene	10.50	100%
20	22.038	Tridecane, 3-methylene-	0.28	99%
21	24.19	Tetrapentacontane	0.23	96%
22	24.386	2-Methylhexacosane	0.06	96%
23	25.331	n-Tetracosanol-1	8.15	100%
24	27.098	1-Decanol, 2-hexyl-	0.12	96%
25	28.554	1-Heptacosanol	6.36	100%
26	29.908	1,3,5-Trisilacyclohexane	0.39	97%
27	34.279	1-Hexacosanol	3.29	100%
Total Fatty Alcohol			24.35%	
Total Hydrocarbons			28.11%	

Table 4.23 GC-MS analysis of cell-free supernatant extract obtained from N gas mixture

S.No.	Run time	Compound	% Area	Match quality
1	5.047	1-Dodecene	2.45	100%
2	6.005	Tetradecane	0.80	89%
3	6.24	Benzoic acid	1.09	85%

4	6.747	Hexadecane	0.29	100%
5	7.204	Naphthalene, 1-methyl-	0.23	98%
6	7.74	Dodecane, 4,6-dimethyl-	0.08	99%
7	9.283	1-Pentadecene	8.13	100%
8	9.399	Tetradecane	0.25	93%
9	10.773	2,6,10-Trimethyltridecane	0.10	99%
10	11.35	Undecane, 2,4-dimethyl-	0.12	96%
11	11.526	Eicosane	0.41	100%
12	12.373	Phenol, 3,5-bis(1,1-dimethylethyl)-	5.02	98%
13	12.545	2-Bromotetradecane	0.21	97%
14	13.204	1-Dodecanol, 2-hexyl-	0.07	98%
15	14.577	Heneicosane	0.07	99%
16	14.715	Benzophenone	0.07	98%
17	15.716	1-Tetradecanol	0.53	100%
18	15.987	Heptadecane	0.21	100%
19	17.71	Eicosanoic acid	0.31	96%
20	20.791	Docosane, 1,22-dibromo-	0.20	94%
21	21.179	Decane, 1-iodo-	0.13	97%
22	21.859	1-Nonadecene	10.94	99%
23	22.049	Tridecane, 3-methylene-	0.33	97%
24	24.194	Tetrapentacontane	0.27	97%
25	25.358	n-Tetracosanol-1	8.49	100%
26	28.578	1-Heptacosanol	6.55	100%
27	29.905	1,3,5-Trisilacyclohexane	0.34	98%
28	30.749	Nonacosane, 3-methyl-	0.20	97%
29	34.297	1-Hexacosanol	4.28	100%
Total Fatty Alcohol			26.34%	
Total Hydrocarbons			25.83%	

Table 4.24 GC-MS analysis of cell-free supernatant extract obtained from CN gas mixture

S.No.	Run time	Compound	% Area	Match quality
1	5.042	1-Dodecene	2.19	100%
2	6.093	Benzoic acid	3.36	95%
3	6.745	Dodecane, 4,6-dimethyl-	0.06	99%
4	7.203	Naphthalene, 1-methyl-	0.19	99%
5	9.263	1-Pentadecene	5.68	100%
6	9.39	Undecane, 4,7-dimethyl-	0.15	96%
7	9.9	Naphthalene, 1,4-dimethyl-	0.05	95%

8	11.342	Undecane, 2,4-dimethyl-	0.05	95%
9	11.395	2,6,10-Trimethyltridecane	0.11	93%
10	12.265	Phenol, 3,5-bis(1,1-dimethylethyl)-	5.39	95%
11	12.549	2-Bromotetradecane	0.10	93%
12	13.576	Eicosanoic acid	0.10	98%
13	14.711	Benzophenone	0.07	98%
14	15.71	1-Tetradecanol	0.32	99%
15	15.981	Heptadecane	0.18	100%
16	16.146	Eicosane	0.16	100%
17	17.702	Tetradecanoic acid	0.13	98%
18	17.785	1-Undecene, 9-methyl-	0.16	96%
19	18.047	Heneicosane	0.13	85%
20	20.361	Decane, 1-iodo-	0.06	98%
21	20.943	2-Isopropyl-5-methyl-1-heptanol	0.05	90%
22	21.828	1-Nonadecene	11.73	100%
23	22.032	Tridecane, 3-methylene-	0.29	97%
24	24.186	Tetrapentacontane	0.11	95%
25	25.176	Octadecanoic acid	0.50	89%
26	25.329	n-Tetracosanol-1	8.40	100%
27	27.088	1-Decanol, 2-hexyl-	0.10	98%
28	28.549	1-Heptacosanol	6.63	100%
29	29.894	1,3,5-Trisilacyclohexane	0.50	100%
30	34.276	1-Hexacosanol	3.61	100%
Total Fatty Alcohol			28.59%	
Total Hydrocarbons			21.97%	

Table 4.25 GC-MS analysis of cell pellet and cell-free supernatant for C, N and CN gas mixtures

Gaseous compositions	Cell pellet		Cell-free supernatant	
	fatty alcohol	hydrocarbons	fatty alcohol	hydrocarbons
C	28.43%	18.47%	24.35%	28.11%
N	21.24%	26.33%	26.34%	25.83%
CN	33.33%	18.64%	28.59%	21.97%

Table 4.26 GC-MS analysis of cell lysate extract obtained from S gas mixture

S.No.	Run time	Compound	% Area	Match quality
1	5.087	1-Dodecene	2.92	99
2	9.222	1-Tetradecene	3.76	100
3	9.383	Tetradecane	0.37	97
4	11.625	Heptadecane	0.29	99
5	12.295	2,4-Di-tert-butylphenol	3.28	99
6	13.686	1-Hexadecanol	5.35	100
7	13.827	Hexadecane	0.43	99
8	15.835	2(3H)-Benzothiazolone	0.29	95
9	16.052	2,6,10-Trimethyltridecane	0.28	95
10	19.94	Heneicosane	0.24	98
11	21.276	Triacontane, 1-iodo-	0.17	95
12	21.539	n-Hexadecanoic acid	1.63	97
13	21.713	1-Nonadecene	6.20	100
14	21.81	Eicosane	1.02	99
15	21.985	1-Dodecanol, 2-octyl-	0.36	90
16	22.045	Cyclic octaatomic sulfur	0.15	78
17	23.738	1-Decanol, 2-hexyl-	0.29	87
18	25.227	1-Heptacosanol	4.55	100
19	25.431	Nonacosane	0.12	100
20	27.059	Tetracontane	0.28	87
21	28.385	Pentadecane, 4-methyl-	0.10	86
22	28.456	1-Hexacosanol	3.41	100
23	28.52	Tetracosane	0.53	100
24	28.624	Dotriacontane	0.35	95
25	29.049	Tetratriacontane	0.22	98
26	29.859	1,3,5-Trisilacyclohexane	2.17	100
27	30.033	Hexatriacontane	0.31	98
28	30.158	Floxuridine	1.10	98
29	32.121	Triphenylphosphine sulfide	0.37	94
30	32.899	Tetrapentacontane	0.32	98
31	35.571	2-Methylhexacosane	0.29	97
Total fatty alcohols			18.87%	
Total hydrocarbons			22.13%	

Table 4.27 GC-MS analysis of cell lysate extract obtained from CS gas mixture

S.No.	Run time	Compound	% Area	Match quality
1	5.127	1-Tridecene	2.46	99
2	9.248	1-Tetradecene	4.09	100
3	9.405	Tetradecane	0.26	95
4	11.642	Octadecane	0.17	100
5	12.304	2,4-Di-tert-butylphenol	3.33	100
6	13.696	1-Hexadecanol	5.56	100
7	13.837	Hexadecane	0.40	99
8	15.959	Heptadecane	0.60	100
9	16.052	Pentadecane	0.23	98
11	17.996	Heneicosane	0.62	100
12	20.338	Tetracosane	0.36	98
13	21.275	Triacontane, 1-iodo-	0.13	95
14	21.549	n-Hexadecanoic acid	3.18	98
15	21.716	1-Nonadecene	6.26	100
16	21.814	Eicosane	1.16	98
17	24.88	11-Methyltricosane	0.10	88
18	25.055	Octadecanoic acid	0.61	94
19	25.228	1-Heptacosanol	4.66	100
20	26.728	Dotriacontane, 1-iodo-	0.75	97
21	27.022	Erucic acid	0.35	96
22	28.127	1-Heptatriacotanol	0.21	91
23	28.456	1-Hexacosanol	3.34	99
24	29.863	1,3,5-Trisilacyclohexane	3.57	100
25	30.034	Dotriacontane	0.49	99
26	30.17	Floxuridine	3.19	99
27	32.9	Hexatriacontane	0.42	97
28	35.575	Tetrapentacontane	0.30	98
29	35.797	Tetracosane, 1-iodo-	0.23	96
Total fatty alcohols			21.24%	
Total hydrocarbons			25.79%	

Table 4.28 GC-MS analysis of cell-free supernatant extract for S gas mixture

S.No.	Run time	Compound	% Area	Match quality
1	5.022	Dithiocarbamate, S-methyl-, N-(2-methyl-3-oxobutyl)-	0.14	96
2	5.097	1-Dodecanol	1.22	99
3	5.234	1-Tetradecene	2.39	99

4	9.29	1-Tetradecanol	3.95	100
5	12.324	2,4-Di-tert-butylphenol	2.60	100
6	13.707	1-Hexadecanol	4.96	100
7	13.846	Hexadecane	0.56	99
8	15.847	2(3H)-Benzothiazolone	0.31	89
9	15.964	Heptadecane	0.82	100
10	18	Eicosane	0.94	100
11	19.281	Hexadecane, 1-iodo-	0.12	100
12	19.948	Heneicosane	0.71	100
13	20.588	Hexadecanoic acid	1.38	99
14	20.814	Benzothiazole, 2-(2-hydroxyethylthio)-	0.20	86
15	21.276	Nonadecane, 2,3-dimethyl-	0.25	95
16	21.54	n-Hexadecanoic acid	1.79	99
17	21.716	1-Nonadecene	5.30	100
18	23.82	Heptadecanenitrile	0.31	98
19	25.226	1-Heptacosanol	3.94	100
20	25.307	Dodecane, 2-methyl-	1.07	96
21	26.486	Tetrapentacontane, 1,54-dibromo-	0.19	92
22	26.729	Triacontane, 1-iodo-	0.84	97
23	27.021	Erucic acid	0.40	95
24	27.507	11-Methyltricosane	0.58	87
25	28.456	1-Hexacosanol	2.87	99
26	29.55	Octadecanoic acid	1.23	99
27	29.644	1,1,1,3,3-Pentaisopropyldisiloxane	0.14	88
28	29.86	1,3,5-Trisilacyclohexane	1.88	99
29	30.038	Dotriacontane	0.80	99
30	30.16	Floxuridine	0.97	94
31	30.88	Tetrapentacontane	0.50	95
32	31.497	Tetracosane	1.06	97
33	32.403	1-(4-Undecylphenyl) ethanone	0.59	94
34	35.795	Tetracosane, 1-iodo-	0.28	98
Total fatty alcohols			20.39%	
Total hydrocarbons			20.95%	

Table 4.29 GC-MS analysis of cell-free supernatant extract for CS gas mixture

S.No.	Run time	Compound	% Area	Match quality
1	5.071	1-Dodecanol	0.40	99
2	5.13	1-Tridecene	2.02	100
3	9.253	1-Tetradecene	3.80	100

4	9.41	Tetradecane	0.26	98
5	12.307	2,4-Di-tert-butylphenol	2.43	99
6	13.7	1-Hexadecanol	4.34	100
7	13.839	Hexadecane	0.60	99
8	15.865	2(3H)-Benzothiazolone	0.97	99
9	15.965	Heptadecane	1.16	100
10	16.057	Pentadecane	0.38	93
11	20.343	Tetracosane	0.41	98
12	20.593	Hexadecanoic acid	1.17	99
13	20.773	Benzothiazole, 2-(2-hydroxyethylthio)-	0.92	97
14	21.13	Tetrapentacontane	0.34	94
15	21.281	Triacontane, 1-iodo-	0.22	95
16	21.579	n-Hexadecanoic acid	3.45	98
17	21.721	1-Nonadecene	4.42	100
18	21.819	Eicosane	1.09	100
19	23.829	Heptadecanenitrile	0.28	95
20	25.101	Octadecanoic acid	1.12	96
21	25.232	1-Heptacosanol	3.32	99
22	25.314	Docosane	0.76	92
23	26.736	Triacontane, 1-iodo-	0.70	96
24	27.027	Erucic acid	0.27	99
25	28.098	Heptadecane, 3-methyl-	0.38	86
26	28.14	Octadecane, 1-chloro-	0.36	87
27	28.466	1-Hexacosanol	2.62	99
28	28.534	Tetracosane	0.77	97
29	29.87	1,3,5-Trisilacyclohexane	2.24	99
30	30.045	Dotriacontane	0.72	96
31	31.504	Hexadecane, 2-methyl-	0.66	92
32	35.124	1-(4-Undecylphenyl) ethanone	0.20	94
Total fatty alcohols			19.12%	
Total hydrocarbons			21.77%	

Fatty alcohols are essential industrial compounds and can be used as biofuels and additives due to their excellent fuel potential. By introducing the heterogeneous enzyme fatty Acyl-CoA reductase in the cyanobacteria system, (Yao et al., 2014) investigated the production of fatty alcohol under various environmental conditions using CO_2 and solar energy. Fatty alcohols with a chain length of C_{12}–C_{14} can be used to make detergents, surfactants, and personal care products. Therefore, therefore in high demand and currently sourced from non-renewable resources (Yao et al., 2014). Fatty acids, a vital component of cell membranes, help in the cell's various metabolic and regulatory activities. The metabolism of fatty acids is capable of producing metabolites such as petroleum distillates. As a result, converting fatty acids to fatty acid methyl ester (FAME) is an attractive method that adds value to the process (Lennen et al., 2013). The bacterium is well-known for its ability to produce hydrocarbons (Ladygina et al., 2006). Lower molecular weight hydrocarbons are assumed to pass across the cell membrane into the culture broth. These can be captured and stored by the hydrocarbons already present in the bacterial cell, increasing their carbon number even more. The elemental composition of kerosene oil, jet fuels, and diesel is found in the range of $C_{12} – C_{20}$ (Ladygina et al., 2006). The bacterial consortium has also shown the production of hydrocarbon in the range of $C_{12} – C_{27}$ that correspondent to light oil and shows potential as a valuable fuel in the present study.

Hence, the bacterial consortium has shown its ability to capture CO_2, NO and SO_2 while using DWW with added minerals as growth media. This can also be utilized in the extraction of a valuable biomolecule such as fatty alcohol and long-chain hydrocarbons as suggested by FT-IR spectroscopy and GC-MS analysis and hence, solving both purposes co-equally.

Table 4.30 GC-MS analysis of cell lysate extract for the bio-fixation of CNS gas mixture

S.No.	Run time	Compound	% Area	Match quality
1	5.073	1-Dodecanol	0.56	99
2	5.129	1-Tridecene	3.16	100
3	9.255	1-Tetradecene	3.99	100
4	12.310	2,4-Di-tert-butylphenol	3.24	99
5	13.839	Hexadecane	0.35	99
7	15.841	2(3H)-Benzothiazolone	0.31	90
8	15.963	Heptadecane	0.44	99
9	20.782	Benzothiazole, 2-(2-hydroxyethylthio)-	0.73	95
10	21.549	n-Hexadecanoic acid	3.62	99
11	21.718	1-Nonadecene	6.01	100
12	21.818	Eicosane	0.93	97
13	25.07	Octadecanoic acid	1.20	97
14	25.231	1-Heptacosanol	4.56	99
15	26.731	Triacontane, 1-iodo-	0.81	99
16	28.462	1-Hexacosanol	3.42	99
17	28.529	Tetracosane	0.51	96
18	30.039	Hexatriacontane	0.45	99
19	30.17	Floxuridine	2.52	99
20	32.788	1,3,5-Trisilacyclohexane	3.11	100
21	45.525	Tetrapentacontane	0.41	97
22	46.287	1-Triacontanol	0.30	92
Total fatty alcohols			16.90%	
Total hydrocarbons			23.73%	

Table 4.31 GC-MS analysis of cell-free supernatant for the bio-fixation of CNS gas mixture

S.No.	Run time	Compound	% Area	Match quality
1	6.861	Hexadecane	1.11	100
2	7.309	Naphthalene, 1-methyl-	0.56	95
3	7.828	Dodecane, 4,6-dimethyl-	0.34	99
4	9.281	1-Tetradecanol	1.74	100
5	9.905	Heptadecane	0.42	96
6	10.805	2,6,10-Trimethyltridecane	0.88	99
7	11.372	2,4-Dimethyldodecane	0.50	99
8	11.548	Eicosane	2.08	100
9	12.324	2,4-Di-tert-butylphenol	3.08	99
10	13.719	1-Hexadecanol	3.51	100
11	14.69	Benzophenone	0.23	98
12	14.891	Pentadecane, 2,6,10-trimethyl-	0.36	98
13	15.684	1-Heptadecene	1.73	100
14	17.9	1-Nonadecene	3.00	100
15	18.895	Dotriacontane	0.52	100
16	20.355	Tetrapentacontane	1.83	100
17	20.503	Tetracosane	0.48	98
18	20.616	Hexadecanoic acid	3.39	100
19	23.528	Octadecane, 3-methyl-	0.44	93
20	23.834	Heptadecanenitrile	0.43	98
21	25.241	1-Hexacosanol	1.72	100
22	27.596	Triacontane, 1,30-dibromo-	0.40	92
23	28.65	Octadecanamide	1.79	99
24	29.872	1,3,5-Trisilacyclohexane	0.68	99
25	30.183	Floxuridine	1.19	99
26	32.917	Hexatriacontane	0.21	99
Total fatty alcohols			13.44%	
Total hydrocarbons			19.18%	

4.5 Material balance

The utilization of CO_2 by the bacterial consortium was established by the approximate carbon balance in the semi-continuous system. Elemental carbon (C) balance was performed as per Eq. 3.16. The total mass of C supplied to the system in the form of CO_2 (g) was estimated using ideal gas law and was derived as 118.92 g. The amount of C left from the system as CO_2 (g) at the bioreactor outlet was obtained as 56.637 g. Based on the biomass molecular formula ($C_6H_{12}O_7N$), the mass of C as biomass was calculated to be 2.133 g (Rittmann, 2012). The total amount of C in the dissolved form was estimated as 0.6288 g. Based on these values, the L.H.S. and R.H.S. of Eq. 3.16 were obtained as 118.92 g and 59.39 g, respectively (Table 4.32). The difference between L.H.S and R.H.S was approximately obtained as 59 g. The % area obtained from GC-MS analysis was approximated to the mass fraction in order to calculate the approximate amount of C present in the product. The mass of C in the product was estimated as 32 g. After adding the approximate amount of C in product formation in L.H.S, the difference between L.H.S and R.H.S was reduced to 27 g. This confirmed the assimilation of CO_2 (g) in the form of fatty acids, fatty alcohols, and long-chain hydrocarbons and was also established by FT-IR and GC-MS analysis.

Similarly, N balance was carried out using Eq. 3.17 to prove the gaseous phase utilization of NO by bacterial consortium. The mass of N supplied and leaving from the bioreactor as NO was estimated as 3.4676 g and 1.0046 g, respectively using the ideal gas law. As per the biomass molecular formula ($C_5H_7O_2N$), the mass of N in biomass was obtained as 1.4988 g (Rittmann, 2012). The total amount of N in dissolved form (nitrate and nitrite) was estimated as 0.418 g. The mass of N in the product was estimated as 0.153 g. These values indicated the difference between L.H.S and R.H.S of Eq. 3.17 to be approximately 0.3926 g (Table 4.32). This may be due to the

assimilation of certain amount of nitrogen to form the products and was confirmed by the FT-IR and GC-MS analysis.

4.6 Fixation mechanism

The CO_2 (g) dissolved in the aqueous media after introducing into the bioreactor system results in the formation of carbonate and bicarbonate ions. The bacterial consortium utilizes bi-carbonate ions as the sole carbon source during the process. The utilization of inorganic carbon in the form of HCO_3^- by bacterial species is a well-established fact (Bharti et al., 2014; Mishra et al., 2016). The experimental results of bio-fixation studies can be used to understand the overall metabolism of CO_2 fixations. The FT-IR and GC-MS results showed the formation of different fatty alcohols, fatty acids, and long-chain hydrocarbons during the bio-fixation process. Three-step reaction mechanisms can describe the bioconversion of CO_2 (l) to fatty alcohols by the bacterial consortium: 1) metabolization of HCO_3^- to fatty acids by ribulose-1,5-bisphosphate carboxylase/oxygenase (RuBisCo) enzyme, 2) reduction of fatty acyl-CoA to the fatty aldehyde in the presence of acyl-CoA reductase as a catalyst, and 3) reduction of fatty aldehyde to fatty alcohol by fatty aldehyde reductase as catalyst (Hofvander et al., 2011) (Fig. 4.34). This suggests that long-chain fatty alcohols can be synthesized by bacteria (Mishra et al., 2018).

NO (g) dissolved in the aqueous media and formed NO_3^- and NO_2^- as the main intermediates in the bioreactor system (Xu et al., 2020). Some parts of the NO (g) may oxidize to NO_2 (g) in the presence of air, followed by a reaction with H_2O in aqueous media to form HNO_3 and HNO_2. However, the pH of the microbial reactor remained greater than 4, and hence, HNO_3 and HNO_2 remained in the form of NO_3^- and NO_2^-, respectively (Hende et al., 2012). The utilization of NO_3^- and NO_2^- as a sole nitrogen source by bacterial consortium (*Bacillus tropicus* and *Bacillus cereus*)

for their growth is a well-established process (Remde et al., 1991; Rout et al., 2017; Uddin et al., 2021; Saha et al., 2022).

The previous studies reported that the main intermediates of SO_2 transformation in bioreactor systems were SO_3^{2-} and SO_4^{2-} (Hende et al., 2012). SO_2 reacts with H_2O in an aqueous media and forms H_2SO_3. The oxidation of H_2SO_3 forms sulfuric acid in the system. As the pH of microbial reactors generally remains greater than 1.9, SO_4^{2-} is the major species in the bioreactor system (Hende et al., 2012). Previous studies have shown the utilization of SO_3^{2-} and SO_4^{2-} as energy and sulfur sources by bacterial species (Zhang et al., 2015b). The obtained experimental results can be used to understand the overall mechanism of SO_2 bio-fixation.

Thus, based on FT-IR and GC-MS results in the current work, it may be established that the bacterial consortium followed the above-mentioned pathway of converting the assimilated fatty acids into fatty alcohol when cultivated in the presence of CO_2, NO and SO_2 (Fig. 4.34).

Table 4.32 Approximate material balance for validation of gaseous phase utilization of CO_2 and NO by the bacterial consortium using elemental C, and N balance

Carbon balance				
$M_{C_{in}}$	$M_{C_{go}}$	$M_{C_{bo}}$	$Dissolved\ C\ as\ (aq)\ CO_2$	Mass of C in product
118.92 g	56.637 g	2.133 g	0.628 g	32 g
Nitrogen balance				
$M_{N_{in}}$	$M_{N_{go}}$	$M_{N_{bo}}$	$Dissolved\ N\ as\ (aq)NO$	Mass of N in product
3.467 g	1.0046 g	1.4988 g	0.418 g	0.153 g

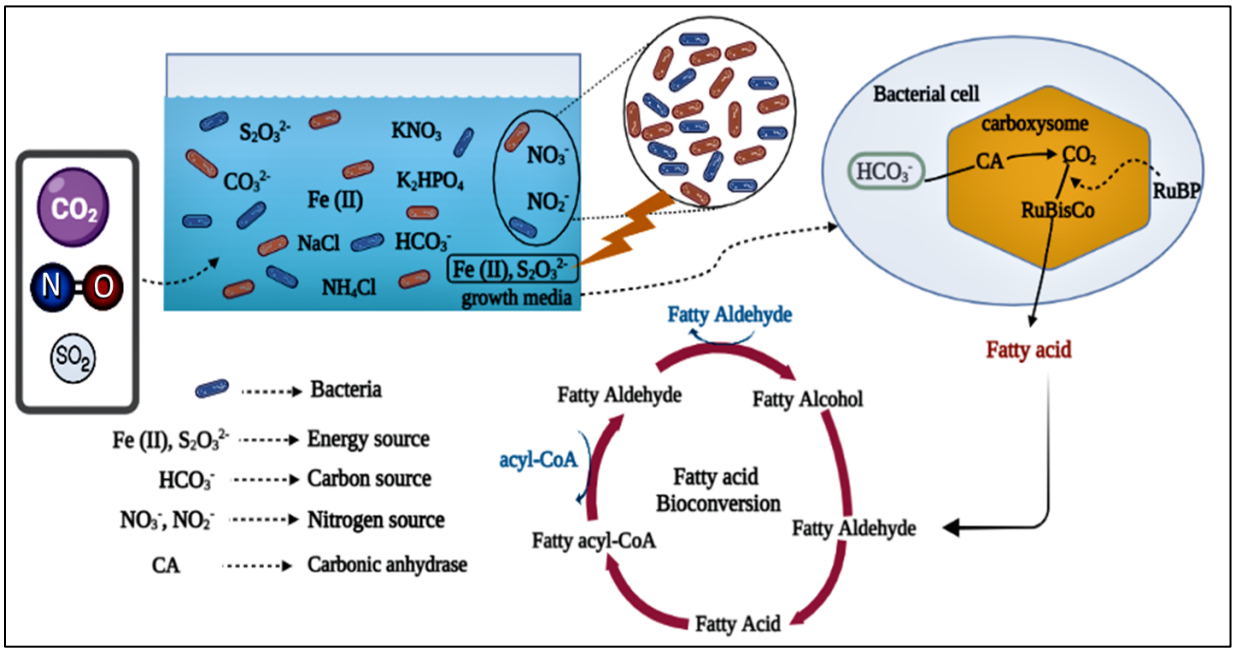

Fig. 4.34 Proposed pathway for flue gas (CO_2, NO, SO_2) bio-fixation by bacterial consortium (RuBP: ribulose –1,5-bisphosphate, (RuBisCo: ribulose-1,5-bisphosphate carboxylase/oxygenase)

4.7 Comparison with existing literature

The performance of bacterial consortium for C, N, S, CN, CS and CNS gas mixture was compared with the reported studies in terms of bio-kinetics parameters such as maximum biomass concentration (X_{max}) (g L^{-1}), maximum biomass productivity (P_{max}) (g L^{-1} d^{-1}), and maximum specific growth rate (μ_{max}) (d^{-1}) and are summarized in Table 4.33. The X_{max}, $P_{max,}$ and μ_{max} were obtained in the range of 0.41 - 3.63 g L^{-1}, 0.07 - 1.55 g L^{-1} d^{-1}, and 0.001 - 3.5 d^{-1}, respectively for different microalgae, cyanobacteria, and bacterial species (Yoshihara et al., 1996; Radmann et al., 2011; Jiang et al., 2013a; Mishra et al., 2018). For the present study values of X_{max}, P_{max} and μ_{max} were obtained in the range of 2.15 - 7.1 g L^{-1}, 2.28 - 4.50 g L^{-1} d^{-1}, and 0.96 - 5.62 d^{-1}, respectively. The obtained values of X_{max}, P_{max} and μ_{max} for the present work are comparatively higher than the reported studies. The X_{max}, P_{max} and μ_{max} for CS gas mixture were found as 2.15 ± 0.51 g L^{-1}, 2.88 ± 0.07 g L^{-1} d^{-1}, and 5.78 ± 1.07 d^{-1}, respectively. The obtained results for CS gas mixture were not comparable due to the lack of previous research on the simultaneous bio-fixation of CO_2 and SO_2.

The growth parameters X_{max}, P_{max} and μ_{max} for CNS gas mixture in the current work were found to be 3.13 g L^{-1}, 4.39 g L^{-1} d^{-1}, and 5.89 d^{-1}, respectively. This is much higher than the values obtained in the previous work (Chiu et al., 2011; Radmann et al., 2011; Du et al., 2019; Duarte et al., 2016) utilizing microalgae as microbial species. The obtained results for CNS gas mixture were either higher than or comparable to the previously reported studies. This suggests the potential of bacterial consortium for the bio-fixation of the simulated flue gases (CO_2, NO and SO_2).

Few studies by Basu et al. (2013) and Zhang et al. (2018) have explained the utilization of bacterial consortium for the synthesis of C_7 to C_{27} carbon compounds and their commercial applications. In the present study, the bacterial consortium was isolated from a hypersaline and halotolerant

environment which might be one of the possible reason for the higher values of growth parameters for simultaneous bio-fixation of CO_2, NO and SO_2. The optimum flowrate, higher gaseous tolerance, potential to grow in DWW along with better CO_2 (g), NO (g) and SO_2 (g) fixation ability of bacterial consortium can make it a sustainable technique for the simultaneous bio-fixation of flue gases (CO_2, NO and SO_2), wastewater treatment and production of value-added products. This can replace conventional fuel as an energy source and indicates the feasibility of the biorefinery concept. The present study also demonstrated the use of DWW as a nutrient and energy source, which further makes this process economically viable and feasible for industrial flue gas treatment.

Table 4.33 Comparison of maximum biomass concentration, biomass productivity, and gas fixation rate at different culture conditions with reported studies

Microbial species	Flue gas composition	Max. biomass conc. (g L^{-1})	Max. biomass productivity (g L^{-1} d^{-1})	Max. specific growth rate (d^{-1})	Reference
Nannochloris sp. NOA- 13	CO_2 -15% (V/V), NO - 300 ppm	2.5	-	3.5 (CO_2) 0.01 (NO)	(Yoshihara et al., 1996)
Dunaliella tertiolecta	NO - 300 ppm	-	0.35	0.5-0.6	(Nagase et al., 2001)
Chlorella sp. MTF-7	CO_2 - 25%, SO_2-0.009%, NO - 0.008%	2.87	0.52	-	(Chiu et al., 2011)
Scenedesmus nidulans	CO_2 -12%, SO_2 - 60 ppm, NO -100 ppm	0.41	0.07	0.001	(Radmann et al., 2011)
H. stevensii	CO_2 - 15% (v/v)	2.16	1.55	1.94	(Mishra et al., 2018)
Chlorella vulgaris	CO_2 - 15% (v/v)	1.976	0.282	0.35	(Mohsenpour et al., 2016)
Scenedesmus dimorphus	CO_2 - 20% (v/v), NO - 500 ppm	3.63	0.485	0.889 (CO_2)	(Jiang et al., 2013a)
Chlorella fusca	CO_2 -10%, SO_2 - 60 ppm, NO – 100 ppm	1.29	0.13	0.18	(Duarte et al., 2016)
Chlorella pyrenoidosa XQ-20044	CO_2 - 15%, SO_2 - 0.03%, NO - 0.03%	0.73	-	-	(Du et al., 2019)

Bacterial consortium	CO_2 - 15.5%, SO_2 - 20 ppm, NO - 1.071 ppm	-	-	-	(Xie et al., 2021)
Bacterial consortium	CO_2 - 15.5%, SO_2 - 7200 ppm, NO-800 ppm	-	-	-	(Xu et al., 2022)
Bacterial consortium	CO_2 - 10% (v/v)	4.92	3.51	4.38	Present study
Bacterial consortium	NO - 750 ppm	7.1	3.73	0.96	Present study
Bacterial consortium	SO_2 - 150 ppm	3.31	2.31	1.99	Present study
Bacterial consortium	CO_2 - 10% (v/v), NO - 750 (ppm)	4.95	4.50	5.62 (CO_2) 1.16 (NO)	Present study
Bacterial consortium	CO_2 - 10 % (v/v), SO_2 - 150 ppm	2.15	2.28	5.78	Present study
Bacterial consortium	CO_2 - 10% v/v, NO - 760 ppm SO_2 - 140 ppm	3.13	4.39	5.89	Present study

Chapter 5

Concluding remarks

In the current chapter, conclusions, major contributions, and future scope for research are discussed.

5.1 Conclusions

The following conclusions are drawn based on the current work results:

5.1.1 CO_2 fixation using *Desmodesmus* species

1. Bio-fixation of CO_2 (g) at three different concentrations (0.03%, 5%, and 10% v/v) by *Desmodesmus* sp. was successfully demonstrated in a 34 L custom-designed loop photobioreactor at a high-temperature range of 30 - 35 ^oC.
2. The maximum values of biomass concentration, specific growth rate, biomass productivity, and CO_2 fixation rate were obtained as 1.903 ± 0.038 g L^{-1}, 0.15 ± 0.04 d^{-1}, 0.185 ± 0.004 g L^{-1} d^{-1}, and 0.333 ± 0.004 g L^{-1} d^{-1}, respectively, at 10% CO_2 concentration.
3. The higher values of carbohydrate (20.7 ± 2.4%), protein (32.3 ± 2.5%), and lipid (42 ± 1.0%) content at 10% CO_2 concentration confirmed the suitability of *Desmodesmus* sp. for the fixation of higher CO_2 concentrations, and the nutrients accumulated in the algal biomass in the form of carbohydrates, lipids, and protein.
4. The higher concentration of Chl b indicated the possibility of more significant photosynthesis activity of *Desmodesmus* sp.
5. The cell concentration in cultures obtained with 5% CO_2 and 10% CO_2 was higher than those with ambient air conditions (0.03% CO_2), which validated the utilization of CO_2 as a carbon source by microalgae.
6. A scaled-up loop bioreactor could be utilized for large-scale fixation of CO_2 emitted from waste management sources and reduce greenhouse gas emissions.
7. The more excellent biochemical constituents in algal biomass can also be utilized as potential feedstocks for biofuel applications.

5.1.2 CO_2 bio-fixation using *H. stevensii*

8. Bio-fixation of CO_2 (g) by *H. stevensii* was successfully demonstrated in a laboratory-scale semi-continuous bioreactor at three different cultivation media [DIW (100 mM $Na_2S_2O_3$), DWW (100 mM $Na_2S_2O_3$), and DWW (no additional sulfate)].
9. The higher values of μ_{max} (1.37 d^{-1}), P_{max} (3.14 g L^{-1} d^{-1}), and CO_2 fixation rate (4.04 g L^{-1} d^{-1}) suggest the possible use of DWW in place of DIW for the preparation of cultivation media.
10. The obtained results indicated that *H.stevensii* has a promising ability to utilize the nutrients (NO_3^-, Cl^-, PO_4^{3-}, SO_4^{2-}, COD, and BOD) present in the DWW as the nutrient and energy source.
11. FT-IR and GC-MS results confirmed the bio-fixation of CO_2 (g) by *H.stevensii* into various value-added compounds, including fatty acids, fatty alcohols, and long-chain hydrocarbons.
12. Carbon balance validated the bio-fixation of CO_2 (g) into biomass utilizing the rPP cycle pathway.
13. Preliminary techno-economic analysis indicates the possibility of replacing pure water with domestic wastewater and utilizing the concomitant inorganic compounds of wastewater as a nutrient and energy source for the growth of *H. stevensii*.

5.1.3 Flue gas (CO_2, NO, SO_2) bio-fixation using bacterial consortium

14. The bacterium present in the water sample procured from SSL was analyzed by 16s rRNA gene sequence analysis and identified as *Bacillus tropicus* SSLMC1 and *Bacillus cereus* SSLMC2.

15. Bio-fixation of individual and simultaneous flue gas mixtures [CO_2 (g), NO (g), and SO_2 (g)] by the bacterial consortium isolated from SSL using DWW as a nutrient and energy source was successfully demonstrated in a laboratory-scale semi-continuous suspended bioreactor.
16. The higher values of μ_{max} (0.96 d^{-1}) and P_{max} (4.50 g L^{-1} d^{-1}) for CN mixture as compared to C mixture (μ_{max} – 0.60 d^{-1}, P_{max} – 3.51 g L^{-1} d^{-1}) and N mixture (μ_{max} – 0.92 d^{-1}, P_{max} – 3.73 g L^{-1} d^{-1}) validated the viability of simultaneous bio-fixation of CO_2 (g) and NO (g) utilizing bacterial consortium as inoculum and DWW as growth media.
17. The maximum values of μ_{max} (5.78 d^{-1}) and P_{max} (2.28 g $L^{-1}d^{-1}$) for CS mixture were comparable to C mixture (μ_{max} – 0.60 d^{-1}, P_{max} – 3.51 g L^{-1} d^{-1}) and S mixture (μ_{max} – 1.99 d^{-1}, P_{max} – 2.31 g L^{-1} d^{-1}).
18. The higher value of biomass productivity (4.39 g L^{-1} d^{-1}) and maximum specific growth rate (5.89 d^{-1}) for CNS mixture validated the utilization of bacterial consortium for the simultaneous bio-fixation of flue gases.
19. The simultaneous utilization efficiency of organic and inorganic components (BOD, COD, PO_4^{3-}, NO_3^-, NO_2^-, CO_3^{2-}, SO_4^{2-} and Fe (II)) present in DWW using bacterial consortium was obtained in the range of 94.3% – 100% for all flue gas mixtures (C, N, S, CN, CS, and CNS).
20. FT-IR analysis of cell pellet and cell-free supernatant obtained from the bio-fixation of flue gas mixtures (C, N, S, CN, CS, and CNS) confirmed the presence of different functional group related to fatty acids, fatty alcohols, and long-chain hydrocarbons.
21. The production of fatty acids (C_7-C_{22}), fatty alcohols (C_{14}-C_{27}) (13.44% - 33.33%), and hydrocarbons (C_{12}-C_{60}) (18.47% - 28.11%) due to the bio-fixation of flue gas mixtures (C, N, S, CN, CS, and CNS) was firmly established by GC-MS analysis of cell pellet and cell-free supernatant.

22. Carbon and Nitrogen balance on all the bio-fixation studies validated the utilization of CO_2 (g) and NO (g) by bacterial consortium for their growth and to produce organic compounds as by-products.
23. The flue gas fixation ability of bacterial consortium at higher gaseous concentration and in the presence of DWW can be understood to be one of the sustainable options for the simultaneous bio-fixation of CO_2 (g), NO (g), and SO_2 (g), wastewater treatment, and production of value-added products.
24. The present study concludes that utilizing DWW as a nutrient and energy source by bacterial consortium indicated the process feasibility for industrial flue gas treatment, and obtained by-products from bio-fixation studies suggest that it can partially replace the requirement of conventional fuels.

5.2 Major contribution

1. Development of custom-designed pilot scale loop photobioreactor for CO_2 (g) (0.03%, 5%, and 10% v/v) fixation study utilizing *Desmodesmus* sp.
2. Development of a cost-effective CO_2 (g) bio-fixation process utilizing the bacterial species *H. stevensii* using growth media prepared in domestic wastewater.
3. Identification of bacterial strains *Bacillus tropicus* SSLMC1 and *Bacillus cereus* SSLMC2 for simultaneous bio-fixation of flue gases [CO_2 (g), SO_2 (g), and NO (g)].
4. Development of a semi-continuous suspended glass bioreactor system for the bio-fixation of flue gas (C, N, S, CN, CS, and CNS) utilizing bacterial consortium as inoculum.
5. Successful utilization of concomitant nutrients present in domestic wastewater for flue gas bio-fixation and simultaneous production of value-added products.

6. Successful demonstration of the conversion of flue gas [CO_2 (g), NO (g), and SO_2 (g)] into value-added products such as fatty acids, fatty alcohols, and long-chain hydrocarbon by bacterial consortium.

5.3 Future Scope

1. Isolation of thermophilic bacteria for bio-fixation of simulated flue gas.
2. Flue gas bio-fixation studies can be performed on a lab scale using industrial flue gas at thermophilic conditions.
3. Flue gas bio-fixation experiments can be performed on the pilot and industrial scale using industrial effluents.
4. Development of an appropriate downstream strategy for recovering the products obtained from bio-fixation studies.

Appendix A

FT-IR results

Table A.1 Band assignments to peaks obtained for cell lysate extract and cell free supernatant extract of *Halomonas stevensii* at three different cultivations medium

Cultivation medium	Wave number (cm^{-1})		Group attribution
	Cell lysate	Supernatant	
DWW (100 mM $Na_2S_2O_3$)	3433.88	3433.97	OH stretching
	2962, 2928	-	CH stretching
	2560.51	2558.07	Thiol stretch
	2000-1900	2066.71, 1924.05	Conjugate double bonds or "pseudo" symmetric alkynes
	1649.19	1631.02	C=O stretch
	1549	-	amide II bands
	1450.80, 1400	-	C=O, CH bending, OH bending
	-	1384.15	Methyl or methylene groups, C–O symmetric stretching of carbohydrates
	1249	1230.45	C-N, C-O, P-O
	1145, 1002	1146, 1002	C-O-C, C-O Stretching of COOH
	834	834	CO_3^{2-} group
	700-600	700-600	C=C bending
DWW (no additional sulfate)	3446.87	3451.20	OH stretching
	2960, 2927	2905.19	CH stretching
	2557.10	2553.52	Thiol stretch conjugate double bonds or "pseudo" symmetric alkynes
	2000-1900	2079.19, 1922.14	Conjugate double bonds or "pseudo" symmetric alkynes
	1649.54	1665.36, 1625.74	C=O stretch
	1547	-	Amide II bands
	1384.43	1382.50	Methyl or methylene groups, C–O symmetric stretching of carbohydrates

	1135, 999	1141, 997	C-O-C, C-O stretching of COOH
	834	834	CO_3^{2-} group
	700-600	700-600	C=C bending
DIW (100 mM $Na_2S_2O_3$)	3434.21	3435.09	OH stretching
	2962.79	-	CH stretching
	2553	2554.41	Thiol stretch
	2070, 1926	2070.02, 1924.90	conjugate double bonds or "pseudo" symmetric alkynes
	1631.40	1631.03	C=O stretch
	1546.24	-	Amide II bands
	1383.42	1383.57	Methyl or methylene groups, C–O symmetric stretching of carbohydrates
	1231	1229.32	C-N, C-O, P-O
	1131, 1000.90	1146, 1001	C-O-C, C-O Stretching of COOH
	834.76	834	CO_3^{2-} group
	700-600	700-600	C=C bending

Table A.2 Band assignments to peaks obtained for cell lysate extract and cell free supernatant extract of *bacterial consortium* for three different gaseous mixture (C, N, CN)

Gaseous mixture	Wave number (cm^{-1})		Group attribution
	Cell lysate	Supernatant	
C	3451	3439	OH stretching
	-	2964	CH stretching
	2000-1900	-	Conjugate double bonds or "pseudo" symmetric alkynes
	1642	1653	C=O stretch
	1565	1552	Amide II bands
	1384	1384	Methyl or methylene groups, C–O symmetric stretching of carbohydrates
	1270	1270	C-N, C-O, P-O
	1119, 1070	1116, 1070	C-O-C, C-O Stretching of COOH
	876, 836	876, 833	CO_3^{2-} group

N	3302	3443, 3136	OH stretching
	2961, 2927	-	CH stretching
	-	2553	Thiol stretch conjugate double bonds or “pseudo” symmetric alkynes
	-	2068, 1919	Conjugate double bonds or “pseudo” symmetric alkynes
	1657	1665	C=O stretch
	1548	-	amide II bands
	1384	1387	Methyl or methylene groups, C–O symmetric stretching of carbohydrates
	1267	1270	C-N, C-O, P-O
	1096	1135, 1071, 997	C-O-C, C-O stretching of COOH
	862, 832	832	CO_3^{2-} group
CN	3449	3460	OH stretching
	2964	-	CH stretching
	2560	2554.41	Thiol stretch
	2070, 1923	2076, 1921	Conjugate double bonds or “pseudo” symmetric alkynes
	1651	1634	C=O stretch
	1549	-	Amide II bands
	1383	1384	Methyl or methylene groups, C–O symmetric stretching of carbohydrates
	1106, 994	1108, 993	C-O-C, C-O stretching of COOH
	834	834	CO_3^{2-} group

Table A.3 Band assignments to peaks obtained for cell lysate extract and cell free supernatant extract of *bacterial consortium* for three different gaseous mixture (C, S, CS)

Gaseous mixture	Wave number (cm^{-1})		Group attribution
	Cell lysate	Supernatant	
C	3451	3439.93	OH stretching
	-	2964.60	CH stretching
	2000-1900	-	Conjugate double bonds or "pseudo" symmetric alkynes
	1642	1653.29	C=O stretch
	1565	1552.32	Amide II bands
	1384	1384.86	Methyl or methylene groups, C–O symmetric stretching of carbohydrates
	1270	1270	C-N, C-O, P-O
	1119, 1070	1116, 1070	C-O-C, C-O Stretching of COOH
	876, 836	875, 833	CO_3^{2-} group
S	3416.45	3464.47	OH stretching
	-	2555.84	Thiol stretch conjugate double bonds or "pseudo" symmetric alkynes
	2031.56	2068.37, 1925.34	Conjugate double bonds or "pseudo" symmetric alkynes
	1640.07	1633.02	C=O stretch
	1535.26	-	Amide II bands
	1384	1384.41	Methyl or methylene groups, C–O symmetric stretching of carbohydrates
	1270	1270, 1203	C-N, C-O, P-O
	1072	1100, 987	C-O-C, C-O stretching of COOH
	834	865, 834	CO_3^{2-} group
	700-600	700-600	C=C bending
	3414.87	3443	OH stretching
	-	2554.94	Thiol stretch

CS	2051.90	2034.97, 1924.97	conjugate double bonds or “pseudo” symmetric alkynes
	1639.95	1638	C=O stretch
	1549.92	1559	Amide II bands
	1383.51	1384	Methyl or methylene groups, C–O symmetric stretching of carbohydrates
	1271.35	1271	C-N, C-O, P-O
	1103.02, 996	1112, 993	C-O-C, C-O Stretching of COOH
	834	834	CO_3^{2-} group
	700-600	700-600	C=C bending

Table A.4 Band assignments to peaks obtained for cell lysate extract and cell free supernatant extract of *bacterial consortium* for CNS gas mixture

Gas mixture	Wave number (cm^{-1})		Group attribution
	Cell lysate	Supernatant	
CNS	3415.82	3455.50	OH stretching
	-	-	Thiol stretch
	2031.58	-	conjugate double bonds or “pseudo” symmetric alkynes
	1639	1642.95	C=O stretch
	1546.09	1554.87	Amide II bands
	1384.65	1384.61	Methyl or methylene groups, C–O symmetric stretching of carbohydrates
	1244.13	-	C-N, C-O, P-O
	1098.28	1124.58, 995	C-O-C, C-O Stretching of COOH
	831.90	834	CO_3^{2-} group
	700-600	700-600	C=C bending

Table A.5 Bio-molecule representation for different Group attribution

Group attribution	Bio-molecule representation
-OH- stretching	Carbohydrates, proteins, lipids (sterols and fatty acids), nucleic acids
-C=O stretch or amide group	Cell-bound fatty acids, amide I band of proteins
C–N stretching of proteins (amide II)	Cell-bound fatty acids, amide II band of proteins
-CH- stretching	Long chain hydrocarbons
-C=O groups/stretching of Carbonate	Carbonate ion
C-H bending of aliphatic group	aliphatic groups
(>P=O) stretching of phosphodiesters	Form of DNA
-C-O-C, -C-O Stretching of -COOH	Lipids, polysaccharides
C-O stretch of alcoholic compounds	hydroxyl/ether
-C=O stretch or amide group	Cell-bound fatty acids, amide I band of proteins
-C-H rock	Long chain alkanes

References

Abid, A., Saidane, F., & Hamdi, M. (2017). Feasibility of carbon dioxide sequestration by *Spongiochloris* sp microalgae during petroleum wastewater treatment in airlift bioreactor. *Bioresource Technology*, *234*, 297–302. doi: 10.1016/j.biortech.2017.03.041.

Abou-Shanab, R. A. I., Ji, M. K., Kim, H. C., Paeng, K. J., & Jeon, B. H. (2013). Microalgal species growing on piggery wastewater as a valuable candidate for nutrient removal and biodiesel production. *Journal of Environmental Management*, *115*, 257–264. doi: 10.1016/j.jenvman.2012.11.022.

Abreu, A. P., Fernandes, B., Vicente, A. A., Teixeira, J., & Dragone, G. (2012). Mixotrophic cultivation of *Chlorella vulgaris* using industrial dairy waste as organic carbon source. *Bioresource Technology*, *118*, 61–66. doi: 10.1016/j.biortech.2012.05.055.

Achinas, S., Achinas, V., & Euverink, G. J. W. (2020). Microbiology and biochemistry of anaerobic digesters: an overview. Bioreactors. INC. doi: 10.1016/b978-0-12-821264-6.00002-4.

Aghaalipour, E., Akbulut, A., & Gullu, G. (2020). Carbon dioxide capture with microalgae species in continuous gas-supplied closed cultivation systems. *Biochemical Engineering Journal*, *163* (July), 107741. doi: 10.1016/j.bej.2020.107741.

Almomani, F., Al Ketife, A., Judd, S., Shurair, M., Bhosale, R. R., Znad, H., & Tawalbeh, M. (2019). Impact of CO_2 concentration and ambient conditions on microalgal growth and nutrient removal from wastewater by a photobioreactor. *Science of the Total Environment*, *662*, 662–671. doi: 10.1016/j.scitotenv.2019.01.144.

Anjos, M., Fernandes, B. D., Vicente, A. A., Teixeira, J. A., & Dragone, G. (2013). Optimization of CO_2 bio-mitigation by *Chlorella vulgaris*. *Bioresource Technology*, *139*, 149–154. doi: 10.1016/j.biortech.2013.04.032.

APHA. (2003). *APHA (American Public Health Association). (2003). Standard methods for examination of water and waste water. 23rd Ed. Washington DC, USA*.

Arbib, Z., Ruiz, J., Alvarez-Diaz, P., Garrido-Perez, C., Barragan, J., & Perales, J. A. (2013). Effect of pH control by means of flue gas addition on three different photo-bioreactors treating urban wastewater in long-term operation. *Ecological Engineering*, *57*, 226–235. doi: 10.1016/j.ecoleng.2013.04.040.

Aslam, A., Thomas-Hall, S. R., Manzoor, M., Jabeen, F., Iqbal, M., uz Zaman, Q., Schenk, P. M.,

& Asif Tahir, M. (2018). Mixed microalgae consortia growth under higher concentration of CO_2 from unfiltered coal fired flue gas: Fatty acid profiling and biodiesel production. *Journal of Photochemistry and Photobiology B: Biology*, *179* (January), 126–133. doi: 10.1016/j.jphotobiol.2018.01.003.

Barahoei, M., Hatamipour, M. S., & Afsharzadeh, S. (2020). CO_2 capturing by *chlorella vulgaris* in a bubble column photo-bioreactor; Effect of bubble size on CO_2 removal and growth rate. *Journal of CO_2 Utilization*, *37* (July 2019), 9–19. doi: 10.1016/j.jcou.2019.11.023.

Barnes, J. M., Apel, W. A., & Barrett, K. B. (1995). Removal of nitrogen oxides from gas streams using biofiltration. *Journal of Hazardous Materials*, *41*(2–3), 315–326. doi: 10.1016/0304-3894(94)00103-N.

Basu, S., Roy, A. S., Mohanty, K., & Ghoshal, A. K. (2013). Enhanced CO_2 sequestration by a novel microalga: *Scenedesmus obliquus* SA1 isolated from bio-diversity hotspot region of Assam, India. *Bioresource Technology*, *143*, 369–377. doi: 10.1016/j.biortech.2013.06.010.

Baumann, H., Talmage, S. C., & Gobler, C. J. (2012). Reduced early life growth and survival in a fish in direct response to increased carbon dioxide. *Nature Climate Change*, *2*(1), 38–41. doi: 10.1038/nclimate1291.

Beedlow, P., Tingey, D., Phillips, D., Hogsett, W., & Olszyk, D. (2004). Rising CO_2 and forests. *Front Ecological Environment*, *2*, 315–322.

Berg, I. A. (2011). Ecological aspects of the distribution of different autotrophic CO_2 fixation pathways. *Applied and Environmental Microbiology*, *77*(6), 1925–1936. doi: 10.1128/AEM.02473-10.

Bernhard S. (2008)*., Infrared and Raman Spectroscopy: Methods and Applications, 3rd edition Wiley, Germany*.

Bharti, R. K., Srivastava, S., & Thakur, I. S. (2014). Production and characterization of biodiesel from carbon dioxide concentrating chemolithotrophic bacteria, *Serratia* sp. ISTD04. *Bioresource Technology*, *153*, 189–197. doi: 10.1016/j.biortech.2013.11.075.

Bligh, E.G. and Dyer, W. J. (1959). A rapid method of total lipid extraction and purification. *Canadian Journal of Biochemistry and Physiology*, *37*(8), 911–917.

Bong, G. M., Stringer, J., Brandvold, D. K., Simsek, F. A., Medina, M. G., & Egeland, G. (2001). Development of integrated system for biomimetic CO_2 sequestration using the enzyme carbonic anhydrase. *Energy and Fuels*, *15* (2), 309–316. doi: 10.1021/ef000246p.

Borkenstein, C. G., Knoblechner, J., Frühwirth, H., & Schagerl, M. (2011). Cultivation of *Chlorella emersonii* with flue gas derived from a cement plant. *Journal of Applied Phycology*, *23* (1), 131–135. doi: 10.1007/s10811-010-9551-5.

Cai, T., Park, S. Y., Racharaks, R., & Li, Y. (2013). Cultivation of *Nannochloropsis salina* using anaerobic digestion effluent as a nutrient source for biofuel production. *Applied Energy*, *108*, 486–492. doi: 10.1016/j.apenergy.2013.03.056.

Carlozzi, P. (2003). Dilution of solar radiation through "culture" lamination in photobioreactor rows facing south-north: A way to improve the efficiency of light utilization by cyanobacteria (*Arthrospira platensis*). *Biotechnology and Bioengineering*, *81*(3), 305–315. doi: 10.1002/bit.10478.

Chae, S. R., Hwang, E. J., & Shin, H. S. (2006). Single cell protein production of *Euglena gracilis* and carbon dioxide fixation in an innovative photo-bioreactor. *Bioresource Technology*, *97* (2), 322–329. doi: 10.1016/j.biortech.2005.02.037.

Chen, C. Y., Kao, P. C., Tan, C. H., Show, P. L., Cheah, W. Y., Lee, W. L., Ling, T. C., & Chang, J. S. (2016). Using an innovative pH-stat CO_2 feeding strategy to enhance cell growth and C-phycocyanin production from *Spirulina platensis*. *Biochemical Engineering Journal*, *112*, 78–85. doi: 10.1016/j.bej.2016.04.009.

Chen, L., Yu, Z., Liang, J., Liao, Y., & Ma, X. (2018). Co-pyrolysis of *chlorella vulgaris* and kitchen waste with different additives using TG-FTIR and Py-GC/MS. *Energy Conversion and Management*, *177* (October), 582–591. doi: 10.1016/j.enconman.2018.10.010.

Chen, Z. Y., Chen, C., Zhang, Y., Xia, Z. M., Yan, K. F., & Li, X. Sen. (2017). Carbon dioxide and sulfur dioxide capture from flue gas by gas hydrate based process. *Energy Procedia*, *142*, 3454–3459. doi: 10.1016/j.egypro.2017.12.229.

Cheng, J., Huang, Y., Feng, J., Sun, J., Zhou, J., & Cen, K. (2013). Mutate *Chlorella* sp. by nuclear irradiation to fix high concentrations of CO_2. *Bioresource Technology*, *136*, 496–501. doi: 10.1016/j.biortech.2013.03.072.

Cheng, J., Li, K., Yang, Z., Lu, H., Zhou, J., & Cen, K. (2016). Gradient domestication of *Haematococcus pluvialis* mutant with 15% CO_2 to promote biomass growth and astaxanthin yield. *Bioresource Technology*, *216*, 340–344. doi: 10.1016/j.biortech.2016.05.095.

Chiang, C. L., Lee, C. M., & Chen, P. C. (2011). Utilization of the cyanobacteria *Anabaena* sp. CH1 in biological carbon dioxide mitigation processes. *Bioresource Technology*, *102* (9),

5400–5405. doi: 10.1016/j.biortech.2010.10.089.

Chiang, T. Y., Yuan, T. H., Shie, R. H., Chen, C. F., & Chan, C. C. (2016). Increased incidence of allergic rhinitis, bronchitis and asthma, in children living near a petrochemical complex with SO_2 pollution. *Environment International*, *96*, 1–7. doi: 10.1016/j.envint.2016.08.009.

Chiarini, A., & Quadrio, M. (2021). The light/dark cycle of microalgae in a thin-layer photobioreactor. *Journal of Applied Phycology*, *33* (1), 183–195. doi: 10.1007/s10811-020-02310-1.

Chinnasamy, S., Ramakrishnan, B., Bhatnagar, A., & Das, K. C. (2009). Biomass production potential of a wastewater alga *chlorella vulgaris* ARC 1 under elevated levels of CO_2 and temperature. *International Journal of Molecular Sciences*, *10* (2), 518–532. doi: 10.3390/ijms10020518.

Chiu, S. Y., Kao, C. Y., Chen, C. H., Kuan, T. C., Ong, S. C., & Lin, C. S. (2008). Reduction of CO_2 by a high-density culture of *Chlorella* sp. in a semicontinuous photobioreactor. *Bioresource Technology*, *99* (9), 3389–3396. doi: 10.1016/j.biortech.2007.08.013.

Chiu, S. Y., Kao, C. Y., Huang, T. T., Lin, C. J., Ong, S. C., Chen, C. Da, Chang, J. S., & Lin, C. S. (2011). Microalgal biomass production and on-site bioremediation of carbon dioxide, nitrogen oxide and sulfur dioxide from flue gas using *Chlorella* sp. cultures. *Bioresource Technology*, *102* (19), 9135–9142. doi: 10.1016/j.biortech.2011.06.091.

Clarke, K., Pugsley, T., & Hill, G. A. (2009). Gas-solid packed and fluidized bed models for bioremediation of volatile organic compounds in air. *Biochemical Engineering Journal*, *46* (1), 34–43. doi: 10.1016/j.bej.2009.04.009.

Dasu, B. N., & Sublette, K. L. (1989). Microbial removal of sulfur dioxide from a gas stream with net oxidation to sulfate. *Applied Biochemistry and Biotechnology*, *20* (1), 207–220. doi: 10.1007/BF02936483.

De Bhowmick, G., Sarmah, A. K., & Sen, R. (2019). Performance evaluation of an outdoor algal biorefinery for sustainable production of biomass, lipid and lutein valorizing flue-gas carbon dioxide and wastewater cocktail. *Bioresource Technology*, *283*, 198–206. doi: 10.1016/j.biortech.2019.03.075.

De Silva, G. P. D., Ranjith, P. G., & Perera, M. S. A. (2015). Geochemical aspects of CO_2 sequestration in deep saline aquifers: A review. *Fuel*, *155*, 128–143. doi: 10.1016/j.fuel.2015.03.045.

Deng, H., Yi, H., Tang, X., Liu, H., & Zhou, X. (2013). Interactive effect for simultaneous removal of SO_2, NO, and CO_2 in flue gas on ion exchanged zeolites. *Industrial and Engineering Chemistry Research*, *52* (20), 6778–6784. doi: 10.1021/ie303319f.

Doucha, J., Straka, F., & Lívanský, K. (2005). Utilization of flue gas for cultivation of microalgae (*Chlorella* sp.) in an outdoor open thin-layer photobioreactor. *Journal of Applied Phycology*, *17* (5), 403–412. doi: 10.1007/s10811-005-8701-7.

Douskova, I., Doucha, J., Livansky, K., MacHat, J., Novak, P., Umysova, D., Zachleder, V., & Vitova, M. (2009). Simultaneous flue gas bioremediation and reduction of microalgal biomass production costs. *Applied Microbiology and Biotechnology*, *82* (1), 179–185. doi: 10.1007/s00253-008-1811-9.

Du, K., Wen, X., Wang, Z., Liang, F., Luo, L., Peng, X., Xu, Y., Geng, Y., & Li, Y. (2019). Integrated lipid production, CO_2 fixation, and removal of SO_2 and NO from simulated flue gas by oleaginous *Chlorella pyrenoidosa*. *Environmental Science and Pollution Research*, *26* (16), 16195–16209. doi: 10.1007/s11356-019-04983-9.

Duarte, J. H., Fanka, L. S., & Costa, J. A. V. (2016). Utilization of simulated flue gas containing CO_2, SO_2, NO and ash for *Chlorella fusca* cultivation. *Bioresource Technology*, *214* (x), 159–165. doi: 10.1016/j.biortech.2016.04.078.

Dubois, M., Gilles, K. A., Hamilton, J. K., Rebers, P. A., & Smith, F. (1956). Colorimetric method for determination of sugars and related substances. *Analytical Chemistry*, *28* (3), 350–356. doi: 10.1021/ac60111a017.

Dworkin, M. (2012). Sergei Winogradsky: A founder of modern microbiology and the first microbial ecologist. *FEMS Microbiology Reviews*, *36* (2), 364–379. doi: 10.1111/j.1574-6976.2011.00299.x.

Dyksma, S., Bischof, K., Fuchs, B. M., Hoffmann, K., Meier, D., Meyerdierks, A., Pjevac, P., Probandt, D., Richter, M., Stepanauskas, R., & Mußmann, M. (2016). Ubiquitous Gammaproteobacteria dominate dark carbon fixation in coastal sediments. ISME Journal, 10 (8), 1939–1953. doi: 10.1038/ismej.2015.257.

Ferreira, A., Ribeiro, B., Marques, P. A. S. S., Ferreira, A. F., Dias, A. P., Pinheiro, H. M., Reis, A., & Gouveia, L. (2017). *Scenedesmus obliquus* mediated brewery wastewater remediation and CO_2 biofixation for green energy purposes. *Journal of Cleaner Production*, *165*, 1316–1327. doi: 10.1016/j.jclepro.2017.07.232.

Figueroa, J. D., Fout, T., Plasynski, S., McIlvried, H., & Srivastava, R. D. (2008). Advances in CO_2 capture technology-The U.S. Department of Energy's Carbon Sequestration Program. *International Journal of Greenhouse Gas Control*, *2* (1), 9–20. doi: 10.1016/S1750-5836(07)00094-1.

Flanagan, W. P., Apel, W. A., Barnes, J. M., & Lee, B. D. (2002). Development of gas phase bioreactors for the removal of nitrogen oxides from synthetic flue gas streams. *Fuel*, *81* (15), 1953–1961. doi: 10.1016/S0016-2361(02)00130-8.

Fu, W., Gudmundsson, S., Wichuk, K., Palsson, S., Palsson, B. O., Salehi-Ashtiani, K., & Brynjolfsson, S. (2019). Sugar-stimulated CO_2 sequestration by the green microalga *Chlorella vulgaris*. *Science of the Total Environment*, *654*, 275–283. doi: 10.1016/j.scitotenv.2018.11.120.

Fuchs, G. (2011). Alternative pathways of carbon dioxide fixation: Insights into the early evolution of life. Annual Review of Microbiology, 65. doi: 10.1146/annurev-micro-090110-102801.

Fulke, A. B., Mudliar, S. N., Yadav, R., Shekh, A., Srinivasan, N., Ramanan, R., Krishnamurthi, K., Devi, S., & Chakrabarti, T. (2010). Bio-mitigation of CO_2, calcite formation and simultaneous biodiesel precursors production using *Chlorella* sp. *Bioresource Technology*, *101* (21), 8473–8476. doi: 10.1016/j.biortech.2010.06.012.

Gasiorek, J. (1994). Microbial removal of sulfur dioxide from a gas stream. *Fuel Processing Technology*, *40* (2–3), 129–138. doi: 10.1016/0378-3820(94)90137-6.

Ghanbari Ghozikali, M., Heibati, B., Naddafi, K., Kloog, I., Oliveri Conti, G., Polosa, R., & Ferrante, M. (2016). Evaluation of Chronic Obstructive Pulmonary Disease (COPD) attributed to atmospheric O_3, NO_2, and SO_2 using Air Q Model (2011-2012 year). *Environmental Research*, *144* (2016), 99–105. doi: 10.1016/j.envres.2015.10.030.

Hall, D. O., Acien Fernández, F. G., Guerrero, E. C., Rao, K. K., & Grima, E. M. (2003). Outdoor helical tubular photobioreactors for microalgal production: Modeling of fluid-dynamics and mass transfer and assessment of biomass productivity. *Biotechnology and Bioengineering*, *82* (1), 62–73. doi: 10.1002/bit.10543.

Han, L., Shaobin, H., Zhendong, W., Pengfei, C., & Yongqing, Z. (2016). Performance of a new suspended filler biofilter for removal of nitrogen oxides under thermophilic conditions and microbial community analysis. *Science of the Total Environment*, *562*, 533–541. doi: 10.1016/j.scitotenv.2016.04.084.

Han, Y., & Zhang, W. (2010). Simultaneous removal of NO_x and SO_2 in exhausted gas through landfill leachate. *Indian Journal of Experimental Biology*, *48* (12), 1237–1242.

Han, Y., Zhang, W., & Xu, J. (2011). A performance study of simultaneous microbial removal of NO and SO_2 in a biotrickling-filter under anaerobic condition. *Brazilian Journal of Chemical Engineering*, *28* (2), 189–196. doi: 10.1590/S0104-66322011000200003.

Herrera, L., Hernandez, J., Ruiz, P., & Gantenbein, S. (1991). Desulfovibrio desulfuricans growth kinetics. *Environmental Toxicology and Water Quality*, *6* (2), 225–237. doi: 10.1002/tox.2530060211.

Ho, S. H., Chen, C. Y., Yeh, K. L., Chen, W. M., Lin, C. Y., & Chang, J. S. (2010). Characterization of photosynthetic carbon dioxide fixation ability of indigenous *Scenedesmus obliquus* isolates. *Biochemical Engineering Journal*, *53* (1), 57–62. doi: 10.1016/j.bej.2010.09.006.

Hofvander, P., Doan, T. T. P., & Hamberg, M. (2011). A prokaryotic acyl-CoA reductase performing reduction of fatty acyl-CoA to fatty alcohol. *FEBS Letters*, *585* (22), 3538–3543. doi: 10.1016/j.febslet.2011.10.016.

Huang, Q., Jiang, F., Wang, L., & Yang, C. (2017). Design of Photobioreactors for Mass Cultivation of Photosynthetic Organisms. *Engineering*, *3* (3), 318–329. doi: 10.1016/J.ENG.2017.03.020.

Hyvonen, R., Agren, G. I., Linder, S., Persson, T., Cotrufo, M. F., Ekblad, A., Freeman, M., Grelle, A., Janssens, I. A., Jarvis, P. G., Kellomaki, S., Lindroth, A., Loustau, D., Lundmark, T., Norby, R. J., Oren, R., Pilegaard, K., Ryan, M. G., Sigurdsson, B. D., Wallin, G. (2007). The likely impact of elevated [CO_2], nitrogen deposition, increased temperature and management on carbon sequestration in temperate and boreal forest ecosystems: A literature review. *New Phytologist*, *173* (3), 463–480. doi: 10.1111/j.1469-8137.2007.01967.x.

IPCC 2021; https://www.CO_2.earth/. (2021).

Hamiit, J. K., Jain, A. K., Adams, J. L., & Wuebbles, D. J. (2020). A welfare-based index for assessing environmental effects of greenhouse-gas emissions. In Nature, 388, 539–547.

Jackson, P., Robinson, K., Puxty, G., & Attalla, M. (2009). In situ Fourier Transform-Infrared (FT-IR) analysis of carbon dioxide absorption and desorption in amine solutions. *Energy Procedia*, *1* (1), 985–994. doi: 10.1016/j.egypro.2009.01.131.

Jiang, R., Huang, S., & Yang, J. (2008). Biological removal of NO_x from simulated flue gas in

aerobic biofilter. *Global Nest Journal*, *10* (2), 241–248.

Jiang, Ran, Huang, S., Chow, A. T., & Yang, J. (2009). Nitric oxide removal from flue gas with a biotrickling filter using *Pseudomonas putida*. *Journal of Hazardous Materials*, *164* (2–3), 432–441. doi: 10.1016/j.jhazmat.2008.08.058.

Jiang, Y., Zhang, W., Wang, J., Chen, Y., Shen, S., & Liu, T. (2013). Utilization of simulated flue gas for cultivation of *Scenedesmus dimorphus*. *Bioresource Technology*, *128* (X), 359–364. doi: 10.1016/j.biortech.2012.10.119.

Jiao, H., Wang, H., Li, B., Huang, Z., Chen, Z., & Wei, Z. (2022). Collaborative removal of NO_x and toluene in flue gas driven by aerobic denitrifying biotrickling filter. *Fuel*, *324* (x). doi: 10.1016/j.fuel.2022.124519.

Joshi, A., & Seth, G. (2011). Hydrochemical profile for assessing the groundwater quality of Sambhar lake City and its Adjoining area. *Environmental Monitoring and Assessment*, *174* (1–4), 547–554. doi: 10.1007/s10661-010-1477-5.

Kaiwan-arporn, P., Hai, P. D., Thu, N. T., & Annachhatre, A. P. (2012). Cultivation of cyanobacteria for extraction of lipids. *Biomass and Bioenergy*, *44*, 142–149. doi: 10.1016/j.biombioe.2012.04.017.

Kalsi, P. S. (2007). *Spectroscopy of organic compounds, 8th edition*.

Kampa, M., & Castanas, E. (2008). Human health effects of air pollution. *Environmental Pollution*, *151* (2), 362–367. doi: 10.1016/j.envpol.2007.06.012.

Kao, C. Y., Chen, T. Y., Chang, Y. Bin, Chiu, T. W., Lin, H. Y., Chen, C. Da, Chang, J. S., & Lin, C. S. (2014). Utilization of carbon dioxide in industrial flue gases for the cultivation of microalga *Chlorella* sp. *Bioresource Technology*, *166*, 485–493. doi: 10.1016/j.biortech.2014.05.094.

Kargupta, W., Ganesh, A., & Mukherji, S. (2015). Estimation of carbon dioxide sequestration potential of microalgae grown in a batch photobioreactor. *Bioresource Technology*, *180*, 370–375. doi: 10.1016/j.biortech.2015.01.017.

Kaufman, E. N. (1997). A biological process for the reclamation of flue gas desulfurization gypsum using mixed sulfate-reducing bacteria with inexpensive carbon sources. *Applied Biochemistry and Biotechnology - Part A Enzyme Engineering and Biotechnology*, *63–65* (1), 677–693. doi: 10.1007/BF02920467.

Kita, J., & Ohsumi, T. (2004). Perspectives on biological research for CO_2 ocean sequestration.

Journal of Oceanography, *60* (4), 695–703. doi: 10.1007/s10872-004-5762-1.

Kumar, K., Banerjee, D., & Das, D. (2014). Carbon dioxide sequestration from industrial flue gas by *Chlorella sorokiniana*. *Bioresource Technology*, *152*, 225–233. doi: 10.1016/j.biortech.2013.10.098.

Kumar, K., & Das, D. (2012). Growth characteristics of *Chlorella sorokiniana* in airlift and bubble column photobioreactors. *Bioresource Technology*, *116*, 307–313. doi: 10.1016/j.biortech.2012.03.074.

Kumar, K., Dasgupta, C. N., Nayak, B., Lindblad, P., & Das, D. (2011). Development of suitable photobioreactors for CO_2 sequestration addressing global warming using green algae and cyanobacteria. *Bioresource Technology*, *102* (8), 4945–4953. doi: 10.1016/j.biortech.2011.01.054.

Kumar, M., Gupta, A., & Thakur, I. S. (2016). Carbon dioxide sequestration by chemolithotrophic oleaginous bacteria for production and optimization of polyhydroxyalkanoate. *Bioresource Technology*, *213*, 249–256. doi: 10.1016/j.biortech.2016.02.038.

Kumaraswamy, R., Van Dongen, U., Kuenen, J. G., Abma, W., Van Loosdrecht, M. C. M., & Muyzer, G. (2005). Characterization of microbial communities removing nitrogen oxides from flue gas: the BioDeNOx process. *Applied and Environmental Microbiology*, *71* (10), 6345–6352. doi: 10.1128/AEM.71.10.6345-6352.2005.

Kwon, H. S., Lee, J. H., Kim, T., Kim, J. J., Jeon, P., Lee, C. H., & Ahn, I. S. (2015). Biofixation of a high-concentration of carbon dioxide using a deep-sea bacterium: *Sulfurovum lithotrophicum* 42BKTT. In RSC Advances, 5 (10), 7151–7159. doi: 10.1039/c4ra07830f.

Ladygina, N., Dedyukhina, E. G., & Vainshtein, M. B. (2006). A review on microbial synthesis of hydrocarbons. *Process Biochemistry*, *41* (5), 1001–1014. doi: 10.1016/j.procbio.2005.12.007.

Lal, R. (2008). Sequestration of atmospheric CO_2 in global carbon pools. *Energy and Environmental Science*, *1* (1), 86–100. doi: 10.1039/b809492f.

Laribi, S., Dubois, L., De Weireld, G., & Thomas, D. (2018). Simultaneous absorption of SO_2 and CO_2 from conventional and partial oxy-fuel cement plant flue gases. *Chemical Engineering Transactions*, *69* (x), 121–126. doi: 10.3303/CET1869021.

Lebrero, R., Estrada, J. M., Munoz, R., & Quijano, G. (2012). Toluene mass transfer characterization in a biotrickling filter. *Biochemical Engineering Journal*, *60*, 44–49. doi:

10.1016/j.bej.2011.09.017.

Lee, C. M., Sublette, K. L., & McInerney, M. J. (1994). Conversion of sulfur dioxide to sulfate and hydrogen sulfide by *Desulfotomaculum orientis*. *Fuel Processing Technology*, *40* (2–3), 123–127. doi: 10.1016/0378-3820(94)90136-8.

Lennen, R. M., & Pfleger, B. F. (2013). Microbial production of fatty acid-derived fuels and chemicals. *Current Opinion in Biotechnology*, *24* (6), 1044–1053. doi: 10.1016/j.copbio.2013.02.028.

LI, F.F., YANG, Z.H., ZENG, R. (2011). Microalgae capture of CO_2 from actual flue gas discharged from a combustion chamber. *Ndustrial and Engineering Chemistry Research*, *50*, 6496–6502.

Li, D., Wang, L., Zhao, Q., Wei, W., & Sun, Y. (2015). Improving high carbon dioxide tolerance and carbon dioxide fixation capability of *Chlorella* sp. by adaptive laboratory evolution. *Bioresource Technology*, *185*, 269–275. doi: 10.1016/j.biortech.2015.03.011.

Li, L., Yang, K., Lin, J., & Liu, J. (2017). Operational aspects of SO_2 removal and microbial population in an integrated-bioreactor with two bioreaction zones. *Bioprocess and Biosystems Engineering*, *40* (2), 285–296. doi: 10.1007/s00449-016-1696-4.

Li, L., Zhang, J., Lin, J., & Liu, J. (2015). Biological technologies for the removal of sulfur containing compounds from waste streams: bioreactors and microbial characteristics. *World Journal of Microbiology and Biotechnology*, *31* (10), 1501–1515. doi: 10.1007/s11274-015-1915-1.

Li, W., Li, M., Zhang, L., Zhao, J., Xia, Y., Liu, N., Li, S., & Zhang, S. (2016). Enhanced NO_x removal performance and microbial community shifts in an oxygen-resistance chemical absorption-biological reduction integrated system. *Chemical Engineering Journal*, *290* (x), 185–192. doi: 10.1016/j.cej.2016.01.044.

Lichtenthaler, H. K., & Buschmann, C. (2001). Chlorophylls and Carotenoids: Measurement and Characterization by UV-VIS Spectroscopy. *Current Protocols in Food Analytical Chemistry*, *1* (1), F4.3.1-F4.3.8. doi: 10.1002/0471142913.faf0403s01.

Lin, J., Li, L., Ding, W., Zhang, J., & Liu, J. (2015). Continuous desulfurization and bacterial community structure of an integrated bioreactor developed to treat SO_2 from a gas stream. *Journal of Environmental Sciences (China)*, *37*, 130–138. doi: 10.1016/j.jes.2015.05.029.

Littlejohns, J. V., McAuley, K. B., & Daugulis, A. J. (2010). Model for a solid-liquid airlift two-

phase partitioning bioscrubber for the treatment of BTEX. *Journal of Chemical Technology and Biotechnology*, *85* (2), 173–184. doi: 10.1002/jctb.2280.

Liu, N., Jiang, Y., Zhang, L., Xia, Y., Lu, B., Xu, B., Li, W., & Li, S. (2014). Evaluation of NO_x removal from flue gas by a chemical absorption-biological reduction integrated system: Glucose consumption and utilization pathways. *Energy and Fuels*, *28* (12), 7591–7598. doi: 10.1021/ef5014852.

Liu, Y., Du, J., Lai, Q., Zeng, R., Ye, D., Xu, J., & Shao, Z. (2017). Proposal of nine novel species of the *bacillus cereus* group. *International Journal of Systematic and Evolutionary Microbiology*, *67* (8), 2499–2508. doi: 10.1099/ijsem.0.001821.

Liu, Y., Lai, Q., Du, J., & Shao, Z. (2017). Genetic diversity and population structure of the *Bacillus cereus* group bacteria from diverse marine environments. *Scientific Reports*, *7* (1), 1–11. doi: 10.1038/s41598-017-00817-1.

Lizzul, A. M., Hellier, P., Purton, S., Baganz, F., Ladommatos, N., & Campos, L. (2014). Combined remediation and lipid production using *Chlorella sorokiniana* grown on wastewater and exhaust gases. *Bioresource Technology*, *151*, 12–18. doi: 10.1016/j.biortech.2013.10.040.

Lopez, J. C., Quijano, G., Souza, T. S. O., Estrada, J. M., Lebrero, R., & Muñoz, R. (2013). Biotechnologies for greenhouse gases (CH_4, N_2O, and CO_2) abatement: State of the art and challenges. *Applied Microbiology and Biotechnology*, *97* (6), 2277–2303. doi: 10.1007/s00253-013-4734-z.

Lopez, M. C. G. M., Sanchez, E. D. R., Casas López, J. L., Fernandez, F. G. A., Sevilla, J. M. F., Rivas, J., Guerrero, M. G., & Grima, E. M. (2006). Comparative analysis of the outdoor culture of *Haematococcus pluvialis* in tubular and bubble column photobioreactors. *Journal of Biotechnology*, *123* (3), 329–342. doi: 10.1016/j.jbiotec.2005.11.010.

Lowry, O. H., Rosebrough, N. J., Farr, A. L., & Randall, R. J. (1951). Protein measurement with the Folin phenol reagent. *Journal of Biological Chemistry*, *193*, 265–275.

Ma, S., Li, D., Yu, Y., Li, D., Yadav, R. S., & Feng, Y. (2019). Application of a microalga, *Scenedesmus obliquus* PF3, for the biological removal of nitric oxide (NO) and carbon dioxide. *Environmental Pollution*, *252*, 344–351. doi: 10.1016/j.envpol.2019.05.084.

Ma, X., Gao, M., Gao, Z., Wang, J., Zhang, M., Ma, Y., & Wang, Q. (2018). Past, current, and future research on microalga-derived biodiesel: a critical review and bibliometric analysis.

Environmental Science and Pollution Research, *25* (11), 10596–10610. doi: 10.1007/s11356-018-1453-0.

Martinez, M. E., Sanchez, S., Jimenez, J. M., El Yousfi, F., & Munoz, L. (2000). Nitrogen and phosphorus removal from urban wastewater by the microalga *Scenedesmus obliquus*. *Bioresource Technology*, *73* (3), 263–272. doi: 10.1016/S0960-8524(99)00121-2.

Mecozzi, M. (2005). Estimation of total carbohydrate amount in environmental samples by the phenol-sulphuric acid method assisted by multivariate calibration. *Chemometrics and Intelligent Laboratory Systems*, *79* (1–2), 84–90. doi: 10.1016/j.chemolab.2005.04.005.

Mishra, S., Chauhan, P., Gupta, S., Raghuvanshi, S., Singh, R. P., & Jha, P. N. (2017). CO_2 sequestration potential of halo-tolerant bacterium *Pseudomonas aeruginosa* SSL-4 and its application for recovery of fatty alcohols. *Process Safety and Environmental Protection*, *111*, 582–591. doi: 10.1016/j.psep.2017.08.013.

Mishra, S., Gupta, S., Raghuvanshi, S., & Pal, P. (2016). Energetic assessment of fixation of CO_2 and subsequent biofuel production using *B. cereus* SM1 isolated from sewage treatment plant. *Bioprocess and Biosystems Engineering*, *39* (8), 1247–1258. doi: 10.1007/s00449-016-1603-z.

Mishra, S., Pahari, S., Siva, K., Mohanty, S., Gupta, S., & Raghuvanshi, S. (2018). Investigation on CO_2 bio-mitigation using *Halomonas stevensii* in laboratory scale bioreactor: Design of downstream process and its economic feasibility analysis. *Journal of CO_2 Utilization*, *24* (March), 274–286. doi: 10.1016/j.jcou.2018.01.018.

Mishra, S., Raghuvanshi, S., Gupta, S., & Raj, K. (2017). Application of novel thermo-tolerant haloalkalophilic bacterium *Halomonas stevensii* for bio mitigation of gaseous phase CO_2: Energy assessment and product evaluation studies. *Process Biochemistry*, *55*, 133–145. doi: 10.1016/j.procbio.2017.01.019.

Mochida, I., Korai, Y., Shirahama, M., Kawano, S., Hada, T., Seo, Y., Yoshikawa, M., & Yasutake, A. (2000). Removal of SO_x and NO_x over activated carbon fibers. *Carbon*, *38* (2), 227–239.

Mohsenpour, S. F., & Willoughby, N. (2016). Effect of CO_2 aeration on cultivation of microalgae in luminescent photobioreactors. *Biomass and Bioenergy*, *85*, 168–177. doi: 10.1016/j.biombioe.2015.12.002.

Molina Grima, E., Belarbi, E. H., Acien Fernández, F. G., Robles Medina, A., & Chisti, Y. (2003).

Recovery of microalgal biomass and metabolites: Process options and economics. *Biotechnology Advances*, *20* (7–8), 491–515. doi: 10.1016/S0734-9750(02)00050-2.

Mondal, M., Ghosh, A., Gayen, K., Halder, G., & Tiwari, O. N. (2017). Carbon dioxide bio-fixation by *Chlorella* sp. BTA 9031 towards biomass and lipid production: Optimization using Central Composite Design approach. *Journal of CO_2 Utilization*, *22* (July), 317–329. doi: 10.1016/j.jcou.2017.10.008.

Moreira, D., & Pires, J. C. M. (2016). Atmospheric CO_2 capture by algae: Negative carbon dioxide emission path. *Bioresource Technology*, *215*, 371–379. doi: 10.1016/j.biortech.2016.03.060.

Mousavi, S., Najafpour, G. D., & Mohammadi, M. (2018). CO_2 bio-fixation and biofuel production in an airlift photobioreactor by an isolated strain of microalgae *Coelastrum* sp. SM under high CO_2 concentrations. *Environmental Science and Pollution Research*, *25* (30), 30139–30150. doi: 10.1007/s11356-018-3037-4.

Mudge, S. M. (2005). Fatty Alcohols – a review of their natural synthesis and environmental distribution. *The Soap and Detergent Association*, *132*, 1–141. Retrieved from http://www.aciscience.org/docs/fatty alcohols mudge 2005. pdf.

Nagappan, S., & Verma, S. K. (2016). Growth model for raceway pond cultivation of *Desmodesmus* sp. MCC34 isolated from a local water body. *Engineering in Life Sciences*, *16* (1), 45–52. doi: 10.1002/elsc.201500024.

Nagase, H., Eguchi, K., Yoshihara, K. I., Hirata, K., & Miyamoto, K. (1998). Improvement of microalgal NO_x removal in bubble column and airlift reactors. *Journal of Fermentation and Bioengineering*, *86* (4), 421–423. doi: 10.1016/S0922-338X(99)89018-7.

Nagase, H., Yoshihara, K. ichi, Eguchi, K., Okamoto, Y., Murasaki, S., Yamashita, R., Hirata, K., & Miyamoto, K. (2001). Uptake pathway and continuous removal of nitric oxide from flue gas using microalgae. *Biochemical Engineering Journal*, *7* (3), 241–246. doi: 10.1016/S1369-703X(00)00122-4.

Nayak, M., Dhanarajan, G., Dineshkumar, R., & Sen, R. (2018). Artificial intelligence driven process optimization for cleaner production of biomass with co-valorization of wastewater and flue gas in an algal biorefinery. *Journal of Cleaner Production*, *201*, 1092–1100. doi: 10.1016/j.jclepro.2018.08.048.

Nayak, M., Karemore, A., & Sen, R. (2016a). Performance evaluation of microalgae for concomitant wastewater bioremediation, CO_2 biofixation and lipid biosynthesis for biodiesel

application. *Algal Research*, *16*, 216–223. doi: 10.1016/j.algal.2016.03.020.

Nayak, M., Karemore, A., & Sen, R. (2016b). Sustainable valorization of flue gas CO_2 and wastewater for the production of microalgal biomass as a biofuel feedstock in closed and open reactor systems. *RSC Advances*, *6* (94), 9111–91120. doi: 10.1039/c6ra17899e.

Negoro, M., Shioji, N., Miyamoto, K., & Micira, Y. (1991). Growth of Microalgae in High CO_2 Gas and Effects of SO_x and NO_x. *Applied Biochemistry and Biotechnology*, *28–29* (1), 877–886. doi: 10.1007/BF02922657.

Ole Kenneth, N. (2019). EMEP/EEA air pollutant emission inventory guidebook 2019: Technical guidance to prepare national emission inventories. *EEA Technical Report*, *12/2019*. Retrieved from https://www.eea.europa.eu/publications/emep-eea-guidebook-2019.

Oremland, R. S., Saltikov, C. W., Stolz, J. F., & Hollibaugh, J. T. (2017). Autotrophic microbial arsenotrophy in arsenic-rich soda lakes. *FEMS Microbiology Letters*, *364* (15), 1–11. doi: 10.1093/femsle/fnx146.

Pal, S., Sar, A., & Dam, B. (2019). Moderate halophilic bacteria, but not extreme halophilic archaea can alleviate the toxicity of short-alkyl side chain imidazolium-based ionic liquids. *Ecotoxicology and Environmental Safety*, *184* (September), 109634. doi: 10.1016/j.ecoenv.2019.109634.

Papi, S., Montalvo, S., Papic, L., & Borja, R. (2018). Biological removal of gaseous sulfur dioxide through the reduction to hydrogen sulfide by means of *Desulfovibrio desulfuricans*. *International Biodeterioration and Biodegradation*, *126* (June), 21–27. doi: 10.1016/j.ibiod.2017.09.023.

Passos, F., Gutierrez, R., Brockmann, D., Steyer, J. P., García, J., & Ferrer, I. (2015). Microalgae production in wastewater treatment systems, anaerobic digestion and modelling using ADM1. *Algal Research*, *10*, 55–63. doi: 10.1016/j.algal.2015.04.008.

Pavia, D. L., Lampman, G. M., Kriz, G. S., & Vyvyan, J. R. (2019). *Introduction to spectroscopy, Ninth edition, 2019.*

Philip, L., & Deshusses, M. A. (2003). Sulfur dioxide treatment from flue gases using a biotrickling filter - Bioreactor system. *Environmental Science and Technology*, *37* (9), 1978–1982. doi: 10.1021/es026009d.

Praveenkumar, R., Kim, B., Choi, E., Lee, K., Cho, S., Hyun, J. S., Park, J. Y., Lee, Y. C., Lee, H. U., Lee, J. S., & Oh, Y. K. (2014). Mixotrophic cultivation of oleaginous *Chlorella* sp. KR-1

mediated by actual coal-fired flue gas for biodiesel production. *Bioprocess and Biosystems Engineering*, *37* (10), 2083–2094. doi: 10.1007/s00449-014-1186-5.

Purbia, D., Khandelwal, A., Kumar, A., & Sharma, A. K. (2019). Graphene-water nanofluid in heat exchanger: Mathematical modelling, simulation and economic evaluation. *International Communications in Heat and Mass Transfer*, *108*(September), 104327. doi: 10.1016/j.icheatmasstransfer.2019.104327.

Puxty, G., Wei, S. C. C., Feron, P., Meuleman, E., Beyad, Y., Burns, R., & Maeder, M. (2014). A novel process concept for the capture of CO_2 and SO_2 using a single solvent and column. *Energy Procedia*, *63*, 703–714. doi: 10.1016/j.egypro.2014.11.078.

Radmann, E. M., Camerini, F. V., Santos, T. D., & Costa, J. A. V. (2011). Isolation and application of SO_x and NO_x resistant microalgae in biofixation of CO_2 from thermoelectricity plants. *Energy Conversion and Management*, *52* (10), 3132–3136. doi: 10.1016/j.enconman.2011.04.021.

Rahman, F. A., Aziz, M. M. A., Saidur, R., Bakar, W. A. W. A., Hainin, M. R., Putrajaya, R., & Hassan, N. A. (2017). Pollution to solution: Capture and sequestration of carbon dioxide (CO_2) and its utilization as a renewable energy source for a sustainable future. *Renewable and Sustainable Energy Reviews*, *71*, 112–126. doi: 10.1016/j.rser.2017.01.011.

Rawat, I., Ranjith Kumar, R., Mutanda, T., & Bux, F. (2011). Dual role of microalgae: Phycoremediation of domestic wastewater and biomass production for sustainable biofuels production. *Applied Energy*, *88* (10), 3411–3424. doi: 10.1016/j.apenergy.2010.11.025.

Razzak, S. A., Ilyas, M., Ali, S. A. M., & Hossain, M. M. (2015). Effects of CO_2 concentration and pH on mixotrophic growth of *Nannochloropsis oculata*. *Applied Biochemistry and Biotechnology*, *176* (5), 1290–1302. doi: 10.1007/s12010-015-1646-7.

Remde, A., & Conrad, R. (1991). Metabolism of nitric oxide in soil and denitrifying bacteria. *FEMS Microbiology Letters*, *85* (1), 81–94. doi: 10.1111/j.1574-6968.1991.tb04700.x.

Rittmann, B.E., *McCarty, P. L.* (2012). *Environmental biotechnology: principles and applications, Tata McGraw-Hill Education (2012).*

Ritz, D. (2002). Biological Roles of Proteases. *Review Literature And Arts Of The Americas*, *15* (1), 275–305.

Robert, H. P., Don, W. G., & James, O. M. (1997). *Perry's chemical engineers' handbook, Mc Graw-Hills New York (1997) 56-64.*

Rosenzweig, C., Karoly, D., Vicarelli, M., Neofotis, P., Wu, Q., Casassa, G., Menzel, A., Root, T. L., Estrella, N., Seguin, B., Tryjanowski, P., Liu, C., Rawlins, S., & Imeson, A. (2008). Attributing physical and biological impacts to anthropogenic climate change. *Nature*, *453* (7193), 353–357. doi: 10.1038/nature06937.

Rout, P. R., Bhunia, P., & Dash, R. R. (2017). Simultaneous removal of nitrogen and phosphorous from domestic wastewater using *Bacillus cereus* GS-5 strain exhibiting heterotrophic nitrification, aerobic denitrification and denitrifying phosphorous removal. *Bioresource Technology*, *244* (August), 484–495. doi: 10.1016/j.biortech.2017.07.186.

Ryu, H. J., Oh, K. K., & Kim, Y. S. (2009). Optimization of the influential factors for the improvement of CO_2 utilization efficiency and CO_2 mass transfer rate. *Journal of Industrial and Engineering Chemistry*, *15* (4), 471–475. doi: 10.1016/j.jiec.2008.12.012.

Sadeghizadeh, A., Farhad dad, F., Moghaddasi, L., & Rahimi, R. (2017). CO_2 capture from air by *Chlorella vulgaris* microalgae in an airlift photobioreactor. *Bioresource Technology*, *243*, 441–447. doi: 10.1016/j.biortech.2017.06.147.

Saha, J., Adhikary, S., & Pal, A. (2022). Analyses of the Heavy Metal Resistance Pattern and Biosorption Potential of an Indigenous *Bacillus tropicus* Strain Isolated from Arable Soil. *Geomicrobiology Journal*, *0*(0), 1–15. doi: 10.1080/01490451.2022.2089781.

Saini, R., Kapoor, R., Kumar, R., Siddiqi, T. O., & Kumar, A. (2011). CO_2 utilizing microbes - A comprehensive review. *Biotechnology Advances*, *29* (6), 949–960. doi: 10.1016/j.biotechadv.2011.08.009.

Salek, S. S., Kleerebezem, R., Jonkers, H. M., Witkamp, G. jan, & Van Loosdrecht, M. C. M. (2013). Mineral CO_2 sequestration by environmental biotechnological processes. *Trends in Biotechnology*, *31* (3), 139–146. doi: 10.1016/j.tibtech.2013.01.005.

Santoro AL., bastviken D., Gudasz C., Tranvik L., (2013). Dark Carbon Fixation: An Importance Process in Lake Sediments. *PLoS ONE*, *8* (6), e65813. doi: 10.1371/journal.pone.0065813.

Sar, A., Pal, S., Islam, S., Mukherjee, P., & Dam, B. (2021). An alkali-halostable endoglucanase produced constitutively by a bacterium isolated from sambhar lake in India with biotechnological potential. *Proceedings of the National Academy of Sciences India Section B - Biological Sciences*, *91* (2), 319–326. doi: 10.1007/s40011-021-01230-5.

Simoneit, B. R. T., Rogge, W. F., Lang, Q., & Jaffe, R. (2000). Molecular characterization of smoke from campfire burning of pine wood (pinus elliottii). *Chemosphere - Global Change*

Science, *2* (1), 107–122. doi: 10.1016/S1465-9972(99)00048-3.

Singh Chauhan, D., Sahoo, L., & Mohanty, K. (2022). Maximize microalgal carbon dioxide utilization and lipid productivity by using toxic flue gas compounds as nutrient source. *Bioresource Technology*, *348* (December), 126784. doi: 10.1016/j.biortech.2022.126784.

Skalska, K., Miller, J. S., & Ledakowicz, S. (2010). Trends in NO_x abatement: A review. *Science of the Total Environment*, *408* (19), 3976–3989. doi: 10.1016/j.scitotenv.2010.06.001.

Solomon, S., Plattner, G. K., Knutti, R., & Friedlingstein, P. (2009). Irreversible climate change due to carbon dioxide emissions. *Proceedings of the National Academy of Sciences of the United States of America*, *106* (6), 1704–1709. doi: 10.1073/pnas.0812721106.

Solovchenko, A., Gorelova, O., Selyakh, I., Pogosyan, S., Baulina, O., Semenova, L., Chivkunova, O., Voronova, E., Konyukhov, I., Scherbakov, P., & Lobakova, E. (2015). A novel CO_2-tolerant symbiotic *Desmodesmus* (*Chlorophyceae, Desmodesmaceae*): Acclimation to and performance at a high carbon dioxide level. *Algal Research*, *11*, 399–410. doi: 10.1016/j.algal.2015.04.011.

Sun, C., Yuan, J., Xu, H., Huang, S., Wen, X., Tong, N., & Zhang, Y. (2019). Simultaneous removal of nitric oxide and sulfur dioxide in a biofilter under micro-oxygen thermophilic conditions: Removal performance, competitive relationship and bacterial community structure. *Bioresource Technology*, *290* (May), 121768. doi: 10.1016/j.biortech.2019.121768.

Sundaram, S., & Thakur, I. S. (2015). Biosurfactant production by a CO_2 sequestering *Bacillus* sp. strain ISTS2. *Bioresource Technology*, *188*, 247–250. doi: 10.1016/j.biortech.2015.01.029.

Sydney, E. B., Sturm, W., de Carvalho, J. C., Thomaz-Soccol, V., Larroche, C., Pandey, A., & Soccol, C. R. (2010). Potential carbon dioxide fixation by industrially important microalgae. *Bioresource Technology*, *101* (15), 5892–5896. doi: 10.1016/j.biortech.2010.02.088.

Tang, D., Han, W., Li, P., Miao, X., & Zhong, J. (2011). CO_2 biofixation and fatty acid composition of *Scenedesmus obliquus* and *Chlorella pyrenoidosa* in response to different CO_2 levels. *Bioresource Technology*, *102* (3), 3071–3076. doi: 10.1016/j.biortech.2010.10.047.

Tang, Y., Yang, R., & Bian, X. (2014). A review of CO_2 sequestration projects and application in China. *Scientific World Journal*, *2014*. doi: 10.1155/2014/381854.

Toledo-Cervantes, A., Morales, M., Novelo, E., & Revah, S. (2013). Carbon dioxide fixation and

lipid storage by *Scenedesmus obtusiusculus*. *Bioresource Technology*, *130*, 652–658. doi: 10.1016/j.biortech.2012.12.081.

Uddin, M., Swathi, K. V., Anil, A., Boopathy, R., Ramani, K., & Sekaran, G. (2021). Biosequestration of lignin in municipal landfill leachate by tailored cationic lipoprotein biosurfactant through Bacillus tropicus valorized tannery solid waste. *Journal of Environmental Management*, *300* (August), 113755. doi: 10.1016/j.jenvman.2021.113755.

Ugwu, C. U., Ogbonna, J. C., & Tanaka, H. (2002). Improvement of mass transfer characteristics and productivities of inclined tubular photobioreactors by installation of internal static mixers. *Applied Microbiology and Biotechnology*, *58* (5), 600–607. doi: 10.1007/s00253-002-0940-9.

Upasani, V., & Desai, S. (1990). Chemical composition of the brines and studies on haloalkaliphilic archaebacteria. *Archives of Microbiology*, *154* (6), 589–590. doi: 10.1007/bf00248841.

Van Den Hende, S., Vervaeren, H., & Boon, N. (2012). Flue gas compounds and microalgae: (Bio-) chemical interactions leading to biotechnological opportunities. *Biotechnology Advances*, *30* (6), 1405–1424. doi: 10.1016/j.biotechadv.2012.02.015.

Varshney, P., Beardall, J., Bhattacharya, S., & Wangikar, P. P. (2018). Isolation and biochemical characterisation of two thermophilic green algal species- *Asterarcys quadricellulare* and *Chlorella sorokiniana*, which are tolerant to high levels of carbon dioxide and nitric oxide. *Algal Research*, *30* (May), 28–37. doi: 10.1016/j.algal.2017.12.006.

Varshney, P., Sohoni, S., Wangikar, P. P., & Beardall, J. (2016). Effect of high CO_2 concentrations on the growth and macromolecular composition of a heat- and high-light-tolerant microalga. *Journal of Applied Phycology*, *28* (5), 2631–2640. doi: 10.1007/s10811-016-0797-4.

Wang, B., & Lan, C. Q. (2011). Biomass production and nitrogen and phosphorus removal by the green alga *Neochloris oleoabundans* in simulated wastewater and secondary municipal wastewater effluent. *Bioresource Technology*, *102* (10), 5639–5644. doi: 10.1016/j.biortech.2011.02.054.

Wang, H., Nche-Fambo, F. A., Yu, Z., & Chen, F. (2018). Using microalgal communities for high CO_2-tolerant strain selection. *Algal Research*, *35* (August), 253–261. doi: 10.1016/j.algal.2018.08.038.

Wang, J., Wu, C., Chen, J., & Zhang, H. (2006). Denitrification removal of nitric oxide in a rotating

drum biofilter. *Chemical Engineering Journal*, *121* (1), 45–49. doi: 10.1016/j.cej.2006.04.004.

Wang, X. C., Bi, X. Y., Sun, P. S., Chen, J. Q., Zou, P., Ma, X. M., Zhang, J., Wang, H. Y., & Xu, X. Y. (2015). Effects of oxygen content on the simultaneous microbial removal of SO_2 and NO_x in biotrickling towers. *Biotechnology and Bioprocess Engineering*, *20* (5), 924–930. doi: 10.1007/s12257-015-0138-5.

Wang, X. W., Liang, J. R., Luo, C. S., Chen, C. P., & Gao, Y. H. (2014). Biomass, total lipid production, and fatty acid composition of the marine diatom *Chaetoceros muelleri* in response to different CO_2 levels. *Bioresource Technology*, *161*, 124–130. doi: 10.1016/j.biortech.2014.03.012.

Wang, X., Xu, X., Zou, Y., Yang, F., & Zhang, Y. (2018). Nitric oxide removal from flue gas with ammonium using Anammox DeNOx process and its application in municipal sewage treatment. *Bioresource Technology*, *265* (June), 170–179. doi: 10.1016/j.biortech.2018.05.096.

Wei, Z. S., Huang, Q. R., Wang, J. B., Huang, Z. S., Chen, Z. Y., & Li, B. R. (2016). Performance and mechanism of nitric oxide removal using a thermophilic membrane biofilm reactor. *Fuel Processing Technology*, *148* (x), 217–223. doi: 10.1016/j.fuproc.2016.03.003.

Wen, X., Xu, H., Huang, S., Sun, C., Tong, N., & Zhang, Y. (2019). Simultaneous removal of sulphur dioxide and nitric oxide at different oxygen concentrations in a thermophilic biotrickling filter (BTF): Evaluation of removal efficiency, intermediates interaction and characterisation of microbial communities. *Bioresource Technology*, *294* (September), 122150. doi: 10.1016/j.biortech.2019.122150.

Widdel, F. (2010). *Theory and Measurement of Bacterial Growth*. 1–11.

Williamson, P. (2016). *Scrutinize CO_2 removal methods*. *530*, 153–155.

www.ncbi. nlm.nih.gov. Date: 15 September 2022

www.Zauba.com. Date: 12 March 2020

Xiao, C., Ma, Y., Ji, D., & Zang, L. (2017). Review of desulfurization process for biogas purification. *IOP Conference Series: Earth and Environmental Science*, *100* (1). doi: 10.1088/1755-1315/100/1/012177.

Xie, P., Li, C. L., Shao, B., Xu, X. J., Chen, X. D., Zhao, L., Zhou, X., Lee, D. J., Ren, N. Q., & Chen, C. (2021). Simultaneous removal of carbon dioxide, sulfur dioxide and nitric oxide in

a biofilter system: Optimization operating conditions, removal efficiency and bacterial community. *Chemosphere*, *276* (x), 130084. doi: 10.1016/j.chemosphere.2021.130084.

Xu, X. J., Li, H. J., Wang, W., Zhang, R. C., Zhou, X., Xing, D. F., Ren, N. Q., Lee, D. J., Yuan, Y. X., Liu, L. H., & Chen, C. (2020). The performance of simultaneous denitrification and biogas desulfurization system for the treatment of domestic sewage. *Chemical Engineering Journal*, *399* (June), 125855. doi: 10.1016/j.cej.2020.125855.

Xu, X. J., Wu, Y. N., Xiao, Q. Y., Xie, P., Ren, N. Q., Yuan, Y. X., Lee, D. J., & Chen, C. (2022). Simultaneous removal of NO_X and SO_2 from flue gas in an integrated FGD-CABR system by sulfur cycling-mediated Fe(II) EDTA regeneration. *Environmental Research*, *205* (X), 112541. doi: 10.1016/j.envres.2021.112541.

Xu, X., Li, C.-L., Xie, P., Yuan, Y., Zhou, X., Ren, N., Lee, D.-J., & Chen, C. (2022). Enhanced removal of nitric oxide and carbon dioxide from flue gas in a biofilter: effect of flue gas recirculation and Fe(II) EDTA addition. *SSRN Electronic Journal*, 1–22. doi: 10.2139/ssrn.4067161.

Xue, S., Su, Z., & Cong, W. (2011). Growth of *Spirulina platensis* enhanced under intermittent illumination. *Journal of Biotechnology*, *151*(3), 271–277. doi: 10.1016/j.jbiotec.2010.12.012.

Yadav, G., Karemore, A., Dash, S. K., & Sen, R. (2015). Performance evaluation of a green process for microalgal CO_2 sequestration in closed photobioreactor using flue gas generated in-situ. *Bioresource Technology*, *191*, 399–406. doi: 10.1016/j.biortech.2015.04.040.

Yadav, G., & Sen, R. (2017). Microalgal green refinery concept for biosequestration of carbon-dioxide vis-a-vis wastewater remediation and bioenergy production: Recent technological advances in climate research. *Journal of CO_2 Utilization*, *17*, 188–206. doi: 10.1016/j.jcou.2016.12.006.

Yang, Q., Li, H., Wang, D., Zhang, X., Guo, X., Pu, S., Guo, R., & Chen, J. (2020). Utilization of chemical wastewater for CO_2 emission reduction: Purified terephthalic acid (PTA) wastewater-mediated culture of microalgae for CO_2 bio-capture. *Applied Energy*, *276* (July), 115502. doi: 10.1016/j.apenergy.2020.115502.

Yang, Y., Huang, S., Zhang, Y., & Xu, F. (2013). Field applications for NO_x removal from flue gas in a biotrickling filter by *chelatococcus daeguensis* TAD1. *Aerosol and Air Quality Research*, *13* (6), 1824–1831. doi: 10.4209/aaqr.2012.12.0352.

Yao, L., Qi, F., Tan, X., & Lu, X. (2014). Improved production of fatty alcohols in cyanobacteria

by metabolic engineering. *Biotechnology for Biofuels*, *7* (1), 1–9. doi: 10.1186/1754-6834-7-94.

Ye, Q., Cheng, J., Guo, W., Xu, J., Li, K., & Zhou, J. (2018). Serial lantern-shaped draft tube enhanced flashing light effect for improving CO_2 fixation with microalgae in a gas-lift circumflux column photobioreactor. *Bioresource Technology*, *255* (January), 156–162. doi: 10.1016/j.biortech.2018.01.127.

Yen, H. W., Ho, S. H., Chen, C. Y., & Chang, J. S. (2015). CO_2, NO_x and SO_x removal from flue gas via microalgae cultivation: A critical review. *Biotechnology Journal*, *10* (6), 829–839. doi: 10.1002/biot.201400707.

Yoshihara, K. I., Nagase, H., Eguchi, K., Hirata, K., & Miyamoto, K. (1996). Biological elimination of nitric oxide and carbon dioxide from flue gas by marine microalga NOA-113 cultivated in a long tubular photobioreactor. *Journal of Fermentation and Bioengineering*, *82* (4), 351–354. doi: 10.1016/0922-338X(96)89149-5.

Youngquist, J. T., Schumacher, M. H., Rose, J. P., Raines, T. C., Politz, M. C., Copeland, M. F., & Pfleger, B. F. (2013). Production of medium chain length fatty alcohols from glucose in *Escherichia coli*. *Metabolic Engineering*, *20*, 177–186. doi: 10.1016/j.ymben.2013.10.006.

Zhang, C., Tang, X., & Yang, X. (2018). Overcoming the cell wall recalcitrance of heterotrophic *Chlorella* to promote the efficiency of lipid extraction. *Journal of Cleaner Production*, *198*, 1224–1231. doi: 10.1016/j.jclepro.2018.07.114.

Zhang, J., Li, L., & Liu, J. (2015a). Temporal variation of microbial population in a thermophilic biofilter for SO_2 removal. *Journal of Environmental Sciences (China)*, *39*, 4–12. doi: 10.1016/j.jes.2015.11.005.

Zhang, J., Li, L., & Liu, J. (2015b). Thermophilic biofilter for SO_2 removal: Performance and microbial characteristics. *Bioresource Technology*, *180*, 106–111. doi: 10.1016/j.biortech.2014.12.074.

Zhang, J., Li, L., & Liu, J. (2017). Effects of irrigation and water content of packing materials on a thermophilic biofilter for SO_2 removal: Performance, oxygen distribution and microbial population. *Biochemical Engineering Journal*, *118*, 105–112. doi: 10.1016/j.bej.2016.11.015.

Zhang, J., Li, L., Liu, J., & Wang, Y. (2018). Effects of oxygen and water content on microbial distribution in the polyurethane foam cubes of a biofilter for SO_2 removal. *Journal of Environmental Sciences (China)*, *63*, 268–276. doi: 10.1016/j.jes.2017.03.017.

Zhang, X., Jin, R., Liu, G., Dong, X., Zhou, J., & Wang, A. (2013). Removal of nitric oxide from simulated flue gas via denitrification in a hollow-fiber membrane bioreactor. *Journal of Environmental Sciences (China)*, *25* (11), 2239–2246. doi: 10.1016/S1001-0742(12)60285-X.

Zheng, M., Li, C., Liu, S., Gui, M., & Ni, J. (2016). Potential application of aerobic denitrifying bacterium *Pseudomonas aeruginosa* PCN-2 in nitrogen oxides (NO_x) removal from flue gas. *Journal of Hazardous Materials*, *318*, 571–578. doi: 10.1016/j.jhazmat.2016.07.047.

Zhou, W., Zou, P., Sun, P., Bi, X., Wang, J., Chen, J., & Wang, H. (2013). Effects of the external carbon sources on the microbes in the simultaneous biological removal of SO_2 and NO_x process. *Environmental Earth Sciences*, *70* (5), 2381–2386. doi: 10.1007/s12665-013-2452-6.

Zhou, W., Wang, J., Chen, P., Ji, C., Kang, Q., Lu, B., Li, K., Liu, J., & Ruan, R. (2017). Bio-mitigation of carbon dioxide using microalgal systems: Advances and perspectives. *Renewable and Sustainable Energy Reviews*, *76* (March), 1163–1175. doi: 10.1016/j.rser.2017.03.065.

Zhu, B., Sun, F., Yang, M., Lu, L., Yang, G., & Pan, K. (2014). Large-scale biodiesel production using flue gas from coal-fired power plants with *Nannochloropsis* microalgal biomass in open raceway ponds. *Bioresource Technology*, *174*, 53–59. doi: 10.1016/j.biortech.2014.09.116.

Zhu, B., Xiao, T., Shen, H., Li, Y., Ma, X., Zhao, Y., & Pan, K. (2021). Effects of CO_2 concentration on carbon fixation capability and production of valuable substances by Spirulina in a columnar photobioreactor. *Algal Research*, *56* (5), 102310. doi: 10.1016/j.algal.2021.102310.

List of publications

International Journals:

1. **Anand, A.**, Raghuvanshi, S., & Gupta, S. (2020). Trends in Carbon Dioxide (CO_2) Fixation by Microbial Cultivations. **Current Sustainable/Renewable Energy Reports**, *7* (2), 40–47. doi: 10.1007/s40518-020-00149-1.
2. **Anand, A.**, Tripathi, K., Kumar, A., Gupta, S., & Raghuvanshi, S. (2021). Bio-Mitigation of Carbon Dioxide Using *Desmodesmus* sp. in the Custom-Designed Pilot-Scale Loop Photobioreactor. 1–16, **Sustainability**, 13, 9882. https:// doi.org/10.3390/su13179882.
3. Khandelwal, A., **Anand, A.**, Raghuvanshi, S., & Gupta, S. (2021). Integrated approach for microbial carbon dioxide (CO_2) fixation process and wastewater treatment for the production of hydrocarbons: Experimental studies. **Journal of Environmental Chemical Engineering**, *9* (3), 105116. doi: 10.1016/j.jece.2021.105116.
4. **Anand, A.**, Raghuvanshi, S., & Gupta, S. (2022). Sustainable approach for simultaneous reducing CO_2 and NO_x emissions from synthetic industrial flue gases using bacterial consortium and domestic wastewater in a suspended glass bio-reactor**, Biomass Conversion and Biorefinery**, 1–16, https://doi.org/10.1007/s13399-023-03934-2.

Book chapter communicated:

1. Rachael J Barla, **Abhishek Anand**, Smita Raghuvanshi, & Suresh Gupta, Life Cycle Assessment (LCA) of renewable diesel production, under review.

Manuscript under preparation:

1. **Anand, A.**, Raghuvanshi, S., Gupta, S. (2022). Performance evaluation of bacterial consortium in suspended glass bioreactor for concomitant wastewater bioremediation, simultaneous bio-fixation of CO_2- SO_2 and lipid biosynthesis for biodiesel production.
2. **Anand, A.**, Raghuvanshi, S., Gupta, S. (2022). Simultaneous removal of carbon dioxide, sulfur dioxide and nitric oxide in a 3-L bioreactor with simulated cement industry composition: Optimization, operating conditions, mitigation efficiency and product analysis.

International conference:

1. **Anand, A.**, Raghuvanshi, S., Gupta, S. (2022), Performance evaluation of bacterial consortium for bio-mitigation of CO_2 + SO_2 utilizing wastewater. "International Conference on Water Technologies (ICWT 22)", December 1-2, 2022, IIT, Bombay.
2. **Anand, A.**, Raghuvanshi, S., Gupta, S. (2022), Simultaneous removal of carbon dioxide and nitric oxide utilizing a mixed bacterial consortium in a glass bio reactor: Evaluation of

removal efficiency, characterization of microbial communities, and value-added products. "Technological Interventions for Sustainability", April 14-16, 2022, MNNIT, Allahabad.

3. **Anand, A.**, Khandelwal, A., Raghuvanshi, S., Gupta, S. (2019), Comparative bio-mitigation studies of CO_2 utilizing *H. stevensii* grown in wastewater and synthetic media. "Advances in Chemical Engineering and Science", 07-88 March 2019, IISER, Bhopal.

Biographies

Biography of the Candidate

Abhishek Anand did his B. Tech degree in Chemical Engineering from Haldia Institute of Technology in 2014. He completed his M.E. degree in Chemical Engineering from Jadavpur University in 2016. He joined BITS-Pilani, Pilani Campus in August 2017 as a Research Scholar. He is currently a PhD Scholar in the Department of Chemical Engineering at Birla Institute of Technology and Science (BITS), Pilani Campus, Rajasthan, India. His current research area includes bio-fixing flue gases (CO_2, NO and SO_2) using the microbial route. His research interests include wastewater remediation, flue gas bio-mitigation, downstream processing, and biofuel production. He got the Best Oral Presentation award at the "2nd International Conference on Water Technology 2022" at IIT Bombay. He was also involved in Teaching Assistant work in various courses such as chemical reaction engineering, process design principles-1, numerical methods for chemical engineering, fluid mechanics, transport phenomena, heat transfer, chemical engineering lab-II, process dynamics and control lab (first and second order system).

Biography of Supervisor

Prof. Smita Raghuvanshi is working as a professor in the Department of Chemical Engineering, BITS-Pilani, Pilani Campus, Rajasthan, India. She did her PhD from BITS-Pilani in the year 2010 in the area of Environmental Engineering. Her research focus is in the area of Biochemical Engineering and Environmental Engineering and specializes in Bio-filtration, Carbon Capture and Utilization in particular CO_2 mitigation utilizing bacterial species. Prof. Smita worked as Assistant Professor till July 2018 and at present is Associate Professor in the Department of Chemical Engineering.

Prof. Smita also works in the area of Anaerobic digestion of food waste. Prof. Smita takes up the courses of Biochemical Engineering, Environmental Management Systems, Chemical Process Technology, Environmental Studies, Chemical Engineering Lab, and few courses such as Heat Transfer, Engineering Chemistry and Chemical Process Calculations. Prof. Smita has completed 3 Projects; DST Fast Track Research Project entitled "Removal of volatile organic compounds, chlorinated VOCs, non-methane hydrocarbons, ethylene glycol) from waste streams using biofiltration" in year 2015. Another project entitled "Removal of Heavy Metals from Industrial Wastewater using Biofiltration" was completed as part of UGC major research project in June, 2015. Prof. Smita has just recently completed CRG – SERB Project of Rs 31.61 Lakhs in the area of Carbon Capture Utilization. The project was entitled as "Process development for bio-mitigation of flue gases (CO_2, SOx, and NOx) using Chemolithotrophs and production of value-added products".

She has around 28 Research Publications in peer reviewed International Journals such as Bioresource Technology, Process Biochemistry, Biodegradation, Journal of CO_2 Utilization. She has also published 5 Book Chapters and invited articles in various books and technical notes. She has around 53 Conference Publications. Prof. Smita has also won 1st prize in the paper presentation on "Removal of Methyl Ethyl Ketone (MEK) using Bio-filtration" in National Conference on Environmental Conservation (NCEC-2006), held at BITS-Pilani in September 1-3, 2006. She is the reviewer of International Journals which include Journal of Physical Sciences, Biodegradation, Journal of Food Processing and Technology and Nano-sciences & Nanotechnology, Journal of Chemical and Environmental Engineering. She has shown exemplary acumen in the application of life cycle engineering concepts i.e. LCA of RO based filtration system in BITS-Pilani and has also carried out LCA of STP, BITS-Pilani, She is a Life Member of Indian Institute of Chemical Engineers (IIChE) and Fellow Member of International Congress of Chemistry and Environment (FICCE). She is also a member of American Institute of Chemical Engineers (AIChE), International Association of Engineers (IAENG) and Institute of Engineers, IEI, India.

She was the former Convener of Department Research Committee (DRC) and the Department Committee of Academics of Chemical Engineering Department. She has been the

Nucleus Member of Practice School Division, BITS-Pilani, Pilani Campus, Rajasthan, India from 2003-2012. She has been actively involved in various departmental activities and involved in laboratory based up gradation work of Engineering Chemistry. She was the Convener of the Work shop on Analytical Instruments for Chemical and Environmental Engineers - WAICEE-2015 and WAICEE - 2019. Prof. Smita has also been the Organizing Committee Member of Life Cycle Engineering Conference held at BITS-Pilani in the year 2015 and 2016. She has guided 1 PhD student as Supervisor, 1 PhD student as Co – Supervisor, and guiding 3 student as Supervisor. She has guided 8 ME dissertation student and 1 student is pursuing ME dissertation. She has been actively guiding several BE Thesis and Project student.

Biography of Co-Supervisor

Prof. Suresh Gupta is a Professor in Department of Chemical Engineering. Prof. Suresh completed his PhD from BITS-Pilani, Pilani Campus, India in the year 2008. Prof. Suresh Gupta's broader Research interests include Environmental Engineering and Separation Processes. He became Assistant Professor in August 2008, Associate Professor in February 2015, and Professor in June 2021. He served as Head of the Department during September 2012 to August 2016. Prof. Gupta served as Associate Dean, Academic - Undergraduate Studies Division (AUGSD), BITS Pilani, Pilani Campus from August 2018 to August 2022.

Prof. Gupta is an excellent academician with total 20 years of teaching and research experience. Prof Gupta is the recipient of DST Young Scientist Project awarded to him by Department of Science and Technology, Govt. of India, New Delhi, India during the year 2013 to 2017. He has successfully implemented several research projects in the field of Environmental Engineering, funded by DST-SERB, UGC, Birla Cellulosic Kharach, BITS Pilani, and Aditya Birla Science & Technology Company Pvt. Ltd. (ABSTCPL). He has published 41 Research Publications in peer reviewed journals, 7 Book Chapters and 68 Conference Proceedings. He has around 60 Conference Proceedings to his credit. He guided 4 PhD (as Supervisor/Co-supervisor) and 19 M.E. Dissertation students. Prof. Gupta is guiding 2 PhD Student at present. Prof. Gupta has been in various Academic and Administrative Committees at BITS-Pilani and various Institutes / Organizations.

Prof. Gupta was invited as a member in die workshop to review the existing scheme of the Engineering Services Examination conducted by the Commission organized by UPSC at the International Management Development Center (IMDC), Indian Institute of Management, Vastrapur, Ahmedabad. Prof. Gupta is a Member of the Board of Studies of Faculty of Bio- and Chemical Engineering, Sathyabama University, Jeppiaar Nagar, Chennai. He has visited various industries such as Ultratech Cement, Reddipalaym Cement Works, Indo Gulf Fertilizers, Birla Cellulosic Kharach, Bhang Aluminum Company Limited and Hindustan Zinc Limited for discussions on BITS Collaborative Programmes on Academic Development in Basic Process Engineering for their Employees. He also served as a Resource Faculty in Practice School

Division, BITS-Pilani. He was also an External Examiner for B. Tech - Chemical Engineering students at Banasthali University. He is currently the reviewer of 16 International reputed Journals. He is a Life Member of Indian Institute of Chemical Engineers (IIChE) and Fellow Member of International Congress of Chemistry and Environment (FICCE).